The surface/atmosphere exchange of ammonia

Mark A. Sutton

A thesis submitted for the degree of Doctor of Philosophy to the University of Edinburgh.

Declaration

This thesis has not been submitted in any other application for a degree and is the result of my own work and composition

October 1990

Abstract

Measurements of the exchange of gaseous ammonia (NH_3) and particulate ammonium (NH_4^+) between the atmosphere and a range vegetated surfaces were made using micrometeorological techniques. The aerodynamic gradient method was applied to estimate fluxes, and these interpreted using a resistance analogy and estimates of surface concentration. The results are used to develop an understanding of exchange processes with a view to estimating annual budgets for different surfaces. NH_4^+ was found to deposit very slowly so that the study focused on the exchange of NH_3.

Over natural and unfertilized vegetation, NH_3 was generally found to deposit rapidly with near zero surface resistance (r_c). Some exceptions were seen for dry vegetation (r_c < 50 s m^{-1}) and over vegetation with exposed calcareous soil (mean r_c = 125 s m^{-1}). Over fertilized agricultural vegetation both emission and deposition fluxes were recorded, with emission being favoured in warm dry conditions, and deposition in cool wet conditions. In wet conditions in summer r_c was variable (0–130 s m^{-1}), whereas in winter r_c was small (< 30 s m^{-1}). During frozen conditions an increased r_c of up to 80 s m^{-1} was observed. In dry summer conditions emission of up to 24 ng NH_3 m^{-2} s^{-1} was recorded. The estimation of the net 'compensation point' for exchange using surface concentration estimates is discussed, and shown to range over 0–7 μg m^{-3} in the study here depending on surface type and environmental conditions.

The different exchange patterns seen over unfertilized and fertilized vegetation are compared and described in terms of the net exchange with the surface resulting from exchange with leaf surfaces, stomata and the soil. Factors affecting these processes are discussed and include environmental conditions (particularly temperature, wetness and humidity), the presence of acidic pollutants, and the status of the surface (including nitrogen status, stomatal opening, soil pH). Implications are drawn for the concentration dependence of exchange rates and approaches to modelling the atmospheric behaviour of NH_3.

In order to estimate annual fluxes, atmospheric concentrations of NH_3 are needed. Background annual concentrations of NH_3 measured in this study at several sites in S. Scotland were in the range 0.4–1.1 μg m^{-3}. Using these and other published data, annual fluxes over different surfaces are estimated. Over an example fertilized surface a small net NH_3 emission is predicted (< 1 kg N ha^{-1} $year^{-1}$), while over unfertilized surfaces larger deposition fluxes are expected (3–55 kg N ha^{-1} $year^{-1}$ for the background sites considered). Comparison with other sources of atmospheric N shows that dry deposition of NH_3 is frequently the dominant N input to unfertilized surfaces.

Acknowledgements

This study was conducted jointly between the Institute of Terrestrial Ecology (ITE), Edinburgh Research Station and the Department of Forestry and Natural Resources (FNR) of the University of Edinburgh. I would like to thank my supervisors in both institutes, Dr. David Fowler (ITE) and Dr. John Moncrieff (FNR), for their guidance and encouragement, as well as all the other friends and colleagues who helped in some way. Particular thanks are due to Gordon Elphinstone of the ITE workshop for the high quality field equipment he produced, and to the staff of the ITE library for coping with my innumerable illegible requests for reading material.

Advice and support in collaborative field measurements were also received from members of other institutes, including Dr. Roy Harrison (University of Essex), Dr. Tom Choularton (University of Manchester Institute of Science and Technology), Dr. Geoff Dollard (Harwell Laboratory) and other colleagues in these institutes. The project was funded by a studentship from the U.K. Natural Environment Research Council (Special Topic Program in Atmospheric Chemistry) and permission for measurements given by several willing landowners. The help of each of these is gratefully acknowledged.

Finally, thanks to Dr. Ken Hargreaves and Robert Storeton-West at ITE for all their support and humour both in the laboratory and the field — not least to Robert, for being ready to fetch a haggis to the hills on a cold winter's night.

List of symbols and other notation

Roman Alphabet

A	cross sectional area of a diffusion tube (m^2)
B	semi-empirical sub-layer Stanton number (dimensionless).
c_p	specific heat capacity of air (1.01 J g^{-1} $°C^{-1}$; approximately constant at usual environmental temperatures)
D	diffusion coefficient of an entrained property in still air (m^2 s^{-1})
d	zero plane displacement. Height of apparent (aerodynamic) ground level due to a rough surface such as vegetation (m)
E	water vapour flux to or away from a ground surface (g m^{-2} s^{-1})
$E\{z\text{-}d\}$	absolute humidity or water vapour concentration at a given height above the zero plane (g m^{-3})
$E_sT\{z_o'\}$	saturated water vapour concentration at the mean temperature of the surface (g m^{-3})
F_χ	flux of trace gas or particulate to or away from a surface (μg m^{-2} s^{-1})
$f\{z\text{-}d\}$	multiplicative stability correction factor, $(\Phi_M.\Phi_H)^{-1}$ (dimensionless)
G	ground heat flux by conduction (W m^{-2})
g	gravitational acceleration (9.81 m s^{-2})
H	sensible heat flux to or away from a ground surface (W m^{-2})
h	height of vegetation surface (m)
K	chemical equilibrium constant. Subscripted: ha, Henry constant for ammonia; a, dissociation constant of NH_4^+; b, dissociation constant of $NH_3.H_2O$; w dissociation constant of water
K	Turbulent diffusion coefficient (eddy diffusivity). Subscripted: M, momentum; H, heat; E, water vapour; χ, gas or particulate exchange (m^2 s^{-1})
k	von Karman's constant. Constant of proportionality of mixing length (l) to height above zero plane in neutral conditions (0.41)
L	Monin-Obukhov stability length. Estimate of atmospheric stability above a surface. Independent of height within the constant flux layer (m)
l	mixing length or mean eddy size at a given height above a surface (m)
M	molecular weight (g mol^{-1})
P	air pressure (Pa). Subscripted: NH_3, partial pressure of ammonia in air
Q	mass of NH_3 captured during a diffusion tube exposure period (μg)
q	mass of NH_4^+ measured in a diffusion tube adsorbent disc (μg). Subscripted: e, exposed tube; b, blank tube
R	general gas constant (8.314 Pa m^3 mol^{-1} K^{-1})
Re_*	turbulent Reynolds number, used in estimating B (dimensionless).

Ri	Richardson number. Estimate of atmospheric stability above a surface. A function of height within the constant flux layer (dimensionless)
$\mathbf{R_n}$	net radiation flux to or away from a surface (W m^{-2})
$r\{z_1, z_2\}$	resistance to atmospheric transport of a trace component between two heights z_1 and z_2 (s m^{-1}).
$r_t\{z\text{-}d\}$	total resistance to deposition of a trace component, from a defined height above the zero plane. Inverse of deposition velocity (s m^{-1}).
$r_{aM}\{z\text{-}d\}$	atmospheric resistance to deposition of momentum (s m^{-1}).
$r_a\{z\text{-}d\}$	atmospheric resistance of a trace component to turbulent transfer between the atmosphere and a surface (s m^{-1})
r_b	resistance to transfer for entrained properties across quasi-laminar sub-layer surrounding roughness elements of a surface (s m^{-1})
r_c	surface or canopy resistance to deposition. A residual or excess resistance between r_t and $(r_a + r_b)$, assuming surface concentration is zero. May be envisaged as a number of component resistances acting together: r_s, stomatal diffusion; r_i, mesophyll uptake; r_{cu}, cuticle diffusion; r_{ep}, epidermal cell uptake; r_p, leaf surface uptake by reaction; r_g, soil uptake (s m^{-1})
r_{sE}	stomatal resistance to water vapour transfer (s m^{-1})
r_{sEb}	bulk stomatal resistance to water vapour transfer (s m^{-1})
s	parts per billion (10^9) volume fraction of a constituent in air, ppbv
Sc	Schmidt number, used in estimating B (dimensionless)
T	temperature (°C or K).
t	time (s and other units)
u	mean horizontal windspeed (m s^{-1}).
u_*	eddy (or friction) velocity (m s^{-1})
$u\{z\text{-}d\}$	mean horizontal windspeed at a given height above the zero plane (m s^{-1}).
$V_d\{z\text{-}d\}$	deposition velocity of gaseous or particulate species at a given height above the zero plane (mm s^{-1})
$V_m\{z\text{-}d\}$	maximum value of the deposition velocity permissible by turbulence, $1/(r_a + r_b)$ (mm s^{-1})
w	mean vertical windspeed (m s^{-1})
w'	instantaneous fluctuations about the mean vertical windspeed (m s^{-1})
z	distance; height above the ground; diffusion tube path-length (m)
z_χ	apparent height above zero plane of predicted zero concentration, from linearized concentration profile (m).
z_o	roughness length. Apparent height above zero plane of predicted zero windspeed, from linearized wind profile. Mean point of absorption of momentum (m)
z_o'	apparent height above the zero plane of the mean point of exchange of entrained properties with a surface, accounting for r_a and r_b (m)
z_o''	as z_o' but also accounting for a surface resistance *e.g.* r_{sEb} (m)

Greek alphabet

Γ	gradient of constituent *versus* $\ln(z\text{-}d)$ in error analysis, Appendix 5
ΔP	pressure difference between ambient pressure and forward pressure of moving air, used in Pitot tube measurement (Pa)
ΔV_d	error in gradient method estimate of V_d arising from concentration changes ($\Delta\chi$) during sampling runs of duration (Δt) (mm s^{-1})
κ	thermal diffusivity of air (m^2 s^{-1})
λ	latent heat of vaporization of water vapour (J g^{-1})
λ E	latent heat flux to or away from a ground surface (W m^{-2})
ν	kinematic viscosity of air (m^2 s^{-1})
ρ	density of air (g m^{-3})
τ	atmospheric residence time of a species. Subscripted V_d: residence time of dry deposition
τ	flux of momentum (shear stress) toward the ground (g m^{-1} s^{-2}, N m^{-2})
$\Phi\{(z\text{-}d)/L\}$	empirically estimated gradient correction factor for non-neutrality in the aerodynamic gradient method. Subscripted: M, momentum; H, heat; χ, trace components (dimensionless)
χ	mean concentration of trace component. Default reference is to ammonia or ammonium (μg m^{-3})
χ'	instantaneous fluctuations about the mean concentration (μg m^{-3})
$\chi\{z\text{-}d\}$	mean concentration of trace gas or particulate in the atmosphere at a defined height $\{z\text{-}d\}$ above the zero plane of the surface (μg m^{-3})
χ_*	eddy concentration (μg m^{-3})
χ_{cp}	compensation point concentration. Supposed concentration in atmosphere in equilibrium with vegetated surfaces (μg m^{-3})
$\psi\{(z\text{-}d)/L\}$	empirically estimated integrated profile correction factor for non-neutrality in the aerodynamic gradient method. Subscripted: M, momentum; H, heat; χ, trace components (dimensionless)

Other notation

The following conventions are adopted in the text:

$[n]$	molar concentration of entity n (mol l^{-1}); parenthesis in mathematical expressions
$a\{b\}$	functional relationship of a upon b in mathematical expressions
$\bar{n}$	mean value of n
$\tilde{n}$	median value of n

Field measurement campaigns are referred to in the text by site and month/year. For example, Huntingdon 8/1987 refers to measurements made at this site in August 1987.

Further conventions are discussed in Appendix 1.

Contents

Chapter 1

Introduction

Ammonia (NH_3) is increasingly becoming recognized as an important atmospheric pollutant. While its source, mainly from agriculture, sets it apart from combustion source pollutants such as sulphur dioxide (SO_2) and nitrogen oxides (NO_x), the scale of its emission results in it being one of the major sources of fixed nitrogen deposited onto natural ecosystems, alongside NO_x. In addition, oxidation of NH_3 to nitrates (NO_3^-) in some soils contributes with these other gases to the acidification of ecosystems. Both these inputs may have undesirable ecological consequences.

Ammonia is an alkaline gas, being readily soluble in water, ionizing to form the ammonium ion (NH_4^+). It occurs naturally as both NH_3 and NH_4^+ and is one of the major components of the nitrogen cycle in the biosphere. It is an important constituent of plants and animals, while in natural ecosystems it derives originally from the atmospheric nitrogen fixed by some bacteria — such as those associated with leguminous plants — and from the biological conversion of NO_3^- fixed as NO_x in electrical storms, as well as a contribution from soils (*e.g.* Söderlund and Svensson, 1976). Biological assimilation generally converts the fixed nitrogen to the reduced (R-NH_2) form. Subsequent decomposition of dead plants and animals, and production of animal excreta, release NH_3, which may then volatilize into the atmosphere. This later returns to earth, either by direct uptake as NH_3 or NH_4^+ (dry deposition), or as NH_4^+ dissolved in precipitation (wet deposition).

It is difficult to ascertain what would be the size of these fluxes in a wholly natural system, although attempts have been made (*e.g.* Söderlund and Svensson, 1976; Dawson, 1977; Delwiche, 1977). What is clear however, is that man has increasingly disrupted the natural levels by the addition of large quantities of fixed nitrogen into the cycle. This is largely due to the increased industrial fixation of NH_3 for fertilizers, and the ensuing intensive agriculture that is consequently possible. The nitrogen produced by the increased use of legumes adds to this effect, while the burning of fossil fuels, particularly coal, releases NH_3 otherwise isolated from the biosphere for millions of years.

In Europe the agricultural losses to the atmosphere are particularly important (*e.g.* Buijsman *et al*, 1987). Losses may occur during production or application of the fertilizer, or be connected with livestock farming. This is especially the case for the intensive farming made possible by the use of additional feeds, these being artificially

produced or resulting from the crop surpluses that are possible as a result of fertilization. The livestock produce large quantities of excreted waste, from which ammonia is lost to the atmosphere. This may occur directly from pastures and feedlots, may be lost during storage, or may result from the application of the waste to fertilize further crops.

The result of these changes is an increased flux of NH_3 into the atmosphere which may then influence tropospheric chemical processes. Neutralization reactions may occur with other anthropogenic acid pollutants, such as SO_2, HNO_3 and HCl to form NH_4^+, which is present in sub-micrometre size aerosol particles or dissolved in cloud droplets. This change of state from gases to aerosols affects the rate at which each of the components return to earth, as dry or wet deposition, and consequently modifies the quantity of each component transported in the atmosphere. Given that NH_3 may affect the rates of conversion of the other components, a change in the pattern of acid deposition received by different localities may result.

Increased deposition of NH_x (NH_3 or NH_4^+) to the ground also contributes to the nitrogen input of an ecosystem. For agricultural crops such inputs may be small compared to fertilizers. However, for natural ecosystems, with no other nitrogen added, this may represent a considerable shift in the nitrogen balance, and correspondingly lead to biological changes associated with eutrophication (*e.g.* Heil and Diemont, 1983; Roelofs *et al.* 1985). The scale of inputs may be raised from less than $\approx$5 to over 50 kg N ha^{-1} $year^{-1}$ deposited in polluted areas. In addition nitrification of the NH_x may occur resulting in soils and water bodies being acidified, exacerbating the effect of the other pollutants (Van Breeman *et al.*, 1982; Nihlgard, 1985).

These observations identify a need for an improved understanding of the processes of NH_x circulation. As well as the more widespread interest associated with air chemistry and acidification, the concern about ecological effects outlined above has been especially prominent in the Netherlands and Belgium, where NH_3 emissions are large. This concern has only fully been realized in the 1980s, yet has already stimulated an increased scientific attention, both in terms of ecological effects studies, as well as in the estimation and modelling of emission, transport, and deposition. There remains, however, a shortage of information from field studies, on which to base such work. This is especially the case with regard to the estimation of NH_x exchange between the atmosphere and the ground, and in the measurement of atmospheric concentrations. Results from such studies would be useful, both to those modelling atmospheric NH_x budgets, and to those interested in ecological effects. It is these, then, which are the subject of this study.

1.1. PROPERTIES OF AMMONIA

As a background to understanding the behaviour of ammonia in the environment, it is important to consider its physical and chemical properties.

Ammonia is a gas at all environmental temperatures, since its boiling point at atmospheric pressure is -33.4 °C. It is colourless and may be detected by its pungent odour when in high concentrations (>50 ppmv, NRC, 1979). Other physical constants and properties of NH_3 are given in Table 1.1. As a base, NH_3 is important in neutralizing acids in the atmosphere where it constitutes the only major gaseous base present. Equilibria with HNO_3 and HCl are known to occur in the gas phase reacting to form NH_4^+ salts (*e.g.* Allen *et al.*, 1989). At low humidities these are present as crystalline particles of approximately 0.1 to 1.0 μm diameter, while at high humidities (above 70% relative humidity) they progressively deliquesce to form aqueous aerosol particles. The dominant NH_4^+ salts in the atmosphere are, however, the sulphates (SO_4^{2-}). These are produced predominantly by aqueous reaction with H_2SO_4 in atmospheric water droplets, such as in clouds, with subsequent droplet evaporation producing particulates. Oxidation of SO_2 to form SO_4^{2-} may itself also be enhanced by NH_3. Atmospheric aerosols are important as they affect atmospheric turbidity (clarity) and also act as cloud condensation nuclei (Seinfeld, 1986).

Ammonia is a reactive gas and will readily adsorb on to dry surfaces (NRC, 1979), as well as being extremely soluble in water (Table 1.1). The solubility of ammonia is particularly important in its environmental circulation. The equilibrium with aqueous solutions depends on both its physical solubility and on removal reactions in solution. Its physical solubility may be described according to the Henry equilibrium:

$$NH_3 + H_2O \overset{K_{ha}}{\Leftrightarrow} NH_3.H_2O \qquad 1.1$$

$$K_{ha} = [NH_3.H_2O] / [NH_3(gas)] \qquad 1.2$$

where K_{ha} is the dimensionless Henry constant (M/M) and square brackets imply molar concentrations (M = mol dm^{-3}). The value of K_{ha} is temperature dependent, with solubility decreasing with increasing temperature.

The total NH_x solubility is much larger than given solely by K_{ha} however, because of ionization in solution to form NH_4^+. This may be described by:

$$NH_3.H_2O \overset{K_b}{\Leftrightarrow} NH_4^+ + OH^- \qquad 1.3$$

$$K_b = [NH_4^+] .[OH^-] / [NH_3.H_2O] \qquad 1.4$$

Property	value
Molecular weight	17.03 g mol^{-1}
Boiling point	-33.35 °C
D (NH_3)	2.29 × 10^{-5} m^2 s^{-1}
D (H_2O)	2.49 × 10^{-5} m^2 s^{-1}
K_{ha} (O_3)	0.23
K_{ha} (CO_2)	0.83
K_{ha} (SO_2)	30
K_{ha} (NH_3)	1.8 x 10^3
K_{ha} (HCl)	6.1 x 10^4
K_{ha} (HNO_3)	5.1 x 10^6

Table 1.1a Selected properties of NH_3 and a comparison of solubility in water (see Table 1.1b) with other gases. Diffusion coefficient (D) for NH_3 in air also compared with H_2O. D and K_{ha} for 25 °C.

T (°C)	K_{ha}	K_b x 10^{-5}	K_w x 10^{-15}
0	5206	1.374	1.138
5	4192	1.479	1.845
10	3353	1.570	2.917
15	2722	1.652	4.508
20	2225	1.710	6.808
25	1832	1.774	10.07
30	1517	1.820	14.69
35	1265	1.849	20.89

Table 1.1b Dimensionless (M/M) equilibrium constants for calculating solubility of NH_3 in water. K_{ha}: Henry constant of NH_3; K_b: dissociation constant of $NH_3.H_2O$; K_w: dissociation constant of water. (Data for both parts of table from NRC, 1979; Seinfeld, 1986; Hargreaves, 1989).

Values for K_b are also given in Table 1.1. Hence NH_3 acts as a base, through the production of hydroxide ions (OH^-). The effect of this upon pH may be quantified by relating this to the ionization of water:

$$H_2O \overset{K_w}{\Leftrightarrow} H^+ + OH^- \qquad 1.5$$

$$K_w = [H^+].[OH^-] \qquad 1.6$$

Substituting the $[NH_3.H_2O]$ and $[OH^-]$ of equation 1.4 with their values from equation 1.2 and 1.6 respectively gives:

$$[NH_3(gas)] = \frac{K_w\ [NH_4^+]}{K_{ha}\ K_b\ [H^+]} \qquad 1.7$$

Hales and Drewes (1979) and NRC (1979) have provided relationships accounting for the temperature dependence of K_{ha} and K_a where $K_a = K_w/K_b$. These may be substituted into equation 1.8 to provide a useful working formula, where temperature (T) is in Kelvin:

$$[NH_3(gas)] = \frac{10^{(-0.09018\ -\ 2729.92/T)}[NH_4^+]}{10^{(1477.7/T\ -\ 1.6937)}\ [H^+]} = 10^{(1.60352\ -\ 4207.62/T)}.\frac{[NH_4^+]}{[H^+]} \qquad 1.8$$

Thus given $pH = -\log_{10}[H^+]$ (using molar concentrations), the interdependence of pH, $[NH_4^+]$, and $[NH_3(gas)]$ may be quantified. It is seen that $[NH_4^+]$ increases proportionately to $[NH_3(gas)]$ and to $[H^+]$. However, given the logarithmic relationship of the latter to pH, the solubility of NH_4^+ will be extremely sensitive to pH. Conversely, this shows that an increased quantity of $NH_3(gas)$ will give rise to an increased pH. These relationships are shown in Figure 1.1 for total dissolved NH_x.

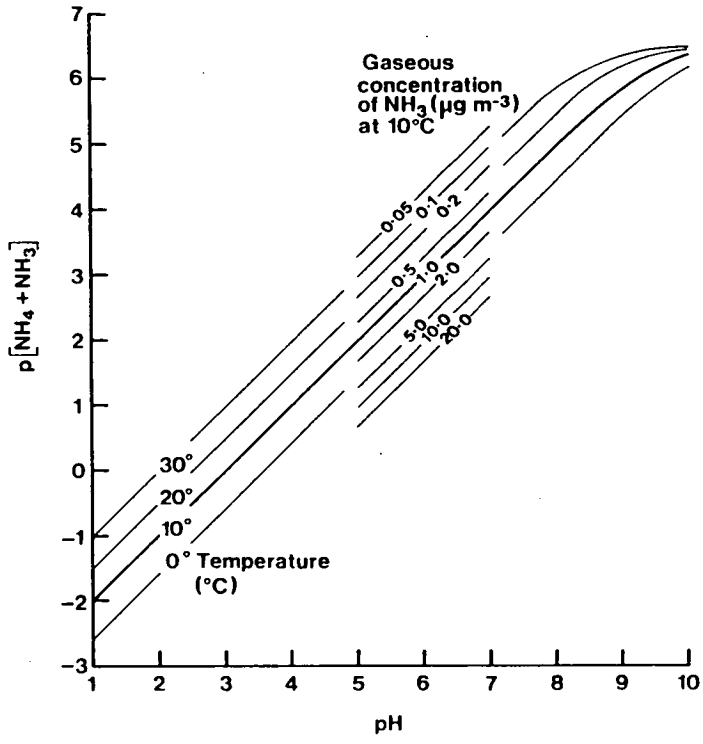

Figure 1.1 Relationships of equilibrium total NH_3 and NH_4^+ in water for different pH, temperature and air concentration of NH_3. Aqueous ammonia concentration plotted as $p[NH_3 + NH_4^+] = -\log_{10}[NH_3 + NH_4^+]$ for comparison with pH. The main curves are for an air concentration of NH_3 of 1 $\mu g\ m^{-3}$. The curvature at high pH is due to the increased proportion from $[NH_3.H_2O]$.

The total $[NH_x]$ in solution may be found by adding the dissolved NH_x components from equations 1.2 and 1.7. However, at all but the highest environmental pH values the NH_4^+ dominates over the NH_3. Court *et al* (1964) have estimated that at a value of pH 9, 40% of the total NH_x is $NH_3.H_2O$, while at pH 8 the value is only 5%. Below this pH the $NH_3.H_2O$ component is negligible. Temperature also affects the equilibrium, primarily through K_{ha}. Over usual environmental temperature ranges the effect is smaller than that due to pH, though still considerable (Figure 1.1).

The parameters that affect NH_3 exchange between aqueous and gas phases may consequently be described. This discussion, however, represents a simplified analysis since it deals only with the solubility in pure solutions. In environmental conditions other species will be present, such as the products of dissolved gases, CO_2, SO_2, HNO_3, HCl or ions from soils such as humic acids or Ca^{2+}. These all have effects on pH and correspondingly modify NH_x solubility. This may be accounted for by a similar, but extended, analysis to the above. Acid species, such as the other air pollutants enhance solubility, while basic ones such as Ca^{2+} reduce it. An example of these interactions occurs in the (O_3 catalyzed) oxidation of SO_2 to SO_4^{2-} noted above. In the absence of NH_3 the production of SO_4^{2-} lowers the pH which limits the

reaction. However, with NH_3 present a high pH is maintained allowing the reaction to proceed (Junge and Ryan, 1958).

In addition to such pH modification of solubility, Hales and Drewes (1979) also noted a further interaction with CO_2 which caused solubility to be less than predicted. They postulated this could be due to the formation of a volatile adduct, such as carbamic acid (NH_3CO_2), the simultaneous loss of which would reduce solubility. In addition, the normal temperature response of the equilibrium was modified. With one exception (Horváth, 1982) this effect appears to have been ignored in work modelling surface atmosphere exchange of NH_3, though it appears to warrant further research, given that CO_2 is present in usual environmental NH_3 equilibria.

In summary, the equilibrium for ammonia depends on levels of $[NH_4^+]$, $[NH_3(gas)]$, pH and temperature, though this may be modified by other ions in the chemical environment. In addition the water balance of a surface affects total quantities dissolved. As a consequence, these factors are expected to be important in the exchange of NH_3 between the ground and the atmosphere, and between phases in the atmosphere itself.

1.2. Historic Review

1.2.1 Early work

Interest in atmospheric ammonia is certainly not new. De Saussure, in France, observed its presence in the atmosphere in 1804 (see Way, 1855). However, it was with the great debate in the mid 19th century, on the source of nitrogen for plants, that interest in ammonia in the atmosphere really started. Full accounts of the debate are given elsewhere (*e.g.* Way, 1855; Russell and Richards, 1919; Eriksson, 1952), however in essence, Liebig (1847) proposed that plants derived their nitrogen as ammonia from the air, in a similar way to carbon dioxide, and also from rain. He suggested a figure of 27 kg NH_x-N ha^{-1} $year^{-1}$ was brought down to meet this need. The debate that ensued however, showed the situation to be more complicated. Boussingault (1856) showed the importance of nitrate in plant nutrition, while the precipitation chemistry measurements of others such as Lawes and Gilbert (1851) at Rothamsted, U.K., showed that a fertilized non-leguminous crop removed far in excess nitrogen than was brought down as ammonium by rain; an amount which they estimated to be $\approx$5 kg NH_4-N ha^{-1} $year^{-1}$.

Many other measurements of ammonium in precipitation followed and these were reviewed by Eriksson (1952). A selection of these is given in Table 1.2. Eriksson notes some of the problems that might be encountered in these measurements, which

would include contamination by dust and bird excreta, as well as problems of microbial decomposition of samples before analysis. He noted that contamination by excreta is usually easy to detect since this gives occasional greatly increased concentrations. Decomposition could be minimized by reducing storage before analysis or by using lead containers to reduce microbial activity (*e.g.* Russell and Richards, 1919). The problem of dust input appeared most intractable. As a result of this and also because of dry deposition to collectors (section 1.2.3), such samples have become known as bulk precipitation. With this restriction, most sites in Table 1.2 gave deposition in the range of 1–15 kg NH_4-N ha^{-1} $year^{-1}$. Much variation was apparent between sites with the highest values associated with major population centres, suggesting emission to be of anthropogenic origin. Conversely, remote coastal sites in high latitudes gave the lowest values.

Other studies were made of ammonia in the air, including the demonstration that plants could absorb NH_3 gas directly from the atmosphere. Studies by Ville (1850) and later by Schlösing(1874) using chlorotic, nitrogen deficient plants showed that they would regain a healthy green colour when put in an NH_3 rich chamber. Many attempts were made to quantify the importance of this absorption, however these were done by indirect means, and mostly considering the soil as the sink. Measurements of absorption of NH_x by dilute acid solutions or soil surfaces with a given area exposed to the air, were used to estimate the deposition flux. Early results using such acid solutions were provided by Bineau (1854; see Hall and Miller, 1911) who recorded 50 kg NH_x-N ha^{-1} $year^{-1}$ at Lyon and 15 kg ha^{-1} $year^{-1}$ at Caluire in France, however contamination by insects and dust was again suspected to be important. Similar experiments of Heinrich (1881) gave 31 kg ha^{-1} $year^{-1}$ at Rostock, while Kellner *et al.* (1886) recorded 11.6 kg ha^{-1} $year^{-1}$ at Tokyo. Bretshneider (1872) provided the first deposition measurements to soil-like surfaces. He found a moist mixture of 95% quartz sand and 5% humic acid absorbed 46 kg ha^{-1} $year^{-1}$.

Conversely, Hall and Miller (1911) at Rothamsted used a fine mesh screen over their collector in an attempt to reduce insect and dust contamination. They obtained results showing a deposition of around 1 kg ha^{-1} $year^{-1}$ to their acid solutions, and correspondingly concluded that this dry deposition process was not important. However, the reduced air access to their dishes due to the mesh is the most likely explanation of their results. The problem of air access to collector surfaces is, nevertheless, a general criticism of the approach. Because of the different aerodynamic properties of collector surfaces compared to rough ground or vegetation, it is likely that deposition rates will also differ. Despite this, authors have continued to use this approach (De Rossi, 1947: 20–25 kg NH_3-N ha^{-1} $year^{-1}$ to soil; Malo and Purvis,

Year	Place	precipitation (mm)	concentration (mg NH_4-N dm^{-3})	flux (kg NH_4-N ha^{-1} $year^{-1}$)
	EUROPE			
	Belgium			
1889–1893	Gembloux	693	1.14	7.9
	Denmark			
1880–1885	Copenhagen	577	1.91	11.0
1922–1927	Askov	740	0.71	5.3
1880..1927	mean 5 sites	628	1.06	6.6
	France			
1877	Methroy	760	0.41	3.1
1876–1900	Montsouris	545	2.13	11.6
1864..1886	Germany, mean 6 sites	509	1.49	7.5
	Great Britain			
1888–1916	Rothamsted	730	0.41	3.0
1906–1909	Garforth, Leeds	685	1.04	7.1
1908–1913	Butt of Lewis, Stornaway	1060	0.04	0.4
1907..1913	NW Scotland: mean 4 sites	1359	0.11	1.6
	Holland			
1910–1912	Groningen	700	0.72	5.1
1932–1937	Hilversum mean 6 sites	—	—	3.8
	Iceland			
1911–1912	Vifelstadir	949	0.09	0.9
1869..1890	Italy, mean 4 sites	924	0.64	6.3
1928–1929	Norway, mean 2 sites	824	0.14	1.2
	ASIA, AUSTRALASIA, AFRICA			
	East Indies			
1891–1892	Pasoeroean, Java	920	0.14	1.3
1891..1942	India, mean 6 sites	2162	0.30	5.8
	Japan			
1883–1884	Tokyo	1337	0.13	1.7
	Australia			
1908	Queensland, mean 2 sites	905	0.32	2.6
	New Zealand			
1884–1887	Lincoln, Canterbury	755	0.08	0.6
1904..1912	South Africa, mean 6 sites	670	0.61	4.0
1938	Mauritius	1002	0.38	3.8
	AMERICA			
	Canada			
1908–1924	Ottawa	860	0.51	4.43
	U.S.A.			
1919..1926	N. Y. State, mean 4 sites	818	1.02	8.4
1930	Goodwell, Oklahoma	390	0.28	1.1
1922–1923	Kentucky, mean 6 sites	1090	1.19	13.0
	West Indies			
1886–1889	Barbados	1620	0.07	1.1
1901–1912	Trinidad	1480	0.16	2.4
	British Guiyana			
1890–1909	Georgetown	2520	0.05	1.1
	Argentina			
1906	Buenos Aires	750	2.96	22.2

Table 1.2 Pre-1950 data on levels of ammonium in precipitation (Bulk precipitation). Typical data from that collated by Eriksson (1952). Note: year..year implies data for selected years through period.

1964: 3–6 kg ha^{-1} $year^{-1}$ to soil; Hanawalt, 1969: 55–74 kg ha^{-1} $year^{-1}$ to soil, with an applied air concentration of 38 μg m^{-3} NH_3; Rodgers, 1978: 4 kg ha^{-1} $year^{-1}$ to an acid surface). Much of the variation between results undoubtedly reflects air concentration differences. However, this was rarely measured in these studies.

The results of Hall and Miller (1911) were interesting however, since they exposed their collectors at two heights above the ground. Their results, expressed as deposit-

	deposition to collectors (kg NH_x-N ha^{-1} $year^{-1}$)							
field(Plot No.)	lawn (1)		Broadbalk (7)		Broadbalk (12)		parkland (4)	
sampler height above ground (m)	1.15	0.05	1.15	0.05	1.15	0.05	1.15	0.05
1908–1909	1.55	0.88	1.25	1.45	1.17	1.29	0.79	0.68
1909–1910	1.77	1.02	1.28	1.98	1.41	2.11	0.95	0.88

Table 1.3 Deposition of NH_x recorded by Hall and Miller (1911) at Rothamsted, U.K. Deposition was recorded to acid solutions in plates of measured area under fine gauze shields. Results are given for measurements above several land surfaces: Plots 1 and 4 were unfertilized grassland; plots 7 and 12 were fields fertilized with ammonium sulphate and chloride in the Spring of each year.

Author and year	Place	μg NH_x-NH_3 m^{-3}	Remarks
Levy (1880)	Montsouris, France	17–24	
Fodor (1881)	Budapest, Hungary	32	average
Müntz *et al.* (1882)	Pic du Midi, summit, France	6–25	
Buenos Aires (1906)	Buenos Aires, Argentina	62–72	monthly average

Table 1.4 Early determinations of total NH_x in air. Samples were collected by bubbling air through acid solutions. Data collated by Eriksson (1952).

ion fluxes, are given in Table 1.3. There was a clear difference in the flux at the two heights, and also between the sites. The fertilized sites showed a greater flux to the collector nearest the ground, which could relate to an emission of NH_x from the soil. The grass sites, however, showed reduced fluxes to the lower collector, which could result from absorption of NH_x by the ground. However, since the air flow over the lower plates would be less, giving a lower sampling rate, the authors felt unable to confirm this. Nevertheless, this did demonstrate that fertilized ground has a greater potential for emission of ammonia than unfertilized.

Some measurements of air concentrations were made in the early years (Table 1.4). The method used, was to bubble a measured volume of air through an acid solution. Correspondingly this measured total NH_x, giving no information on the relative importance of NH_3 and NH_4^+. However, some caution must be taken with this small amount of data, especially for the Montsouris and Buenos Aires sites. Since both sites showed high concentrations in precipitation compared to other sites (Table 1.2.), it is possible the NH_x was also high. Hence, typical air concentrations may have been lower than these.

Following this early interest, the number of investigations declined in the early 20th century, and while precipitation composition was often measured, there was almost an absence of air concentration determinations. Attention was revived in the 1950s as a result of both the agricultural and air pollution importance of ammonia.

1.2.2 Recent agricultural interest in ammonia

With the increased use of nitrogen fertilizers and manures, and analysis of the efficiency of their use, it was apparent that much nitrogen was not being recovered either in the crop or remaining in the soil after harvest. Reviewing the literature, Allison (1955) concluded that both leaching of nitrate and gaseous loss of ammonia were important. He suggested that several environmental conditions would affect the degree of ammonia release. These were that: 1) a high pH soil will be more liable to volatilization; 2) losses from wet soils are likely to be small unless 3) it is a drying alkali soil with much NH_x near the soil surface; 4) losses will be greater at higher temperatures; 5) soils of low cation exchange capacity will suffer greater losses and 6) losses may occur from decomposing nitrogenous material, even if the soil is acid since the NH_3 produced will raise the pH locally. It is not unexpected that these relate closely to the parameters affecting ammonia solubility listed in section 1.1.

Many studies have since examined the factors promoting volatilization of ammonia by different fertilizers and this has been reviewed by Vlek and Crasswell (1980), Freney *et al.* (1983), and Ryden (1984). In addition to the factors above, these authors stress the importance of atmospheric turbulence, which affects the rate of diffusion away from the surface, and also of vegetation cover, since soil released NH_3 may be re-absorbed by a plant canopy above (Denmead *et al.*, 1976).

1.2.3. Recent interest in ammonia as a pollutant

Egner and Eriksson (1955) started the first large scale monitoring network of precipitation and air chemistry (European Air Chemistry Network), and this included NH_x measurements. The UK results of this network were analysed by Stevenson (1968), and the NH_x values from this are given in Table 1.5. For several of these sites, *viz.* Leeds, Rothamsted and Stornaway, there is also precipitation data from the turn of the century (Table 1.2.). Although comparison is difficult, since the data here are medians, the values are similar or possibly slightly higher in the later period. Comparing the air concentration data with that for Table 1.4, the EACN values are rather low. However, if the precipitation for each site is compared the pattern is the same, suggesting that this may reflect site differences. Overviews of the EACN data have also been provided by Söderlund (1977) and Söderlund and Granat (1982).

Many other monitoring networks have since been set up. On a global scale the World Meteorological Organization (*e.g.* WMO, 1984) has initiated its Background Air chemistry and Precipitation Monitoring Network (BAPMoN), while in Europe, aside from various national networks, the European programme for Monitoring and Evaluat-

site	medians, 10 and 90 percentiles					
	NH_4^+-N in precipitation (mg dm^{-3})			total NH_x-N in air (μg m^{-3})		
	10	50	90	10	50	90
Aberdeen, N.E. Scotland	0.1	0.3	0.6	1.4	2.6	5.3
Aldergrove, N. Ireland	0.3	0.5	1.5	1.1	1.9	3.5
Cambourne, S.W. England	0.1	0.3	0.8	1.2	2.0	2.9
Edinburgh, C. Scotland	0.0	0.2	1.0	1.8	3.3	5.3
Eskdalemuir, S. Scotland	0.1	0.2	0.7	0.7	1.6	3.1
Leeds, N. England	0.4	1.1	2.9	2.8	4.3	6.7
Lerwick, Shetland, N. Scotland	0.0	0.1	0.6	0.4	1.0	1.9
Newton Abbot, S.W. England	0.3	1.4	4.8	2.4	4.0	6.0
Rothamsted, S.E. England	0.2	0.5	1.3	2.4	3.9	6.7
Stornaway, Lewis, N.W. Scotland	0.1	0.2	1.1	—	—	—

Table 1.5 NH_x in bulk precipitation and air in the U.K. 1959–1964. Data from Stevenson (1968).

ion of the long range transmission of air Pollutants (EMEP) has monitored extensively (Schaug *et al.*, 1987). Buijsman and Erisman (1988) have drawn together the various data sets for NH_4^+ to estimate a wet deposition and precipitation concentration field for Europe. Deposition ranges from less than 3 to over 14 kg NH_4-N ha^{-1} $year^{-1}$, with the highest deposition centring on the low countries of north west Europe.

One of the major improvements with some of the more recent monitoring programmes has been the introduction of wet-only sampling; collectors that only open during precipitation events. Hence the problem of contamination by dust, of concern to Eriksson (1952), and also dry deposition of pollutants to the collector (Fowler and Cape, 1984) that occur in bulk samples, may be minimized. Buijsman and Erisman (1988) have estimated correction factors for this, and also for biological decay during storage, and conclude the 1960s EACN data may over-estimate by a factor of 1.1.

The degree of monitoring for NH_x in the air has, however, been much less. More importantly, many of the measurements that have been made, as above, have not discriminated between NH_3 and NH_4^+, despite their different environmental behaviour.

Junge and Ryan (1958) highlighted this difference by demonstrating the role of NH_3 in promoting the aqueous oxidation of SO_2 to SO_4^{2-}, producing $(NH_4)_2SO_4$ (see section 1.1). They envisaged this reaction to be important in clouds and fogs, a suggestion that has since been supported by field studies. An example is the case of Tees-side in the 1960s where Eggleton and Atkins (1972) showed that high NH_3 and SO_2 pollution from industry and combustion encouraged the formation of high levels of $(NH_4)_2SO_4$, which being present as particles reduced visibility. In addition, because of the hygroscopic nature of the particles, they acted as condensation nuclei which, associated with high humidity sea breezes, encouraged fog formation.

Hence NH_4^+ is considered to be a secondary pollutant resulting from reaction of NH_3. In addition, as is discussed later (section 1.4), the deposition rates of NH_3 and NH_4^+ differ considerably. Because of these differences, the importance of separate monitoring has been realized, and methods have been developed to do this.

1.2.4 Developments in separate NH_3 and NH_4^+ sampling methods

An early method of separating NH_3 and NH_4^+, as used in the Tees-side Investigation, was by a dual filter sampling system. Particulate matter, including NH_4^+, was caught on a prefilter (in this case a Whatman 41 cellulose fibre filter), while NH_3 gas was presumed to pass through to be caught on an acidified Whatman 41 filter. However, this method has not been without criticism, and it has been suggested that some NH_3 may be caught on the first filter. Conversely, where high loadings on the prefilter occur, some of the particulate may evaporate, since the equilibrium of NH_4NO_3 particulate with gaseous NH_3 and HNO_3 is disturbed (section 1.1; Ferm, 1979; Appel *et al.*, 1980; Cadle, 1985).

In response, Ferm (1979) developed an alternative sampling system, known as a denuder tube, where NH_3 is caught by diffusion as it is passed through a narrow bore tube with acidified sides. The NH_4^+ containing particles have a much slower diffusion rate so that these are supposed to pass through unaffected, allowing subsequent capture on a filter. Unfortunately, in order to maintain the required laminar flow, this system suffered from a limitation of very low flow rates. Recently however, the method has been modified so as to sample through the gap between two larger tubes, arranged concentrically. This 'annular denuder' enables faster flow rates (similar to filter packs) and therefore shorter sampling times (Allegrini *et al.*,1984; Høv *et al.*, 1988). However, denuders are very laborious to use and also suffer problems at the extremes of humidity. In addition sampling artifacts are possible with the deposition of large particles to denuder walls (Sickles *et al.*, 1990). Many authors have therefore preferred dual filter systems ('filter packs'). It is argued that in temperate conditions interferences are minimal when using an inert prefilter, such as PTFE, and low flow rates and filter loadings (Goldan *et al.*, 1983; Dollard *et al.*, 1987; Allen *et al.*, 1988). Other authors have shown good agreement between filter packs and denuders (Vibelu-Anderson, 1989, pers. comm.; Sickles *et al.*, 1990).

Progress has also been made in the development of passive NH_3 samplers or 'diffusion tubes' (Hargreaves and Atkins, 1987). This is an improvement on the old passive flux collector; here the diffusive resistance to the acid surface is quantified and used to calculate air concentrations (Chapter 6). The tubes are set out for periods of about two weeks, and are convenient since they require no electricity supply on site.

In addition to these chemical methods, gaseous NH_3 may be measured by a number of physico-chemical methods, with rapid response times of the order of seconds, and these have been reviewed by Quinn *et al.* (1987). They include systems which oxidize NH_3 to NO_x, followed by measurement of the latter, and flame derivitization. Measurement may also be made by spectroscopy, and early work in this field has been reviewed by Junge (1963). More recently tunable diode lazer absorption spectroscopy (TDLAS) has enabled much lower detection limits ($\approx$0.1 $\mu g\ m^{-3}$), comparable to those possible by chemical methods and enabled confirmation of the latter (Anlauf *et al.*, 1987; Sickles *et al.*, 1990). However, the high cost of these machines precludes their widespread use.

1.2.5 Concentrations of NH_3 and NH_4^+ in the atmosphere

In accordance with the above points, most authors have used the chemical methods for NH_3 detection, with the additional advantage that NH_4^+ may be collected in the same sampling train. A selection of results from various authors are given in Tables 1.6a. and 1.6b. Comparing the two data sets, NH_3 shows a much greater intersite variability than NH_4^+, although the range of values possible at given sites is equally wide. In accordance with the precipitation data, the values are lowest in remote or oceanic sites. Additionally, the NH_3 on land shows very low concentrations in an afforested area, and the highest values in some urban areas, or areas with livestock agriculture. This again suggests that industry and agriculture are sources of atmospheric NH_3, and this is discussed in the next section.

1.3. Sources of atmospheric ammonia

1.3.1 Identification of the sources

While the presence of NH_x in the atmosphere has been known for many years, it has only been recently that some degree of consensus has emerged over its sources. Perhaps the earliest hypothesis, suggested by Boussingault (1856), was that the sea was the source. This idea was strongly supported by Schlösing (*e.g.* 1875) and even later still favoured by Ingham (1950). The body of opinion, however, was against this. Monitoring of precipitation in remote coastal sites, such as that of Miller (1913; see Table 1.2: sites in N.W. Scotland and Iceland) showed that the level of NH_4^+ was much lower than at inland sites. More recent data have also shown lower levels of NH_x (Georgii and Muller, 1974) and NH_3 (Ayers and Gras, 1983) in marine air masses compared to continental air. It is therefore more likely that the sea should rather be acting as a sink for NH_x. An exception to this has been provided by Georgii and Gravenhorst (1977), who showed that the Sargasso Sea may act as a source of

Author and year	Place	Conc. NH_3 ($\mu g\ m^{-3}$) mean	range	Remarks
	EUROPE			
Eggleton and Atkins (1972)	UK, July–Oct. 1968			tandem (paper prefilter), Su
	Tees-side, Stockton (urban)	33.7		
	Eston	11.0		
	Tees-side Airport	9.9		
	Kew, (S.W. London area)	8.2		
	Harwell, Oxfordshire (rural)	5.4		
Allen *et al.* (1988)	Essex, UK, 1985–1986			tandem (PTFE prefilter), Su
	overall mean:19 sites	4.87		
	mean: 12 mid range sites	2.60	0.6–5.0	(monthly
	mean: 2 livestock farms	24.3	3–66	means)
	roof top, rural area, Colchester	1.36	0.1–29.4	(24 hour runs)
Erisman *et al.* (1988)	Cabauw, the Netherlands, 1985			denuder
	(livestock agr. area) height: 2 m	8.3	0.8–49.4	Samplers on met-
	25 m	6.2	0.7–18.0	eorological tower
	100 m	3.6	0.1–12.1	(12 hour runs)
	200 m	2.1	0.1–10.1	
Lenhard and Gravenhorst (1980)	Frankfurt region, W. Germany			tandem (PVC
	(mixed rural) height:100 m summer	4.8		prefilter), from
	winter	1.9		aircraft
	700 m summer	2.5		
	winter	1.5		
	AMERICA			
Tjepkema *et al.* (1981)	Petersham, Mass., USA, 1980			denuder, Su
	(afforested area, few livestock)			
	Spring (March–May)	0.05		
	Summer (June–Aug.)	0.16		
	Autumn (Sept.–Nov.)	0.05		
	Winter (Dec.–Feb.)	0.01		
Cadle (1985)	Detroit, Mitchigan, USA,			denuder, Su
	1981–1982 (urban)			
	Spring (March–May)	0.16		
	Summer (June–Aug.)	0.85		
	Autumn (Sept.–Nov.)	0.37		
	Winter (Dec.–Feb.)	0.10		
Alkezweeny *et al* (1986)	Kentucky, USA, 1 month, 1983			tandem (PTFE/ glass prefilter)
	(livestock agr. area)		0.04–5.6	Su
			0.0–0.55	from aircraft
Le Bel *et al.* (1985)	Bermuda, 1982	0.34		WO_3 denuder, from aircraft
	ASIA, PACIFIC and ANTARCTIC			
Pang and Tong (1985)	Beijing area, 1984			tandem (membrane
	agricultural areas (3 sites)		40–450	prefilter), Su,
	industrial areas (9 sites)		0.9–50	(range of single
	residential areas (4 sites)		3–65	daily values)
Yamamoto *et al.* (1988)	Yokohama, Japan, 1982–1986			tandem (PTFE
	(urban)	5.54	0.5–29.8	prefilter) Su + 14 m
	Summer (April–Sept.)	10.7		(monthly means)
	Winter (Oct.–March)	4.0		
Ayers and Gras (1983)	C. Grim, Tasmania, 1978–1980			tandem, Su
	(remote) Continental air	0.34	0.01–0.85	
	Marine air	0.06	0.01–0.10	
Gras (1983)	Antarctica, summer 1980			denuder, Su
	Wright Valley, NZ sector	0.01		
	South Pole	0.02		

Table 1.6a Examples of reported gas phase NH_3 concentrations in air. Tandem samplers refer to dual filter packs and pre-filtered bubble meters. Denuders are acid coated unless otherwise stated. Su implies surface measurements (generally 1.5–2.5 m height height above ground).

Author and year	Place	Conc. NH_4^+ ($\mu g\ m^{-3}$) mean	range	Remarks
	EUROPE			
Eggleton and Atkins (1972)	UK, July–Oct. 1968			high vol. (paper prefilter), Su
	Tees-side, Stockton (urban)	4.7		
	Eston	3.8		
	Tees-side Airport	4.7		
	Kew, (S.W. London area)	3.5		
	Harwell, Oxfordshire (rural)	3.5		
Allen *et al.* (1988)	Essex, UK, 1985–1986			tandem (PTFE prefilter), Su (monthly means)
	overall mean:19 sites (inter site differences small)	4.04	1.0–9.5	
	roof top, rural area, Colchester	4.29	0.05–69.9	(24 hr. runs)
Erisman *et al.* (1988)	Cabauw, the Netherlands, 1985			post denuder filter Samplers on met-eorological tower (12 hr. runs)
	(livestock agr. area) height: 2 m	5.6	1.2–20.3	
	25 m	5.0	1.2–15.6	
	100 m	5.0	1.0–15.4	
	200 m	4.1	0.8–13.6	
Lenhard and Gravenhorst (1980)	Frankfurt region, W. Germany			tandem (PVC prefilter), from aircraft
	(mixed rural) height:100 m summer	4.9		
	winter	2.6		
	700 m summer	2.9		
	winter	2.0		
	AMERICA			
Tjepkema *et al.* (1981)	Petersham, Mass., USA, 1980 (afforested area, few livestock)			post denuder filter Su
	Spring (March–May)	1.3		
	Summer (June–Aug.)	2.4		
	Autumn (Sept.–Nov.)	1.0		
	Winter (Dec.–Feb.)	0.8		
	PACIFIC and ANTARCTIC			
Yamamoto *et al.* (1988)	Yokohama, Japan, 1982–1986 (urban)	1.7	0.5–4.0	tandem (PTFE prefilter) Su + 14 m (monthly means)
	Summer (April–Sept.)	1.7		
	Winter (Oct.–March)	1.8		
Gras (1983)	Antarctica, summer 1980			post denuder filter Su
	Wright Valley, NZ sector	0.04		
	South Pole	0.05		

Table 1.6b Examples of reported particulate NH_4^+ concentrations in air. Tandem samplers refer to dual filter packs and pre-filtered bubble meters. Su implies surface measurements (generally 1.5–2.5 m height height above ground).

atmospheric NH_3, as the concentrations they measured over this area were much greater than the surrounding ocean ($\approx$8 as compared to 1 $\mu g\ m^{-3}$). However, this source would presumably only be important on a local scale in the marine cycle, a subject which has been reviewed by Liss (1983) and Quinn *et al.* (1987).

Thus the major sources of NH_x appear to be continental. Several possibilities have been suggested: emission from coal or other combustion sources, volatilization from the decay of animal excrements and from fertilizer volatilization, and losses from transformations in natural soils. Other minor sources are listed by Buijsman *et al.* (1987). It is generally agreed that for each of these, emission occurs in the form of NH_3 gas; it is then through subsequent reaction in the atmosphere that NH_4^+ is produced (*e.g.* Healy *et al.*, 1970).

In reviewing the literature, Eriksson (1952) favoured combustion of coal as the major source of ammonia. In this respect he cites the work of Russell and Richards (1919), who calculated the potential quantity of NH_x released into the atmosphere by burning of coal to be about 5 times the quantity brought down in rain — despite the fact that these authors did not consider this ratio would occur in practice. Eriksson used this theory to explain the higher levels of NH_4^+ observed in rain in Europe compared to the rest of the world, and also in cities compared to rural areas (see Table 1.2), since it is these places where most combustion occurs. Indeed, his view receives some support from modern measurements of NH_3 levels (Table 1.6a), which are also often high in urban areas.

Russell and Richards (1919), however, believed the soil to be the main source of the ammonia. This was based mainly on the work of Hall and Miller (1911), who showed fertilized soils could emit NH_x (Table 1.3), and also on the observation that precipitation NH_4^+ was highest in summer, when biological activity of the soil would be greatest. These authors were not specific about the source of this soil NH_3, however, later workers have attempted to assess the importance of the different possibilities: volatilization from natural soils, fertilizers and animal waste.

The literature on emission of NH_3 from natural soils appears at first sight to be somewhat contradictory. In section 1.2.1 soils were discussed as a sink for atmospheric ammonia. Other authors, such as Robinson and Robbins (1970) and Dawson (1977) considered natural soils to be a source. While the latter admits that "emission from uncultivated, unfertilized vegetated land has never been measured", he nevertheless proceeds to model the emission on the basis of decomposition and nitrification rates, solubility equilibria and a simple diffusion equation. To add to this controversy, Georgii and Lenhard (1978) have since measured emission from "natural soils", with values in the range equivalent to 0.0–1.8 kg NH_3 ha^{-1} $year^{-1}$, depending on soil pH and temperature. However their study, which measured NH_3 enrichment in a chamber over different soils, used bare soil surfaces, and soils which had been fertilized at some point, although details of this are not given. Hence the flux recorded could relate to the presence of fertilizer residues in the soil, and would not take into account the effect of vegetation, which would usually be present in a natural system. As will be seen, however, even if their estimate is taken as an upper limit for natural soil emission the figures are small compared to other sources.

Compared to the above, the losses of NH_3 from fertilizers and animal wastes have been well documented. Interest in fertilizer losses has focused on quantifying the loss of nitrogen that would otherwise be available for crops. Attention has focused

particularly on the situation concerning alkaline soils, as in such conditions the high pH reduces NH_x solubility, favouring NH_3 losses. Thus while losses from neutral mineral fertilizers, such as $(NH_4)_2SO_4$ and NH_4NO_3, are normally small, in alkaline soils they may become important. The use of urea fertilizer also promotes losses, since its hydrolysis in the soil liberates NH_3, which raises the pH locally, reducing solubility, and favouring emission (Vlek and Crasswell, 1981). A similar process occurs during the decay of livestock urine, so that losses from this source may also be large. In accordance with the solubility equilibria, in wet conditions emission is low, but becomes large in drying conditions and at higher temperatures. The exception is where urea is present, in which case wet conditions promote its hydrolysis which may result in increased emission.

A major source of evidence suggesting the loss of fixed nitrogen from agricultural surfaces has been the study of crop balance sheets (*e.g.* reviews by: Allison, 1955; Wetselaar and Farquahar, 1979). Other studies include those of Fenn *et al.* (1981), who studied the percentage loss of N as NH_3 for different soils and fertilizer type, while Sommer *et al.* (1984) have reviewed percent losses from the storage of manure. Buijsman *et al.* (1987) give an overview of these and other loss mechanisms, which also include field losses from urine and faeces, and losses after application as manure.

Studies using micrometeorological methods have also provided useful information (*e.g.* Denmead *et al.*, 1974; Beauchamp *et al.*, 1982; Leuning *et al.*, 1984; Ryden *et al.*, 1987; Lockyer *et al.*, 1989). The approach consists of measuring the fluxes in the air above a surface, typically up to 2 m, and from this inferring the net exchange at the surface (see Chapter 2.). Using a gradient approach, Denmead *et al.* (1974) measured fluxes over a grazed sheep pasture. The mean estimate from their measurements (made in summer) was 0.30 $\mu g\ NH_3\text{-}N\ m^{-2}\ s^{-1}$ ($\equiv$95 kg N $ha^{-1}\ year^{-1}$). More recently, other measurements have been made using the micrometeorological mass balance method (see Chapter 2; Denmead, 1983) and field enclosures (or wind-tunnels). Recent studies include those of Jarvis *et al.* (1989), Pain and Thompson (1989), Van den Abbeel *et al.* (1989), and Van der Molen *et al.* (1989). Much variation is apparent in the measured fluxes; for example Jarvis *et al.* (1989) estimated values lower than those above, of 7–25 kg N $ha^{-1}\ year^{-1}$, from cattle grazed pastures. In addition to environmental variables, differences in results arise from stocking density, animal species and sward fertilization, as well as grazing management.

1.3.2 Estimation of emission

Many attempts at quantifying emissions have been made using the limited number of experimental results. One approach has been the calculation of "emission inventories",

in which the contributions from the different sources are identified and summed to provide total emission estimates. Global surveys have been made by Robinson and Robbins (1970), Söderlund and Svensson (1976) and Mészáros (1981), while European inventories include those of Bonis *et al.* (1980) and more recently Buijsman *et al.* (1987). National inventories have also been made, such as those of Healy *et al.* (1970) and ApSimon *et al.* (1987) for Great Britain, Cass *et al.* (1982) for California, Buijsman *et al.*(1984) for the Netherlands, and Möller and Schieferdecker (1989) for the GDR.

The general method of this approach is to estimate individual emission factors for the different source types, and then sum occurrences of these sources over the region of study. The totals for each source type are finally summed to estimate overall total emission. As a result of such studies it has generally been agreed that for Europe agricultural sources represent the bulk of the emission, with animal wastes contributing most of this, and a smaller proportion from fertilizers. Losses from combustion sources appear to be only of small importance on a regional scale. For example Healy *et al.* (1970) estimated this to contribute less than 8% for the U.K., with animal urine providing 66% of the emission. The recent estimate of Buijsman *et al.* (1987) suggests a total emission of 6.4 Mt NH_3 $year^{-1}$ over the whole of Europe giving a range of 2–40 kg NH_3 ha^{-1} $year^{-1}$ for grid elements of 150 x 150 km (mid 1980s values). Of this, over 80% was attributed to livestock and 17% to fertilizers. Emission due to combustion sources and natural soils was assumed insignificant and ignored. However, for the second of these, on the basis of the results of Georgii and Lenhard (1978) and assuming that 75% of the land area of Europe consists of natural soils, they estimated a natural soils emission of 0.75 Mt $year^{-1}$ for Europe to justify its exclusion. Since it has been noted above that natural soil emission is probably even less than this, its exclusion may be supported.

Estimates were also given for individual countries. For the U.K. a total emission of 405 kt $year^{-1}$ was calculated, while the figure for the Netherlands was 150 kt $year^{-1}$. Accounting for the different agricultural areas of countries, these authors also devised an 'emission density' (= agricultural emission/agricultural area, t km^{-2} $year^{-1}$). The mean for Europe was 2.6, with the highest and lowest values from the Netherlands (6.4) and Norway (0.3), respectively. The figure for the U.K. was 2.1.

Such emission inventory calculations have proved useful in identifying the sources. However, some degree of caution is needed in using the results, since the calculations are poorly coupled to the physical environment where the emissions occur. For example livestock emission factors are calculated for an average animal of a given

species, and multiplied up by the number of animals in a given area, to estimate the total emission for that species. In reality however, this linearity may be complicated by the relationship to emission and deposition in the locality of emission. Much of the emitted NH_3 may be redeposited in the immediate vicinity on to vegetation or soils. If this is the case the type of vegetation environment of the animals is also important, such as the presence of long or short grass in pastures (Denmead *et al.*, 1974, 1976).

There is consequently a need to define what is meant by emission. It could be defined as purely gaseous loss from a surface. Conversely, it could be seen as net release above the vegetation canopy, or at a defined height in the atmosphere above this. The choice of this definition depends on the method used and the scale of exchange of interest. The use of an atmospheric reference height, as in micrometeorological studies is favourable since in this way an average figure for a large area is derived. This may be of the order of 1 m, where exchange over an area of several tens of metres is of interest, so as to understand the budget of different surface types. Results from this may also be used to sum emissions from different surface types to help understand the net exchange with the atmosphere.

Another approach has been to use reference heights of the order of hundreds of metres, so that the effects of different land uses are integrated, and a net flux to the atmosphere estimated. Micrometeorological gradient methods have also been used here, making measurements either from aeroplanes (Georgii and Müller, 1974; Georgii and Lenhard, 1978; Lenhard and Gravenhorst, 1980; Alkezweeny *et al.*, 1986) or towers (Erisman *et al.*, 1988). For example, the study of Erisman *et al.* was made in the central Netherlands, in an area of livestock agriculture (see Table 1.6). They calculated a net emission of 0.12 $\mu g\ NH_3\ m^{-2}\ s^{-1}$ (38 kg N $ha^{-1}\ year^{-1}$), which is large but not surprising for this site, given the high density of livestock in the Netherlands (Buijsman *et al.*, 1987). This method also has restrictions, however, since on such large scales, chemical conversions and advection may mean that the gradients cannot be interpreted as fluxes toward or away from the surface.

1.4. Sinks of atmospheric ammonia

NH_x is present in the atmosphere as NH_3 gas, NH_4^+ in cloud and precipitation, and NH_4^+ particles. For each of these, different removal mechanisms apply. It has been suggested that NH_3 gas may be oxidized in the atmosphere (*e.g.* McConnell, 1973; Levine *et al.*, 1980), however, this reaction is slow, and accounts for only a small fraction of the loss from the atmosphere (Söderlund and Svensson, 1976; Høv *et al.*, 1988). The bulk of the removal is therefore by deposition back to earth. Wet

deposition and early work on total NH_x dry deposition have been considered in section 1.2. For the latter, however, it was noted that the collectors used were unlikely to give good deposition estimates, as well as not separating the processes of NH_4^+ and NH_3 dry deposition. The improvements in recent measurements of deposition processes are therefore considered in the following sections.

1.4.1 Direct measurements of NH_x dry deposition

Various attempts have been made to measure deposition directly, and yet overcome the problems of flat collectors. This has either been done by analyzing washings of artificial or real leaves, or by using precipitation events to do the washing, and estimating dry deposition as the difference between the wet deposition and throughfall fluxes.

For example, Tjepkema *et al.*(1980) estimated a deposition of 0.6–2.5 kg NH_x-N ha^{-1} $year^{-1}$ to a remote forest area of Massachussets, USA, with low air concentrations of NH_3, on the basis of leaf washing experiments. They attributed the capture to NH_4^+ and could show no difference between real or artificial leaves, though it is probable NH_3 also contributed to the deposition. Other studies have been made (*e.g.* Ingham, 1950; Bytnerowicz *et al.*, 1987; Dasch, 1987), however, a general criticism is the difficulty in scaling up over an area basis, especially when a complex surface such as a forest is being considered.

Mainly for this reason throughfall measurements have been the most popular technique. For example, Van Breeman *et al.* (1982) made throughfall measurements in two forests in the Netherlands, in intensive farming areas, and estimated a deposition of 64 kg NH_x-N ha^{-1} $year^{-1}$. For comparison they reviewed the work of several other experiments in Europe and N. America. These gave deposition fluxes in the range 3–20 kg NH_x-N ha^{-1} $year^{-1}$, which being much smaller highlighted the large size of the NH_x input at the Dutch site. Indeed it was partly as a result of this study that the current concern over the direct effects of NH_x pollution began. Further Dutch work has emphasized this problem. For example Draaijers *et al.*(1987) recorded a deposition of 133 kg NH_x-N ha^{-1} $year^{-1}$ to a forest in throughfall compared to 14 kg ha^{-1} $year^{-1}$ in precipitation. These authors also looked at initial throughfall concentrations after dry periods and found the concentration to be correlated with the duration of the intervening dry period. They believed the period of greatest uptake was for the first few days after the last rain event. However, after a long dry period of 4 weeks they found a very high throughfall concentration of 82 mg NH_x-N dm^{-3}, which was approximately 30 times the mean precipitation $[NH_4^+]$ at the site. In neither study was NH_x in the air measured, however, given the proximity of both sites

to intensive agriculture it may be assumed to have been large (*c.f.* Erisman *et al.*, 1988: 8 $\mu g\ m^{-3}$. See Table 1.6a).

Such measurements may, however, be subject to errors because of canopy exchange of the ions studied. For example, Heil *et al.* (1987) measured throughfall over heathland vegetation and found some periods where throughfall deposition was less than precipitation, which they attributed to the possibility of canopy uptake. An additional criticism is that the method assumes no emission from soil beneath, which might contribute to the NH_x deposited, while as with all such measurements it is not possible to use the results to predict deposition at other sites. To do this an understanding of the factors controlling deposition is needed.

1.4.2 Dry deposition of NH_4^+

The deposition of airborne particles has been intensively studied and this has been reviewed by Chamberlain and Little(1981), Sehmel (1980) and Nicholson (1988). Atmospheric turbulence transports the particles close to the surface, from where deposition may occur through either sedimentation or impaction — processes more efficient with large particles — and Brownian diffusion, which is more efficient with small particles. Atmospheric NH_4^+ aerosol particles occur predominantly in the size range 0.1–1 μm diameter (*e.g.* Kadowaki, 1976). This is both too small for sedimentation or impaction to be important, yet too large for efficient Brownian diffusion (Chamberlain and Little, 1981). Hence these particles are expected to deposit slowly.

The rate of deposition is often expressed as a deposition velocity (V_d), which is considered to be independent of air concentration, and is referenced at a particular height (z) above the depositing surface:

$$V_d\{z\} = \text{Deposition flux} / \text{concentration}\{z\} \qquad 1.9$$

(See also chapter 2.) A typical upper value for particles in the the same size range as NH_4^+ is of the order of $V_d\{1\ m\} = 1\ mm\ s^{-1}$ (Chamberlain and Little,1981), with values being largest in windy conditions over rough surfaces. Such values have on the whole been confirmed by other laboratory and field studies (*e.g.* McMahon and Denison, 1979; Nicholson and Davies, 1987). As a result, only a small proportion of the atmospheric NH_x will be lost as NH_4^+ particulate dry deposition. Assuming a typical NH_4^+ concentration of 2 $\mu g\ m^{-3}$ and deposition velocity of 0.1 $cm\ s^{-1}$, gives an annual flux of 0.5 kg N $ha^{-1}\ year^{-1}$, which is small compared to precipitation input.

NH_4^+ is present in cloud or fog droplets owing to the action of the particulates as cloud condensation nuclei, and as a result of droplet scavenging of NH_4^+ and NH_3.

Such droplets are mostly present in the size range 5–30 μm. At this size impaction and sedimentation both become important, so that deposition is much more efficient. Thus where fog or ground level cloud are present, deposition of the order of 1–10 cm s^{-1}, may occur, depending on windspeed and surface roughness. This has been demonstrated for example, by Yosida (1953) who measured fog deposition, while Dollard *et al.* (1983) and Gallagher *et al.* (1988) have measured deposition of surface clouds at high elevation sites. As a consequence of this rapid droplet deposition an additional input of NH_4^+ is possible for some sites (Fowler *et al.*, 1989; Saxena and Lin, 1990), which may exceed 1 kg NH_x-N ha^{-1} $year^{-1}$, although, as a regional loss mechanism for the atmosphere this will usually be small.

As a result of the slow dry deposition rate of NH_4^+ particles, most is eventually removed as precipitation, or in some cases cloud droplet deposition. Similarly, given the large amounts of total NH_x dry deposition often recorded (section 1.4.1), it is expected that the bulk of this is due to NH_3 deposition, rather than NH_4^+ as has sometimes been suggested (*e.g.* Ingham, 1950; Tjepkema *et al.*, 1981).

1.4.3 Dry deposition/exchange of NH_3

Until recently there were no actual measurements of NH_3 deposition suitable for quantifying rates, such as by a deposition velocity. Thus Söderlund and Svensson (1976), in compiling their global budget for nitrogen compounds, assumed a value of V_d = 8 mm s^{-1} based on supposed similarity of NH_3 to SO_2. However, since it has been noted above that NH_3 may be both emitted from or deposited to the ground, it is clear that a more rigorous approach is needed. The question, then, is to understand the bi-directional surface exchange process as a whole. The role of animals and fertilizer loss as emission sources has been considered above. In this section the background exchange of land surfaces is considered, including both natural (or unfertilized) vegetation and fertilized ecosystems, though not considering the emission immediately following fertilizer application. Progress has been made both through controlled environment studies, and micrometeorological field measurements. These are considered and a summary of experiments given in Tables 1.7 and 1.8.

- *Controlled environment studies*

Porter *et al.* (1972) provided the first modern demonstration of foliar absorbtion of NH_3. Using ^{15}N labelled NH_3 they showed that NH_3 was absorbed into the plant and metabolized (See also section 1.2.1. for early work). Lockyer and Whitehead (1986) and Whitehead and Lockyer (1987), also using ^{15}N, applied air concentrations in the range 14–709 μg NH_3 m^{-3} and showed that plant enrichment was proportional

to air concentration, with up to 77% of the plant N deriving from the air at 709 μg m^{-3}. In some of their treatments they also washed leaf surfaces before analysing for N, but could detect no difference as compared to unwashed leaves. From this they concluded that leaf surface adsorption of the NH_3 was insignificant in comparison.

Hutchinson *et al.* (1972) made the first study of uptake rates of NH_3. Using concentrations of 24–44 μg m^{-3}, they showed a clear relationship between uptake and stomatal opening, by comparison with the flux of CO_2 in light and dark periods. This is a feature that has since been demonstrated in other similar studies (*e.g.* Aneja *et al.*, 1986; Van Hove *et al.*, 1987a). In the study of Hutchinson *et al.*, while much of the NH_3 passed through stomata, a proportion (not calculated) was deposited on the leaf surface. These authors also compared deposition fluxes to plants with different levels of fertilization, but could see no trends associated with this. However, a trend was seen by Whitehead and Lockyer (1987), with lower fluxes to plants with greater fertilization. Since this was supplied as NO_3^-, the change must have been a result of altered plant metabolism, rather than simply the presence of fertilizer residues.

All these experiments, however, used large air concentrations (Table 1.7). By contrast Meyer (1973) also used NH_3 free air. Whereas he found a similar pattern to the above using 27–417 μg m^{-3}, when NH_3 free air was applied NH_3 emission occurred, with the outgoing airstream of his chamber containing between 1.3 and 12 μg m^{-3}, depending on plant species. He considered 27 μg m^{-3} to be a normal air concentration and therefore did not think this would be important in practice. However, since air concentrations are usually much lower than this, other workers soon revived the idea of bi-directional fluxes by using both chamber studies (Farquahar *et al.*, 1979, 1980; Hooker *et al.*, 1980) and fieldwork (Lemon and Van Houtte, 1980). Farquahar *et al.*(1980), in a study that has become well known, formalized the idea of an NH_3 'compensation point' concentration (denoted here χ_{cp}). They observed deposition to occur when air concentrations were above this level, and emission to occur when they were below it; at the χ_{cp} itself no net exchange would occur. They explained this as being the concentration in equilibrium with the intercellular fluid of the plant tissue, accessible through the stomata. As a consequence of this study, these authors considered the previous high concentration studies to be in error. They also observed an increase in χ_{cp} with temperature, which was consistent with the solubility equilibria (section 1.1.), assuming dissolved NH_x concentration to be constant with temperature. For *Phaseolus vulgaris* at 25 °C they found a χ_{cp} of 1.7 μg NH_3 m^{-3}, while at 33 °C this was 3.7 μg m^{-3}. Using the lower concentration to predict dissolved NH_4^+ at an estimated pH, they plotted the

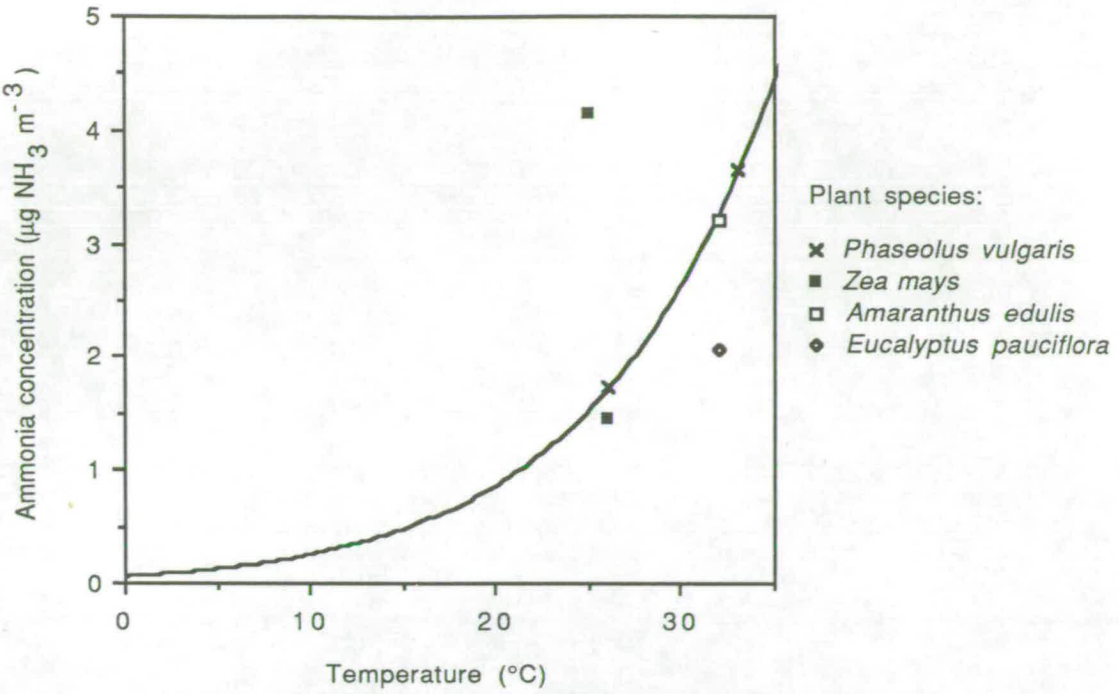

Figure 1.2 Ammonia compensation point determinations of Farquahar *et al.* (1980). The graph is redrawn to show compensation point concentrations (χ_{cp}) using μg NH_3 m^{-3} for all their reported results, with the lowest temperature limit extended from 10 to 0 °C. The curve represents modelled values of the χ_{cp} of *P. vulgaris* at different temperatures, according to the NH_3 solubility equilibria, given the experimentally derived value at 26 °C, and an estimated leaf pH of 6.8. The ordinate may be rescaled directly to fit any of the points. See also footnote *.

response of χ_{cp} to temperature, and found the upper value to be close to that predicted (Figure 1.2) *.

Many authors have adopted this idea, to the extent that it has even been included in a model of atmospheric transport (Derwent, 1987). However this author, as with many others, assumed a constant value χ_{cp} (here 1.5 μg m^{-3}), regardless of temperature. Such a simplification may well be convenient in modelling, however the relationship should not be ignored in explaining observed exchange results. It may also be noted that Derwent's estimate,which is for N.W. Europe, is too high. Based on a more typical temperature of 10 °C, the result for these conditions would be 0.28 μg m^{-3}, although, given the range of temperatures possible, it is clear that such an approach is of limited use. Similarly, the estimate is for *P. vulgaris* well supplied with nutrient solution. Figure 1.2 gives some indication of species variability (not graphed in the original), however, again all plants were well fertilized. There appears to be no χ_{cp} data for unfertilized plant species. An example of the effect of N status was noted

* Some caution nevertheless needs to be applied to this temperature response given the possibility of interactions with atmospheric CO_2 equilibria as demonstrated by Hales and Drewes (1979; section 1.1). An example temperature response for the χ_{cp} of a water surface accounting for this effect has been calculated by Horváth *et al.* (1982).

above (Whitehead and Lockyer, 1987). Additionally, in a wind tunnel experiment Whitehead and Lockyer (1989) showed emission from moist decomposing cut grass herbage, yet only where the grass had previously been well fertilized. This supports N status as being an additional factor affecting the size of the χ_{cp}.

More recently Parton *et al.* (1988) have examined the effect of plant nitrogen status on exchange. They found NH_3 emission to occur for both low and high N treatments of winter wheat at the relatively high concentrations of 6–24 $\mu g\ m^{-3}$ with day-time temperatures of 24 °C. This suggests a much higher χ_{cp} than found by Farquahar *et al.* (1980). In addition, while per plant emission was less from the low N treatments, on a leaf area basis emission was similar. In further experiments, over the course of a growing season, Morgan and Parton (1989) confirmed this larger χ_{cp}. At their usual experimental concentration of 8 $\mu g\ m^{-3}$ emission was recorded in all cases. This varied with time and was greatest following anthesis and during leaf senescence (grain ripening). For most of the time emission was in the range 5–40 ng m^{-2} leaf area s^{-1}, though during these periods values of up to 60 and 80 ng $m^{-2}\ s^{-1}$ respectively were recorded. Three determinations of χ_{cp} were made, at early and late grain filling and at stiff dough (grain ripening). These gave values of 13, 25 and >25 $\mu g\ m^{-3}$ respectively. This confirmed the greater emission during senescence observed by Farquahar *et al.* (1979) and Hooker *et al.* (1980), although both these groups found much smaller fluxes (Table 1.7).

These studies show that the stage of plant growth is also important in exchange. The different biology of perennials and annuals is probably also relevant given that above ground senescence of perennials usually results in translocation of N to roots. This is not a major process in annuals where N is predominantly transferred to grain, or lost entirely from balance sheets (Wetselaar and Farquahar, 1980). It is therefore possible that NH_3 emission during senescence from perennial plants is less than from annuals. Experiments are needed to examine this.

Another complication is the role played by the leaf surface. Van Hove *et al.* (1987b) showed this to act as a capacitor for NH_3 uptake in an experiment using concentrations of 4 to 400 $\mu g\ NH_3\ m^{-3}$. They found that the size of the capacitance increased with humidity, suggesting that, even when no free water (*e.g.* rain or dew) was visible, some sort of bound water layer was present. In their conditions, however, they still found this to be small compared to transport *via* the stomata.

Conversely, there is the evidence from the throughfall studies noted earlier (*e.g.* Van Breeman *et al.*, 1982; Draaijers *et al.*, 1987) that large quantities of NH_x are adsorbed

Authors	χNH_3 ($\mu g\ m^{-3}$)	NH_3 exchange results (Results expressed on a leaf area basis)	Plant species and notes
^{15}N-NH_3 studies			
Porter *et al.* (1972)	760–15000	Deposited NH_3 metabolized.	*Zea mays*
Lockyer & Whitehead (1986), Whitehead & Lockyer (1987)	16–520 14–709	Deposited NH_3 metabolized. Uptake proportional to χ. Less uptake in high N status plants. Stomatal deposition implied.	*Lolium perenne*
Deposition studies using NH_3 only			
Hutchinson *et al.* (1972)	24–44	Deposition mostly through stomata; some surface uptake. No difference of uptake to different N status plants seen. V_d = 2–6 mm s^{-1} (day) and < 2 mm s^{-1} (night).	*Z. mays, Glycine max, Helianthus annuus, Gossypium hirsutum*
Aneja *et al.* (1986)	38–760	Deposition through stomata; negligible cuticle uptake. Approx. V_d = 4 mm s^{-1} (day) and 0.2 mm s^{-1} (night)	*Z. mays, G. max, Phaseolus vulgaris,* grasses
Van Hove *et al.* (1987 a and b)	4–400	Deposition through stomata; small cuticle uptake greater at high humidities. Surface resistance r_c = 50–500 s m^{-1}, depending on light intensity (stomatal opening)	*P. vulgaris*
Emission / deposition studies			
Meyer (1973)	0 26–417	Emission of NH_3 Deposition of NH_3: uptake proportional to χ	*Z. mays, Pinus* sp. *P.vulgaris, G. max*
Farquahar *et al.* (1979)	2–3.5	Healthy leaves: emission 0.68 ng m^{-2} s^{-1} Senescent leaves: emission 9.69 ng m^{-2} s^{-1}	*Z. mays*
Farquahar *et al.* (1980)	0–34	χ_{cp} = 1.7 $\mu g\ m^{-3}$ (26 °C) and 3.7 $\mu g\ m^{-3}$ (33 °C) Emission if $\chi > \chi_{cp}$; Deposition if $\chi < \chi_{cp}$	*P. vulgaris* (see Figure 1.1)
Hooker *et al.* (1980)	0	Pre-anthesis: emission 0.5–1.2 ng m^{-2} s^{-1} post-anthesis: emission 1.4–1.8 ng m^{-2} s^{-1} (temperature raised from 4 to 25 °C over the growing season)	*Triticum aestivum*
Parton *et al.* (1988)	6–24 (48)	growing plants: emission 70–150 ng m^{-2} s^{-1} senescing plants: emission 240–360 ng m^{-2} s^{-1} Leaf area fluxes similar for low and high N plants. Day: 24 °C, night 10 °C	*T. aestivum*
Morgan and Parton (1989)	≈10	background: emission 6–50 ng m^{-2} s^{-1} at anthesis: emission 50–70 ng m^{-2} s^{-1} senescence: emission 35–95 ng m^{-2} s^{-1} early grain filling: χ_{cp} = 16 $\mu g\ m^{-3}$ late grain filling: χ_{cp} = 28 $\mu g\ m^{-3}$ grain ripe (leaves senescent) χ_{cp} > 30 $\mu g\ m^{-3}$	*T. aestivum*
Deposition studies using NH_3 and SO_2			
Adema *et al.* (1986)	300–600 NH_3, SO_2	Deposition to water surface. Uptake of each gas enhanced by presence of the other. At fixed pH 5–7 both gases deposit at maximal rates.	SO_2 oxidation to SO_4^{2-} increased.
Van Hove *et al.*(1989)	NH_3: 56–100; SO_2: 53–84	Deposition of each gas enhanced by presence of the other. Mechanism is cuticle adsorption saturated after several hours (see below).	*P. vulgaris, Populus* sp.
Van Hove *et al.*(1990)	NH_3: 100 SO_2: 100	Stomatal uptake dominates in steady state conditions. At 15 °C high humidities increase deposition. Little effect at 20, 25 °C.	*P. vulgaris*

Table 1.7 Summary of modern controlled environment studies of NH_3 exchange with plants. V_d = deposition velocity, r_c = surface resistance to uptake (see Chapter 2), χ = concentration, χ_{cp} = compensation point concentration (see text). Fluxes and concentrations expressed as NH_3.

on leaf surfaces, which are later washed off by rain. In these cases it is stomatal uptake which is assumed to be negligible. Perhaps crucially however, these authors also recorded large quantities of SO_4^{2-}. This suggests that a pH neutralization of depositing NH_3 by SO_2, and *vice versa*, was occurring, with subsequent oxidation of the SO_2 to SO_4^{2-}, which would enable greater deposition of both species. It seems reasonable that in the chamber studies, with levels of NH_3 dominating, there would be less leaf surface NH_3 deposition as the pH is raised and dissolution limited (section 1.1), resulting in stomatal uptake dominating.

Controlled environment studies have been made to look at this possibility. In a wind tunnel study, Adema *et al.*(1986) confirmed this enhancement process to occur over water surfaces, recording increased deposition velocities in the presence of both NH_3 and SO_2. Van Hove *et al.* (1989), examined this for dry leaf surfaces and found a stimulation of deposition when both gases were present, which as before was enhanced at high humidities. However, for their experimental conditions (56–100 μg NH_3 m^{-3} and 53–83 μg SO_2 m^{-3}) they still found the bulk of the deposition to occur through stomata, with the leaf surface acting as a capacitor, which was filled after 5–10 hours. It is interesting to compare this to the results of Draaijers *et al.* (1987), whose highest throughfall concentrations followed a dry period of a month. This suggests that in field conditions this process may last much longer. Van Hove *et al.* (1989) also found SO_2 to be more soluble than NH_3, which is surprising considering the Henry equilibria of each would suggest the reverse (Seinfeld, 1986; Table 1.1). However, this may relate to their use of large air concentrations with an equivalent ratio of approximately 2 NH_3 : 1 SO_2 (4 : 1 moles), so that NH_3 was in excess.

- ***Micrometeorological field measurements***

Examples of regional scale micrometeorological studies have been considered earlier (section 1.3.2), and appear to show a general emission from the land areas studied. To understand the process of exchange over different surface types however, field scale micrometeorological studies are appropriate. Measurements of background exchange have used the gradient method exclusively, since this allows for a large time period (1–3 hours) needed for ammonia detection. The studies have been stimulated from both agricultural and pollution interests.

The agricultural work has been an extension of the interest in crop N-balances and has therefore been linked to the literature dealing with N-losses following fertilization or grazing, experiments in which NH_3 concentrations are very high. Traditionally therefore, only total NH_x has been measured, on the assumption that NH_4^+ is negligible in comparison. However, for the background surface exchange, NH_4^+ is

significant, and the two concentration gradients are confounded. The result is that valid deposition velocities and resistances cannot be calculated. Nevertheless, given that NH_4^+ deposits very slowly, the NH_x gradient is dominated by NH_3 exchange; since it is this that is used to calculate the flux, it may be concluded that the flux estimates are reasonably valid.

The results of these studies are given in Table 1.8. The experiment, by Harper *et al.* (1983), is included for comparison to show the initial emission after addition of a fertilizer (urea). The initial period of elevated losses was estimated to last between 4 and 14 days depending on environmental conditions. After this period, a background exchange was observed, showing a number of possible responses. One example showed day-time emission and night-time deposition, which appeared to be related to low air concentrations and dew during the night. In another example deposition occurred during the day giving way to a small rate of exchange at night during a period of high air concentrations. Surface wetness and air concentrations are therefore again shown to be important in controlling the exchange process.

Other background crop exchange studies support this pattern. Lemon and Van Houtte (1980), interpreted their results in terms of a bi-directional exchange from the crop, depending on air concentration, while Dabney and Bouldin (1985) in a study over Alf alfa found emission to predominate but suspected deposition to dew at night, although this could not be confirmed because of advection problems in these cases. Denmead *et al.* (1978) appear to have observed the reverse over a maize crop, with deposition occurring when the soil was dry, and emission from a wet soil. These authors used a deposition velocity analysis and found, that for some runs, deposition was too rapid to be through the stomata alone, suggesting leaf surface absorption to be occurring. Since the measurements were for total NH_x, this implies that NH_3 deposition rates were in fact even higher which supports their conclusion.

These studies measured the net exchange with the atmosphere. In addition, Denmead *et al.* (1976) studied the soil crop interaction. They found a large soil emission to be occurring, but most of this was recaptured by deposition to the canopy above, so that above canopy emission was small, with even some net deposition at night. They calculated deposition to the canopy by the difference between the two fluxes. Here also, they suspected leaf surface uptake to be occurring.

More recently, Harper *et al.* (1987) examined the exchange of NH_x over a growing season for a wheat crop fertilized with ammonium nitrate. The net exchange they observed was seen to fall into 4 different phases, while they also explored the origin

Author	χNH_x ($\mu g\ m^{-3}$)	deposition fluxes ($\mu g\ NH_x\text{-}N\ m^{-2}\ s^{-1}$)	V_d and resistances	Notes
Agricultural studies				
Denmead *et al.* (1976)	NH_x-N *e.g.* 2	at soil: -1.6 – -0.08 above canopy: -0.1 – -0.03		Ungrazed pasture; 0.7 m grass sward with *Trifolium* sp. below. Flux largest when soil drying. (D+N)
Denmead *et al.* (1978)	NH_x-N 1–10 mean: 4.6	diurnal cycle: wet soil -0.77 dry soil 0.18	some runs $r_c < 50$ $s\ m^{-1}$	*Z. mays* 1–1.8 m, fertilized 10 weeks before. 21–33 °C. (D+N)
Lemon and Van Houtte (1980)	NH_x-N 1–40	-0.92–0.59		*G. max*, *Elymus repens* Interpreted as χ dependent exchange, χ_{cp}, (D+N)
Harper *et al.* (1983)	NH_x-N 570 2.5–15 13–28	-9.4 (max. fertilizer loss) -0.4–0.2 (background -0.1–0.9 exchange)		Low density sub-tropical pasture (4 cows ha^{-1}) 370 kg N ha^{-1} applied as urea. Fertilizer loss period: 4–14 days. (D+N)
Dabney and Bouldin (1985)	NH_x-N 1.0–5.4	-0.69–0.14		*Medicago sativa*, emission most after hay cutting. Deposition to dew at night. (D+N)
Harper *et al.* (1987)	NH_x-N ≈10 ≈10 20–30 8–15	1) -0.26 pre-fertilization 2) -0.87–0.06 post-fertilization (2 weeks) 3) 0.06 growing stage (foliar N shortage) 4) -0.65–0.02 (mean ≈ 0.15, leaf senescence)		*T. aestivum*. 112 kg N ha^{-1} applied as NH_4NO_3. 4 phases of exchange over growing season. Plant height ranged over 0.2–0.8 m.
Pollution studies				
Horváth (1982, 1983), Mészáros and Horváth (1984)	NH_3 2.74{4 m} 0.96 mean annual	mean: 0.019	V_d = 1.4 mm s^{-1}	Grass surface χ dependent exchange: $V_d\{4\ m\} = 1 - 0.93/[NH_3]$ (cm s^{-1}) ($\mu g\ m^{-3}$) 50–100 m fetch.
Duyzer *et al.* (1987)	NH_3 mean: 3.9	mean: 0.046 (-0.03–0.19) mean wet surfaces: mean dry surfaces:	mean V_d = 19 mm s^{-1} r_c = 0.09 $s\ m^{-1}$ 0.28 $s\ m^{-1}$	Natural vegetation: mainly moorland + some forest. Deposition independent of air concentration implied. (mostly day-time runs)
Harrison *et al.* (1989)	NH_3 mean: 1.5	mean: -0.031 (-0.10–0.02)	not calculated	Various grassland and crop surfaces. Fertilization details not given. (day-time only)

Table 1.8 Micrometeorological studies of background NH_3 exchange over vegetated surfaces. Negative fluxes imply emission. Agricultural measurements are for total NH_x, though the flux is dominated by NH_3 (see text). V_d = deposition velocity, r_c = surface resistance to uptake (see Chapter 2). D+N = both day and night-time measurements made. χ = concentration.

of sources and sinks using within-canopy concentration profiles. These phases are shown in Table 1.8. Prior to fertilization net emission was seen with the source being the vegetation tops, while the soil acted as a sink. Emission was larger for a period of 1 week following fertilization, with both the soil and the vegetation acting as sources (accounting for an estimated total of 8.3 kg N ha^{-1}). This subsequently declined so that net deposition was seen from 2 weeks after fertilization through the growing stage (a total of 0.7 kg N ha^{-1}), although the soil continued to emit NH_3 which was absorbed by the canopy. Finally a period of net emission was again seen from the inflorescence stage to grain maturity and leaf senescence (an estimated total of 7 kg N

ha^{-1}). They attributed the post-fertilization emission to an excess of nitrogen in leaf tissues, and the period of deposition to foliar nitrogen shortages. However, their data show higher air concentrations during the latter period which, if χ_{cp} was exceeded, may also have contributed to the deposition observed. They related the final period of emission to inefficient translocation of N in filling grain, and an excess of NH_3 in tissues due to protein break-down during leaf senescence.

There has been little study of exchange where NH_3 has been measured separately; what there is relates to interest in the gas as a pollutant (see also table 1.8). Horváth (1982, 1983) believed his results over short grassland (conditions unspecified) to show both emission and deposition depending on air concentration, and interpreted this as a soil χ_{cp}. However, a number of criticisms may be made of this study. In particular the measurements were made using only a very limited fetch (13–25 × maximum measurement height), and only two reference heights, so that observed gradients may not solely reflect surface exchange. Harrison *et al.* (1989) have recently reported measurements over several canopy types, and find most grass and crop surfaces to give emission, although as with Horváth, they do not relate this to crop fertilization. However, studying their data, emission seems to be favoured by high temperatures and dry conditions. While they found some deposition results, they dismiss the idea of using a deposition velocity, since the bi-directional exchange suggests the exchange is not independent of air concentration.

The only studies of exchange over natural (or unfertilized) surfaces have been made recently by Duyzer *et al.* (1987). These authors found a consistent pattern of deposition to be occurring over different heathland surfaces in the Netherlands, and support the use of deposition velocities. They found deposition to be too rapid for uptake by stomata alone, which implies that the main site of uptake was the leaf surfaces. In wet conditions this uptake was considered to have no surface resistance so that deposition was limited solely by aerodynamic transport to the surface.

Comparing these studies it seems that land use is important in the exchange process that occurs. This probably relates to the nitrogen status of the community. Exchange also seems to depend on environmental conditions, with temperature, humidity and wetness playing important roles. This may be related to the controlled environment studies. The idea of a compensation point concentration, χ_{cp}, for exchange is supported in the field measurements for the crops by Lemon and Van Houtte (1980) and for soils by Horváth (1982). However this seems to be complicated by environmental conditions as noted above. With the only study on natural surfaces of

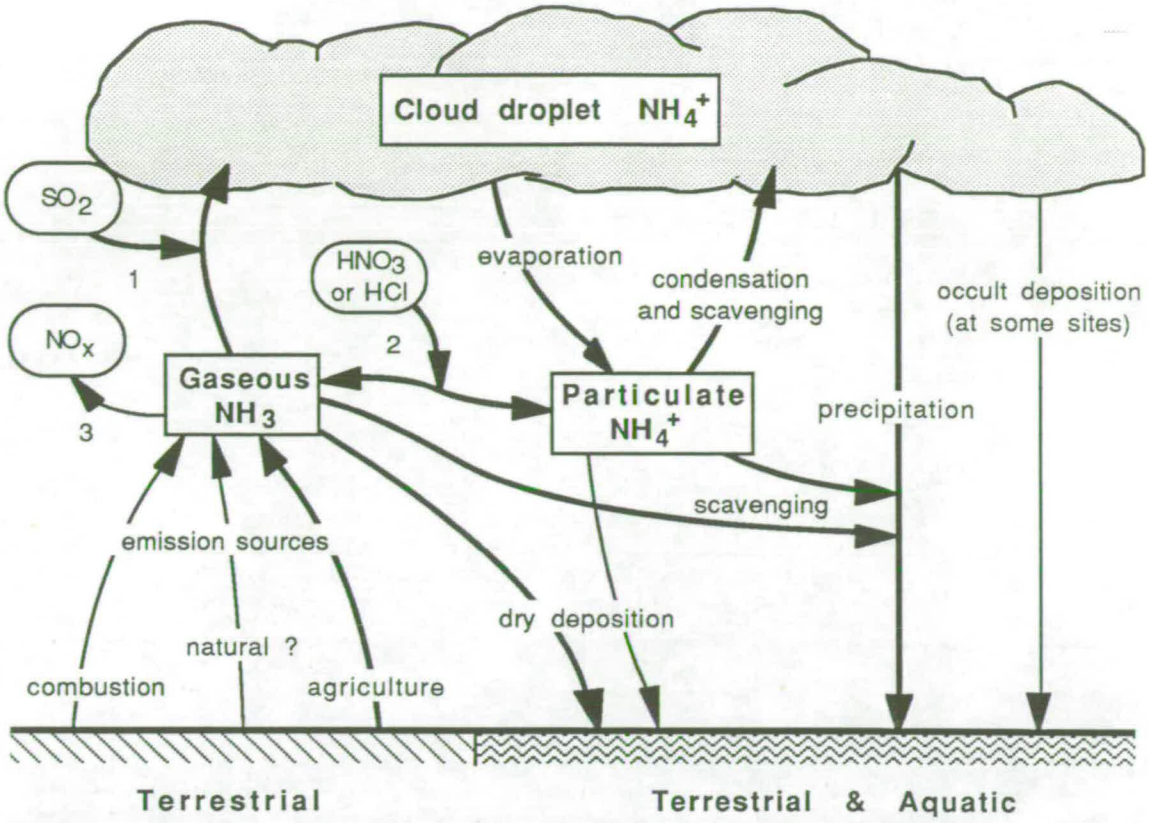

Figure 1.3 Simplified scheme of the surface/atmosphere circulation of NH_x. Major fluxes are shown by bold lines. The three reactions noted are: 1) SO_2 oxidation to SO_4^{2-} and neutralization by NH_3 to give ammonium sulphate (*e.g.* $(NH_4)_2SO_4$); 2) Equilibria of the gases NH_3, HCl and HNO_3 to form particulate NH_4NO_3 and NH_4Cl; 3) Oxidation of NH_3 by $OH^\bullet$ to form NO_x.

Duyzer *et al.* (1987) no relationship to χ_{cp} was considered, and the idea of concentration independent deposition supported. Their work supports the existence of leaf surface deposition and agrees with the throughfall measurement results of Van Breeman *et al.* (1982) and Draaijers *et al.* (1987). Conversely, the chamber work of Van Hove *et al.* (1989) suggests that this sink is filled in several hours.

It is difficult to see how these different observations and concepts may be reconciled. It is therefore clear that there is a need for more work which accounts for each, in order to develop a coherent picture of NH_3 exchange over both natural and crop surfaces.

1.5. AN OVERALL CYCLE FOR ATMOSPHERIC NH_X

From the discussion above a picture of the overall cycle of NH_x between the earths surface and the atmosphere may be built. A simplified representation is given in Figure 1.3. Although attempts have been made to model and quantify budgets for the different aspects of this cycle, given the uncertainty in many of the routes, only an approximate indication of importance is given. A number of budget studies have

already been mentioned in the context of estimating emissions (section 1.3.2). In addition Mészáros and Horváth (1984) have estimated a deposition budget over Hungary, while Möller and Schieferdecker (1985) have estimated the relative importance of the sinks for a typical mid European atmosphere.

Such budgets have often calculated the mean atmospheric residence time of the species (τ), a process which is reviewed by Seinfeld (1986). τ may be found by relating an assumed constant air concentration to emission or deposition, or by summing the individual process residence times as parallel resistances (reciprocal summation). For their global budget, Söderlund and Svensson (1976) estimated species residence times for NH_3 and NH_4^+ of 1-4 and 7–19 days respectively. Möller and Schieferdecker (1985) also used this analysis in their study, and gained values of 0.8 and 7.7 days respectively. These estimates agree well with each other given the approximations inherent in such a calculation. In addition, such residence times are supported by the high degree of local variability seen in field monitoring, characteristic of a species with a short τ. However, these values depend on field estimates of process rates for which there is considerable uncertainty. Möller and Schieferdecker used the dry deposition rates of Mészáros and Horváth (1984) (see Table 1.8). If these are replaced by those of Duyzer *et al.* (1987) the estimated process residence time of NH_3 dry deposition (τ_{V_d} = (assumed mixing height = 1000 m)/(V_d = 0.0014 m s^{-1}) = 200 hours) would be an order of magnitude smaller (τ_{V_d} = 15 hours) and τ = 0.4 days. Since these processes also vary with land surface and meteorological conditions the estimation of τ must only be considered approximate.

Long range transport models of NH_3 and NH_4^+ have been provided by Asman and Janssen (1987), Derwent (1987) and Fisher (1987), and are based largely on calculations such as that given above applied on a geographical basis. These authors have used this to provide maps of air concentrations and deposition over Europe. Large scale area differences, reflecting the specificity of input data are generally shown well by these studies. However, on this scale and using large approximations, the large degree of local variability due to the short residence times and variability in dry deposition is inevitably not seen.

Asman and Drukker (1988) have also applied their model to look at the change in deposition for Europe over the last century. This is achieved by supplying the relevant emission data for given dates in the past, on the assumption that agricultural emissions predominate. Since these sources have increased over this period, the model shows a corresponding increase in deposition. This gets some support from observations of wet deposition increasing with time (*e.g.* Söderlund and Granat, 1982), however as

Skeffington and Wilson (1988) point out, there is a great deal of variability, with many sites showing reductions. This is not unexpected, as changes in the pattern of emission have undoubtedly also occurred. However, it seems that in many areas, such as the Netherlands, increases have been large, with the result that ecological responses appear to be occurring.

1.6. EFFECTS OF NH_X ON THE ENVIRONMENT

Deposition of atmospheric NH_X may affect ecosystems by increasing nitrogen inputs, causing soil acidification, or by direct toxic effects on organisms. Toxicity effects have been reviewed by Van der Eerden (1982) for plants and by NRC (1979) for animals and are associated with very high levels of NH_3. Although the effects may be serious, since such concentrations (>500 $\mu g\ m^{-3}$) are only found near strong sources, these are only local effects. The greatest environmental concern seems to have focused on increased nitrogen inputs and soil acidification.

- Increased nitrogen supply

The 19th century interest in the deposition of atmospheric NH_X as a beneficial source of N to plants has been considered earlier (section 1.2.1). There is indeed evidence that where very high local concentrations occur, crop growth may be stimulated (*e.g.* Malo and Purvis, 1964; Cowling and Lockyer, 1981). Most of the recent interest has, however, been concerned with the effects on natural (unfertilized) ecosystems, where natural levels of deposition are important to the nutrient economy (Rosswall, 1976). As a result any increase in deposition associated with polluted atmospheres represents a considerable shift in nutrient balances. Observed effects have been centred on the Netherlands and Belgium where NH_X pollution is widespread, and have included water bodies, heathlands and forests (Van Breeman and Van Dijk, 1988).

Deposition to oligotrophic waterbodies has been recognized as a possible problem for some time leading to eutrophication and increased possibility of algal blooms (*e.g.* Hutchinson and Viets, 1970), however, most concern revolves around the concurrent acidification observed (see below).

The eutrophication of heathlands is a major issue. Deposition of atmospheric NH_X is blamed for a decline in ericaceous communities (*e.g. Calluna vulgaris*, *Erica tetralix*) and their replacement by grassland communities (*e.g. Molinia caerulea*, *Deschampsia flexuosa*, *Festuca ovina*) observed over much of the Netherlands (Schneider and Bresser, 1987), and the causality of this seems to have been confirmed in fertilization experiments (Heil and Diemont, 1983). Roelofs (1986) has suggested such changes

are apparent when total N inputs exceed 20 kg ha^{-1} $year^{-1}$. The changes may also be exacerbated by an interaction with the heather beetle (*Lochmaea suturalis*), the growth of which is favoured by the increased nitrogen status of the vegetation. Plant death opens up the canopy while decay of the dead heather releases more nitrogen, favouring increased growth of the grasses (Brunsting and Heil, 1985).

Concern has also recently extended to species rich calcareous grasslands. The area of such communities has decreased in recent years due to conversion to arable farming and changes in livestock management. In addition, it has been suggested that the increased N deposition favours the growth of taller rough grasses, such as *Brachypodium pinnatum* , which out-compete the short grassland species (Bobbink, 1989)

Increased deposition NH_x may also exacerbate the poor health of forests. Over 50% of forests in the Netherlands are recorded as being less than vital (Van Breeman and Van Dijk, 1988). The distribution of damaged trees follows that of intensive livestock breeding, which being the major source of NH_3, supports this hypothesis. Nihlgard (1985) formulated an hypothesis for this decline, whereby the increased nitrogen supply can result in imbalances of the other nutrients (K, Mg, Ca, P), and also make shoots more sensitive to frost damage and consequently fungal infection. The role of ammonia in acidifying soils (see below) may exacerbate this. Nutrient imbalances related to high foliar N and large atmospheric NH_x have, for example, been observed by Van Dijk and Roelofs (1988), while increased fungal infection has been discussed by De Temmerman *et al.* (1987) and Istas *et al.* (1988).

- ***Acidification***

The processes and proton exchanges by which an increased NH_x supply can also result in acidification are summarized in Figure 1.4. These may occur in both soils and water bodies. The most important step is the nitrification of NH_4^+ to NO_3^-, by the soil bacteria (*e.g. Nitrobacter* spp), which liberates two H^+ ions:

$$NH_4^+ + 2O_2 \Rightarrow NO_3^- + H_2O + 2H^+$$

Clearly the degree of acidification that occurs depends on the fate of the NH_x. Acidification, may occur from an input of NH_4^+ without oxidation, but only results from NH_3 where nitrification occurs. Leaching of the NO_3^- exacerbates this, while associated loss of nutrient cations may heighten the problems of plant nutrient shortages. This is part of the 'ammonium hypothesis' for forest decline of Nihlgard (1985).

The concern over N eutrophication and acidification of water bodies, resulting from NH_x deposition, has focused on the decline of poorly buffered water pools in the Netherlands. Formerly these supported a characteristic aquatic plant community

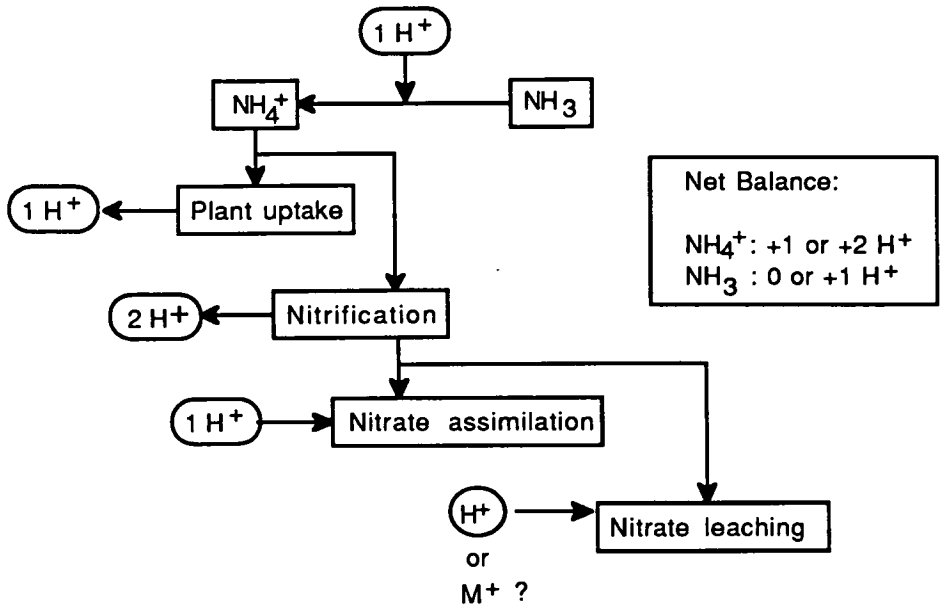

Figure 1.4 Effects of atmospheric NH_3 or NH_4^+ input on soil or water proton balances. The level of production of H^+ depends on the form of NH_x input and the fate of the NH_4^+ ion. M^+ represents a metal ion that might be leached from a soil. Diagram modified from Binkley and Richter (1987).

including *Littorella uniflora*, *Lobelia dortmanna*, and *Isoetes* spp. Most have now vanished, being replaced by acid tolerant, nitrophilous plants such as *Sphagnum* spp., *Drepanocladus fluitans*, and *Juncus bulbosus* (Roelofs 1986). In addition to this, there is the general problem of increased levels of NO_3^- entering ground and river water supplies, however here, the direct effect of infiltration and run off from agricultural residues is more important. Both these nitrification issues and the effects of N eutrophication have been reviewed by Van Breeman and Van Dijk (1988) and Skeffington and Wilson (1988).

1.7. Objectives of Study and Thesis Plan

It is clear from the above discussion that ammonia is important both because of its direct ecological effects, and because of its more widespread role in acid pollution chemistry. At the same time it is also clear that, while some aspects of the surface/atmosphere ammonia cycle appear to be well categorized, such as the quantity and distribution of wet deposition, other aspects are poorly understood or quantified. In addition, much of what has been described above has only become available since the initiation of this study. The objectives of this project were therefore as follows:

1. To make field measurements of the surface/atmosphere exchange of ammonia over a range of vegetated surfaces.

The sparseness of field data on the exchange of NH_3 is particularly noticeable. Consequently, the main body of this study is devoted to this area. Field micro-

meteorological techniques (aerodynamic gradient method) are applied with separate NH_3/NH_4^+ samplers, in order to differentiate between the exchange processes of each component. The fluxes are interpreted using deposition velocity and resistance analyses and related to other environmental factors. Measurements are made over a wide range of vegetated surfaces, including both natural (unfertilized) surfaces and arable crop surfaces (not including the initial period of fertilizer emission). These are then used to develop an understanding of ammonia surface exchange processes.

2. *To monitor the atmospheric NH_3 concentrations at several sites in S. Scotland.*
There is also comparatively little data on the ambient levels of NH_3. This is especially the case in Scotland, where the only published data is the total NH_x results of the EACN (Stevenson, 1968). Ammonia concentrations are provided from monitoring at several sites for periods of up to 18 months. The passive diffusion tube method of Hargreaves and Atkins (1987) is used.

3. *To estimate exchange budgets of ammonia over different surfaces.*
The results from the field studies above are used, with other published data, to estimate the annual fluxes of NH_3 and NH_4^+ exchange over different land surfaces. These are compared with other inputs of fixed nitrogen.

The following chapters are presented as follows:

Chapter 2. theory of field micrometeorological exchange analysis to be used in surface/atmosphere exchange studies;

Chapter 3. field and analytical methods used in the surface exchange studies;

Chapter 4. presentation of the results of the surface exchange studies made over 'natural' and unfertilized ecosystems, including moorland, grasslands and a forest site;

Chapter 5. presentation of the results of the background surface exchange studies made over agricultural (fertilized) crops, including forage grass and cereals;

Chapter 6. report of diffusion tube monitoring of atmospheric NH_3 in S. Scotland;

Chapter 7. general discussion of the surface/atmosphere exchange of ammonia and the estimation of exchange budgets;

Appendices.

Chapter 2

Micrometeorological theory

2.1. INTRODUCTION

Field measurements that allow the quantification of trace gas exchange between vegetated surfaces and the atmosphere may be made either by chamber methods, where fluxes are found from the changes in gas concentration in an enclosure over the ground, or by micrometeorological methods, where the flux is measured in the free air above the surface, and equated with exchange at the surface.

Although chamber methods have found extensive use in controlled environment studies of ammonia exchange, they have a number of disadvantages for use in field conditions. The chamber may modify the surface environment, and hence alter exchange patterns, and only represents a small area (often less than 1 m^2) so that replication over a site is needed to obtain large area averages of fluxes. In addition, deposition of NH_3 to field chamber walls may become important, especially if condensation of water vapour occurs in the system. Thus micrometeorological methods are in principle more favourable. Here the surface is not disturbed and field processes can continue unaffected, while the net exchange is measured, since measurements are made above the surface. This may be important where a number of opposing processes are occurring in a plant/soil system. The method also samples over a large area, so that variations in exchange over the site are averaged out. Consequently, it is the micrometeorological approach that is applied in this study.

Micrometeorological methods fall into two groups. Most are based on the use of large homogeneous surfaces, so that the boundary layer of air flowing over the surface is assumed to be in equilibrium with the surface up to a given height above the ground. Within this layer the vertical fluxes are assumed to be constant with height and a one dimensional analysis of transport made. Various estimates exist as to the relative depth of this constant flux layer, but as an approximate rule, 100 m of upwind fetch over a uniform surface are needed for it to fully develop to a height of 1 m (Monteith, 1973). In practice given practical measurement restrictions, a depth of 2–5 m is often used, so that a uniform land surface of several hundred metres upwind is required.

An alternative procedure is the mass balance method (Denmead, 1983). Here measurement is made of the modification of a developed boundary layer by a small upwind patch (*e.g.* fetch 20 m), that has markedly different exchange pattern to the background

exchange. An example for NH_3 is the estimation of emission from a fertilizer treated plot (Denmead, 1983). The outgoing downwind horizontal flux, found from integrating the products of horizontal windspeed and excess concentration over the height of the affected layer, is assumed to balance that being lost from the ground. This is a useful technique, but is clearly not suitable for measurements of background exchange; in this case constant flux layer techniques are appropriate.

2.2. METHODS ASSUMING A CONSTANT FLUX LAYER

Theoretically the simplest approach is the eddy covariance technique. This method correlates the instantaneous vertical windspeed with the instantaneous concentration of individual eddies, at a given point above the surface. The flux of a trace gas (F_χ) is given by:

$$F_\chi = \overline{w'\chi'} \qquad 2.1$$

where w' and χ' are the instantaneous fluctuations about the mean vertical windspeed (w) and concentration (χ) respectively. The method is favoured for its conceptual simplicity and lack of empiricism, however, the scale of some of the eddies transporting the gas necessitates sampling at least at 5–10 Hz. The technical difficulty of sampling at such rates for NH_3 at environmental concentrations means that at present eddy covariance is not a viable option for measuring NH_3 exchange (Denmead, 1983).

Alternative approaches are based on the principle of diffusion of an entrained property along its mean concentration gradient. These permit the long sampling times (generally at least one hour) required for the precise determination of low levels of ammonia. Emission or deposition sets up a gradient of concentration with height above the surface, corresponding to either enrichment or depletion at the surface. The gradient may be characterized by measurement of mean concentrations at several heights above the surface in the constant flux layer. The flux toward or away from the surface is then found as the product of this gradient and the turbulent diffusion coefficient of trace gas or particulate exchange (K_χ):

$$F_\chi = K_\chi \, \partial\chi/\partial z \qquad 2.2$$

where z is height above the surface. The estimation of K_χ may be made either by comparison with the eddy diffusivity for momentum (K_M), found from windspeed profiles (aerodynamic method) or from the energy balance of a surface (energy balance method). The aerodynamic method is used in this study and is described in full in the sections following, though brief consideration may first be given to the energy balance method.

The energy balance of a ground surface is given as:

$$\mathbf{R_n} = \mathbf{H} + \lambda\mathbf{E} + \mathbf{G} \qquad 2.3$$

where net radiation flux ($\mathbf{R_n}$) balances the sensible and latent heat fluxes ($\mathbf{H}$ and $\lambda\mathbf{E}$ respectively) and the ground heat flux ($\mathbf{G}$).

$\mathbf{H}$ and $\lambda\mathbf{E}$ may be defined in similar form to equation 2.2:

$$\mathbf{H} = K_H \rho c_p \partial T/\partial z \qquad 2.4$$

$$\lambda\mathbf{E} = K_E \lambda \partial E/\partial z \qquad 2.5$$

where K_H and K_E are the appropriate eddy diffusivities, ρ is the density of the air, c_p is the specific heat capacity of the air, λ is the latent heat of vaporization of water vapour, and E is the absolute humidity. There is good field evidence of the equality of eddy diffusivities for heat and entrained properties, such as gases and sub-micron particles, in all stabilities (*e.g.* Thom, 1975), so that combining these with equation 2.3 gives:

$$\mathbf{R_n} - \mathbf{G} = K_\chi [(\rho c_p \partial T/\partial z) + (\lambda \partial E/\partial z)] \qquad 2.6$$

Hence K_χ, and consequently the flux, may be found from the net radiation, ground storage and gradients of temperature and water vapour. A more detailed analysis, including development of the Bowen ratio formula, is provided by Monteith (1973), Thom (1975), and Denmead (1983).

The method is to be preferred to the aerodynamic method in conditions of very low windspeed, where windspeed profiles are difficult to measure accurately, or in conditions of extreme non-neutrality, where large empirical stability corrections are needed to calculate the flux in the aerodynamic method. Conversely, the energy balance method performs poorly in conditions of small heat flux, such as at night and in near neutral cloudy day-time conditions. Thus where the cycle of diurnal variation in exchange is of interest, as in this study, the aerodynamic method is to be preferred.

2.3. AERODYNAMIC GRADIENT METHOD

2.3.1 Basic theory

As noted in the previous section K_χ appears to equal K_H in all stability conditions. In addition in neutral and stable conditions (*e.g.* Thom, 1975):

$$K_M = K_H = K_\chi \qquad 2.7$$

In unstable conditions the equality with K_M does not hold, however, empirical relationships exist so that it is possible to use K_M to estimate K_χ and obtain trace gas fluxes. K_M may be found from an equation similar to equation 2.2, describing the

momentum flux (τ):

$$\tau = \rho K_M \partial u/\partial z \qquad 2.8$$

where ρ is air density and u is mean horizontal windspeed. τ may also be defined by a notional 'eddy velocity' (u_*), which is analogous to the velocity fluctuations of w' of the eddy covariance technique (equation 2.1):

$$\tau = \rho u_*^2 \qquad 2.9$$

The term u_* may be defined in terms of gradient theory such that:

$$u_* = l \partial u/\partial z \qquad 2.10$$

where l is the mixing length, or mean eddy size, at a given height above the ground. Thus u_* is also equivalent to the mean windspeed change over one mixing length. Within the boundary layer u_* is constant with height, though both l and $\partial u/\partial z$ are not. The mixing length for momentum may be given by:

$$l = \frac{k(z-d)}{\Phi_M} \qquad 2.11$$

where k is the von Karman constant (0.41), defined by this formula as the ratio of mean eddy size to height above the surface, Φ_M is the empirically estimated correction for effects of non-neutrality upon this ratio, while d is the zero plane displacement — or apparent increase in aerodynamic ground level — that occurs over vegetated surfaces. In effect $(z-d)$ is the height above the aerodynamic ground level.

K_M may be found from equations 2.8–2.11:

$$K_M = l^2 \frac{\partial u}{\partial z} = \frac{k(z-d)u_*}{\Phi_M} = \frac{k^2(z-d)^2}{\Phi_M^2} \frac{\partial u}{\partial z} \qquad 2.12$$

This formula may be used to estimate K_χ in neutral and stable conditions. The difference between K_M and K_χ in unstable conditions is due to the stability correction for heat (Φ_H) or entrained properties (Φ_χ) not equaling Φ_M. Given the equality of Φ_H and Φ_χ, a general form of K_χ may be defined by analogy with equation 2.12:

$$K_\chi = \frac{k(z-d)u_*}{\Phi_H} \qquad 2.13$$

which may then be substituted into the flux equation 2.2:

$$F_\chi = \frac{k(z-d)u_*}{\Phi_H} \frac{\partial \chi}{\partial z} \qquad 2.14$$

This may be used to calculate the flux, but in practice it is often more convenient to dispense with K_χ and deal solely with u_* and an analogous term χ_* (eddy

concentration). From equations 2.10 and 2.11 and by comparison with 2.14:

$$u_* = \frac{k(z-d)}{\Phi_M}\frac{\partial u}{\partial z} \qquad 2.15$$

$$\chi_* = \frac{k(z-d)}{\Phi_H}\frac{d\chi}{dz} \qquad 2.16$$

$$F_\chi = u_* \chi_* \qquad 2.17$$

Equation 2.17 is comparable with the equation describing the eddy covariance technique (equation 2.1).

2.3.2 Approximate log-linear approach: integrating Φ as a constant.

Although the flux may be calculated using the formulae above, since the gradients with height are non-linear, this not particularly convenient. Curve fitting procedures could be used or, as is often done, the gradients treated as the difference between two heights (*e.g.* Thom,1975). A more useful approach, however, is to linearize the profiles, which are approximately logarithmic, by integration. The simplest approach, and one which is often used (*e.g.* Garland, 1977), treats Φ as a constant.

Integration of equation 2.15 above gives:

$$u\{z-d\} = \frac{u_* \Phi_M}{k}\int_0^z \frac{1}{(z-d)}\,\partial z \qquad 2.18$$

$$u\{z-d\} = \frac{u_* \Phi_M}{k}\ln\left(\frac{z-d}{z_0}\right) \qquad 2.19$$

Similarly by analogy, for concentration:

$$\chi\{z-d\} = \frac{\chi_* \Phi_H}{k}\ln\left(\frac{z-d}{z_\chi}\right) \qquad 2.20$$

These are often treated as linear functions, though strictly this is only the case in neutral conditions. The constant of integration for the wind profile (equation 2.19), z_0, represents the height above d at which windspeed is predicted to be zero — although in practice a finite windspeed usually exists here — and is often termed the roughness length, as it is a function of surface roughness. z_χ is the analogous term for concentration, being the height above d at which concentration is predicted to be zero. The effect of the slight curvature of these profiles in non-neutral conditions is that valid estimates of z_0 or z_χ can only be made in neutral conditions using these equations. Nevertheless, linear regression provides a good approximation for the gradient, and is often used (*e.g.* Garland, 1977). The gradients from equation 2.19 and 2.20 may be seen to be:

$$\frac{\partial u}{\partial \ln(z-d)} = \frac{u_* \Phi_M}{k}; \qquad \frac{\partial \chi}{\partial \ln(z-d)} = \frac{\chi_* \Phi_H}{k}; \qquad 2.21,\ 2.22$$

Substituting these values of u_* and χ_* into equation 2.17 gives the flux as:

$$F_\chi = k^2 \frac{\partial u}{\partial \ln(z-d)} \frac{d\chi}{\partial \ln(z-d)} (\Phi_M \Phi_H)^{-1} \qquad 2.23$$

Precise estimation of the gradients may be made by fitting second order polynomials (*e.g.* Saugier and Ripley, 1978). However, the error in not doing so at most amounts to only a few percent, which is often small compared to other sources of error. In practice, the linear analysis is usually made. The term $(\Phi_M \Phi_H)^{-1}$ is often termed the stability factor (Thom, 1975) and in later sections is denoted f.

2.3.3 Corrections for non-neutral conditions

The empirical estimation of Φ for different conditions has been the subject of much investigation. The results of Businger (1966) and Dyer and Hicks (1970) for unstable conditions and those of Webb (1970) for stable conditions are strongly supported in the literature (*e.g.* Paulson, 1970; Denmead, 1983) and are consequently used here. For unstable conditions this gives:

$$\Phi_M^2 = \Phi_H = \Phi_\chi = \left[1 - 16\frac{z-d}{L}\right]^{-0.5} \qquad 2.24a$$

$$\text{where } \frac{z-d}{L} \approx \text{Ri} \qquad 2.24b$$

while for stable conditions:

$$\Phi_M = \Phi_H = \Phi_\chi = \left[1 + 5.2\frac{z-d}{L}\right] \qquad 2.25a$$

$$\text{where } \frac{z-d}{L} = \frac{\text{Ri}}{1 - 5.2\text{Ri}} \qquad 2.25b$$

Here the terms L and Ri are the Monin-Obukhov stability length and the Richardson number respectively. These are measures of stability and may be calculated from wind and temperature profiles. In the above equations Φ is described indirectly in relation to Ri. Direct relationships are given by Thom (1975), but since Ri is a function of height and L is not, the above analysis using $(z-d)/L$ is more convenient.

L may be defined as:

$$L = \frac{u_*^3 \rho c_p T}{k g \mathbf{H}} \qquad 2.26$$

where T is absolute temperature (Kelvin), g is gravitational acceleration and c_p is the specific heat capacity of the air. Since both $\mathbf{H}$ and L are needed to calculate one another, L cannot be found directly from equation 2.26 when using the aerodynamic

method alone. It may however be found by its relationship to Ri. This describes the relative importance of buoyancy (free convection) in unstable conditions, or thermal stratification in stable conditions, as compared to the forced convection of the wind. It is usually expressed (*e.g.* Thom, 1975) as:

$$\mathrm{Ri} = \frac{g\,\partial T/\partial z}{T\,(\partial u/\partial z)^2} \qquad 2.27$$

Here T is again in Kelvin. Both Ri and L are positive in stable and negative in unstable conditions. The general form of their relationship, from which equations 2.24b and 2.25b are derived may be seen to be:

$$\mathrm{Ri} = \frac{(z-d)\,\Phi_H}{L\ \Phi_M{}^2} \qquad 2.28$$

As it stands equation 2.27 involves the estimation of slopes of curves, which is not convenient. However, the same arguments of section 2.3.2 may be applied to derive a more useful equation. Substituting the relationship for $\partial u/\partial z$ given in equation 2.15 and an analogous expression for $\partial T/\partial z$ into equation 2.27, then substituting back with logarithmic gradients of the form in equation 2.21 gives:

$$\mathrm{Ri} = \frac{(z-d)\,g\,\partial T/\partial \ln(z-d)}{T\,[\partial u/\partial \ln(z-d)]^2} \qquad 2.29$$

This formula does not appear to have been used elsewhere, however, as with equation 2.23 a good approximation may be made by linear regression of these gradients, thus simplifying analysis.

Estimation of wind and temperature profiles allow Ri and then L to be calculated from which appropriate values of Φ may be found. These may then be applied with measured concentration and wind profiles to estimate a corrected flux on the basis of equation 2.23. However, it is important to remember that Φ relies on empirical estimation, and as such, where its contribution to the magnitude of the flux is large, the uncertainty in the flux will also be large. With this in mind, results in extreme non-neutrality must be considered with caution.

2.3.4 Log-linear approach: integrating Φ as a function of height

The reason for the slight non-linearity of the profile equations (2.19 and 2.20) in non-neutral conditions is because strictly the stability correction is a function of height, $\Phi\{(z-d)/L\}$, rather than a constant as treated in these equations. The profiles may, therefore, be properly linearized by including Φ in the integration of equation 2.18. This is often not done because of the increased complexity of the analysis, and because good estimates of the flux may be made by the simpler method. However, the

linearization achieved by integrating $\Phi\{(z\text{-}d)/L\}$ allows z_0, and other related parameters (see section 2.4.5), to be estimated directly even in non-neutral conditions. It also provides a check on the stability correction, since it is possible to assess the improvement of profile linearity that occurs when the stability correction is applied.

- ***Stable conditions***

Integration is straightforward in the stable case (Thom, 1975; Biscoe *et al.*, 1975). Substitution of equation 2.25a into 2.15 gives:

$$\frac{\partial u}{\partial z} = \frac{u_*}{k(z\text{-}d)}\left[1 + \frac{5.2(z\text{-}d)}{L}\right] \qquad 2.30$$

Rearranging this and integrating gives:

$$u\{z\text{-}d\} = \frac{u_*}{k}\int_0^z \left[\frac{1}{(z\text{-}d)} + \frac{5.2}{L}\right]\partial z \qquad 2.31$$

$$u\{z\text{-}d\} = \frac{u_*}{k}\left[\ln\left(\frac{z\text{-}d}{z_0}\right) + \frac{5.2(z\text{-}d)}{L}\right] \qquad 2.32$$

This may be rearranged to the standard format of a straight line and a similar concentration profile given on the basis of similarity of Φ_H and Φ_M in stable conditions (equation 2.25):

$$u\{z\text{-}d\} = \frac{u_*}{k}\left[\ln(z\text{-}d) + \frac{5.2(z\text{-}d)}{L}\right] - \frac{u_*}{k}\ln(z_0) \qquad 2.33$$

$$\chi\{z\text{-}d\} = \frac{\chi_*}{k}\left[\ln(z\text{-}d) + \frac{5.2(z\text{-}d)}{L}\right] - \frac{\chi_*}{k}\ln(z_\chi) \qquad 2.34$$

Thus the stability correction is effected by a rescaling of the height axis in equations 2.33, 2.34.

- ***Unstable conditions***

The integration accounting for $\Phi\{(z\text{-}d)/L\}$ in unstable conditions is somewhat more complicated. Panofsky (1963) suggested the use of an integrated stability function $\psi\{(z\text{-}d)/L\}$. Thus integrating the windspeed gradient (equation 2.15):

$$u\{z\text{-}d\} = \frac{u_*}{k}\int_0^z \left[\frac{1}{(z\text{-}d)} \cdot \Phi_M\left\{\frac{z\text{-}d}{L}\right\}\right]\partial z \qquad 2.35$$

$$u\{z\text{-}d\} = \frac{u_*}{k}\left[\ln\left(\frac{z\text{-}d}{z_0}\right) - \psi_M\left\{\frac{z\text{-}d}{L}\right\}\right] \qquad 2.36a$$

$$\text{where} \quad \psi_M\left\{\frac{z\text{-}d}{L}\right\} = \int_0^{z/L} \frac{1 - \Phi_M\{(z\text{-}d)/L\}}{(z\text{-}d)/L}\,\partial\left[\frac{z\text{-}d}{L}\right] \qquad 2.36b$$

The corrected wind profile (equation 2.36a) may again be re-arranged into the standard form for a straight line, and a similar equation for concentration provided:

$$u\{z\text{-}d\} = \frac{u_*}{k}\left[\ln(z\text{-}d) - \psi_M\left\{\frac{z\text{-}d}{L}\right\}\right] - \frac{u_*}{k}\ln(z_o) \qquad 2.37$$

$$\chi\{z\text{-}d\} = \frac{\chi_*}{k}\left[\ln(z\text{-}d) - \psi_H\left\{\frac{z\text{-}d}{L}\right\}\right] - \frac{\chi_*}{k}\ln(z_\chi) \qquad 2.38$$

Dyer and Hicks (1970) calculated and tabulated values of ψ for their data, which covered a wide range of instability, so that ψ may be found from interpolation of their values. Alternatively, Paulson (1970) provided the integrals of equation 2.36b for the Dyer and Hicks stability correction (equation 2.24):

$$\psi_M\left\{\frac{z\text{-}d}{L}\right\} = 2\ln\left[\frac{1+x}{2}\right] + \ln\left[\frac{1+x^2}{2}\right] - 2\tan^{-1}(x) + \frac{\pi}{2} \qquad 2.39$$

$$\psi_H\left\{\frac{z\text{-}d}{L}\right\} = 2\ln\left[\frac{1+x^2}{2}\right] \qquad 2.40$$

$$\text{where} \quad x = \left[1 - 16\frac{z\text{-}d}{L}\right]^{0.25} \qquad 2.41$$

Here x is in radians for the $\tan^{-1}$ term. A derivation of this integration is given by Miranda (1982).

Thus given L from the equations in section 2.3.3, values of ψ may be found for the heights at which the quantities are measured in sampling by using the equations above. Linear regression may then be performed for the values of χ or *u versus* stability corrected $\ln(z\text{-}d)$ from equations 2.33 and 2.34 or equations 2.37 and 2.38, depending on atmospheric stability. This provides u_* and χ_*, which may then be substituted into equation 2.17 to give the flux.

2.3.5 Practical considerations

The effect of non-neutrality on the standard logarithmic profiles (equations 2.19, 2.20) may be seen from Figure 2.1, where different wind profiles are given for the hypothetical conditions of $z_o = 0.05$ m, and $u_* = 0.25$ m s^{-1}. The linear neutral profile ($L = |\infty|$) is compared with examples of moderately strong instability ($L = -10$ m) and stability ($L = 10$ m), for both of which the non-linearity is clear. In the simpler analysis, integrating Φ as a constant in relation to z (section 2.3.2.), an estimate of u_* (or equally χ_*) is made by treating each of the plots as linear and the slope as $u_*\Phi/k$. In the analysis with Φ integrated as a function of z (section 2.3.4), the stability correction ($\psi\{(z\text{-}d)/L\}$) is applied at each measurement height to provide corrected $\ln(z\text{-}d)$, that is $[\ln(z\text{-}d) - 5.2(z\text{-}d)/L]$ or $[\ln(z\text{-}d) - \psi_M\{(z\text{-}d)/L\}]$, with the effect that

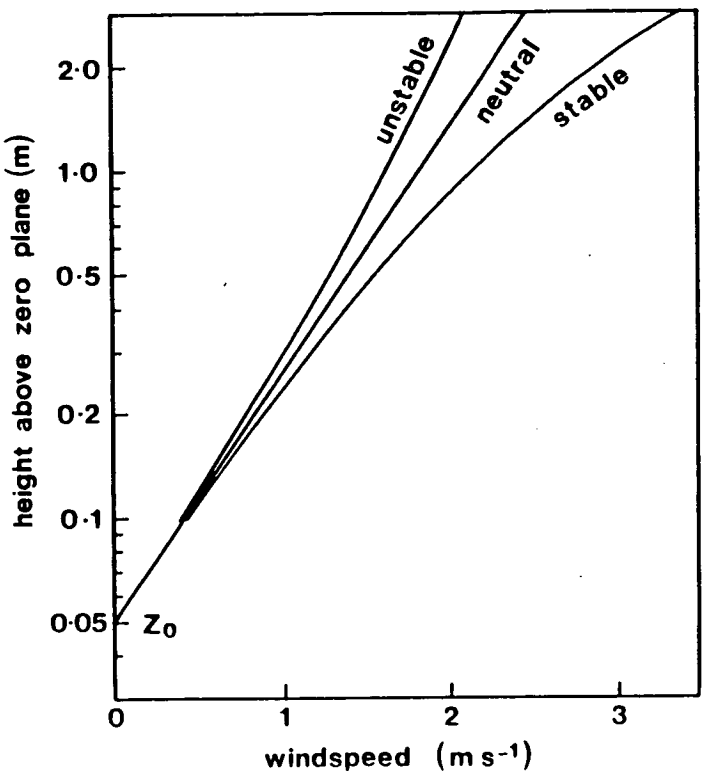

Figure 2.1 Effect of non-neutrality on windspeed profiles. The examples given are for an hypothetical fully developed boundary layer with $z_0 = 0.05$ m and $u_* = 0.25$ m s^{-1}. L = -10, |∞|, 10 m for the three cases of unstable, neutral, and stable conditions respectively. Correction of the non-neutral profiles by the integrated Φ approach produces lines co-linear with the neutral profile.

the corrected profiles fit the linear neutral condition profile. u_* is then found by treating the slope as u_*/k.

It is clear from Figure 2.1 that the magnitude of this correction increases with height, so that in strong non-neutrality it is wise not to measure over too deep a boundary layer. This may be demonstrated by the relationship between Ri and the stability factor, f, in stable conditions. For example, at 10 m above the ground with L = 10 m then Ri = 0.16 and f = 0.026, which dominates the estimate of the flux (see equation 2.23). Conversely at 2 m, Ri = 0.098 and f = 0.24, which is an order of magnitude less than that at 10 m. The corrections may be viewed as relating to the comparative importance of forced turbulence and temperature stratification, so that the greater proportion of forced turbulence near the surface results in the stability correction being less. In comparison the correction at z_0 is generally negligible.

Profile curvature is also relevant to the estimation of d when working over vegetated surfaces. As an approximate guide, relationships between the height of a crop (h) and both d and z_0 are often suggested (*e.g.* Jones, 1983):

$$z_0 = 0.1h \qquad d = 0.6h \text{ to } 0.7h \qquad \text{2.42a, 2.42b}$$

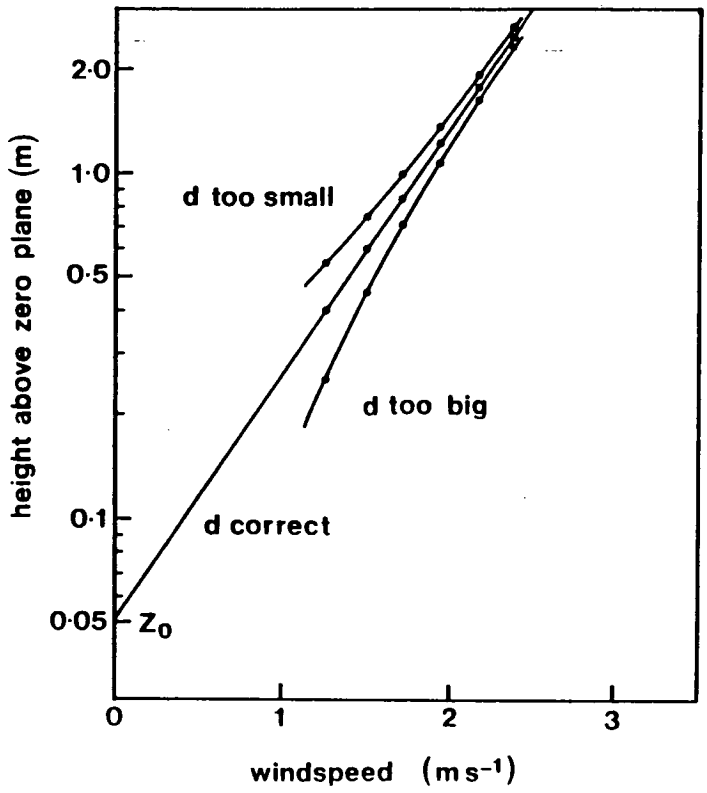

Figure 2.2 Effect of the estimate of zero plane displacement on the logarithmic wind profile in neutral conditions. Curvature may be detected by an array of anemometers at several heights (here six) above the ground. In this example $z_0 = 0.05$ m and $u* = 0.25$ m s^{-1}.

A more precise estimate of d may however be found by analysis of the wind profile, particularly for heights nearest the ground (Figure 2.2). Where a correct value of d is used, the profile is logarithmic towards z_0, as described in the preceding analysis; however, if d is too large or small the profile is curved. Consequently, the value of d may be found as that which linearizes the profile toward z_0 for a logarithmic plot. Given the non-linearity of profiles in stable and unstable conditions, it is clear this estimation should be restricted to neutral runs, although theoretically an iterative approach with stability linearized profiles might be possible.

It is also clear from the above that an accurate determination of z_0 depends on an equally good estimate of d, because of the inter-relationship between these two quantities. Where d is overestimated z_0 is underestimated and *vice versa*. Hence the estimation of d may be a potential source of error. Over short vegetation with a small z_0, such as grasslands and crops, the curvature toward z_0 is easily detected with good measurement of wind profiles, so that this is not a great problem. However, over very rough surfaces such as forests, estimation of d is more approximate, since the available measurement range (see Appendix 8) is further from the surface and this curvature is less clear. Some caution is therefore needed in considering such flux estimates.

In practice the value of d derived from windspeed measurements, is used to estimate d for the concentration profile, since the precision of the trace gas concentration, such as

ammonia, is usually not good enough to allow independent determination. An error might be suggested to result from this procedure where deposition of momentum and the trace component occurs to different sites, such as to roughness elements and soil respectively. However, this is by no means clear, and requires experimentation. Errors in d also affect the values of F_χ, the deposition velocity (V_d) and the surface resistance (r_c, see following section). However, while F_χ is fairly sensitive to such errors, the sensitivity is much less for V_d and r_c. This is demonstrated for a wide range of d for example data collected in this study and given in Appendix 2 (Fala Moor, Harwell).

2.4. RESISTANCE ANALYSIS

2.4.1 General

In addition to the analysis of fluxes described above, it is also of interest to be able to view transfer in terms of rates and resistances which identify the controlling factors in exchange. This may be done by the analogy of trace gas fluxes to current in an electrical circuit as described by Ohm's law (resistance = potential difference/current), and is relevant to all the constant flux layer methods of estimating surface exchange:

$$r\{z_1, z_2\} = (\chi\{z_1\} - \chi\{z_2\})/F_\chi \qquad 2.43$$

where z_1 and z_2 are two heights above the surface and $r\{z_1, z_2\}$ the resistance to transfer of the trace compound between these levels. In measurements of the dry deposition of trace gases, such as SO_2, the absorbing surface is often assumed to have a zero air concentration, and the flux therefore viewed as being dependent on the atmospheric concentration (*e.g.* Garland, 1977; Fowler and Unsworth, 1979). In this case, if z_2 is considered to be the notional height of the absorbing surface, where concentration is zero, and a zero plane displacement is accounted for, a total resistance from a defined height to the surface ($r_t\{z\text{-}d\}$) may be defined:

$$r_t\{z\text{-}d\} = \chi\{z\text{-}d\}/F_\chi = 1/V_d\{z\text{-}d\} \qquad 2.44$$

The inverse of r_t is the deposition velocity V_d, which was introduced briefly in Chapter 1.

This total resistance may be viewed as the sum of a number of resistances in series and parallel as shown in Figure 2.3a. In addition, the resistances may be considered as applying between notional heights above d as shown in Figure 2.3b. Turbulent transfer operates from the free atmosphere down to z_0 — the theoretical point of zero windspeed and absorption of momentum — and is accounted for by the aerodynamic resistance r_a. This is estimated from momentum transport using the wind profile

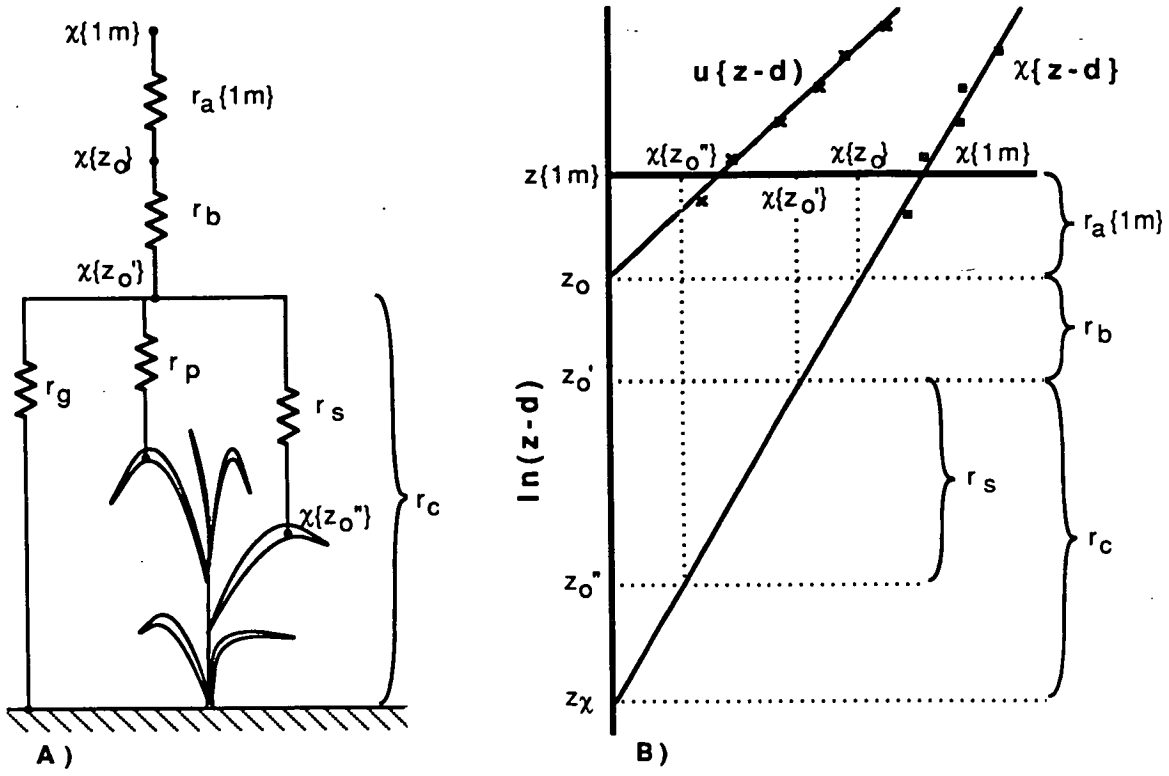

Figure 2.3 Resistance analogy of trace gas transfer between the atmosphere and vegetation.

A) For a gas of concentration χ the component resistances to transfer are given as: r_a, atmospheric resistance; r_b, laminar boundary-layer resistance, r_c, surface or canopy resistance. r_c may be considered as several parallel resistances: r_g, resistance to soil uptake; r_p, resistance to leaf surface uptake by pollutant reaction; r_s, resistance to uptake through stomata. The notional surface concentrations at z_o, z_o' and z_o'' are given for different points between resistances.

B) The resistances may be viewed as accounting for the transfer between notional heights above the surface. For this hypothetical example, deposition would be recorded with a value of r_c which is greater than r_s. For further details of this analysis see text.

(Figure 2.3b). However, for trace gases and other entrained properties atmospheric transport to surface roughness elements involves a further resistance. This is because friction and bluff body forces, which allow momentum deposition, set up a quasi-laminar layer of air immediately surrounding roughness elements. Properties must diffuse through this layer of air, and this is accounted for by the laminar boundary-layer resistance, r_b. Therefore, the notional height of the surface for entrained properties, referred to as z_o', is less than z_o. The difference between z_o and z_o' depends on the value of r_b. Finally, a resistance to transfer at the surface may exist and, using the assumption of equation 2.44 that the concentration at the surface is zero, a surface or canopy resistance, r_c, may be defined for the residual concentration change between z_o' and z_χ.

Equation 2.44 may be expanded to account for these component resistances, which are considered as operating in series between each of the notional heights above d:

$$r_t\{z\text{-}d\} = \frac{[\chi\{z\text{-}d\} - \chi\{z_o\}] + [\chi\{z_o\} - \chi\{z_o'\}] + [\chi\{z_o'\} - \chi\{z_\chi\}]}{F_\chi} \quad 2.45$$

$$= r_a\{z\text{-}d\} + r_b + r_c \quad 2.46$$

Thus $\chi\{z_o\}$ represents the concentration at the junction of the laminar and turbulent boundary layer and $\chi\{z_o'\}$ the concentration at the base of the laminar boundary layer, at the surface. By definition $\chi\{z_\chi\}$ equals zero. It must be remembered, however, that these concentrations are the product of extrapolating mean profiles measured above the canopy and therefore do not imply that such values occur in practice at these heights above *d*.

The usefulness of this approach is that the surface resistance (r_c) may be found by micrometeorological methods. Since r_c is independent of the aerodynamic terms, it may be explained in terms of processes affecting surface uptake. In addition, r_a and r_b may be estimated for given surface roughness and windspeed conditions. Consequently, having characterized r_c, the analysis may be modelled in reverse to predict V_d and for different circumstances. Total deposition fluxes may then be estimated from equation 2.44 using the predicted V_d with an estimate of atmospheric concentration. r_c may be viewed as the sum of different resistances for exchange acting in parallel (Figure 2.3a). Identification and characterization of these is useful in understanding the behaviour of r_c, and this may be used in modelling exchange.

In the following sections (sections 2.4.2–2.4.4) a consideration of the resistances r_a, r_b and r_c (and its components) is given from the stand-point of the aerodynamic gradient method. In addition, an alternative analysis considering surface resistances in terms of concentrations is developed in section 2.4.5.

2.4.2 Atmospheric resistance, r_a

The value of r_a for trace component exchange may be found by analogy to the resistance to the deposition of momentum (r_{aM}) from wind profile measurements. The momentum flux (τ) from equations 2.8–2.9 may be included in a similar Ohm's law analysis to the above, which can be simplified, since by definition windspeed at the surface is zero:

$$r_{aM}\{z\text{-}d\} = \frac{\rho(u\{z\text{-}d\} - u\{z_o\})}{\rho\, u_*^2} = \frac{u\{z\text{-}d\}}{u_*^2} \quad 2.47a,\ 2.47b$$

In neutral and stable conditions heat and entrained properties are transported through the atmosphere at the same rate as momentum (equations 2.7, 2.25a) so that this formula may also be used for the r_a of these properties. However, in unstable conditions this equality fails because of a difference in the value of Φ (equation 2.24a),

so that modification of the equation is needed. In the case of r_a for trace gas exchange, analogy is made between $\tau = \rho\, u_*^2$ (equation 2.9) and $F_\chi = u_*\, \chi_*$ (equation 2.17) as the denominator for equation 2.47b. Hence for trace gas exchange, $f_\chi = (\Phi_M\, \Phi_H)^{-1}$ rather than $f_M = (\Phi_M\, \Phi_M)^{-1}$ is used in equation 2.47.

Following the analysis of Monteith (1973) and Thom and Oliver (1977), equation 2.47b may therefore by expanded for u_* using equation 2.36a and a similar equation including $\psi_H\{(z-d)/L\}$ as the stability corrector:

$$r_a\{z-d\} = \frac{\left[\ln\left(\frac{z-d}{z_0}\right) - \psi_M\left\{\frac{z-d}{L}\right\}\right]\left[\ln\left(\frac{z-d}{z_0}\right) - \psi_H\left\{\frac{z-d}{L}\right\}\right]}{u\{z-d\}\, k^2} \qquad 2.48$$

The application of the different stability correctors is clear in this equation. In practice, however, given that u_* includes the ψ_M correction, the expansion of just the ψ_H corrected u_* of equation 2.47 is arithmetically simpler. Hence:

$$r_a\{z-d\} = \frac{\ln\left(\frac{z-d}{z_0}\right) - \psi_H\left\{\frac{z-d}{L}\right\}}{u_*\, k} \qquad 2.49$$

Garland (1977) has further rearranged this formula to provide the numerically equivalent expression:

$$r_a\{z-d\} = \frac{u\{z-d\}}{u_*^2} - \frac{\psi_H\left\{\frac{z-d}{L}\right\} - \psi_M\left\{\frac{z-d}{L}\right\}}{u_*\, k} \qquad 2.50$$

This may be used in all stabilities. The latter term on the right hand side represents the discrepancy between momentum and entrained property transfer which occurs in unstable conditions, and is consequently omitted in neutral and stable conditions.

2.4.3 Laminar boundary-layer resistance, r_b

The resistance to diffusion of entrained properties through the quasi-laminar layer of air immediately surrounding the roughness elements of a surface may also be considered in a form similar to equation 2.49. Notionally this is seen as occurring through the layer from z_0 to z_0' (Monteith, 1973). This gives:

$$r_b = \frac{\ln\left(\frac{z_0}{z_0'}\right) - \psi_H\left\{\frac{z_0}{L}\right\}}{u_*\, k} \qquad 2.51$$

The value of r_b, however, cannot be found directly from this, since z_0' is unknown. Hence another approach is needed.

A number of semi-empirical relationships have been developed to describe r_b, based on

an assumption of molecular diffusion to the roughness elements. Owen and Thomson (1963) proposed the estimation of a sub-layer Stanton number (B), which could be used to calculated r_b:

$$r_b = (Bu_*)^{-1} \qquad 2.52$$

Garland (1977) reviewed this study and those of Chamberlain (1966, 1968), and concluded that for exchange over fibrous surfaces, such as vegetation B^{-1} may be described by:

$$B^{-1} = 1.45\ Re_*^{0.24}\ Sc^{0.8} \qquad 2.53$$

Here Re_* is the turbulent Reynolds number given as $Re_* = z_0\ u_*/\nu$ and Sc is the Schmidt number given as $Sc = \nu/D$, where ν is the kinematic viscosity of air and D is the diffusion coefficient of the entrained property in air.

This estimation is useful for both heat and trace gases, however, since the transfer of particulate material also involves gravitational settling and impaction (see section 1.4.2), especially for large particles, equation 2.52 may not fully account for observed processes. For sub-micron particles both these processes are inefficient. In addition, Brownian diffusion is many times slower than the diffusion of gases. Hence r_b is large, resulting in the small deposition rates observed. Seinfeld (1986) gives a value of D of 7×10^{-10} to 3×10^{-11} m^2 s^{-1} for particles in the size range 0.1–1.0 μm diameter, which applies to most of the NH_4^+ aerosol. By comparison Hargreaves and Atkins (1987) have reviewed the literature on values of D_{NH_3} and use 2.09×10^{-5} m^2 s^{-1} at 10 °C. Values for D_H and ν are given by Monteith (1973).

It must be noted however, that this analysis is based on empirical estimation, and as such should be treated with some caution. Other formulations for the same purpose exist and include those given by Wesely and Hicks (1977) and Monteith and Unsworth (1990). These are considered further in sections 3.8 and 7.3, and Appendix 8.

2.4.4 Surface resistance, r_c, and component surface resistances

Once r_a and r_b are known, r_c may be estimated by difference from equation 2.46 and as such this is often referred to as the residual or excess resistance. r_c may be considered as the sum of several component resistances to uptake, such as to leaf surfaces, through the stomata of leaves, or uptake by the soil. It is sometimes possible to identify the importance these routes. For example measurements of deposition of SO_2 by Fowler and Unsworth (1979) showed reduced deposition in dry night-time conditions, which they attributed to stomatal closure, implying that the stomatal uptake was important. Similarly, in conditions of dewfall they found increased uptake (r_c diminished), suggesting that wet leaf surfaces would be an efficient sink of SO_2.

The different components of r_c may be related as parallel resistances:

$$r_c = (r_s^{-1} + r_p^{-1} + r_g^{-1})^{-1} \qquad 2.54$$

where the resistances are for: r_s = stomatal transfer; r_p = leaf surface reaction; r_g = soil transfer. Other paths may also be important. For example, Unsworth (1981) gives other resistances which account for: cuticle and epidermis transfer ($r_{cu} + r_{ep}$) and a resistance for mesophyll transfer in the substomatal cavity (r_i) in series with r_s.

In cases where stomata are implicated as the major route of uptake, such as in the example for SO_2 above, it is of interest to be able to estimate r_s. This may be found by identifying the stomatal resistance to water vapour transfer (r_{sE}). r_{sE} may be found where transpiration through stomata is known to be the only major source of evaporation, as in controlled environment studies. However in micrometeorological studies, other sources such as evaporation from wet surfaces may also be important. In this situation the net r_{sE} is referred to as the bulk stomatal resistance (r_{sEb}), since in dry conditions transpiring vegetation dominates the water vapour flux. r_{sEb} is accessible since water may be assumed to evaporate at the mean temperature of the surface, which is given by $T\{z_0'\}$(see following section), so that the saturated vapour concentration at the surface, $E_S T\{z_0'\}$, may be found. Given the predicted vapour concentration at the surface, $E\{z_0'\}$, may be calculated in a similar manner to $T\{z_0'\}$, r_{sEb} is given as:

$$r_{sEb} = \frac{E\{z_0'\} - E_S T\{z_0'\}}{E} \qquad 2.55$$

Over vegetation in dry conditions this may be used to estimate r_s for pollutant transfer. For many gases this needs a correction factor to account for the different molecular diffusivities (Monteith, 1973); given the similarity of D for NH_3 and H_2O (Table 1.1a) such corrections are minimal for NH_3. Another possible difference is that r_i is assumed to be negligible for water vapour transfer, whereas this may not be the case for pollutants. Little information is available for values of r_{iNH_3}, however, on the basis of unpublished data by Raven and Farquahar for leaf slices of *P.vulgaris*, Farquahar *et al.* (1983) conclude that this is also negligible in comparison to the other resistances.

2.4.5. Estimation of extrapolated values

In the analysis described above, the difference (or excess) between r_t and ($r_a + r_b$) is interpreted as another resistance, r_c (equation 2.46), by assuming zero concentration at the surface (equations 2.44–2.45). However, an alternative analysis may equally be made, where r_c is assumed to be zero, and the excess is represented as a surface concentration. In this case, given that only r_a and r_b are accounted for, the surface concentration is $\chi\{z_0'\}$ (*c.f.* equation 2.45 and Figure 2.3). By re-arrangement of

equation 2.45–2.46 and setting $r_c = 0$, this may be given as:

$$\chi\{z_o'\} = \chi\{z\text{-}d\} - [F_\chi (r_a\{z\text{-}d\} + r_b)] \qquad 2.56$$

Alternatively, in neutral conditions or where stability effects are accounted for by linearization of profiles (equations 2.34, 2.38), $\chi\{z_o'\}$ may be found by extrapolation of the concentration profile to z_o'. From equations 2.51 and 2.52, z_o' may be found as:

$$z_o' = z_o \, . \, e^{-(k/B + \psi_H\{z_o/L\})} \qquad 2.57$$

though in practice the stability effect at this this height is negligible and may be ignored (Thom, 1975; Chamberlain, 1968).

In cases of deposition it is impossible from the micrometeorological analysis alone to determine which of the two interpretations of the excess (r_c or $\chi\{z_o'\}$) is the more physiologically appropriate. However, the interpretation as r_c is only valid where deposition occurs, since in the case of emission, the surface concentration cannot be zero. Hence, where emission occurs only $\chi\{z_o'\}$ may be calculated, whereas for deposition either r_c or $\chi\{z_o'\}$ may be the more appropriate.

The interpretation using r_c is commonly used for describing pollutant transfer where deposition occurs. In cases such as that for SO_2, described in the previous section, the resistance interpretation appears appropriate due to the relationship of r_c with the component resistances such as r_s and r_p. As a result V_d is treated as being independent of concentration, which is convenient for modelling purposes.

In cases where r_c results from the existence of a concentration at the surface, V_d may still be calculated. However, this loses its usefulness since it is no longer independent of air concentration. For a fixed value of $\chi\{z_o'\}$ and an air concentration much larger than this, the value of r_c is small. Conversely, at progressively lower air concentrations the value of r_c becomes larger until surface and air concentrations are equal, at which point no net exchange occurs and r_c is infinite. Where air concentrations are less than the surface concentration, emission results, and it is clear that a surface concentration is controlling exchange rather than r_c. This interaction also acts in reverse, so that for a fixed value of r_c, much lower estimates of $\chi\{z_o'\}$ are predicted at lower air concentrations, and *vice versa*. These observations are useful in analysing field data collected over periods of different air concentrations and may help to identify whether r_c or $\chi\{z_o'\}$ is the factor limiting deposition.

Other cases are more straight forward. Where no surface resistance is expected, as for heat exchange with a vegetation canopy, the value of $T\{z_o'\}$ — calculated by an equivalent expression to equation 2.56 — may be taken as representing the mean temperature of the surface.

In some cases the use of either r_c or $\chi\{z_o'\}$ may, however, be a simplification of the exchange process, since it is possible that both resistance and concentration components contribute to the difference between r_t and $(r_a + r_b)$. For example, this is the case with the transpiration of water, which was considered in the previous section. Here exchange is predominantly through the stomata while the surface concentration in the sub-stomatal cavity is $E_s T\{z_o'\}$. In this case $E\{z_o'\}$ — again found from a similar expression to equation 2.56 — is not the concentration at the site of exchange but that predicted at the leaf surfaces, this being the junction of r_b and r_{sE} (*c.f.* Figure 2.3a). $E\{z_o'\}$ is nevertheless required in order to estimate r_{sEb} in equation 2.55.

The exchange of NH_3 with vegetation has also been suggested as an example where both surface resistances and concentrations are important (*e.g.* Farquahar *et al.*, 1980; section 1.4.3). As a result of studies on plants in enclosed chambers, these authors concluded that NH_3 is transferred through the stomata exchanging with the intercellular fluids of the sub-stomatal cavity, for which an equilibrium air concentration or 'compensation point' exists (denoted here χ_{cp}). They therefore considered studies assuming zero surface concentration to be in error. On the assumption that other routes of exchange are small in comparison to that through stomata, χ_{cp} may be estimated from micrometeorological measurements using $\chi\{z_o''\}$, where this is defined as:

$$\chi\{z_o''\} = \chi\{z\text{-}d\} - [F_\chi (r_a\{z\text{-}d\} + r_b + r_s)] \qquad 2.58$$

(See also Figure 2.3b.) Hence if r_s is found using equation 2.55 it is possible to estimate $\chi\{z_o''\}$ and consequently χ_{cp} by the above formula. Should it be possible to characterize χ_{cp} sufficiently well, this equation could therefore be used to predictively model the flux in a similar manner as that described in section 2.4.1.

A number of restrictions may, nevertheless, be applied to $\chi\{z_o''\}$. Where deposition to leaf surfaces is important (r_p small), then $\chi\{z_o''\}$ may represent an under-estimate the stomatal χ_{cp}. Conversely, soil χ_{cp} may also exist. In cases where emission from soil occurs, $\chi\{z_o''\}$ represents an over-estimate of a stomatal χ_{cp}.

In the absence of estimates of r_s, examination of $\chi\{z_o'\}$ remains useful. In cases of emission $\chi\{z_o'\}$ represents the minimum surface concentration possible, since further resistances to more remote sources increase the surface concentration estimates. By comparison, in cases of deposition $\chi\{z_o'\}$ represents the maximum surface concentration possible (Figure 2.3b). Hence, where deposition occurs at the maximum deposition velocity, such that $r_t = (r_a + r_b)$, then by definition both r_c and $\chi\{z_o'\}$ equal zero. In this case no net χ_{cp} of the surface is possible, and deposition may be modelled assuming V_d to be independent of concentration.

Chapter 3

Micrometeorological studies: methods and analysis

3.1. INTRODUCTION

The major part of this study is devoted to the estimation of ammonia exchange between vegetated surfaces and the atmosphere. The aerodynamic gradient method is used (Chapter 2) and requires the simultaneous measurement of profiles of windspeed, temperature and ammonia concentration above a uniform surface to estimate fluxes of ammonia. Background site information was also collected, while in some of the later studies this is supported by flux measurements of water vapour and other pollutants, in order to help interpret the ammonia exchange. The following sections consider the methods used in the collection and analysis of the data, and the restrictions and errors associated with the results.

3.2. FIELD SAMPLING

Measurements were generally made over sites with an upwind fetch of at least 200 m over an homogeneous surface to allow profile measurement within a fully developed constant flux layer of approximately 2 m (section 2.1). Profile measurements were made on separate masts, located close to one another (generally 3–5 m apart), orientated so that each mast had undisturbed access to the air flow. Masts were built from 25 mm diameter steel scaffold tubing and joints (Tubeclamps Ltd., Cradley Heath, West Midlands, U.K.), being 3 m high, held with guy lines from the top, and with side arms (0.6 m) of adjustable height, orientated to face into the wind (Figure 3.1). The profiles were measured using up to 5 ammonia samplers, and up to 6 anemometers, spaced exponentially with height away from the ground surface so as to measure at points evenly spread over the approximately logarithmic profile. A number of different systems and arrays of temperature measurement were used during the study (see section 3.5).

An exception to this system was for measurements over a forest area (Dunslair Heights, Peebles), where a fetch of at least 500 m was available allowing measurement up to approximately 5 m above the zero plane. In this experiment a 9 m scaffold tower was used to fix the sampler masts at the required heights. However, because important minimum measurement heights apply over very rough surfaces, such as forests — for example, one estimate suggesting a minimum of 10 z_0 above the zero plane (Raupach, 1979) — the minimum height was limited to 3 m above d at this

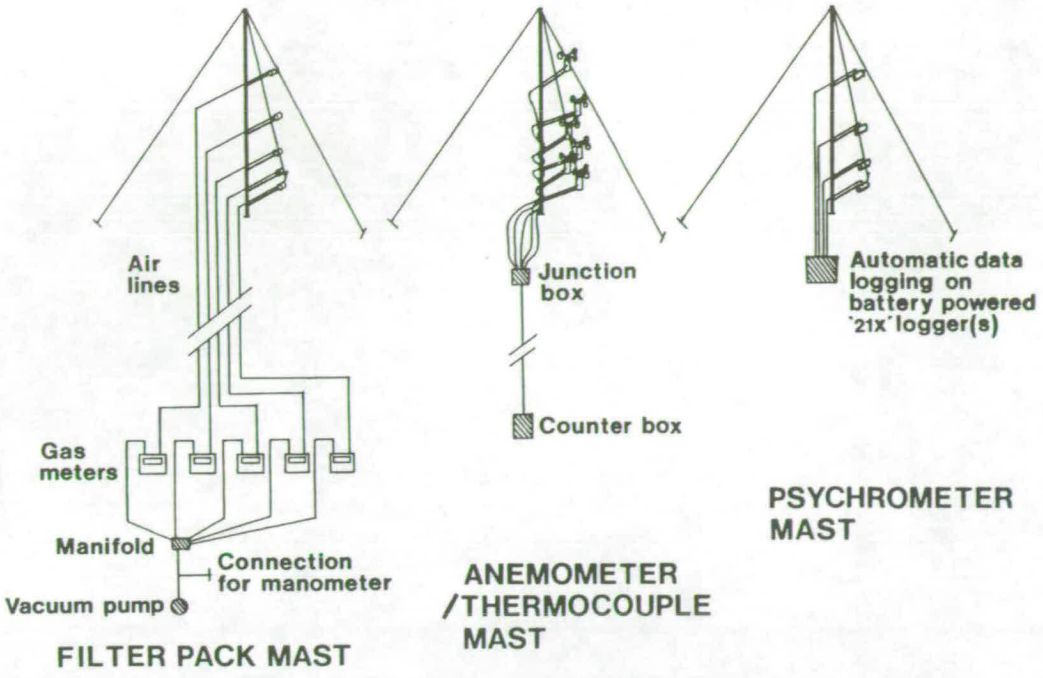

Figure 3.1 Schematic diagram of field sampling equipment. For further details see text.

site. Because of this limitation, the maximum concentration changes within the available measurement band over such sites are very small (see Appendix 8), so that in this situation the ammonia samplers were grouped at the two extreme available measurement heights to increase the ability to detect the gradient.

3.3. AMMONIA MEASUREMENT

3.3.1. Filter pack system

Concentrations of ammonia in this study were measured using a filter pack system similar to that described by Allen *et al.* (1988) and Harrison *et al.* (1989) with advice given by Harrison (1986, pers. comm.). The advantage of such a filter pack system over the main alternative of denuder tubes is that of greatly increased field convenience, although the method also enables a relatively good precision and low detection limits (section 1.2.4).

The principle is to separate the particulate NH_4^+, also present in the air, from the NH_3 by prefiltering the air with an inert filter, allowing NH_3 to pass through and be subsequently caught on an acidified filter (Figure 3.2). The prefilter may then be analysed for NH_4^+ or any other particulate species of interest. In the system used here the prefilter was an hydrophobic PTFE (Teflon) membrane filter on a polypropylene grid backing, with 1 μm pore size (Microfiltration Systems, Dublin, Calif., U.S.A.; U.K. distributors: CP Instrument Co. Ltd., Bishops Stortford, Herts.,). By sampling air using two prefilters in series it was shown that a single filter would fully capture the

NH_4^+ particulate as no NH_x was captured on the second filter. Since NH_3 was also recorded on the acid filter, this result also showed that the prefilter did not capture NH_3. The acidified filter used to capture the NH_3 was a Whatman 42 (high density) cellulose filter paper, impregnated with 75 g dm^{-3} ortho-phosphoric acid (H_3PO_4) solution in water (7.5 % w/v). Tests putting these filters in series showed the first filter to capture at least 95% of the NH_3 gas, so that in practice only one filter was needed for analysis. Prepared filters were clamped in place onto a PTFE support. In addition to the particulate and NH_3 supports, a third support, set between the other two, was also available in this design for inclusion of a nylon membrane filter (0.45 μm pore size, Sartorius Instruments Ltd., Belmont, Surrey, U.K.), which could be used to capture gaseous nitric and hydrochloric acids.

The filter packs were built in the Institute of Terrestrial Ecology workshop (Bush Estate, Edinburgh) and designed to hold 90 mm diameter filters, giving an open-face sampling diameter of 84 mm. This large size, as compared to the more usual 47 mm diameter filter packs was chosen so as to increase the possible sampling rate for a given face velocity, and hence increase sensitivity. Filter packs were sampled facing into the direction of air flow, at a sampling rate of approximately 0.17 $dm^3\ s^{-1}$ and within a range of 0.13–0.23 $dm^3\ s^{-1}$ (according to pump available). These low flow rates were used, so as to minimize the pressure drop over the prefilter which was approximately 1 kPa (8 mm Hg). This is important as it has been suggested that large pressure drops may disturb the equilibrium of captured NH_4NO_3 and NH_4Cl with the gaseous phase components and result in volatilization of some of the salts (see section 1.2.4). In addition, the low flow rates and short sampling duration (from 1 hour up to 12 hours) kept filter loadings low, so as to avoid this problem. The possibility of such filter interactions occurring in the measurements here is considered further in Chapter 4.

Rain shields were also constructed so as to fit over the open face of the sampler in showery conditions. These were constructed from polypropylene filter funnels and clamped on to the filter pack case by a circular groove cut in the latter (Figure 3.2). No measurable effect was detected of the cowl upon recorded concentrations of NH_3; for NH_4^+ a small loss of less than 5% was seen when the cowl was used. This is not considered a major problem, since when the cowls were in use, they were used on all the filter packs, and it is the concentration differences between filter packs which requires the greatest accuracy. However, more important losses exist when sampling aerosol/particulate within cloud or fogs where the rain shield is used. In this case the filter packs fail to catch most of the larger drops, which make up the bulk of the aerosol present in these conditions. Conversely, the cowl serves to protect the prefilter from getting wet with cloud water, so that its aim is fulfilled.

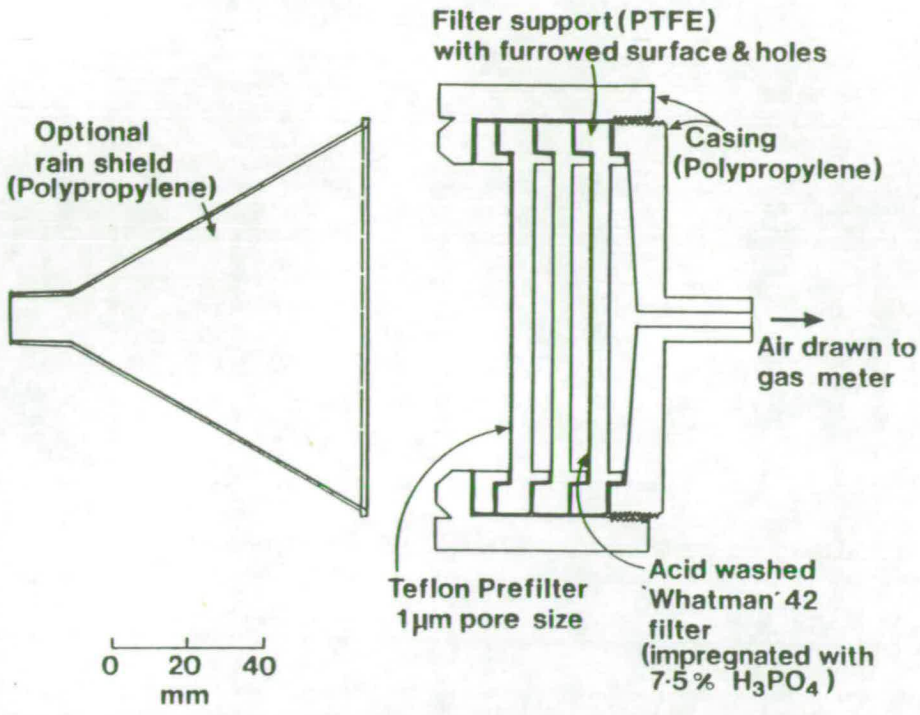

Figure 3.2 Cross-sectional view through a filter pack and rain shield.

For field sampling, the filter packs were set out on the mast and air drawn through them from a single vacuum pump (Edwards High Vacuum Ltd., Crawley, Sussex, U.K.) or 2 diaphragm pumps (Charles Austin Pumps Ltd., Weybridge, Surrey, U.K.) powered either by mains electricity or from a generator located downwind of the measurement point. A hose of 5 PVC tubing lines (12 mm internal diameter) 15 m long was used to connect samplers and gasmeters ('Remus' dry gas meter; distributors: Charles Austin Pumps Ltd.). The tubing lines down-stream of the gas meters were then joined with a manifold and connected to the vacuum pump (Figure 3.1). This system utilized the resistance of the filters to balance the flows, so that flow rates also acted as a check to ensure that the filter packs were not leaking, a feature to which they are commonly prone. However, the design also resulted in the gas meters being placed under negative pressure, giving an over-estimation of the volume of air passed. The pressure drop was therefore measured by means of a water filled U-tube manometer, and the values corrected. In addition each gas meter was calibrated against a bubble meter so that volumes would be accurate to within 1%.

Several causes of air leakage into filter packs were observed with the system used here, though measures could be taken to avoid this. Leakage through the screw thread and around the base of the bottom filter support stage was found to be a major problem. This could be stopped by winding PTFE thread sealing tape over these parts. Leakage also occurred where filters were not seated or clamped properly. In order to ensure the acid paper filters were clamped tightly, it was necessary to always insert two filters into

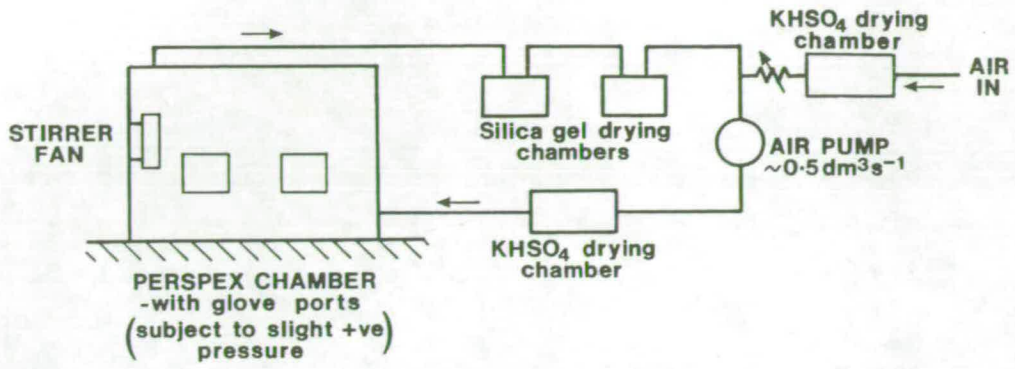

Figure 3.3. Schematic diagram of the clean air chamber system for drying filters.

this position of the stage support, although only the front filter was needed for concentration determinations. Improper seating of filters was the cause of occasional leaks, which could be detected by flow imbalances, and corrected by reseating the affected filters.

3.3.2. Cleaning of filters and equipment

Given the very low air concentrations encountered in the field (Table 1.6) it is important that blank (unexposed) filters have as low and as uniform NH_x contents as is possible. To do this requires pre-extraction of the filters before use.

Two different methods of extracting the Whatman 42 papers were used. In both procedures the filters were washed several times in de-ionized water and then several times in the 75 g dm^{-3} H_3PO_4 aqueous solution, which also served to impregnate the filters ready for use. Batches of up to 100 filters were prepared and then dried spread out on racks in a perspex glove box, from which NH_3 had been removed (Figure 3.3). This is important since laboratory air generally contains high levels of NH_3 (Chapter 6). Air was recycled through the glove box at approximately 0.5 dm^3 s^{-1}, being dried through silica gel towers and scrubbed of gaseous ammonia by a tower filled with potassium hydrogen sulphate granules ($KHSO_4$). A small fan in the chamber served to circulate the air during the drying period, which lasted approximately 8 to 10 hours.

The initial method used to pre-extract the filters was to wash them individually in a Buchner funnel, over a flask under negative pressure. Here 3 short rinses in de-ionized water were followed by 3 in the H_3PO_4 solution, with the whole apparatus placed inside the clean air chamber. However, this method proved to be very laborious and was replaced by washing up to 100 filters together in an ultrasonic bath. In this case three rinses in water, of at least 30 minutes were followed by 5 rinses in the H_3PO_4 solution. The whole batch was subsequently compressed to remove excess water and dried in the usual manner. Both methods gave blank filter NH_4^+ contents of

equally good quality, though values varied between batches (*e.g.* Stenton 6/1989: 0.27 ± 0.03 μg filter^{-1}, n=9; Wether Law 6/1989: 0.36 ± 0.05 μg filter^{-1}, n=14; Errors are sample standard deviations, σ_{n-1}).

Blanks of the PTFE filters were found to have relatively low and consistent NH_4^+ contents so that there was no need for pre-extraction before use. However, at a cost of approximately £6 per filter (U.K. 1987 prices) it was desirable that the filters could be re-used. This did not appear to be done by other authors, since these filters may lose their shape in storage or during extraction by becoming folded or curled up. In the method used here folding of the filters in storage was therefore avoided, and a procedure of rolling up the filters into the storage tubes was used. After analysis was completed it was found these could be carefully unrolled using forceps, and stacked flat in a dish of propan-2-ol, so as to keep the hydrophobic PTFE surface wet. These were then extracted in the ultrasonic bath for at least 6 rinses replacing the propan-2-ol with de-ionized water over the runs. These were finally dried in an oven at 80 °C, with the stack pressed flat, the high temperature serving to soften the filters. It was found that by then cooling the filters in this position they generally kept a reasonable shape. This procedure produced good blanks (*e.g.* 0.021 ± 0.017 μg filter^{-1}, n=10, errors = σ_{n-1}) although an approximate loss of 10–15% of the filters occurred in recycling by either being holed or torn at some stage. Nevertheless such filters were still useful for blanks.

To keep blank values low it is also important to have all equipment which comes into contact with the filters as clean as possible. Filter packs and storage tubes for the filters were therefore washed before use in dilute detergent solution (Decon 90), rinsed several times in de-ionized water and dried at 70–80 °C in a fan oven.

3.3.3 Exposure and storage of filters

The filters were loaded in the filter packs, using carefully cleaned spatula-ended microscope slide forceps, so as not to contaminate the filters or damage the PTFE membranes. The filter packs were then assembled and tightened as much as possible to prevent leaks. Following exposure the filters were removed and carefully rolled up using two sets of clean forceps and placed in the storage tubes. These were then capped ready for storage until analysis. Polypropylene centrifuge tubes of 18 ml capacity (Nalgene Labware, Rochester, N.Y., U.S.A.; U.K. distributors: Techmate Ltd., Milton Keynes) were chosen for the storage of filters since this plastic is inert and has a low diffusivity for gases. They were very satisfactory in protecting the filters and were convenient for laboratory manipulation, keeping storage volume to a minimum.

This manipulation of the filters was generally done in a well ventilated outdoor location, so as to avoid the contamination by deposition, that would occur in the high NH_3 concentrations of the laboratory. In practice, the tailgate of a pick-up vehicle was used as a work area, with manipulations being performed in a large open top box to avoid wind disturbance.

For the acidified Whatman 42 filters, sets of 5 blanks were taken every 3–4 runs by loading the filter packs and then directly unloading the filters and putting them into the storage tubes without sampling. Other Whatman 42 blanks were made by simply loading unexposed filters directly into the storage tubes, so as to check whether there was any contamination arising from contact with the filter packs. Blanks of the PTFE filters were made only on an occasional basis, (*e.g.* 5 or 10 per sampling campaign) because of their low and consistent values.

After preparation, batches of filters were stored in sealed glass or polymethylpentene petri dishes, kept inside an NH_3 clean environment. This was provided by placing the petri dish in a polythene grip-seal bag surrounded by an acid impregnated ($KHSO_4$) paper bag, itself placed in another grip-seal bag. In this way NH_3 diffusing through the outer polythene bag would be captured by the acid paper bag and the filters protected from recapture of NH_3 before sampling.

Working with trace levels of NH_3 is well known to be susceptible to contamination because of its presence in high levels on skin and in breath. In addition to the need for clean air chambers, the wearing of protective gloves is extremely desirable. In this study heavy duty rubber gloves were used, both in the laboratory and in fieldwork, and were regularly washed with de-ionized water. Similarly the forceps for filter handling were washed immediately before each use.

3.3.4 Analysis of filters

The NH_3 in the air is captured by the acidic paper filters by reaction to form ammonium phosphate salts. Hence the analysis of both prefilter and acid filters was for NH_4^+. This was done by extracting the filters in a defined volume of liquid, and then analyzing the solution. For NH_4^+ this is done by an 'indophenol blue' reaction, implemented on continuous flow analysis (CFA). Other ions, such as SO_4^{2-}, Cl^- and NO_3^-, which might be of interest, were analyzed for some runs using ion chromatography in the Chemistry Departments at the Bush and Merlewood stations of ITE.

Extraction of paper and nylon filters was initially done in de-ionized water, while the PTFE filters were extracted in 10% v/v propan-2-ol solution, following Allen *et al.* (1988). The latter extractant solution was used since the hydrophobic PTFE filters

need to be wet up, which may be done by adding a small quantity of propan-2-ol to a filter. Water was then added to dilute this down to 0.1 dm^3 dm^{-3} propan-2-ol in water (10 % v/v). In the analysis here, however, it was found that the sensitivity of the CFA was improved by using 10 % propan-2-ol, so that this was also used (premixed) as an extractant for the other filters. A total of 5 cm^3 of extractant was added to each tube, so that for the PTFE filters, 0.5 cm^3 of propan-2-ol was followed by 4.5 cm^3 of de-ionized water. Filters were then extracted on a wrist shaker for 20 minutes.

The NH_4^+ analysis was implemented on a Chemlab CFA system (Chemlab Inst. Ltd., Hornchurch, Essex, U.K.), utilizing the reaction between dichloroisocyanurate (DCICU) and salicylate, catalyzed by nitroprusside to form a blue indophenol die in the presence of NH_3. All the reagents used were present as the sodium salts, and the reaction carried out at a pH of 12-14, maintained by the presence of sodium hydroxide. In the reaction, the DCICU acts as a hypochlorite source, and the salicylate as a phenol source, which are both required for the reaction, however, by supplying these indirectly, the need to work with these somewhat toxic chemicals is avoided. The reaction mechanisms and different implementations have been extensively reviewed by (Searle, 1984), while the method used here approximately follows that of Bietz (1974). Advice on procedural matters was received from Thomas (1986, pers. comm.). A schematic representation of the CFA system and the composition of reagents are given in Appendix 9.

In the CFA, reagents and either wash or sample solution were passed continuously through the flow cell, where light absorption by the indophenol dye at 660 nm was measured by a spectrophotometer. The system was timed to alternatively draw up wash solution (70 seconds) and sample solution (50 seconds) giving an approximate turn-over time of 2 minutes per analysis when running. The additional NH_4^+ in the samples as compared to the wash, was detected by the spectrophotometer and relayed to a chart recorder to give concentration peaks, the height of which, within 2 orders of magnitude, was virtually linear in relation to concentration. Concentration was therefore calculated by linear regression of peak height *versus* known standard concentrations. However, because of the slight curvature of this response, different standard curves were used for each sensitivity scale used. For analysis of the filter pack filters the most frequent sets of standard used were: 0, 50, 100, 200, 500 μg NH_4^+ dm^{-3} wash solution and 0, 200, 500, 1000, 2000 μg dm^{-3}. Groups of standards were run approximately every 15 samples.

Standards were made up in 10 % propan-2-ol, although the effect of adding H_3PO_4 equivalent to that present in the acid filters was also tested. No change in sensitivity was observed, but a slight increase in all standard peak heights occurred irrespective of

concentration. This was most probably due to the NH_4^+ present in the acid. The acid was therefore not included in the solution.

Samples were supplied to the system by an automatic sampling carousel, taking up approximately 0.2 cm^3 of sample solution from 2 cm^3 polystyrene cups laid out on the carousel ready for sampling. However, because of the problem of deposition of NH_3 onto open samples in the laboratory, the whole carousel, as well as standards and samples ready for analysis, was placed in a clean air chamber. This consisted of an inflated heavy duty polythene bag with glove ports and a sealable entrance ('Atmos bag', Aldrich Chemical Co, Gillingham, Dorset, U.K.). Air was passed through a $KHSO_4$ granule tower, to remove NH_3, and supplied to the glove bag. The air was recycled through this system under slight positive pressure, with a small quantity of new air each time to replace leaks (*c.f.* figure 3.3, but without silica gel). Deposition to sample cups containing de-ionized water, in the open laboratory was found to be ≈8 pg NH_4^+ s^{-1}, which was reduced in the glove bag when well sealed, to ≈1 pg s^{-1}. In addition to this a maximum of up to 10 prepared samples or standards were set out on the carousel at any one time, so as to reduce total deposition. This gave a maximum exposure of 20 minutes, and an air concentration elevation equivalent to 2.3 ng NH_3 m^{-3} (given a 0.5 m^3 sample), which is acceptably small.

Sample cups were rinsed with de-ionized water in the glove bag immediately before use so as to minimize contamination. A sample was then filtered and transferred to each cup. This was done by drawing up the extracted sample from the storage tube, using a 2.5 cm^3 syringe fitted with a short length of narrow bore CFA pump tubing, and then passing it through a syringe tip filter assembly (13 mm diameter, 0.45 μm pore size polyvanilidenedifluoride membrane filter; Acro LC13, Gelman Sciences Ltd., Northampton, U.K.) into the sample cup. Two 0.5 cm^3 quantities of sample served to flush the system and further rinse the sample cups, while a third 1 cm^3 quantity was used as the sample for analysis. The syringe and filter were subsequently flushed with approximately 2 cm^3 of de-ionized water before the next sample. The sampling was started at least 1 hour after starting the system running with the reagents and wash solution, to allow time for it to settle. Once started each sample would take 25 minutes to reach the flow cell and be recorded.

A number of problems occasionally occurred with the CFA system. The most usual was a trapped or blocked tube. (The latter was most usual in the analysis of diffusion tubes where samples were not filtered, Chapter 6.) In addition 'surging' of the reaction mixture sometimes occurred through the flow cell, resulting in a poor base line. This could be usually avoided by keeping the debubbler waste line outlet above the level of

the flow cell. When the system was running evenly, with a good base line the aqueous sample detection limit was approximately 2–5 mg NH_4^+ m^{-3}.

3.3.5 Calculation of air concentrations

Given that filters were extracted in 5 cm^3 of liquid, and accounting for the NH_x in blank filters and the volume of air sampled, then the air concentration of NH_3 in $\mu g\ m^{-3}$ is given as:

$$\chi_{NH3} = \frac{0.005\ ([NH_4^+{}_{sample}] - [NH_4^+{}_{blank}])}{V} \frac{M_{NH3}}{M_{NH4^+}}$$

where aqueous concentrations are in $\mu g\ dm^{-3}$, V is the volume of air sampled (m^3), and M is molecular weight. The ratio of M_{NH3}/M_{NH4^+} is omitted when calculating χ_{NH4^+}.

The sampling precision was assessed on a number of occasions by 'co-sampling' all five filter packs at one height (at least 1.5 m) above the ground. This procedure gives an overall precision of the method including the effect of all constituent errors in measurement. The precision varied between campaigns, however, typical precision for both NH_3 and NH_4^+ was 5% (Coefficient of variation: $100\sigma_{n-1}$/mean, n=5) at $\approx$1 $\mu g\ m^{-3}$, for samples of $\approx$1 m^3 of air. The minimum significant concentrations may also be calculated for single filter pack samples. Assuming a flow rate of 0.2 $dm^3\ s^{-1}$, and given that a filter value is significantly different (95% confidence) from the set of blanks where its concentration is greater by typically 0.05–0.1 $\mu g\ filter^{-1}$ (section 3.3.2), gives a sensitivity of $\approx$0.07–0.13 $\mu g\ NH_3\ m^{-3}$ hour. For NH_4^+ this is $\approx$0.05–0.12 $\mu g\ m^{-3}$ hour.

3.4. WINDSPEED MEASUREMENT

Windspeed profiles were measured with sensitive cup anemometers (Vector Instruments Ltd. Rhyl, Clwyd, U.K.), which were attached vertically onto the side arms of a mast. The anemometers were supplied as a set complete with a 6 anemometer junction box, and a 30 m cable to connect to a battery powered counter box. Pulse output anemometers were used, with one count being recorded per rotation. During ammonia sampling anemometer counts were recorded at the start and end of each run, and the precise start and stop times noted. From this anemometer counts per minute were calculated.

To be able to convert counts per minute into windspeed, the anemometers were calibrated, against a Pitot tube in a windtunnel (in the Department of Forestry and Natural Resources, University of Edinburgh). Windspeeds between 0.1 and 10 $m\ s^{-1}$ as well as calm conditions, were used and this related to the anemometer output in

counts per minute. The Pitot tube measures windspeed by the difference between ambient pressure and the forward pressure due to the windspeed. To do this the pressure difference was measured by a precision micro-manometer. From this, windspeed was calculated according to the following formula:

$$u = \sqrt{2\,\Delta P/\rho} \qquad 3.1$$

where u is windspeed (m s^{-1}), ΔP is pressure difference (Pa), and ρ is air density (kg m^{-3}). Air pressure and temperature were recorded at the time of calibration in order to calculate ρ. The anemometers were found to be very sensitive, responding to very low windspeeds. The stalling speed was found to be $\approx$0.2 ms^{-1}, while the starting speed was $\approx$0.4 m s^{-1}.

3.5. TEMPERATURE AND HUMIDITY MEASUREMENT

A number of systems were used to measure temperature profiles. For the first part of the study (1987–88) fine thermocouples (type 'T') were used, with a self referencing system in a CR21X data logger (Campbell Scientific Ltd., Sutton Bonnington, Loughborough, U.K.). The logger was set up to record temperature measurements every 5 seconds, and to use these to calculate 10 minute means which were then logged. Once this was set up in the field it could be left sampling until the end of each campaign. Temperature profiles for given ammonia sampling runs were then calculated by taking means of the appropriate group of 10 minute runs.

During 1989 a number of campaigns were made using a system of ventilated psychrometers, so as to provide both temperature and humidity profiles. Four psychrometers were used, with data being recorded by two 21X loggers, the system being designed and built by J.B.Moncrieff (Department of Forestry and Natural Resources, University of Edinburgh). Dry bulb temperature was measured by a platinum resistance thermometer, and the difference between the dry and wet bulb temperature by two differential thermocouples. Air was drawn over the sensors by means of a small battery powered fan in each psychrometer, so as to fully aspirate the sensors. This system was again logged as 10 minute runs in the same manner as before. The sensors were calibrated in an ice bath at 0 °C and in a thermostated water bath at 25 °C.

The third system available during one campaign in 1989 was a thermocouple and cooled mirror dew-point system, with two height levels, for precise temperature and humidity measurement. This was part of a Bowen ratio system (Campbell Scientific Ltd.) for measuring fluxes, in use at the site during this period, although in this study the measurements were used as inputs to the aerodynamic gradient method.

Temperature values for each of the systems were generally precise to ≈0.05 °C, while humidity was generally precise to ≈0.05 g m^{-3} absolute humidity (or ≈0.1 °C dew point temperature).

3.6. ANALYSIS OF GRADIENT RESULTS

The profile results were used to derive fluxes according to the aerodynamic gradient method described in Chapter 2. The approximate log-linear form of the Richardson number (equation 2.29) was used to quantify stability, from which the Monin-Obukhov length was found according to equations 2.24b and 2.25b. These were then used in the full treatment of the log-linear approach (section 2.3.4.), and linear regressions calculated of windspeed and concentration *versus* stability corrected logarithm of height (equations 2.33–34, 2.37–38) so as to be able to estimate u_* and χ_* and hence find the flux (equation 2.17). Resistance analysis and estimation of extrapolated values was then performed on the results as described in section 2.4.

These calculations were implemented in a Pascal computer program so that given an estimate of d (section 2.3.5), and profiles of wind, temperature, concentration and in some cases absolute humidity, the analyses above could be made. The program also included estimates of random error, due to scatter in the regressions (section 3.8.3).

3.7. OTHER SUPPORTING INFORMATION

In addition to the micrometeorological flux estimation, other background information was collected. Plant community type and dominant species were recorded, as well as information on the site management. At most sites soil pH (in water) was also measured. Weather conditions during runs were also noted, including cloud cover, wind direction, precipitation and the presence of dew. Special attention was paid to the dryness and stage of development of the plant canopy.

In the absence of micrometeorological measurement of water vapour fluxes, at one site (Bush, 6/1988), measurements of leaf area r_{sE} were made by means of a portable 'Parkinson' leaf chamber and water vapour analyzer (ADC Ltd., Hoddesdon, Herts, U.K.). Samples of 10 plants were measured every 1–2 hours for several periods, and mean r_{sE} calculated according to equation 2.55, but assuming chamber conditions apply at the leaf surface (*i.e.* z_0'). A similar procedure with an automatic porometer (Delta-T devices Ltd., Cambridge, U.K.) to estimate r_{sE} was also used during one campaign (Stenton 6/1989), to supplement other measurements. Leaf area index, was estimated at both sites by harvesting a small known ground area of the vegetation (≈0.3 m^2) and measuring the leaf area using a Li Cor leaf area meter (Lambda Instr. Corp., Lincoln, Nebraska U.S.A.). This was then used to estimate r_{sE} for ground area.

3.8. RESTRICTIONS AND ANALYSIS OF ERRORS

3.8.1 Micrometeorological restrictions

In addition to the fetch requirements, the development of the constant flux layer requires that conditions do not vary significantly during a run. As a result run duration is effectively restricted to a few hours, since environmental changes occur where much longer periods are used. Similarly the trace gas concentrations should remain constant during a run, although in practice variations occur. Garland (1977) considered the errors arising from this source and provided an approximate relationship for a typical upper limit in the error in the deposition velocity, ΔV_d:

$$\Delta V_d < \frac{\Delta\chi}{\chi\{z_1-d\}} \frac{(z_1-d)}{\Delta t} \qquad 3.2$$

where z_1 = mid height of measurement, $\Delta\chi$ = net change in concentration over a sample run of duration Δt. Hence taking an example of (z_1-d) = 1 m, Δt = 2 hours, and a typical upper value of $\Delta\chi/\chi\{z_1-d\} = 1$, gives $\Delta V_d < 0.1$ mm s^{-1}. Since this is small compared to expected V_d of NH_3 (section 1.4.3) it is clear that this is not normally an important source of error. However, the size of ΔV_d increases with measurement height, so that it may be important for measurements over forests.

Another requirement for the development of the constant flux layer is that the fluxes are conserved — that is, that there is no production or loss of the trace components in the atmosphere as they exchange with the ground. The possibility that fluxes of NH_3 are not conserved arises because of its equilibrium with HNO_3 and HCl to form NH_4NO_3 and NH_4Cl respectively (Huebert *et al.*, 1988; Brost *et al.*,1988; Harrison *et al.*, 1989). Deposition or emission of these components, shifts the position of the dissociation, so that reaction occurs to restore the equilibrium. For example, where NH_3 and HNO_3 are both depositing, and NH_4NO_3 is depositing only very slowly, the depletion of the gases may result in a dissociation of the salt, with the apparent results of a greater NH_4NO_3 gradient, and reduced gaseous gradients and fluxes. The question, then, is whether the restoration of equilibrium is sufficiently rapid to be important during the time scale of deposition in the measured first few meters.

Estimates of the lifetime of the dissociation have been reviewed by Harrison *et al.* (1989), who gives values ranging between 100 s to many minutes, while Brost *et al.* (1988) considered that values of less than 100 s may give appreciable effects on the measured gradients. However, in a study of the gradients and concentration products of these species over a number of surfaces, Harrison *et al.* (1989) were unable to detect any deviation from normal surface exchange patterns, therefore favouring a slower

value of the dissociation lifetime. In agreement with this, Heubert and Robert (1985) and Huebert *et al.* (1988) also found negligible effect over a grass surface. However, in the presence of very large quantities of ammonia (near a strong ammonia source), the reactions became important. In this study therefore, where background exchange is measured, this process is considered not to be important in the gradients measured (see also section 4.3–4.4), although the possibility should not be ignored for situations of severe displacement of the equilibrium.

The filter pack measurements made in this study record component density *in situ*. In this case another restriction applies. Webb *et al.* (1980) have shown that gradients of temperature and water vapour over a surface can modify the apparent flux, with the effect of temperature being most important. (The effect of water vapour is usually less than 10% of the temperature effect.) The effects of these gradients, and the need for a correction, may be avoided by pre-drying samples and bringing them to a common temperature. However, this is not possible for ammonia since the gas is removed in drying, while heating may disturb the gas/particle equilibria. Hence the need for a correction must be considered.

Webb *et al.* provide corrections for these errors, given temperature and water vapour flux estimates. The importance of the corrections depends on the relative size of the flux to the trace component concentration. Thus for gases with large exchange rates and low concentrations (in the case of deposition, large V_d), such as NH_3 the corrections are small, and may generally be ignored (Denmead, 1983). In comparison, Denmead also gives typical corrections and fluxes for other nitrogenous gases. For some, like N_2O, where high concentrations and small fluxes often occur, corrections may be several orders of magnitude larger than the uncorrected flux, making this a major restriction on the application of micrometeorological methods. (The corrections may also be significant for individual runs of particulate deposition, however, in the limited analysis of mean values given here, this largely averages out.)

3.8.2. Sources of systematic error

In addition to the restrictions noted above, a number of other possibilities for systematic error exist in the analysis. This is the case for the semi-empirical stability corrections and the estimation of r_b.

The corrections for non-neutrality used in this study (section 2.3.3) are well supported in the literature, comparing well with the energy balance method in comparisons of several different correction estimates (*e.g.* Paulson, 1970; Denmead, 1983). Nevertheless, there is undoubtedly potential for error, which increases in more extreme non-neutrality. It is difficult to assess this error strictly where the aerodynamic method

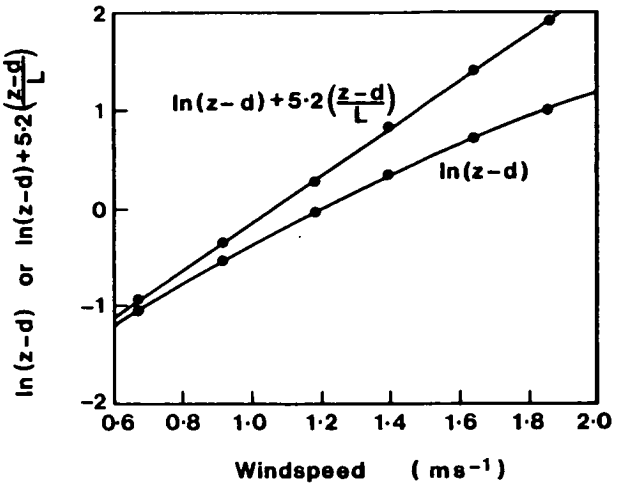

Figure 3.4. Application of the integrated stability correction to a wind profile measured in stable conditions. The good profile linearity achieved by using the correction factor $5.2(z\text{-}d)/L$, suggests reasonable confidence in the correction. The data is for run 5, Stenton 6/1989.

is used alone, however, by using the integrated stability correction approach (section 2.3.4), the correction may be checked by assessing the improvement on profile linearity. An example of this is given in Figure 3.4 for a wind profile measured in conditions of moderately strong stability. The improvement in linearity is very good, suggesting a reasonable confidence in the correction factors.

The error in r_b is more difficult to assess. This could be checked in the field by measuring resistances to water vapour loss over a freely evaporating wet crop surface, assuming $r_s = 0$ and $E\{z_0'\} = E_s\{T\{z_0'\}\}$, as described by Thom (1972, 1975). However, in the absence of this approach, some idea of the expected error may at least be found by comparing the results of different formulations for r_b. This is done in Figure 3.5, where the estimation of Garland (1977), used in this study, is compared with two alternatives — that of Wesely and Hicks (1977) and of Monteith and Unsworth (1990; derived from Thom, 1972) for different values of u_*. The size of r_a for different conditions is also given for comparison. The Garland estimate, has some dependence on z_0, so several curves are given.

It can be seen that, for all but the smallest values of u_*, the difference between estimates of r_b is mostly $\approx$10 s m^{-1} or less. This is quite acceptable given that the main purpose of the resistance analysis is to see if a significant r_c exists and the range of possible r_c is much larger than this. For example, where surface uptake is efficient $r_c \approx 0$, whereas for uptake controlled by stomata, $r_c \approx$ 50–1000 s m^{-1} (Wallace *et al.*, 1981). Hence these differences in r_b are small. In calm conditions greater differences in r_b occur. This combines with an increased random error due to larger values of both r_a and r_b, as well as the possibility of anemometer stalling, so that results in

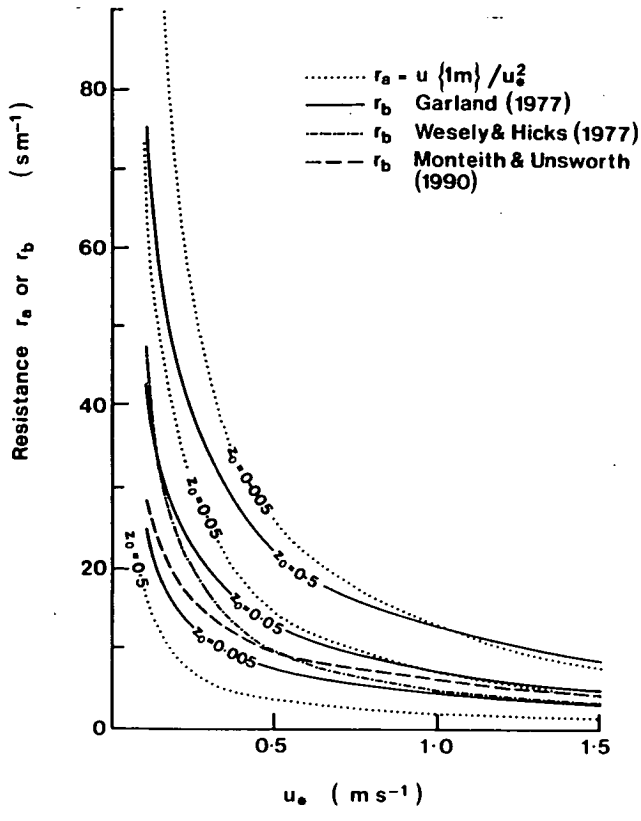

Figure 3.5 Comparison of different semi-empirical estimations of r_b with changing $u*$. Values of r_a (neutral conditions) are also given. The different formulations of r_b are: Garland (1977), $1.45/u* Re*^{0.24} Sc^{0.8}$; Wesely and Hicks (1977), $(2/u*k)(\kappa/D)^{0.67}$; and Monteith and Unsworth (1990), for properties with similar D, to water vapour, after Thom (1972), $6.2\ u*^{-0.67}$.

such conditions should be treated with caution. Conversely, in windy conditions, small r_a and r_b result in a more precise estimation of r_c.

Greater differences in r_b also occur over very rough surfaces such as forests, although Garland (1977) limited the use of his formulation to short vegetation.* Nevertheless, results over forests are approximate anyway because of a number of other constraints on the method. The limitation on the estimation of d in these conditions has been noted in section 2.3.5. In addition to this, the constraints of minimum measurement height above which gradients accurately reflect the flux (Thom *et al.*, 1975; Raupach, 1979), and of maximum height permitted by the fetch, allow little gradient detection (Appendix 8) resulting in a large random error attaching to the flux estimate.

---

* Garratt and Hicks (1973) analyzed the results of both wind tunnel and atmospheric studies of B^{-1} for a wide range of surface roughness (from water surfaces to forests) as a function of Re*. They concluded that the dependence of B^{-1} on z_0 found for surfaces with bluff elements in windtunnel studies (Chamberlain, 1966, 1968) is not applicable for fibrous vegetated surfaces, where individual elements retain similar dimensions with increasing canopy roughness. The formulation of Garland (1977), based on the results of Chamberlain, diverges from the atmospheric results reviewed by Garratt and Hicks at approximately Re* > 2000, beyond which the approximation used by Wesely and Hicks (1977) gives improved estimates. This is the case for forests, where typically Re* > 5000.

3.8.3 Sources of random error

Sources of random error in the results arise from the sampling variability of sensors. Since for most profiles readings were taken at several levels, the random error may be assessed by looking at the scatter of the regressions. Standard errors or confidence limits for the regression parameters may be estimated, and these combined for the different regressions to estimate the error in combined quantities such as F_χ, V_d, r_c and $\chi\{z_o'\}$. A full analysis of this type is given in Appendix 5. It is clear from this that in all cases the error is dominated by the scatter in the trace component concentration profile; in comparison, the random error from the wind profile and stability correction is generally very small. The treatment of the errors may therefore be simplified by ignoring errors due to these sources. (However, because of simplicity the error from the wind profile is included in the error of F_χ and V_d, Appendix 5, equation A5.2). In the flux gradient data presented in Appendices 2–4, 95% confidence limits (which are necessarily approximate because of the small samples) are given for F_χ, V_d, r_c, and $\chi\{z_o'\}$. For the trace component concentration data, where more than one sample analysis in a profile failed, the results are treated with caution and noted with an asterisk. It may be noted that the high degree of scatter for many of the individual runs results in the gradients not being significantly different from zero. This is a perennial problem in trace flux measurement. However, given the consistency of values over series of runs, and the significance of many of these, it is clear the gradients are real.

Chapter 4

Surface exchange results: Natural and unfertilized ecosystems

4.1. INTRODUCTION

Measurements of ammonia exchange between the atmosphere and vegetation were made over a wide variety of surfaces in order to identify the patterns and variability of exchange with surface type. The measurements were made on a campaign basis, sampling intensively over periods of one to several days, to see the effect of diurnal and other environmental changes, with the field campaigns being carried out at different times of year, to observe any seasonal effects.

Sites are divided in this report into two categories: 'natural' and unfertilized ecosystems, and fertilized agricultural ecosystems *. The results of measurements over the natural and unfertilized surfaces are described in this chapter, while those over fertilized agricultural surfaces given in Chapter 5. In each of the chapters, an overview of the sites and results is presented along with a detailed examination of measurement results of particular interest. The full data set of individual flux measurements for the two surface categories is given in Appendices 2 to 4.

4.2. STUDY SITES: NATURAL AND UNFERTILIZED SURFACES

All measurements were made in the United Kingdom, and included studies over grasslands, moorlands and a forest site. Information on the name, location and description of each site is given in Table 4.1. This is supported by Table 4.2, where dates and site information relevant to the different campaigns are described.

The sites were chosen to represent background exchange patterns away from specific sources. Given that livestock are considered the major source of ammonia (section 1.3), none of the sites used were located near to major livestock installations. However, at each of the sites, except for Dunslair Heights, grazing animals are present in low density on an occasional basis. At the moorland sites hill sheep have free access, but generally keep to better ground; the grassland at Huntingdon is

* The term natural is used in a general sense to refer to communities which have developed by natural succession of species, while accepting the importance of low level management practices in the development of that system (*e.g.* hay cutting, burning), but not including sites with fertilization or heavy grazing. Other unfertilized ecosystems are distinguished from this by having a planted or seeded vegetation (*e.g.* plantation forest).

site name used in study	site location	National grid ref.	height AMSL (m)	fetch (m)	soil type and pH (in H_2O)	Vegetation community (dominant species underlined)
MOORLAND						
Great Dun Fell *	N. Pennines, Cumbria	NY705 312	680	>250	peat pH 3.92	Eriophorum vaginatum, *Juncus squarrosus, Nardus stricta*
Fala Moor	M. Lothian, Scotland	NT423 580	330	>250	peat pH 3.95	E. vaginatum, Calluna vulgaris, *Deschampsia flexuosa, Sphagnum* spp. *N. stricta*
Wether Law	E. Lothian Scotland	NT651 609	410	>500	peat (no pH)	Calluna vulgaris, *D. flexuosa*
GRASSLAND						
Huntingdon †	Cambridge-shire, England	TL203 723	15	≈200	neutral-calcareous alluvial (no pH)	unimproved species rich grassland *e.g. Dactylus glomerata, Holcus lanatus, Briza media, Sanguisorba officinalis, Filipendula vulgaris, Centaurea nigra, Orchis morio*
Harwell	Oxfordshire, England	SV468 861	130	130–150	calcareous (chalk) pH 8.43	*e.g.* Agrostis spp., Poa spp., *Ranunculus* spp. *Taraxicum* spp., *Trifolium repens*
FOREST						
Dunslair Heights	Peebles, Borders, Scotland	NT288 435	590	≈500	mineral soil	Picea sitchensis, *Larix decidua, Pinus contorta, Abies procera*

Table 4.1. Sites used for flux measurement studies. * located in Moorhouse National Nature Reserve (NNR); † located in Brampton Race Course Site of Special Scientific Interest (SSSI); AMSL = above mean sea level.

site name	season	sampling dates	canopy height (m)	d * (m)	mean z_0† (mm)	air temp-eratures (°C)	State of canopy/soil during measurements
MOORLAND							
Great Dun Fell	Summer	27/5/87	0.05–0.10	0.05	14	13	AG, canopy dry, soil damp
	Spring	29–30/3/88		0.03	8	-0–4	PG, mostly wet
	"	21/4/88	"	0.03	12	9	PG, canopy dry, soil wet
	"	25/4/89	n/a	0.14	1	-1–2.5	under snow
Fala Moor	Autumn	5–6/11/87	≈0.25	0.15	28	2–8	PG, wet and dry
	Summer	24–25/5/88	20	0.05	31	5–13	AG, *E. vaginatum* flowering wet and dry
Wether Law	Winter	21–23/2/89	0.24–0.30	0.23	27	-2–3	PG, damp, snow or frozen
GRASSLAND							
Huntingdon	Summer	11–13/8/87	0.15–0.20	0.12	17	15–20	AG, cut for hay in June, wet and dry
Harwell	Spring	15–18/3/88	≈0.04	0.03	4	4–10	PG, recently harrowed, soil on leaf surfaces, wet and dry
FOREST							
Dunslair Heights	Autumn	12–17/11/88	≈4.3	3.2	200	4–7	PG, wet and dry

Table 4.1. Dates of campaigns and conditions during measurement periods. * In cases were d is small its value will also depend on the choice of ground reference position used to measure heights. A value of d also arises over snow since heights were measured from soil level. † Calculated from the mean of $\ln(z_0)$ since z_0 is not normally distributed. AG = actively growing vegetation; PG = vegetation senescent or dormant from previous season.

occasionally used for the grazing of horses, while at Harwell, although no livestock are given access, a large population of rabbits is present.

The other main criteria for choice of site were vehicular accessibility, often provided by a farm track, and a surface providing an adequate fetch over uniform terrain. In the latter respect the Great Dun Fell and Dunslair Heights sites provided extensive fetches over uniform vegetation, but were not ideal according to usual micrometeorological criteria because of an undulating land surface at each. However, as Gallagher *et al.* (1988) and Fowler and Duyzer (1989) discuss, these sites can nevertheless provide suitable conditions for flux measurement, demonstrated by the existence of good logarithmic wind profiles.

4.3. PROFILE RESULTS AND INTERPRETATION

Examples of measured wind, temperature and ammonia profiles are given for two example runs, from Great Dun Fell and Fala Moor, in Figures 4.1 and 4.2. In addition the longer term NH_4^+ particulate profiles (recorded over several NH_3 sampling runs) are shown. Profiles of concentration are the most approximate and therefore dominate the sources of error.

On the assumption that the exchange process of NH_3 and NH_4^+ is chemically conserved (section 3.8.1), the decrease in NH_3 concentration towards the ground implies deposition to be occurring. The small concentration gradients of NH_4^+ are typical and suggest a greatly reduced rate of exchange for this species.

The possibility that the fluxes are not conserved, however, also needs to be considered. The most likely cause is perturbation of the gas/particle equilibria in the NH_4^+, NO_3^- and Cl^- system in the air near the ground. In the case here, over natural surfaces, where NH_3 appears to be depositing, and given that the acid gases, HNO_3 and HCl, are expected to be depositing (*e.g.* Huebert and Robert, 1985; Dollard *et al.*, 1987), a reduced gaseous concentration product near the surface might be expected to shift the gas/particle equilibrium and result in particulate evaporation. This would give greater apparent deposition gradients of NH_4^+, and reduced gradients of NH_3. These changes and those for the NH_3 emission situation are shown graphically in Figure 4.3.

Since it is well established that the sub-micron aerosols that make up the NH_4^+, deposit only very slowly (section 1.4.2.), the rates of exchange of NH_4^+ may be used as a check to see if this process is occurring. This is considered in the next section.

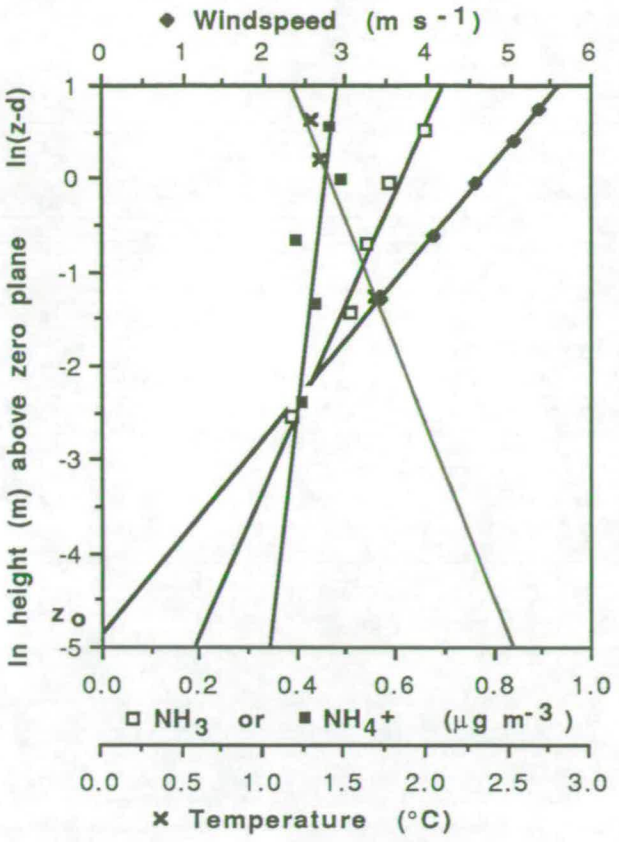

Figure 4.1 Example profiles at Great Dun Fell (Run 3, 3/1988).

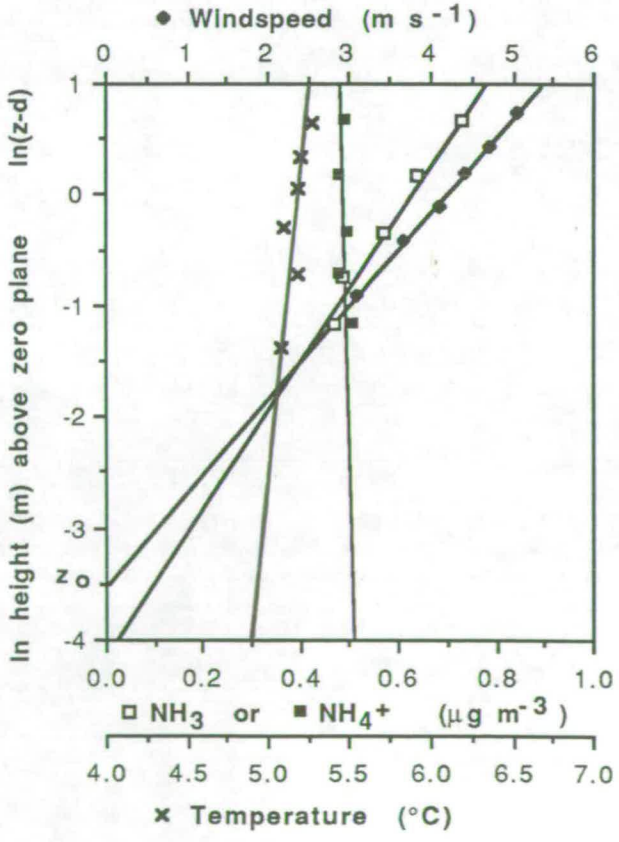

Figure 4.2 Example profiles at Fala Moor (Run 3, 5/1988).

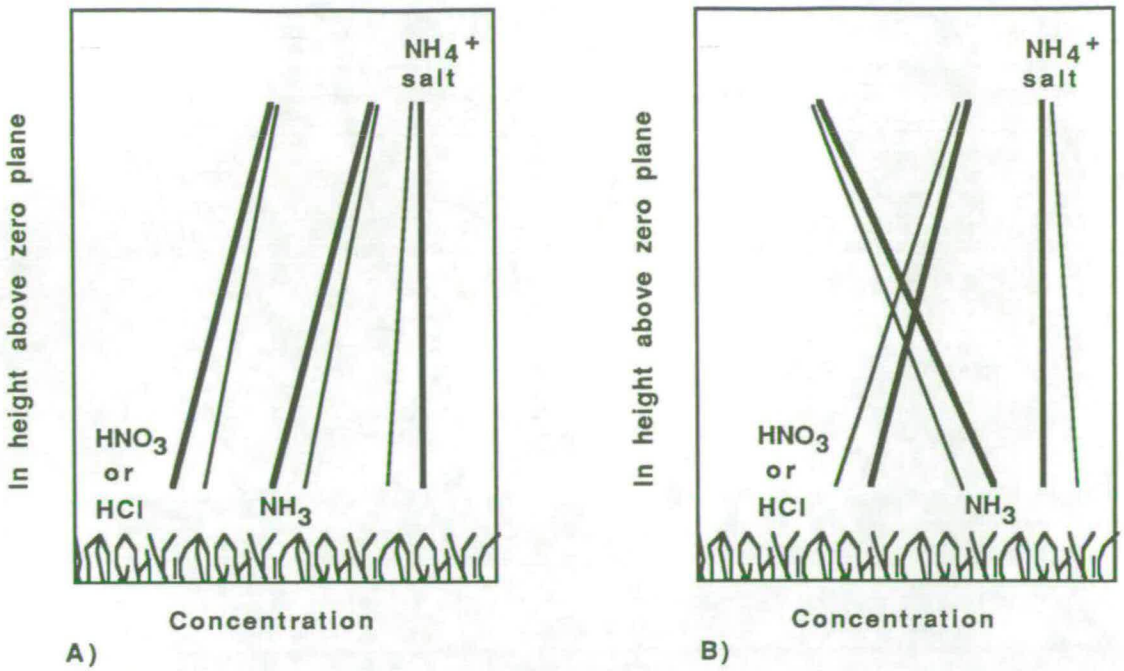

Figure 4.3. Possible effects of gas-particle conversion on observed gradients of NH_3 and NH_4^+ over an extensive homogeneous surface. Bold lines represent profiles where fluxes are conserved. Light lines show profile modification where fluxes are not conserved. A) NH_3 deposition, B) NH_3 emission from the ground surface. For both cases it is assumed that surface exchange of NH_4^+ is negligible in comparison to the gas exchange.

4.4. Surface exchange of NH_4^+

Given the long run periods of much of the NH_4^+ sampling, often encompassing several NH_3 sampling runs, the measurements are not strictly suitable for flux calculation, since environmental conditions and concentrations may vary during sampling. However, since the scatter of the individual NH_4^+ profiles is greater than the variation expected due to environmental changes, a limited flux analysis of general trends may be made.

The full data set of calculated NH_4^+ fluxes is given in Appendix 4. Results of the NH_4^+ exchange for both unfertilized and fertilized ecosystems are shown in a frequency distribution of $V_d\{1\ m\}$ in Figure 4.4. The arithmetic mean of these values is a deposition of 1.9 ± 2.5 mm s^{-1} (95% confidence limits of mean). The mean value of r_a/r_t is 0.05, showing that the main restriction to deposition relates to transfer at the surface (r_b or r_c), which is consistent with the literature on sub-micron particle deposition (section 1.4.2). A small number of measurements of major anion fluxes were also made. Histograms of these are given in Appendix 4. The arithmetic mean values of $V_d\{1\ m\}$ were Cl^-: 9.1 ± 9.7; NO_3^-: 3.7 ± 5.4; SO_4^{2-}: -0.1 ± 5.6 mm s^{-1} (95% confidence limits).

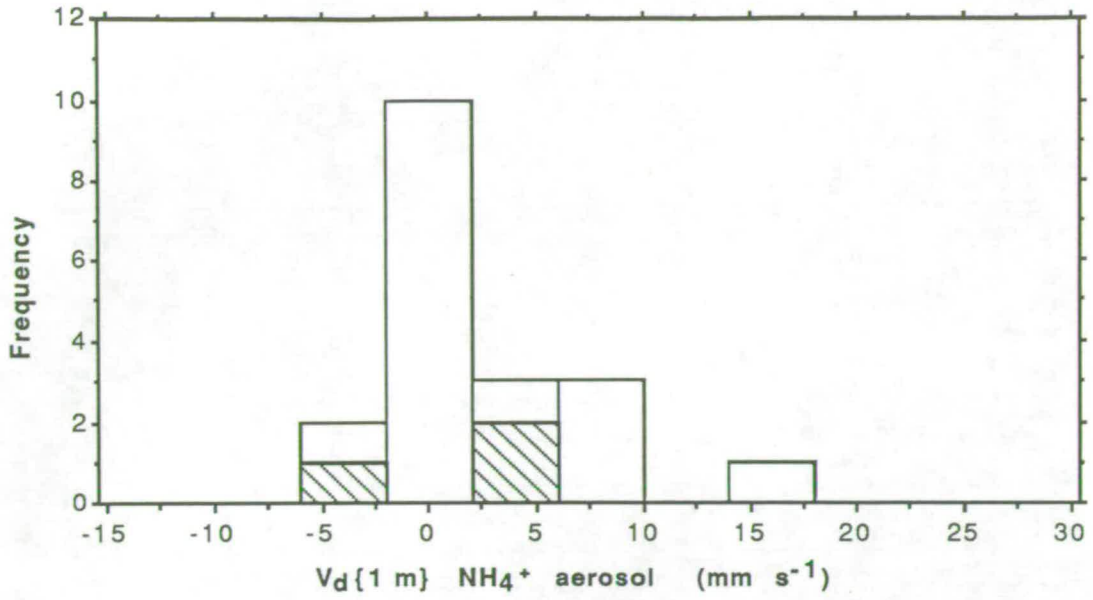

Figure 4.4. Frequency distribution of measured deposition velocities of ammonium aerosol. The hatched component represents values over intensive agricultural sites where NH_3 emission was recorded. All other values are where NH_3 deposition was recorded. Forest results are not included.

Some question exists as to the use of arithmetic means for derived quantities such as deposition velocities. An alternative is to calculate the arithmetic means of the flux and χ and divide these to give a mean V_d (Fowler, 1976). The resulting estimates of V_d and r_a/r_t are similar to the above and are given with the other calculations in Appendix 4.

In Figure 4.4, the majority of values are for situations where NH_3 deposition was occurring. Only a few values are available for measurements over fertilized agricultural surfaces, where emission was recorded, and these are cross hatched in the diagram. If fluxes were non-conserved the bulk of the NH_4^+ data, over natural surfaces, would therefore tend to apparent high deposition velocities (Figure 4.3a). Conversely for the few NH_3 emission runs apparent particle emission might be expected (Figure 4.3b). However, no clear trends of this kind are apparent from Figure 4.4. In addition most of the values of the fluxes are not statistically significant, so that much of the variation seen in Figure 4.4 may be attributed to random variation. Given these observations it is difficult to assess strictly the possibility of non-conservation of fluxes. However, as a whole, the consistency of the data with the expected low value of V_d would suggest that the process is not of major importance in this background exchange situation. Consequently the surface exchange methods for conserved fluxes are used for the NH_3 data here.

This does not negate the possibility of non-conservation, and in a few instances in our data this may be occurring. Thus for Great Dun Fell 4/1988 Run 2, deposition velocities were: NH_3 5.3 mm s^{-1}, NH_4^+ 14.5 mm s^{-1} and NO_3^- 15.8 mm s^{-1}. In this case the large values of V_d for the aerosol are matched by a low value for NH_3, which

is consistent if conversion is occurring. However, this appears to be the exception. Since much of the data show maximal NH_3 deposition velocities (next section) it may be confirmed that this is not generally important. Clearly more work is needed here.

As a result of the much smaller deposition velocities of NH_4^+ compared to NH_3, it is clear that, apart from when NH_4^+ concentrations are very much greater than NH_3, the dry deposition of NH_3 will be much more important. It was because of this, and the greater uncertainty in NH_3 surface exchange, that the main part of this study was designed to examine the exchange of the gaseous fraction.

4.5. SURFACE EXCHANGE OF NH_3

A summary of the conditions and ammonia exchange parameters measured over natural and unfertilized surfaces is given in Table 4.3. Values are means of all the data excluding only runs where fluxes were not accessible. Other mean values, where runs with very poor characterization of the NH_3 profiles are excluded, are calculated in Appendix 2, however the general trends are very similar to those given here.

Estimates in Table 4.3 are arithmetic means of the actual quantity, except for resistances, which are averaged as reciprocals (conductances) so as to reduce skewness. Mean r_c is found as the difference between the mean values of r_{a+b} and r_t. Alternative mean values of V_d and r_c are also provided in Appendix 2 by the method of Fowler (1976), but as with the NH_4^+ data they generally provide similar results to that in Table 4.3.

Deposition was recorded at all of the sites with the mean fluxes for the different campaigns ranging from 2–34 ng NH_3 m^{-2} s^{-1} (equivalent to 0.4–8.8 kg NH_3-N ha^{-1} $year^{-1}$). These values are, however, dependent on both the atmospheric concentrations of ammonia and the turbulent conditions prevailing during the experiments (*i.e.* $\chi\{z\text{-}d\}$, $u\{z\text{-}d\}$ and z_0). Assuming deposition to be independent of concentration — a question considered in section 4.7. — the effect of χ is cancelled out in the deposition velocities, the mean values of which were in the range 5–33 mm s^{-1} for each of the groups in Table 4.3. By the same assumption, the value of the surface resistance r_c is considered to be independent of the site turbulence and the air concentrations occurring during the experiment. For most of the sites the mean value of r_c is much less than the atmospheric resistances, suggesting that in these cases the main limitation of deposition is the prevailing turbulence at a site.

For some sites a negative mean r_c (and also $\chi\{z_0'\}$, see later) is recorded, which is clearly not possible. In this case the V_d estimate exceeds V_m, but from the error analysis these differences are shown to be insignificant, hence r_c approximates to zero.

site, month/year (surface type)	no of runs	$u\{1\ m\}$ ($m\ s^{-1}$)	$T\{z_o'\}$ (°C)	r_{a+b} {1 m} * ($s\ m^{-1}$)	$\chi\{1\ m\}$ ($\mu g\ m^{-3}$)	Deposition flux NH_3 ($ng\ m^{-2}\ s^{-1}$)	$V_d\{1\ m\}$ ($mm\ s^{-1}$)	r_c † ($s\ m^{-1}$)	$\chi\{z_o'\}$ ($\mu g\ m^{-3}$)
Huntingdon 8/1987 (neutral grassland)	9	2.5	(18)	58.2	2.00	33.9	16.3	3.1	-0.14
Harwell 3/1988 (calcareous grass'd)	6	3.3	8	63.5	1.77	14.3	5.3	125	1.01
Great Dun Fell (all) (*Eriophorum* moor)	12	3.9	(7)	45.0	0.67	17.3	19.6	5.9	0.01
Fala Moor 11/1987 (*Eriophorum* moor)	7	1.7	5	65.6	0.23	5.04	21.5	-19.1	-0.06
Fala Moor 5/1988 (mixed spp moor)	8	5.2	13	23.2	0.64	23.5	30.3	7.1	0.07
Wether Law 2/1989 (*Calluna* moor)	8	7.0	-0	19.0	0.08	1.71	27.7	17.1	0.05

Table 4.3 Mean values for NH_3 exchange measurement campaigns over natural and unfertilized surfaces. Values are arithmetic means of runs (unweighted) apart from where noted: * reciprocal mean, from arithmetic mean of V_m; † difference of mean r_{a+b} and mean r_t (reciprocal of arithmetic mean V_d). Positive fluxes imply deposition of NH_3. Values in brackets are means of available data. Data abstracted from Appendix 2.

Chemical species	no of runs	$u\{1\ m\}$ ($m\ s^{-1}$)	$T\{z_o'\}$ (°C)	r_{a+b} {1 m}* (NH_3)	$V_m\{1\ m\}$ (NH_3) ($mm\ s^{-1}$)	$\chi\{1\ m\}$ ($\mu g\ m^{-3}$)	Deposition Flux ($ng\ m^{-2}\ s^{-1}$)	$V_d\{1\ m\}$ ($mm\ s^{-1}$)	r_c † ($s\ m^{-1}$)	$\frac{V_d(\chi)}{V_m(NH_3)}$
NH_3	4	3.3	(6)	9.7	103	0.20	11.0	65.9	5.5	0.64
NH_4^+	5	3.5	(6)	10.0	100	1.14	9.7	16.6	—	0.17

Table 4.4 Mean values for NH_3 and NH_4^+ exchange measurement over coniferous forest at Dunslair Heights. r_b calculated according to the method of Wesely and Hicks (1977). Equivalent $V_m(NH_3)$ given for NH_4^+ data so as to compare rates by V_d/V_m. Other notes as for Table 4.3.

Only one site, a calcareous grassland surface at Harwell, gave a large surface resistance, the mean value being 125 $s\ m^{-1}$. This reflects a consistent difference in these runs to the other sites such that r_c dominates over r_a and r_b at this site.

The results over forest at Dunslair Heights are given in Table 4.4. The data are limited and approximate because of the failure of some of the runs and the low NH_3 concentrations during the experiment. Additionally the large roughness of forests and restricted sampling height range, result in small measurable gradients even for rapidly depositing compounds (Appendix 8). The value given in the table shows negligible r_c in agreement with the other sites. However, some uncertainty must attach to this estimate since the inclusion of one dubious run would result in a large surface resistance. Nevertheless, both estimates using the alternative averaging method give small r_c, so that rapid deposition seems most likely. The deposition velocities of NH_4^+ are also approximate, with a mean $V_d\{1\ m\}$ of 17 $mm\ s^{-1}$. This is large compared to the results over short vegetation (Figure 4.4), though may simply arise

because of the small amount of data; the general trend of $V_d(NH_4^+) < V_d(NH_3)$ is maintained. For the means presented in Table 4.4, $V_d(NH_3)/V_m(NH_3) = 0.64$. By comparison $V_d(NH_4^+)/V_m(NH_3) = 0.17$.

Mean values of the estimated average surface concentration of NH_3, $\chi\{z_o'\}$, are also given for each of the sites. This, as described in section 2.4.5, is another way of examining processes at the surface, and is analogous to r_c. The usefulness of $\chi\{z_o'\}$ is that in cases of deposition it represents the maximum possible mean concentration at the surface of the canopy elements. (Conversely in cases of emission it represents the minimum mean concentration). This is relevant where the possibility of concentration dependent exchange is of interest, which would occur with the existence of an ammonia compensation point (χ_{cp}, section 1.4.3). Given this interdependence of r_c and $\chi\{z_o'\}$, it may be seen that for most of the data, since r_c is not significantly different to zero, neither is $\chi\{z_o'\}$.

In the case of a compensation point, with the potential driven from beneath the stomata, the extra resistance to transfer through the stomata, r_{st}, would mean that the compensation point was even less than the $\chi\{z_o'\}$ estimate (see section 2.4.5., $\chi\{z_o''\}$). Since for much of the data $\chi\{z_o'\}$ approaches zero this would imply negative concentrations. It is therefore clear that such a substomatal χ_{cp} is not relevant here.

4.6. Effects of environmental conditions on NH_3 exchange

By comparison with NH_4^+ deposition, the larger gradients of NH_3 make it possible in many cases to characterize the flux of individual runs and to relate this to environmental conditions. This is examined for the data by following the course of exchange over time in relation to changing environmental conditions. Four sites are considered, Great Dun Fell, Fala Moor (5/1988), Huntingdon and Harwell. The low air concentrations occurring during the campaigns at Fala Moor 11/1987, Dunslair Heights 11/1988 and Wether Law 2/1989 result in larger uncertainty in the fluxes limiting the quality of data for this analysis.

For each site, graphs of NH_3 exchange parameters and environmental conditions are plotted against time. Graphs are given for: $u*$, $\chi\{1\text{ m}\}$, F_χ, $V_d\{1\text{ m}\}$, r_c, $\chi\{z_o'\}$ and $T\{z_o'\}$. Surface wetness and night-time/day-time are also represented diagrammatically. Four qualitative wetness classes were used, and note made of frozen conditions (see Figure 4.5b). In an attempt to quantify these environmental measurements, water vapour fluxes were recorded in the later campaigns, which includes the data collected at Wether Law.

So as to retain clarity, error bars are not shown. However, the precision of the flux, the main restriction, has 95% confidence limits of approximately the same order as individual values. Confidence limits are provided for F_χ, $\chi\{1\,\mathrm{m}\}$, r_c and $\chi\{z_o'\}$ in Appendix 2. In the graphs here values with large uncertainties are given in brackets.

4.6.1 Great Dun Fell

The course of NH_3 exchange and environmental conditions over time for the Great Dun Fell data is given in Figure 4.5. A clear pattern of NH_3 deposition to the surface is seen throughout the data.

By definition, both the flux and $V_d\{1\,\mathrm{m}\}$ are positively related to $u*$. However, in addition so is $\chi\{1\,\mathrm{m}\}$, which is treated as independent of $u*$ in the analysis. The observation may be a result of the deposition process itself where the source of NH_3 is the air aloft. A greater $u*$ steepens the surface gradient such that the concentrations at the 1 m reference height are less depleted by the surface. This is not definite however, since for our data periods of higher $u*$ occurred at the same time as periods of warmer conditions. It is therefore possible that the cause of variation of the NH_3 levels is the changing temperature throughout the day. This would be consistent with both NH_3 solubility equilibria and gas/particle equilibria which favour increased gas concentrations at increased temperatures (section 1.1).

The value of r_c is generally small, with NH_3 depositing to the surface at rates limited by turbulence. However there are a few exceptions. Two of these runs (3/1988 Run 6, 4/1989 Run 1) occurred during very cold conditions ($T\{z_o'\} \approx 0$ °C), and low NH_3 levels ($\chi\{1\,\mathrm{m}\} \approx 0.1\ \mu g\ m^{-3}$). This could relate to the freezing conditions, or could be just scatter at the low concentrations. The third example of a large r_c (4/1988 Run 2) was the run noted earlier (section 4.4) where NH_4^+ deposition was unusually rapid, possibly being an example of non-conservation favoured by the large temperature gradient (L = -11 m) occurring during the run.

Considering the excess resistance (r_c) as a concentration ($\chi\{z_o'\}$), apart from the third exception above, all the values are very close to zero. The runs for the 3/1988 campaign are particularly consistent with a mean $\chi\{z_o'\}$ of 0.09 $\mu g\ m^{-3}$. It is possible this relates to an equilibrium surface concentration over the leaf surfaces, albeit a very small one. In connection with the comment above, relating $\chi\{1\,\mathrm{m}\}$ to temperature, it is interesting that there is no relationship between $\chi\{z_o'\}$ and temperature.

The pattern of rapid deposition is seen both in day and night-time runs. This is reasonable since the small values of r_c imply that the sink for the NH_3 must be the surface roughness elements — the leaf surfaces. Hence deposition will not be under

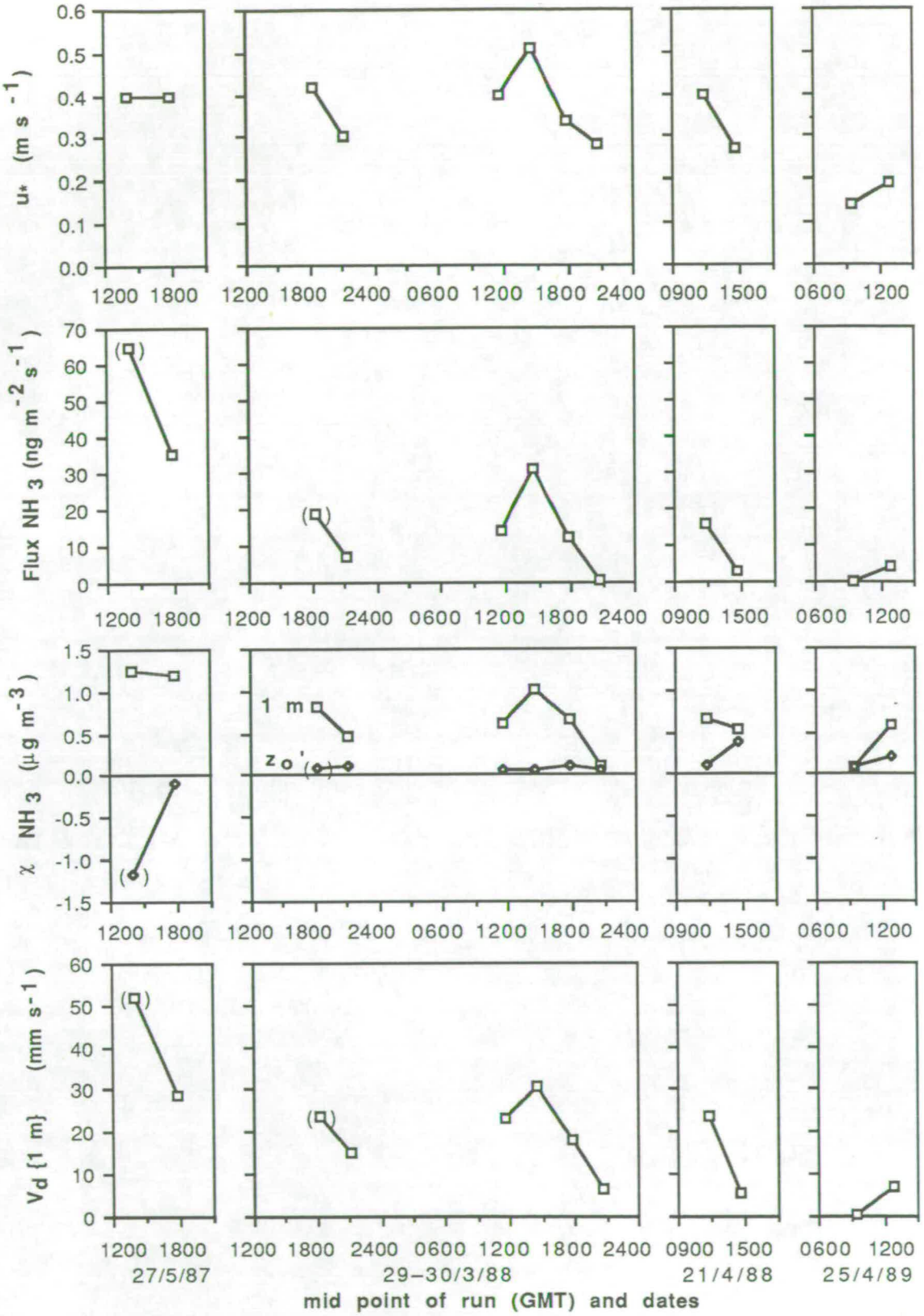

Figure 4.5a Course of ammonia exchange and environmental conditions over time at Great Dun Fell. Note: positive fluxes of NH_3 denote deposition. Figure continued overleaf.

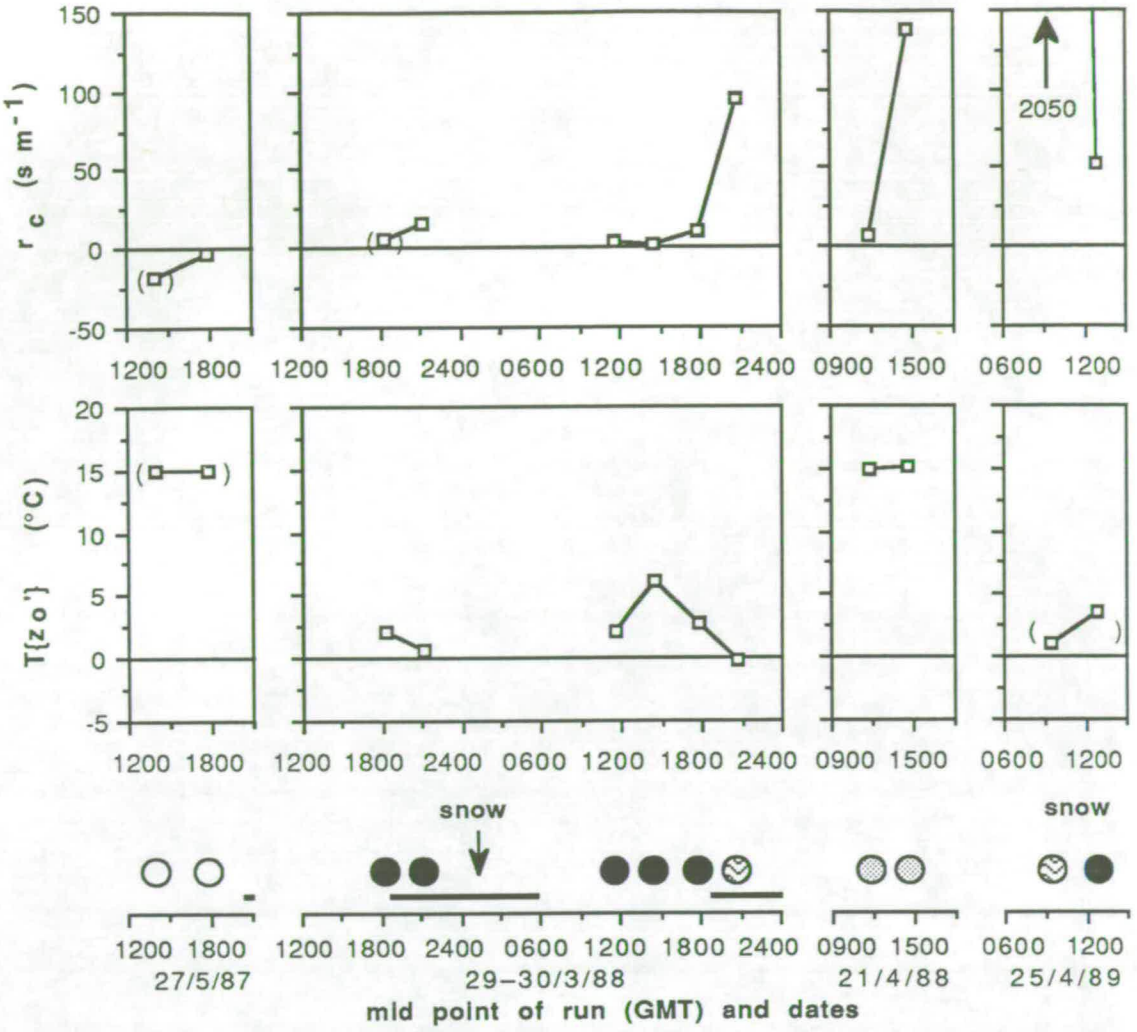

Figure 4.5b Course of NH_3 exchange and environmental conditions over time at Great Dun Fell.

In these and the succeeding graphs vegetation canopy wetness and dryness are divided qualitatively into four classes shown right.

In addition a symbol for frozen surfaces is given. Vertical arrows denote precipitation events, while a horizontal solid bar denotes night-time.

dry
slightly wet
moderately wet
completely wet
frozen surface
precipitation
night-time

the control of biological factors, such as stomatal closure, that might otherwise restrict deposition velocities at night.

4.6.2 Fala Moor 5/1988

The results for the campaign at Fala Moor in May 1988 are given in Figure 4.6. In agreement with the results at Great Dun Fell, NH_3 is again seen to deposit to the surface. For all except two runs $r_c < 10$ s m^{-1}, showing the vegetation to be an efficient sink of the NH_3. The measurements were made during a period of high windspeed and turbulence, with $u*$ in the range 0.5–0.8 m s^{-1}. Consequently large deposition velocities were possible with some values over 50 mm s^{-1}.

The two runs providing exceptions to this trend were poorly characterized profiles (only 3 NH_3 points available) so that it is likely, given the consistency of the other good data that these runs do not reflect exchange processes at the surface.

At Great Dun Fell most of the data were for a wet ground surface. In that example it could be argued that, because NH_3 is a soluble gas, rapid deposition would occur to the water on the leaf surfaces. The results here, however, present data for both dry and wet vegetation, although the ground was still damp throughout. An interesting period is that following the course of vegetation drying in the morning of 25/5, where surface temperature increased from approximately 5 to 20 °C. Both these effects might be expected to favour a reduced equilibrium level of NH_4^+/NH_3 in solution, and so limit NH_3 deposition. In the dry conditions present after midday it might result in only very limited uptake. However, only a small change is evident, accounting for a difference in r_c of 15 s m^{-1}. The consistently small values of r_c suggest that the NH_3 is efficiently bound to the leaf surfaces even when the surfaces appear dry.

4.6.3 Huntingdon 8/1987

A similar pattern of surface exchange to the moorland sites, above, is also shown for the natural grassland site at Huntingdon (Figure 4.7). The estimates of both r_c and $\chi\{z_o'\}$, while showing a larger variation, still approximate to values about zero. Consequently given the higher air concentrations of NH_3 during this experiment (1–3.5 μg m^{-3}) the fluxes were larger than the other sites, ranging from 10–60 ng m^{-2} s^{-1} (mean: 34 ng m^{-2} s^{-1}). This is despite the relatively small wind speeds which restricted $V_d\{1\,m\}$ to a maximum of 27 mm s^{-1}. Temperature measurements were unavailable during the first part of the experiment, although conditions were generally warm, reaching a minimum of around 15 °C near midnight on 12/8.

It is difficult to see whether trends with environmental variation occur, given the degree of scatter. As with the Great Dun Fell measurements, both $u*$ and surface temperature are positively correlated over the measurement period, yet there is no clear response to these variables by $\chi\{1\,m\}$ as discussed there.

Trends may however exist between the vegetation dryness, surface temperature and the NH_3 surface parameters r_c and $\chi\{z_o'\}$. The period between 1600 (GMT) 12/8 and 0500 13/8 shows dry conditions at the start, with a possible limitation to deposition (Run 5, 1700 GMT, r_c = 49 [-6, 900] s m^{-1}; $\chi\{z_o'\}$: 0.76 ± 0.84 μg m^{-3}, 95% confidence limits). This is lost later in the cooling of the evening and subsequent dew-

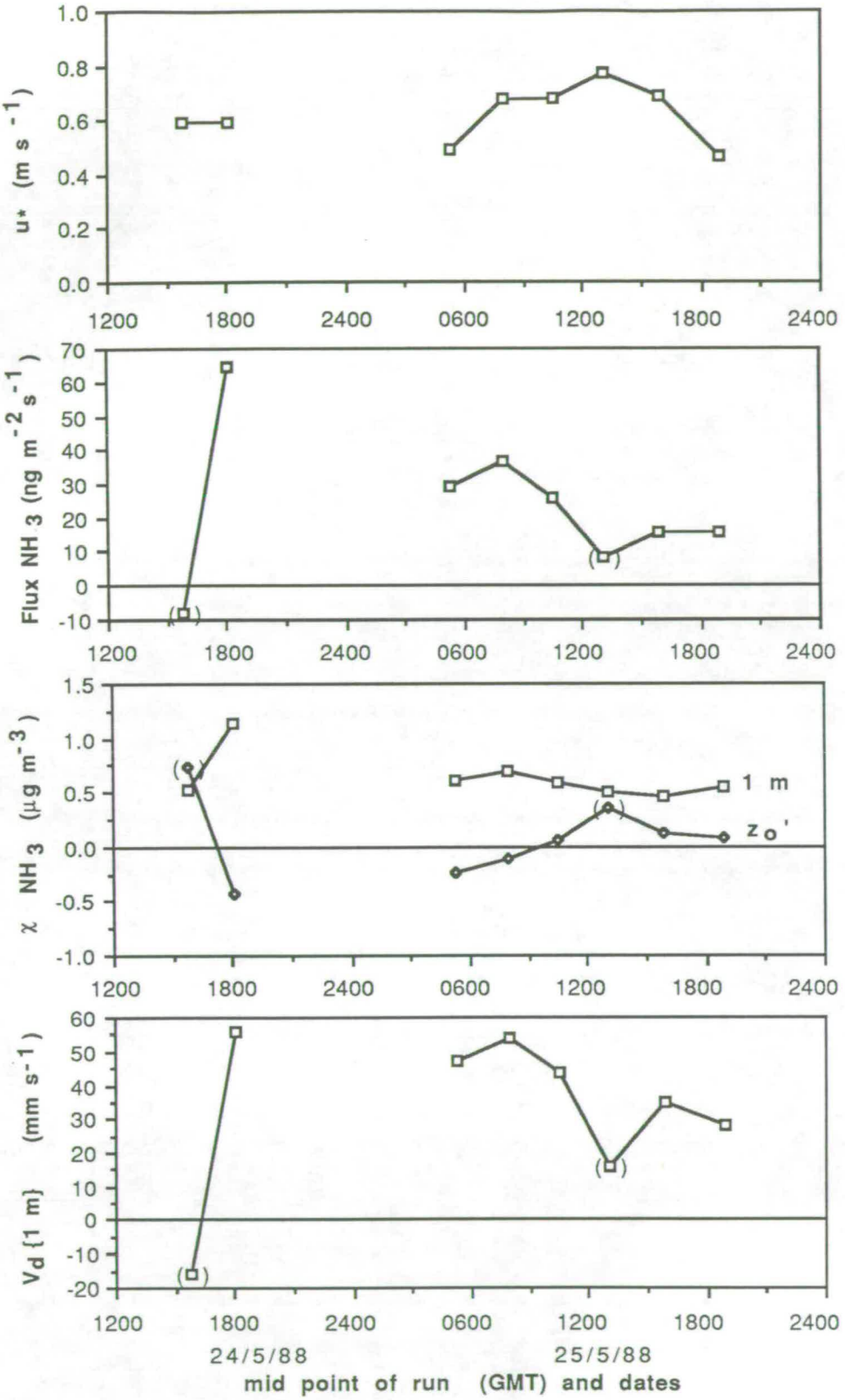

Figure 4.6a Course of ammonia exchange and environmental conditions over time at Fala Moor 5/1988. Note positive fluxes denote deposition. Figure continued overleaf.

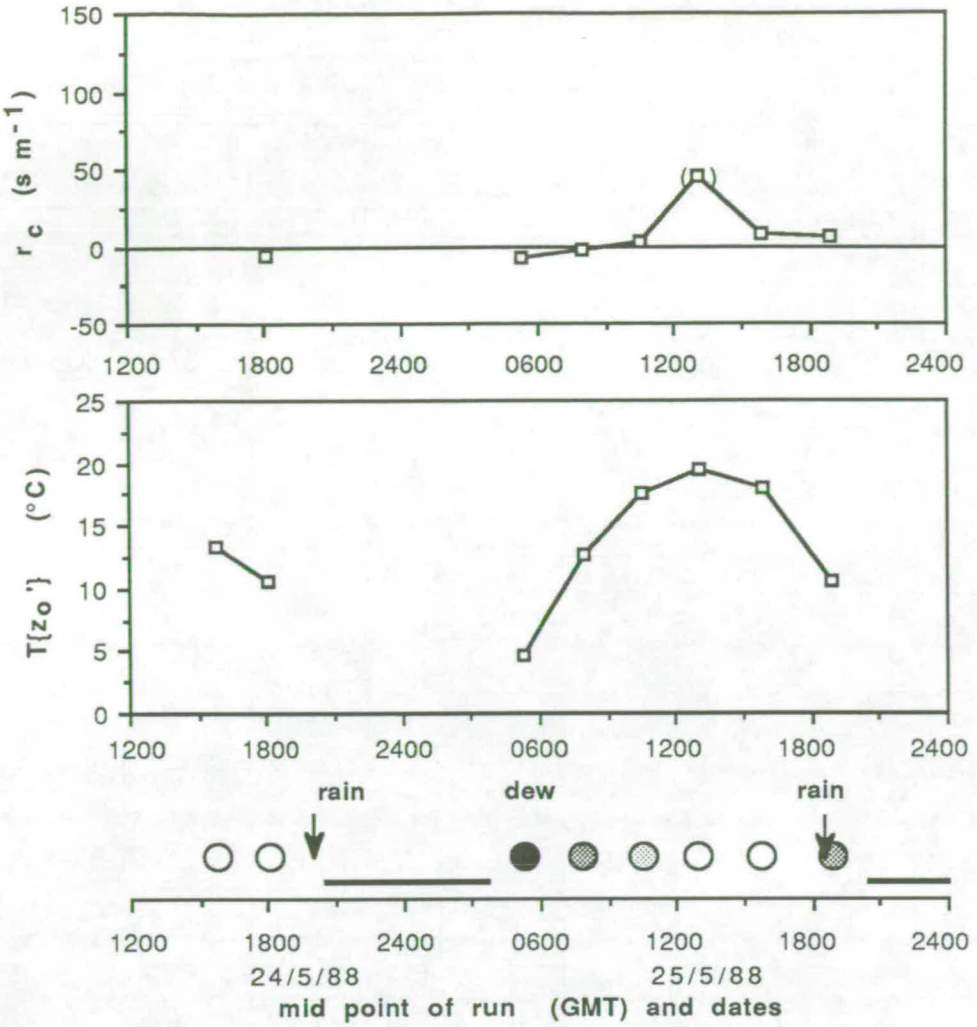

Figure 4.6b Course of NH_3 exchange and environmental conditions over time at Fala Moor 5/1988. Explanation of surface conditions symbols given in Figure 4.5.

fall. It is probable that this is related to an increased leaf surface sink provided by the dew into which the NH_3 could dissolve. Interestingly however, Run 6 (1930 GMT, 12/8) shows minimal surface resistance even before the onset of dew.

This effect of surface wetness is also supported by Runs 1 and 2, although for Run 9 (1040 GMT, 13/8) a significant value of r_c (120 [9.4, emission] s m^{-1}, 95% confidence limits) is recorded over wet vegetation following rain. It is possible this relates to the rainwater having already reached NH_3/NH_4^+ equilibrium with the atmosphere.

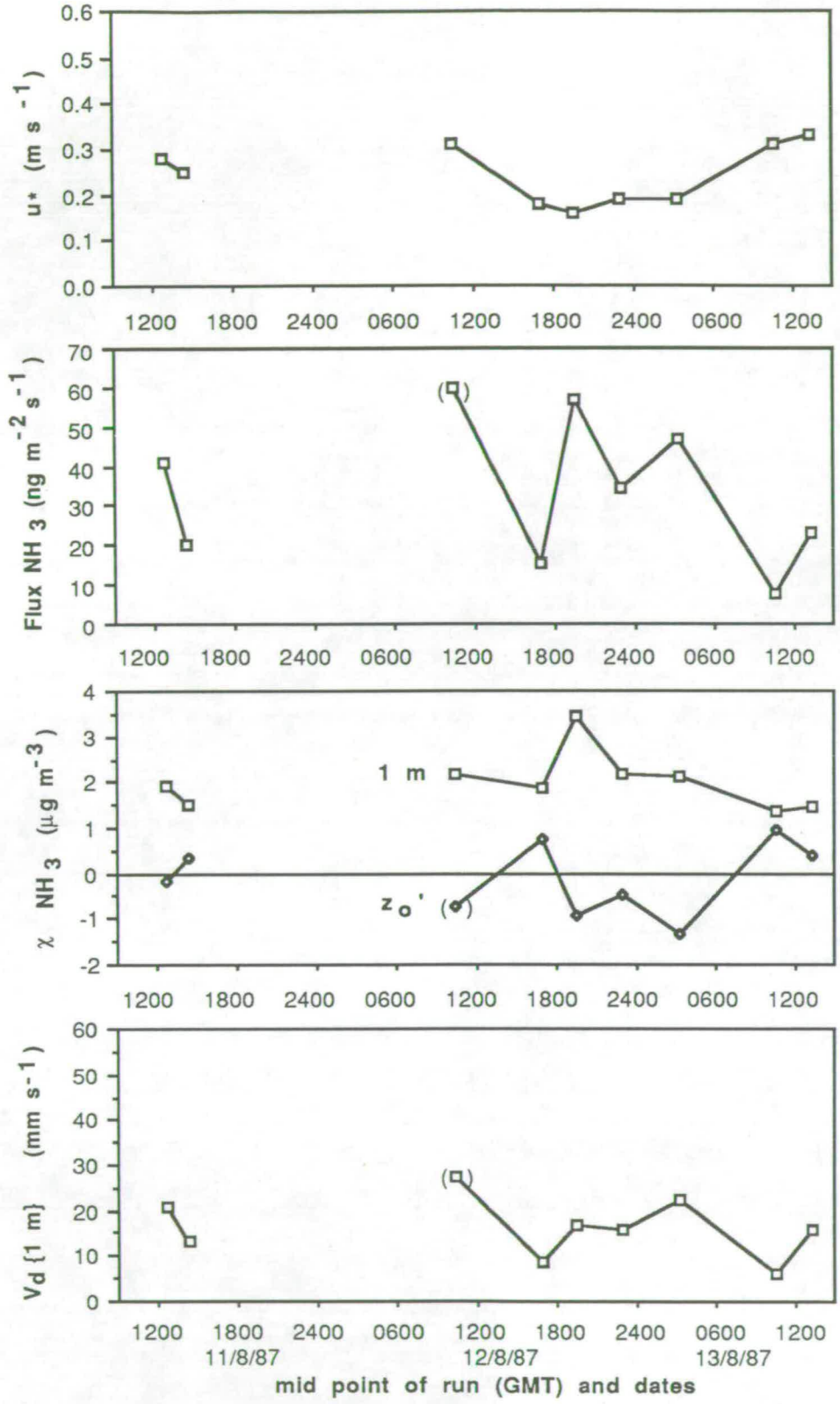

Figure 4.7a Course of ammonia exchange and environmental conditions over time at Huntingdon 8/1987. Note: positive fluxes of NH_3 denote deposition. Figure continued overleaf.

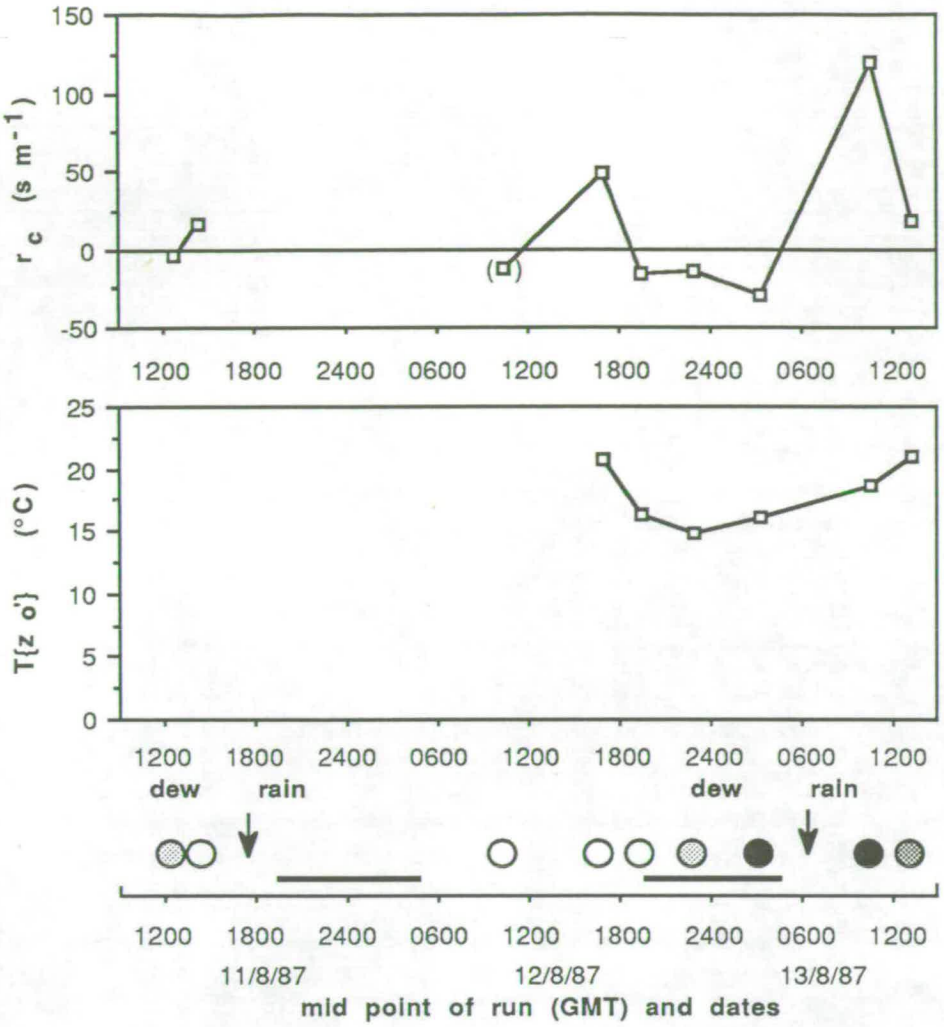

Figure 4.7b Course of NH_3 exchange and environmental conditions over time at Huntingdon 8/1987. Explanation of surface conditions symbols given in Figure 4.5b.

4.6.4 Harwell 3/1988

In contrast to the above sites, the results at Harwell show a very different pattern of surface exchange (Figure 4.8). Here r_c is consistently large with values ranging between 30–1300 s m^{-1} (mean: 125 s m^{-1}). Within this, several of the individual results show significant surface resistance (*e.g.* Run 1, r_c = 87 [31, 430] s m^{-1}, 95% confidence interval). Consequently the values of V_d\{1 m\} are small, ranging 1–11 mm s^{-1}.

The results for this site may be split into two groups. On the first day (Runs 1–3) NH_3 air concentrations were approximately 3–4 μg m^{-3}. However, for the rest of the experiment (Runs 4–8), corresponding to a change in wind direction, concentrations became much lower, around 0.1–0.3 μg m^{-3}. The fluxes in this latter period are not well quantified, since restricted access to the site at night, and the necessity to group

Runs 5–7 because of low concentrations, resulted in rather long run times. However, despite this uncertainty the overall trends are still large enough to be of value.

As has been discussed, r_c and $\chi\{z_0'\}$ represent the same excess in the micrometeorological calculations and it is impossible from these alone to see which is the most physiologically appropriate. From the measurements here r_c was noted to be consistently large. When plotted on a logarithmic scale, appropriate when dealing with such a large range of values of r_c, this consistency appears clearer (see Figure 4.8).

By contrast, the values of $\chi\{z_0'\}$ separate distinctly between the two air concentration groups. If it is taken that $\chi\{z_0'\}$ represents a real concentration maintained by equilibrium with the surface, then it would follow that it ought to be independent of air concentration. However, this is not the case, and the values of $\chi\{z_0'\}$ fall into two separate groups, giving high and low estimates according to $\chi\{1\ \mathrm{m}\}$. Given that r_c does not separate in this manner, it seems likely that r_c represents the more realistic measure of limitation of uptake in this case. That is, the deposition is rather limited by a resistance to uptake at the surface, with a minimal equilibrium surface concentration.

It is interesting to speculate why this site shows such a different pattern of uptake of NH_3. A possible reason could be the low soil acidity (pH 8.4) of the calareous soil, since immediately before the experiment, the site was harrowed, distributing the soil particles over the leaf surfaces. In such alkaline conditions NH_3 is known to have a very low solubility (see Figure 1.1), so that it is possible the leaf surface sink exhibited at the other sites was not available to the same extent. It is feasible that NH_3 deposition was restricted to uptake through the stomata, and in this context it is interesting that the values of r_c are of the same order as stomatal resistances.

Profiles of the acid gases HNO_3 and HCl were also measured at this site, and although very approximate, showed a general pattern of rapid deposition, with a negligible mean r_c. The data for these are given in Appendix 4.

4.7. Discussion

The results here present a clear picture of ammonia deposition throughout the selection of natural and unfertilized ecosystems studied. At none of the sites was there any good evidence of ammonia emission over the range of temperate conditions investigated.

The fluxes were calculated according to the aerodynamic gradient method assuming that gaseous NH_3 is conserved as it deposits. From a consideration of the particulate NH_4^+ exchange processes it is concluded that this assumption is generally valid throughout the data, since the recorded deposition velocities of this component conform to the low values established for such sub-micron particles.

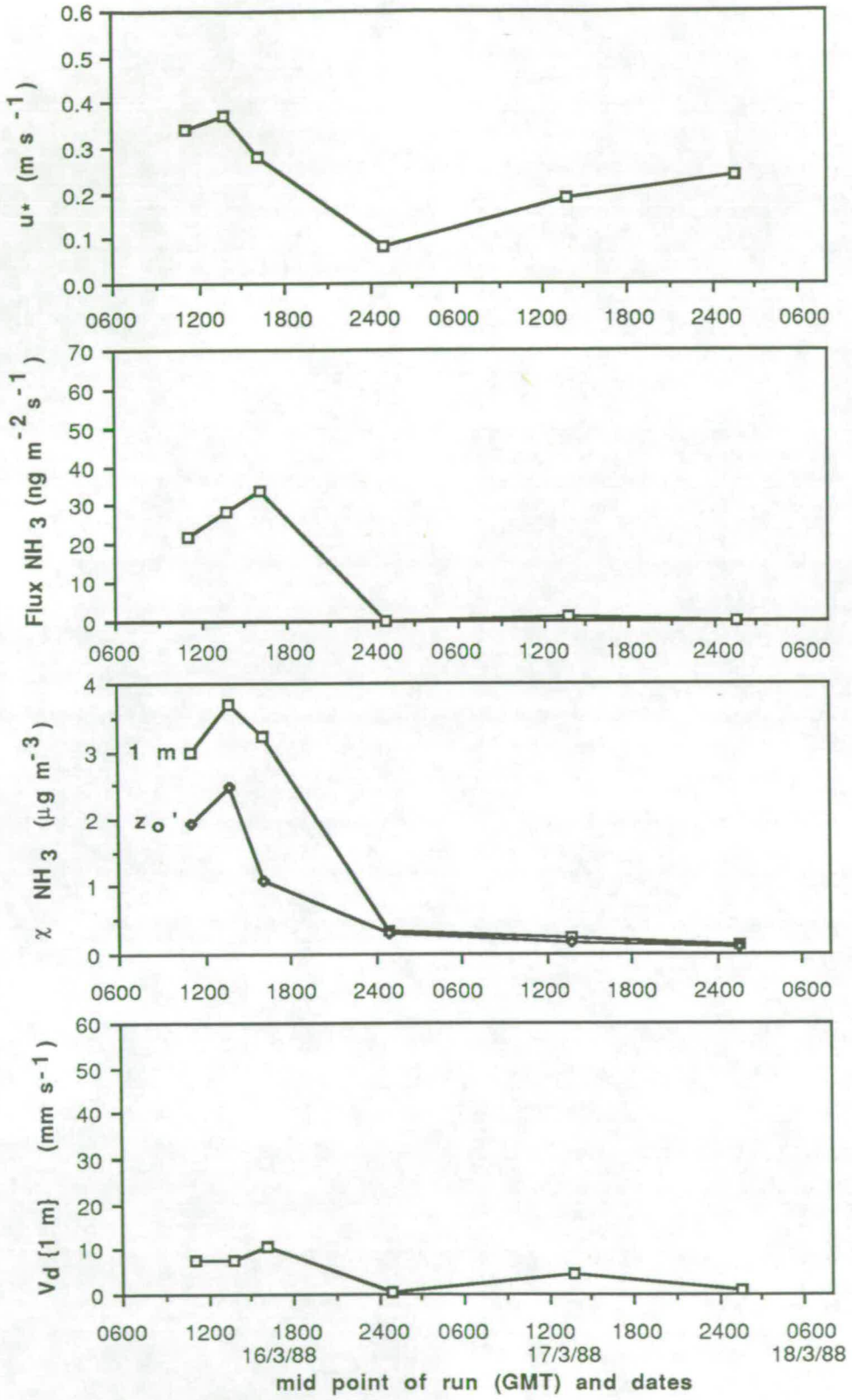

Figure 4.8a Course of ammonia exchange and environmental conditions over time at Harwell 3/1988. Note: positive fluxes of NH_3 denote deposition. Figure continued overleaf.

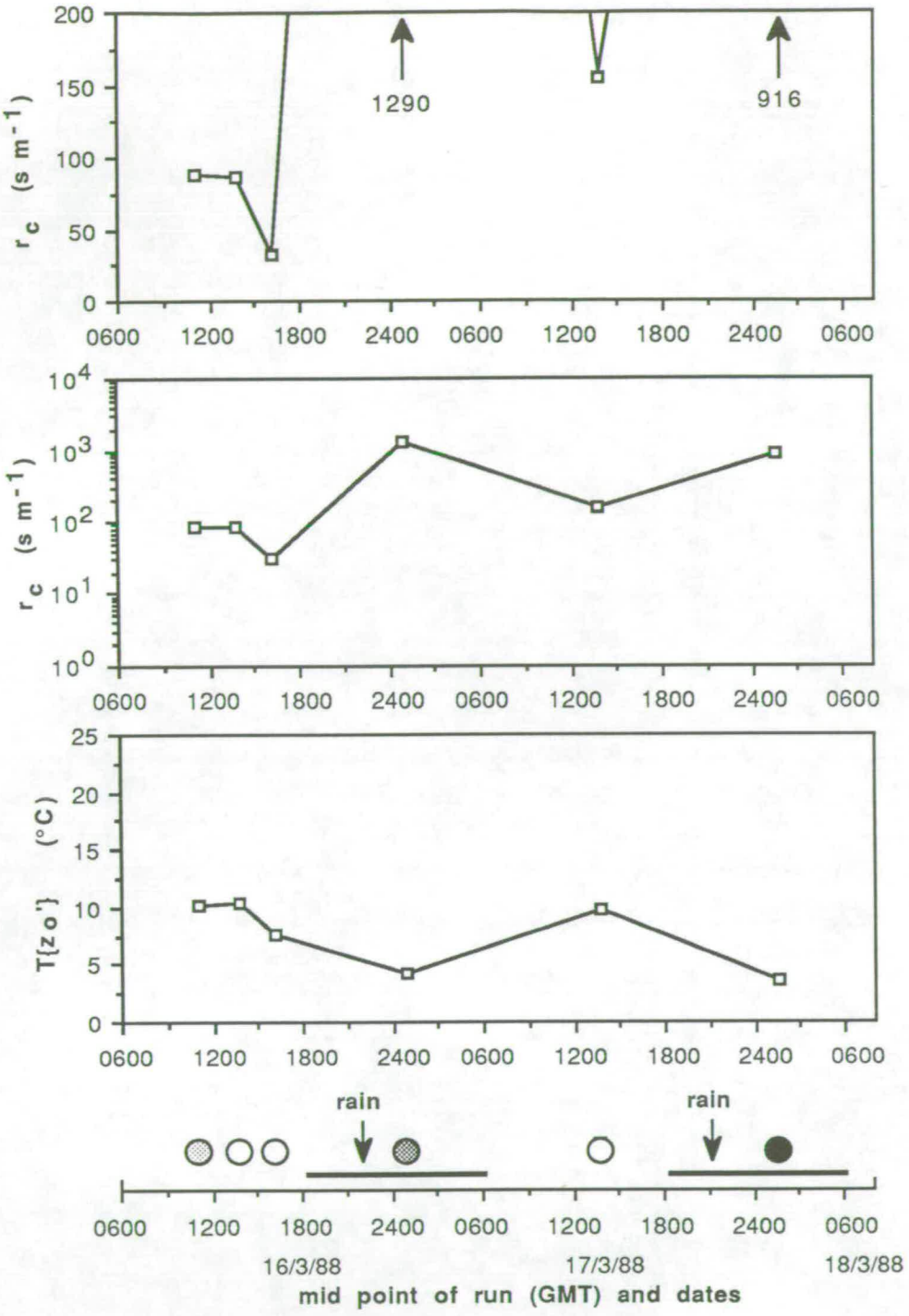

Figure 4.8b Course of NH_3 exchange and environmental conditions over time at Harwell 3/1988. Explanation of surface conditions symbols given in Figure 4.5b.

Another possibility not mentioned above is that filter artifacts may occur and give rise to modified NH_3/NH_4^+ gradients. As discussed in section 3.3.1, this might arise if some of the NH_3 is captured on the particulate prefilter, or alternatively, if some of the collected NH_4^+ volatilizes and is captured downstream on the NH_3 filter. However, the same reasoning as above can be applied, that since the gradients of NH_4^+ conform to the expected small gradients, it is unlikely that this is an important source of error.

If the prefilters were to capture NH_3, it is likely that the steep gradients of the gas would be reflected with increased gradients of the particulate. In support of this tests mentioned in section 3.3.1, using two prefilters in series, showed negligible NH_4^+/NH_3 to be captured on the second filter. Conversely since many of the NH_3 gradients were maximal it is unlikely that NH_4^+ volatilization was important, as the addition of a contribution from the NH_4^+ fraction would serve to reduce the observed NH_3 gradients.

In all, it seems that with this sampling system, and for the environmental conditions of these experiments, the complications to the gradient interpretation, *via* non-conservation of fluxes or sampling artifacts, are not of major importance in the results. The treatment of the data by straightforward flux-gradient analysis is therefore appropriate.

Within the consistent pattern of NH_3 deposition, there is a clear distinction between the Harwell measurements and all the other natural and unfertilized sites studied. For the other sites, of which Great Dun Fell, Fala Moor (5/1988) and Huntingdon have been considered in detail, a pattern of rapid deposition is exhibited, with generally very small surface resistances. Although the precision of the measurements at other campaigns (Fala Moor (11/1987), Dunslair Heights, and Wether Law) does not permit detailed analysis, they also show a pattern consistent with this.

At these rapid deposition sites some excess resistance or concentration (r_c or $\chi\{z_0'\}$), does nevertheless occur in a number of the runs. In these cases it is not immediately clear which is the more physiologically appropriate measure of the excess described by these values. If it is wholly r_c this suggests the deposition process occurs independent of air concentration, even down to zero air concentration, since the potential of the ground is considered to be zero. Since no emission occurs throughout the data collected here, even at low concentrations, this is supported. The interpretation of the excess as $\chi\{z_0'\}$ can also be interpreted similarly if this is considered as simply representing a virtual concentration among the series of resistances to deposition (Figure 2.3). However, if r_c is assumed to be zero, $\chi\{z_0'\}$ represents the concentration in the air at the surface, which is presumably maintained by equilibrium with the surface. In this case the deposition process would be dependent on air concentration, so that when air concentrations were above $\chi\{z_0'\}$, deposition would occur, and when below it emission would occur.

Interpreting the data at Great Dun Fell, it is interesting that a small value of $\chi\{z_0'\}$ is present, which is more consistent than the value of r_c. The estimate for the wet

conditions of the 3/1988 data has a mean of 0.09 $\mu g\ m^{-3}$. It is possible that this is the equilibrium value of the wet surface occurring during this period. However, since air concentrations did not drop below this very small level this hypothesis could not be tested. In addition the pH and concentration of NH_4^+ in the surface water from this site were also measured, so that using solubility theory (section 1.1), it is possible to calculate the gaseous NH_3 concentration that would be in equilibrium with the surface. Given values of pH 3.92 and 4.4 $\mu mol\ dm^{-3}$ NH_4^+ in solution, and assuming a temperature of 5 °C, the equilibrium gaseous NH_3 concentration would be 2×10^{-5} $\mu g\ m^{-3}$. Even accounting for an order of magnitude in uncertainty due to CO_2 effects (section 1.1) this concentration is negligible. If this value is representative of the surface as a whole it is likely that the value of $\chi\{z_0'\}$ given above is simply an approximation to zero. However, even the estimated value of $\chi\{z_0'\} = 0.09\ \mu g\ m^{-3}$ is small. In practice with air concentrations generally much greater than this (Chapter 6) it is reasonable to describe both $\chi\{z_0'\}$ and r_c as approximating to zero.

The results at Harwell provide a marked contrast to the other sites through the existence of a consistently large r_c (mean: 125 $s\ m^{-1}$). The occurrence of both high and low air concentrations (due to a change in wind direction) was fortunate as it provides information as to whether r_c or $\chi\{z_0'\}$ is the more appropriate interpretation. Given that $\chi\{z_0'\}$ depends on $\chi\{1\ m\}$ to such a large extent, it is clear that this does not represent a concentration maintained by equilibrium with the surface. The interpretation as r_c seems more likely. It is, nevertheless, still possible that a smaller equilibrium concentration exists in addition to an uptake resistance, below which emission could occur. However, this would be less than $\chi\{z_0'\}$, and therefore less than $\approx 0.1\ \mu g\ m^{-3}$. This again is small enough to be of negligible importance in practice (Chapter 6).

A possible explanation for the difference in the results at this site to the others, was noted earlier. It was suggested that the difference is the result of harrowing the calcareous soil, so that leaf surface moisture is buffered to a high pH, reducing the potential to dissolve NH_3. Given that equilibrium $[NH_4^+]$ is directly proportional to $[H^+]$ (section 1.1), it is clear a major effect on leaf surface capacitance of $[NH_4^+]$ is possible. Comparing the pH values for this site and the Great Dun Fell data, gives a $\Delta pH = 4.5$, which in otherwise identical conditions would amount to a factor of difference in NH_4^+ capacity of 3×10^4. The high pH of this site therefore seems to be a likely explanation of the difference in surface exchange. However, it would be desirable to confirm these exchange measurements, by measuring fluxes over a similar calcareous surface, both before and after harrowing, or by looking at uptake by soils of different pH.

The other feature of interest is the effect of wetness/dryness and temperature, which promotes a small value of r_c and $\chi\{z_o'\}$. It is difficult to see which of these is the most important, as they tend to occur together in the environment, with an increase in solar radiation causing both heating and drying. However, if the controlling process is taken as being the NH_3/NH_4^+ solubility in water, the effect of drying will be expected to be the most important feature, as in comparison temperature is a second order effect (Figure 1.1).

It is clear though that even in the dry runs in warm conditions the value of r_c is still smaller than might be expected by stomatal transfer alone, given that the minimal r_{st} for these surfaces is ≈ 50 s m^{-1} (Jarvis, 1981). Additionally, if transfer was through stomata a greater r_c would be expected at night. This was not seen at any of the sites (except perhaps Harwell), although in the data presented here there is a lack of dry night-time runs needed to confirm this. Nevertheless, the small values of r_c even in dry conditions imply that the deposition must be to the leaf surfaces, as these are the roughness elements to which the resistance analogy (r_a, r_b) models transfer.

The mechanism by which the NH_3 is fixed to the leaf surfaces could be either adsorption of the gas to the surface directly, or association with bound water even in dry conditions. This is considered further in the discussion of Chapter 7. However, if it is associated with water, the capacity for deposition might increase with humidity corresponding to an increase in bound water (section 1.4.3). It is interesting that, with the increased relative humidity during the evening of 12/8/1987 at Huntingdon, zero r_c was established even before the onset of dew. Similarly with the results of rapid deposition at Fala Moor 5/1988, while the canopy dried out thoroughly, the ground below was still damp, presumably maintaining a high relative humidity. Unfortunately humidity was not measured in that experiment. Given the possibility of humidity effects it would be informative to measure the NH_3 exchange in very dry, or droughted conditions to clarify its importance and see if larger r_c or $\chi\{z_o'\}$ do develop.

Chapter 5

Surface exchange results: Fertilized agricultural ecosystems

5.1. INTRODUCTION

As a complement to the studies over natural and unfertilized ecosystems, ammonia exchange was also investigated over fertilized agricultural ecosystems. Previous studies have shown that NH_3 emission may occur in this case, especially from grazed surfaces and during the period immediately following fertilizer application (see section 1.3). However, little study has been made of the NH_3 exchange over ungrazed grassland and arable surfaces at periods other than immediately following fertilizer application. Consequently, these background exchange patterns are taken as the focus for the measurements here. In addition, most of the studies over agricultural surfaces have been made using total NH_x sampling as an approximation to NH_3. This is sufficient where very large quantities of NH_3 occur, immediately after fertilizer application, although, for the background situation, the NH_4^+ component may be expected to be important. Hence in this study, as with the measurements over natural surfaces, samplers separating NH_3 and NH_4^+ were used.

5.2. STUDY SITES: INTENSIVE AGRICULTURAL ECOSYSTEMS

Measurements were made at two sites, Bush and Stenton, both located in S. Scotland, the details of which are given in Table 5.1. Both sites were visited twice. At Bush sampling was made both in Summer and Winter, with the latter period including measurements over snow. The measurements at Stenton were made during Summer, with the different campaigns measuring over barley and wheat crops in adjacent fields. Further details of the conditions and sampling dates are given in Table 5.2.

Both sites received typical agricultural fertilization, with ammonium nitrate based compounds. The Bush site was fertilized with 150 kg N ha^{-1} as a single batch in mid April 1988, hence the 6/1988 measurements were approximately 8 weeks after fertilization. The grass at this site was cut in July, following which no further treatment was made before the 2/1989 campaign. The Stenton sites were fertilized as 3 and 4 batches of 43 kg N ha^{-1} for the barley and wheat respectively (totals: 130, 170 kg N ha^{-1}). The last dressing for the barley was on 15 May, and that for the wheat on the 3, 8 May 1989, providing $3\frac{1}{2}$ and 6–7 weeks between fertilization and the measurements. Thus for both sites the results may be expected to reflect background exchange processes.

site name used in study	site location	National grid ref.	height AMSL (m)	fetch (m)	soil type and pH (in H_2O)	Vegetation community (dominant species underlined)
GRASSLAND Bush	Penicuik Midlothian Scotland	NT245 639	200	200	loam pH 6.1	*Lolium multiflorum*, *Phleum pratense*, *Poa* spp, *Trifolium repens*
CEREALS Stenton	Dunbar East Lothian Scotland	NT615 768	45	>300	loam pH 5.4, 6.1	a) *Hordeum vulgare* (Barley) b) *Triticum aestivum* (Wheat)

Table 5.1. Sites used for flux measurement studies. AMSL = above mean sea level.

site name	season	sampling dates	canopy height (m)	d * (m)	mean z_o† (mm)	air temp-eratures (°C)	State of canopy / soil during measurements
GRASSLAND Bush	Summer	14–17/6/88	0.85	0.5	4.2	10–19	AG, nearing anthesis, canopy both wet and dry, soil damp
	"	20/6/88	"	—	—	17–20	Within-canopy profiles only AG, anthesis, canopy dry
							Grass cut for hay in July.
	Winter	27–28/2/89	(≈0.1) snow: 0.07–0	0.06– 0.10	range 0.3–6	2–4	Snow melting, frozen at night and complete melt after rain
CEREALS Stenton	Summer	a) 8–9/6/89	0.45	0.26	60	5–16	AG, spikes emerging, canopy dry and wet (dew), soil dry
	"	b) 20–21/6/88	0.90	—	—	10–22	Within-canopy profiles only AG, grain filling, lower leaves senescing, canopy mostly dry.

Table 5.2. Dates of campaigns and conditions during measurement periods. * In cases were d is small its value also depends on the choice of ground reference position used to measure heights. A value of d also arises over snow since heights were measured from soil level. † Calculated from the mean of $\ln(z_o)$ since z_o is not normally distributed. AG = actively growing vegetation.

5.3. PROFILE RESULTS AND INTERPRETATION

Consideration was given in Chapter 4 to the interpretation of concentration profiles and the possibility of non-conservation of fluxes or sampling artifacts. It was concluded that these effects are not of great importance in the results here. Consequently, in this section the profiles are interpreted solely in terms of surface exchange processes.

Example profiles measured over these surfaces are given in Figures 5.1 and 5.2. As with the results over natural surfaces, the wind and temperature profiles provided the most precise data so that concentration profiles dominate the sources of error. In addition for Bush 2/1989 and Stenton 6/1989, water vapour fluxes were also measured and the profiles are shown. For Bush 2/1989 temperature and humidity were measured using four aspirated psychrometers, while at Stenton the psychrometers were again used (only two psychrometers available) and compared with measurements

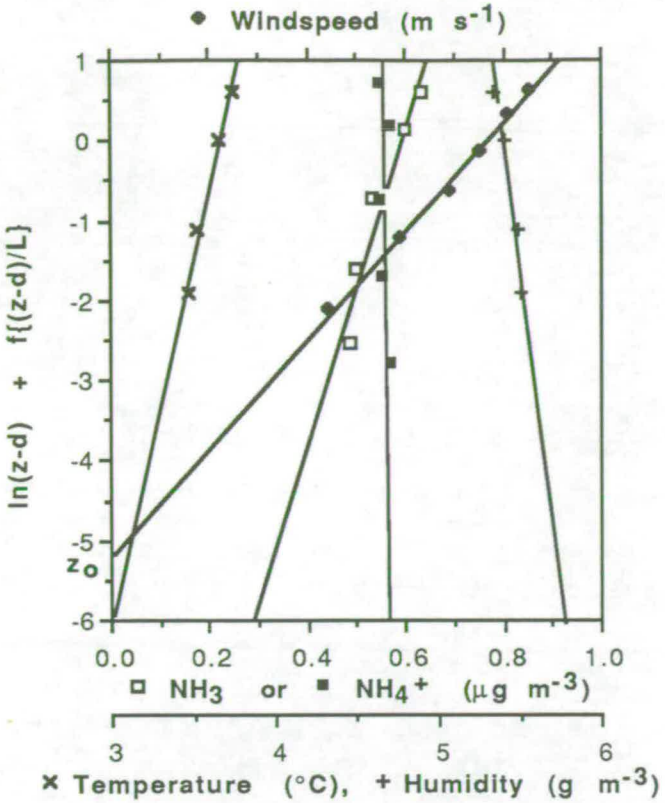

Figure 5.1 Example profiles at Bush 2/1989. Temperature and water vapour profiles measured by aspirated psychrometry. Data are for Run 6 except NH_4^+ which is for Runs 1–6 combined. For height axis, z is in meters; $f\{(z-d)/L\}$ accounts for stability correction.

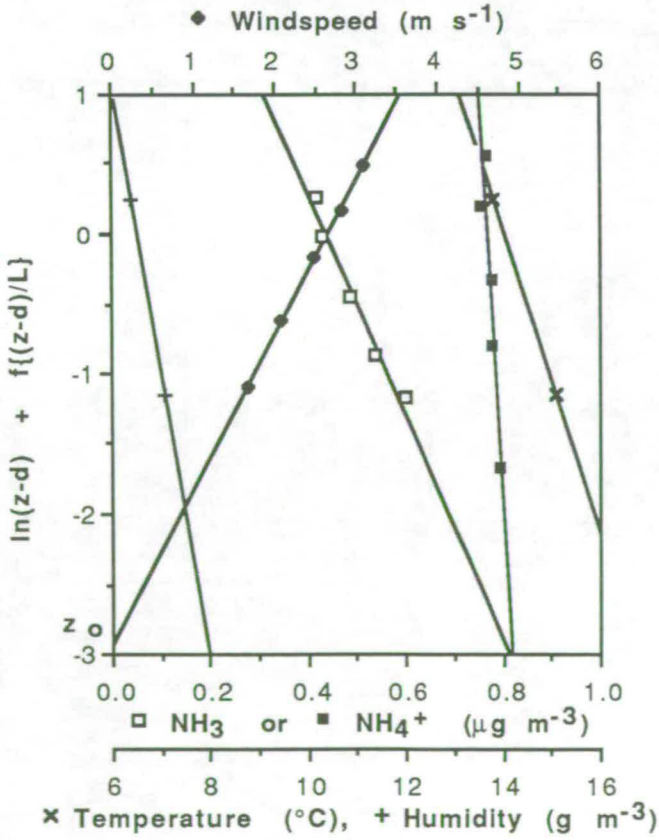

Figure 5.2 Example profiles over barley at Stenton 6/1989. Temperature and water vapour profiles measured by fine thermocouples and a dewpoint hygrometer system. Data are for Run 1 except NH_4^+ which is for Runs 1–8 combined. Height axis as for Figure 5.1.

from a fine thermocouple and dew-point meter system (section 3.5.).

As discussed in section 4.4. the profiles of NH_4^+ show only very small gradients, reflecting a slow rate of surface exchange (see also Appendix 4). The NH_3 profiles, however, show both clear upward and downward gradients, reflecting a bi-directional exchange pattern of both emission and deposition according to environmental conditions. An example of each is given in the figures. In the run shown in Figure 5.1 deposition was recorded, while that in Figure 5.2 gave emission.

5.4. SURFACE EXCHANGE OF NH_3

A summary of the conditions and ammonia exchange measurements over the agricultural surfaces is given in Table 5.3. Arithmetic means are given, but as noted above, clear relationships exist with environmental conditions so that the means of ammonia exchange are only relevant for the experimental conditions encountered. The degree of variation is shown in the table by the inclusion of minimum and maximum values for each of the campaigns.

The results in Table 5.3 show a clear distinction between those made in winter, Bush 2/1989, and those made in summer, Bush 6/1988 and Stenton 6/1989. For the winter measurements there is a consistent pattern of deposition to the snow covered or wet surface, with r_c ranging from near zero to 80 s m^{-1} (mean: 25 s m^{-1}). Conversely, for the measurements in summer, there is an overall trend toward emission of NH_3, with a mean flux of 6–8 ng m^{-2} s^{-1} (equivalent to 1.6–2.1 kg NH_3-N ha $year^{-1}$), for both the grass and barley surfaces. However, for both these sites, deposition is recorded during wet and cool periods.

In the results section for natural and unfertilized ecosystems, the question was raised of the interpretation of the excess in the resistance analogy, as r_c or $\chi\{z_0'\}$ (section 4.5). In those cases surface concentrations approached zero, even where large values of r_c occurred, so that it was concluded deposition would occur independent of air concentration, and that r_c was the most suitable interpretation of the excess. In the winter measurements here this could also be the case, and this is considered in section 5.5.2. However, for the summer measurements, where emission occurs, it is clear that the simple resistance analogy using r_c is not appropriate. Here, the assumption of zero surface concentration of the r_c interpretation breaks down, since a surface concentration must exist for emission to occur. Additionally in these cases, V_d is dependent on air concentration, and though it may be calculated (with negative values denoting emission), it loses its usefulness, so that it is not given here. The values of

site, campaign	no of runs	$u\{1\ m\}$ ($m\ s^{-1}$)	$T\{z_o'\}$ (°C)	r_{a+b} {1 m} * ($s\ m^{-1}$)	$\chi\{1\ m\}$ ($\mu g\ m^{-3}$)	Deposition Flux NH_3 ¶ ($ng\ m^{-2}\ s^{-1}$)	$V_d\{1\ m\}$ ($mm\ s^{-1}$)	r_c † ($s\ m^{-1}$)	$\chi\{z_o'\}$ ($\mu g\ m^{-3}$)	$\chi\{z_o''\}$ ($\mu g\ m^{-3}$)
Bush 6/1988 (cut forage grass)	17	1.47	14.0	58.8 *min.:* *max.:*	0.21 *0.00* *0.96*	-7.7 *-22.2* *1.3*	emis. *emis.* *12.8*	emis. *-15* *emis.*	0.59 *-0.02* *1.82*	3.1 *-0.9* *7.3*
Bush 2/1989 (cut forage grass)	6	6.08	0.6	56.0 *min.:* *max.:*	1.29 *0.54* *3.14*	14.5 *5.1* *35.1*	12.3 *6.5* *20.6*	25 *-7.5* *80*	0.19 *-0.26* *0.42*	— — —
Stenton 6/1989 (barley) ‡	9	1.70	12.7	48.8 *min.:* *max.:*	0.99 *0.47* *1.30*	-6.3 *-23.9* *4.7*	emis. *emis.* *5.3*	emis. *121* *emis.*	1.24 *0.57* *1.69*	2.3 *0.6* *7.4*
Stenton 6/1989 (wheat) §	4	—	16.1	—	1.51	—	—	—	—	—

Table 5.3 Summary of NH_3 exchange and environmental conditions for measurement campaigns over fertilized agricultural surfaces. Values in standard type are arithmetic means of runs (unweighted) apart from where noted. Minimum and maximum values occurring during measurement periods are given in italics. Notes: * reciprocal mean from arithmetic mean of V_m; † difference of mean r_{a+b} and mean r_t (mean r_t = 1/mean V_d); ¶ negative fluxes imply NH_3 emission; ‡ Values calculated using stability corrections from psychrometer temperature values; § within-canopy profiles only, reference height 1.1 m above ground level. Data abstracted from Appendix 3.

V_d and r_c are nevertheless given for the summer runs showing deposition to compare with the results in Chapter 4.

The emission flux may therefore be envisaged as depending upon the concentration at the site of emission, as well as the air concentration and resistances to transfer. The surface concentration at the emission site is presumably maintained by equilibrium with the surface, and as such may be referred to as a compensation point concentration, χ_{cp} (sections 1.4.3, 2.4.5).

The simplest estimate of χ_{cp} is the interpretation of the excess in the resistance analogy as $\chi\{z_o'\}$. This is valid for both deposition and emission situations. In the case of emission this represents the minimum mean concentration at the surface of the canopy elements, since it accounts solely for the transfer through the atmospheric resistances (r_a, r_b). Values of $\chi\{z_o'\}$ are given in Table 5.3 and range from 0.0–1.8 $\mu g\ m^{-3}$ for both the summer campaigns.

However, if further resistances exist in the emission pathway then the value of χ_{cp} will be greater than that predicted by $\chi\{z_o'\}$. In section 1.4.3 the concept of a compensation point driven from equilibrium with the intercellular solution of plants was introduced. In this case r_s provides an additional restriction to transfer. The estimate $\chi\{z_o''\}$ (equation 2.4.6) accounts for the extra resistance and values of this are also given in Table 5.3. At Bush 6/1988 stomatal resistance to water vapour, r_{sE}, which is similar to that for NH_3 (given similar molecular diffusivities), was estimated

by leaf chamber measurements (Appendix 3), while at Stenton bulk stomatal resistance, r_{sEb}, was measured by micrometeorological methods (equation 2.54). The values of $\chi\{z_o''\}$ were in the range -0.9–7.4 μg m^{-3} for both summer campaigns.

The estimate $\chi\{z_o''\}$ nevertheless needs qualification. Where other pathways for deposition occur, for example to leaf surfaces as might be expected from the results of Chapter 4, the estimated value will be less than a substomatal χ_{cp}. Alternatively, where emission occurs from the soil, $\chi\{z_o''\}$ overestimates a substomatal χ_{cp}. However, given that the resistance to diffusion though the canopy to the soil is greater than that to the leaf surfaces, $\chi\{z_o'\}$ may still be considered a minimum value.

Such distinctions cannot be made by the gradient method alone. An attempt to clarify the sources and sinks within the soil/plant system was therefore made by measuring profiles of NH_3 within the canopies. This was done at Bush 6/1988 and for the barley and wheat crops at Stenton.

In the next sections the results of ammonia exchange from each of the campaigns are considered in detail and related to environmental conditions. The results of the within-canopy profiles are also given to aid the interpretation of the exchange process.

5.5. Effects of environmental conditions on NH_3 exchange

Each of the flux measurement campaigns over agricultural surfaces provided data of sufficient quality to examine the time course of exchange and relate it to environmental conditions. The data shown for Bush 6/1988 were the most approximate of the campaigns, since air concentrations of NH_3 were small for most of the experiment (≈0.15 μg m^{-3}), however, the general trends here were still evident. Conversely, the data at Bush 2/1989 were particularly good, due to higher air concentrations of NH_3 (≈0.5–3 μg m^{-3}) as well as good performance of the sampling system. In this experiment all of the individual flux determinations were significantly different to zero (≈95% confidence limits). In order to show the precision that can be obtained under these circumstances, the confidence limits for $\chi\{1\text{ m}\}$, F_χ, r_c, and $\chi\{z_o'\}$ are given with the graphs for this site. Confidence limits of these variables for this and the other sites are also given in Appendix 3. For the graphs for the data collected at Bush 6/1988 and Stenton, confidence limits are not shown so as to retain clarity; in these graphs very approximate or unsure values are given in brackets.

As with the results in Chapter 4, surface wetness and night-time/day-time are shown diagrammatically (see Figure 5.3b). However, in addition at Bush 6/1988 chamber measurements of r_{sE} are given, while at Bush 6/1989 and Stenton, micrometeorological estimates of heat fluxes, r_{sEb} and humidity measurements are given, in order to

improve the quantification of surface conditions. At Bush 6/1988 and Stenton the values of r_{sE} and r_{sEb} are used to estimate $\chi\{z_o''\}$.

5.5.1 Bush 6/1988

The course of ammonia exchange and environmental conditions at Bush for the measurements made in 6/1988 are shown in Figure 5.3. The trend toward emission fluxes, noted above, is clear, with the maximum emission occurring in day-time runs when the crop surface was dry and at its warmest. These runs, however, also correspond to the most turbulent conditions, with highest $u*$, so that V_m is also at its largest. Since a large V_m increases the magnitude of the flux, it is not immediately clear from looking at the flux alone whether turbulence or surface conditions are the more important.

The surface conditions may be expected to control the flux by defining the equilibrium concentration, or compensation point (χ_{cp}), of the surface. $\chi\{z_o'\}$ provides an estimate of this, and removes the effect of turbulence, assuming that the exchange site is the roughness elements of the vegetation. Since $\chi\{z_o'\}$ shows the same pattern as the flux, of high values in warm dry conditions and low values when cool and wet, it may be concluded that these surface environmental conditions are important to the resulting flux. In addition it may be noted that V_m only affects the magnitude of the flux, so that this cannot account for the switch to deposition in wet conditions.

The direction of the flux depends on the difference between χ_{cp} and the concentration in the air, in this case referenced as $\chi\{1\ m\}$. As a consequence it might be expected that in low air concentration conditions emission would predominate, while in high air concentration conditions deposition would predominate. However, this is not seen in the results here. The period of highest air concentration, at the start of the experiment, corresponds to large emission fluxes; for the rest of the data, although air concentrations were consistently small, a range of emission and deposition fluxes occurred. It is clear that the major effect is the value of χ_{cp} at the surface, which varies considerably according to surface conditions.

In order to clarify the distribution of sources and sinks in the canopy, within-canopy profiles were measured at the end of the experiment on 20/6/1988. Two profiles of NH_3 were made in the day-time in warm conditions, the first with a dry canopy and the second with the canopy partly wet. These are shown in Figure 5.4 alongside the combined NH_4^+ profile for both runs. Unfortunately, because of logistical restrictions to the location of the sampling masts and a change in wind direction, only minimal fetch over the grass was available, so that the top height measurements do not reflect exchange over this surface.

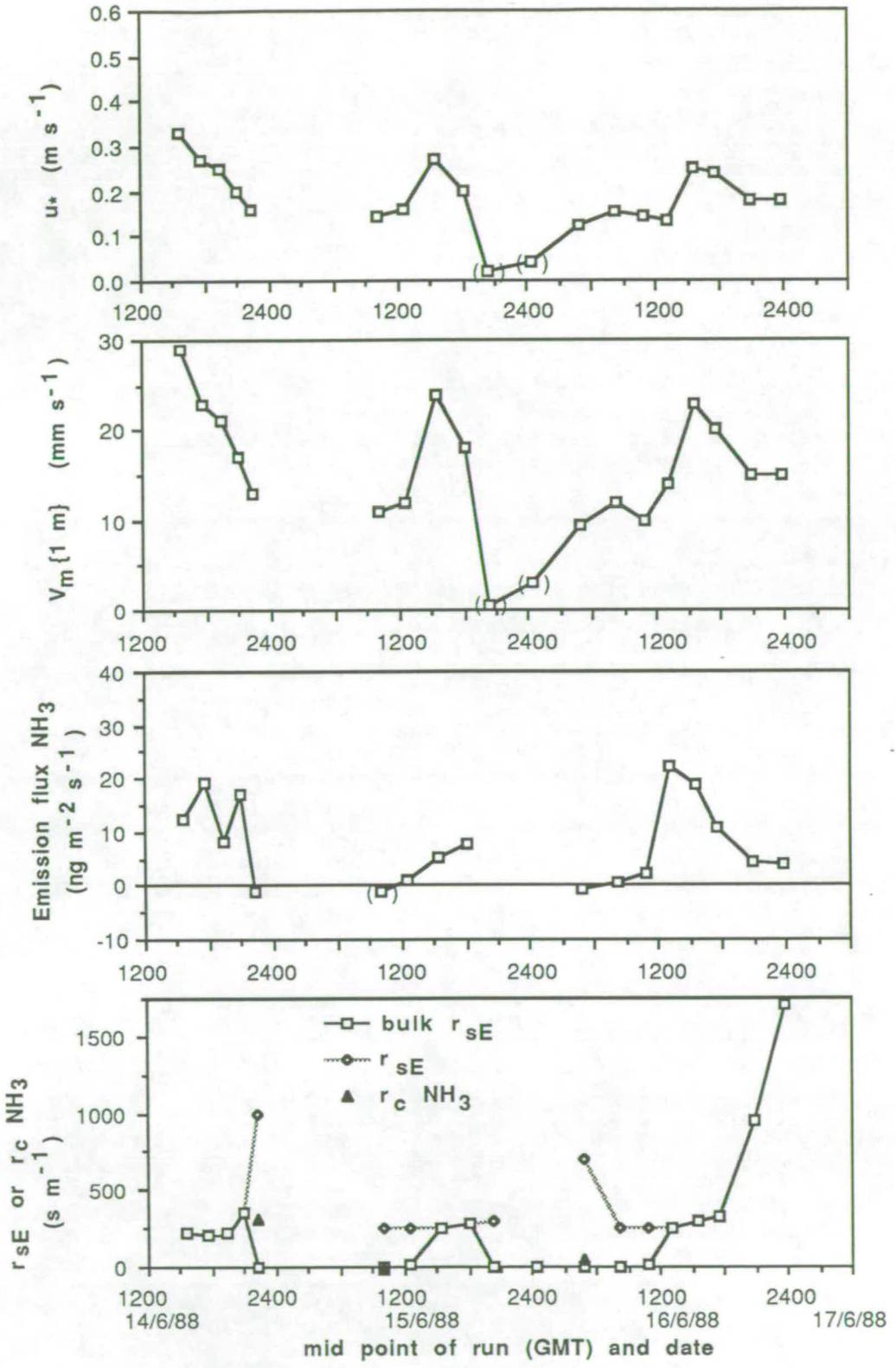

Figure 5.3a Course of ammonia exchange and environmental conditions over time at Bush 6/1988. Note: positive fluxes denote NH_3 emission. Figure continued overleaf.

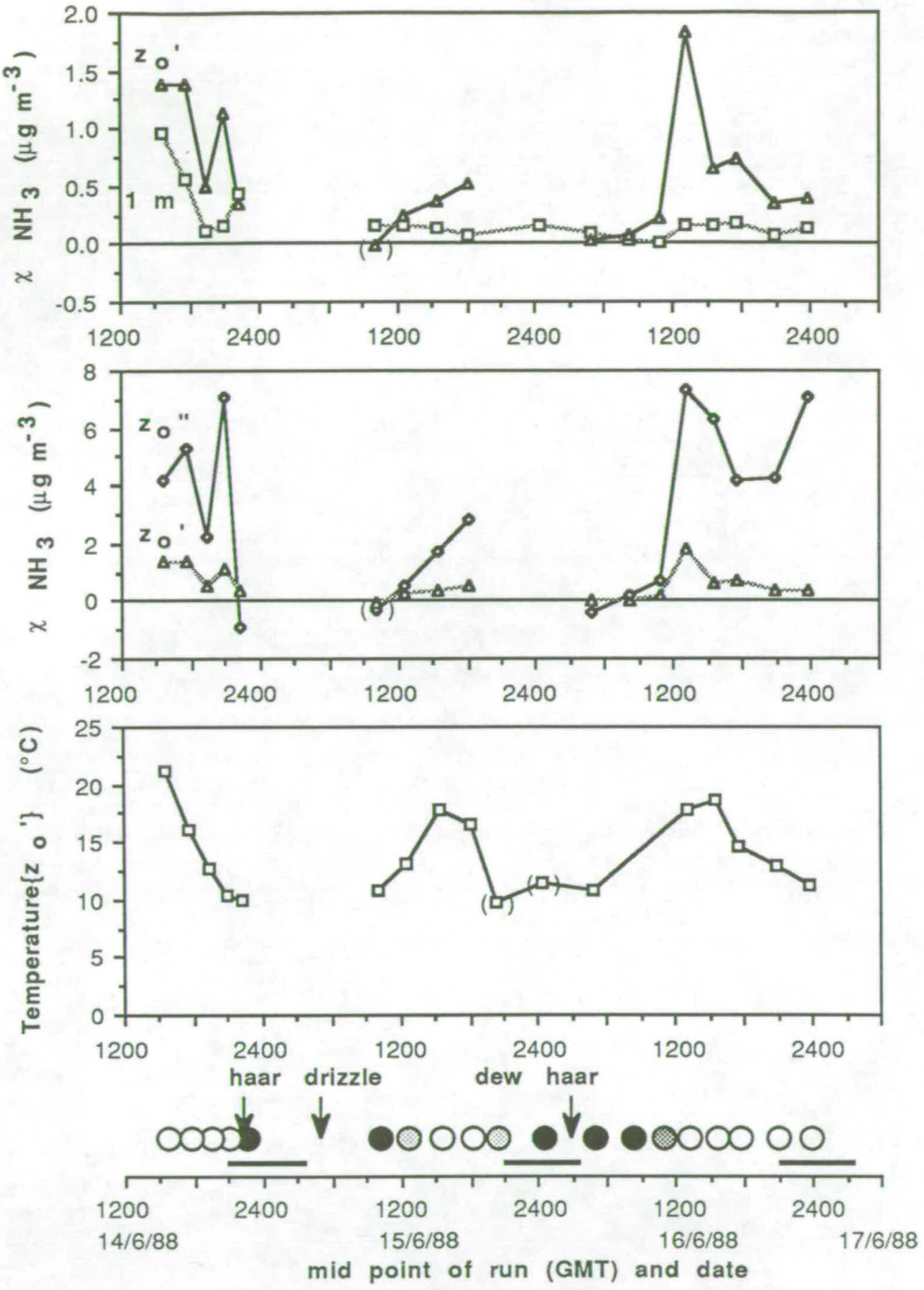

Figure 5.3b Course of NH_3 exchange and environmental conditions over time at Bush 6/1988. In these and the succeeding graphs vegetation canopy wetness and dryness are divided qualitatively into four classes shown right.

In addition a symbol for frozen surfaces is given. Vertical arrows denote precipitation events, while a horizontal solid bar denotes night-time.

dry
slightly wet
moderately wet
completely wet
frozen surface
precipitation
night-time

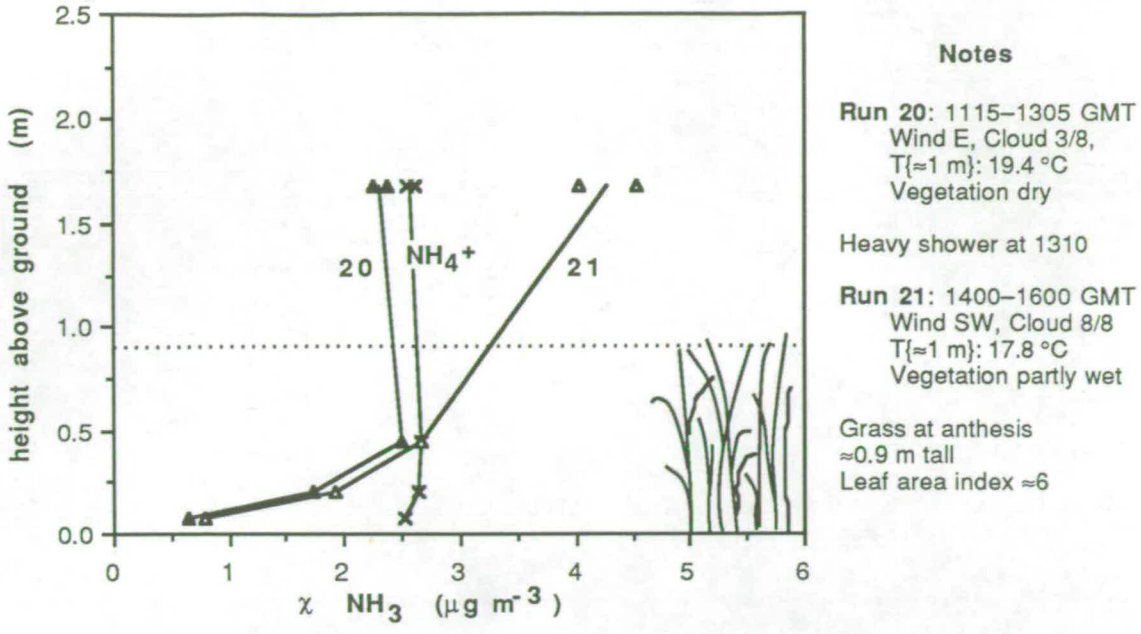

Figure 5.4 Within-canopy profiles of NH_3 and NH_4^+ at Bush 20/6/1988. Due to limited wind fetch, measurements at 1.7 m do not reflect exchange processes of the surface.

In accordance with the surface exchange results, discussed earlier (section 4.4.), the NH_4^+ profile shows only minor changes with height. Conversely, the NH_3 concentrations within the canopy in both runs decrease steeply towards the ground. This implies NH_3 deposition, although it is not clear from the profiles whether the soil or lower vegetation was the main sink. It is clear however, that if emission of NH_3 were occurring, as would be expected at least for the conditions of the first run, the soil would not be the source of that emission. By default then, the vegetation itself must be the source of emission in this campaign — the most likely mechanism for this being a substomatal compensation point.

Given this reasoning, stomatal conductances were measured in order to estimate χ_{cp} by $\chi\{z_o''\}$. Values of leaf r_{sE} found from chamber measurements (Appendix 3), were divided by the leaf area index to give estimated canopy r_{sE}. The values of canopy r_{sE} are graphed in Figure 5.3 alongside values of r_c for NH_3 where deposition occurred. The r_{sE} results were then used to estimate $\chi\{z_o''\}$, which is also given in Figure 5.3. For dry conditions the value of $\chi\{z_o''\}$ was in the range 2–7 $\mu g\ m^{-3}$. For the wet conditions values are close to zero, reflecting a greater tendency to deposition in these conditions. However, in wet conditions r_{sEb} approaches zero. If a zero value is used in these cases, the estimate $\chi\{z_o''\}$ simply becomes $\chi\{z_o'\}$, though this has little effect in the data here. In this case, the overall canopy or net χ_{cp} is estimated, and any substomatal χ_{cp} is clearly inaccessible, as the exchange with the wet surface dominates.

5.5.2 Bush 2/1989

The surface exchange results for the measurements over the same field at Bush in 2/1989 are given in Figure 5.5. The measurements were made largely over snow, which was melting for much of the time, and over the wet vegetation surface after most of the snow had melted. A consistent pattern of deposition is seen throughout these runs, which agrees well with the summer 6/1988 measurements where deposition occurred in cool wet conditions. The deposition was mostly rapid with small r_c, though exceptions are considered below. However, despite high windspeeds, $V_d\{1$ m$\}$ remained small (6–20 mm s^{-1}) as a result of the small roughness length, z_0, of the snow which limited V_m.

In addition to the qualitative assessment of surface wetness, surface conditions estimated by the gradient method are also shown in Figure 5.5. The wetness of the surface is confirmed by surface relative humidities (RH$\{z_0'\}$) of ≈100%, and near zero saturation vapour concentration deficits (SVCD$\{z_0'\}$) throughout the campaign. Values of r_{sEb} were also estimated, though for much of the period the vapour fluxes were very small, so that these are rather approximate. The small fluxes result from the cooling of the air at the surface by the snow, so that evaporation was reduced, even causing vapour deposition in some runs. The flux was greater for the final run, after most of the snow had melted, making the r_{sEb} estimate more precise. As expected for the wet surface, this is close to zero.

As a consequence of these conditions, surface wetness, which was a major factor in the exchange pattern at Bush 6/1988, is not a factor in the variation of the results here. Conversely, a relationship between exchange and surface freezing may be present in the data. For most of the runs the surface was either melting snow or wet vegetation, however, during two runs in the night a light frost was observed. This cooling is confirmed in the estimates of $T\{z_0'\}$, although for the runs as a whole temperatures did not drop much below zero. During this period significant values of r_c and $\chi\{z_0'\}$ were recorded (r_c up to 80 s m^{-1}), whereas for the other runs these were mostly not significantly different from zero (≈95% confidence limits, see Figure 5.5.). It is possible that the limitation to deposition was the result of the frozen conditions, although it is not clear from the micrometeorological analysis which of the two estimates of the excess is the more appropriate. However, given that the trend is more clearly seen in r_c, and that this was the favoured interpretation in the other deposition results of Chapter 4, it is more likely to be a concentration independent exchange with an r_c operating.

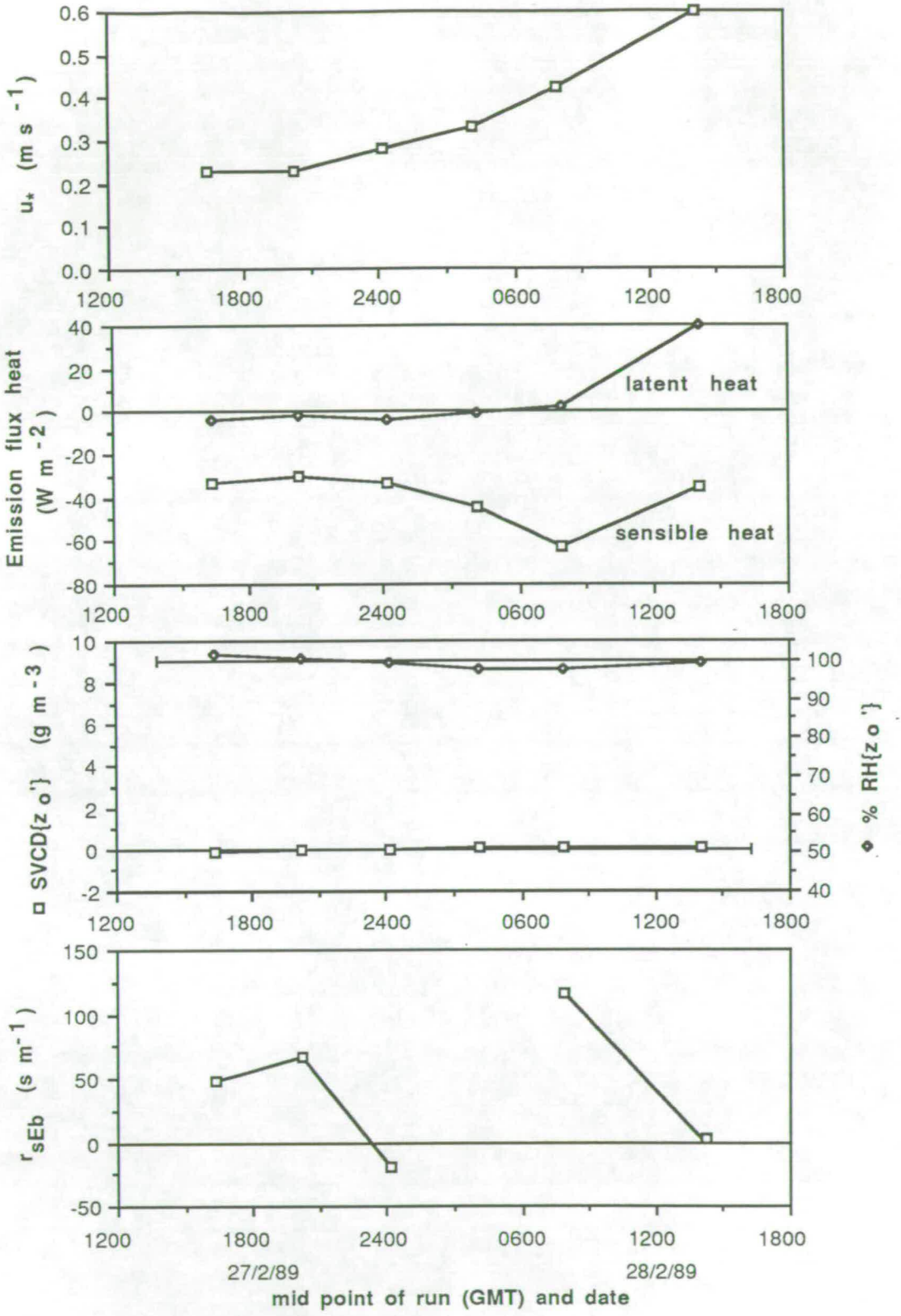

Figure 5.5a Course of ammonia exchange and environmental conditions over time at Bush 2/1989. Notes: positive heat fluxes denote emission; SVCD = saturated vapour concentration deficit; RH = relative humidity. Figure continued overleaf.

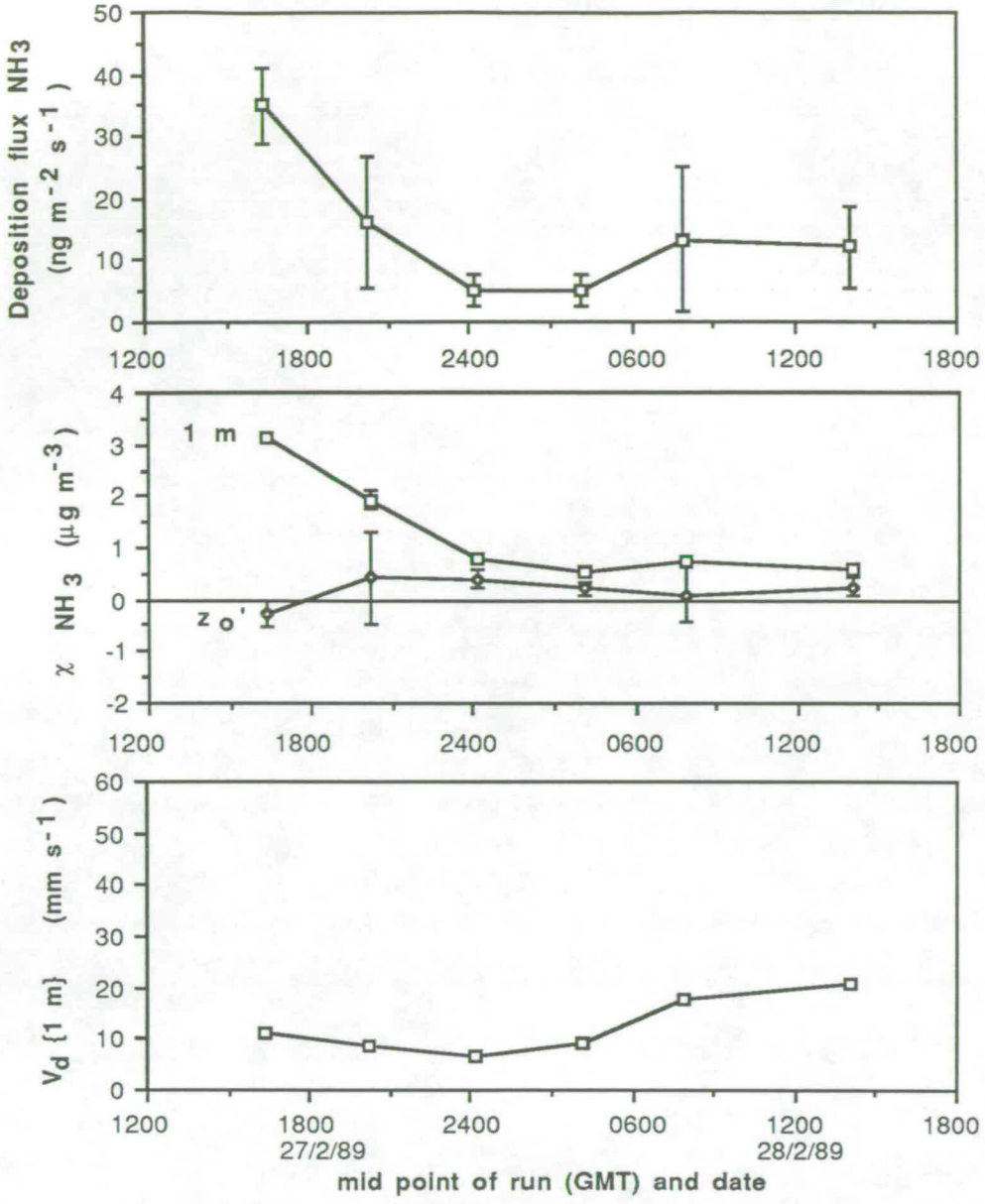

Figure 5.5b Course of NH_3 exchange and environmental conditions over time at Bush 2/1989. Note: positive fluxes of NH_3 denote deposition. Error bars are 95% confidence limits. Figure continued overleaf.

5.5.3 Stenton 6/1989: barley

The results of the measurements over the barley crop at Stenton are given in Figure 5.6. The measurements were made during a period of warm weather and present a similar overall pattern of surface exchange to the study at Bush 6/1988, with emission fluxes for most of the runs between 2–20 ng m^{-2} s^{-1}. For one run the canopy was wet from dewfall and deposition occurred, although a surface resistance was present here of ≈130 s m^{-1}.

As noted in section 5.3, temperature and humidity were measured by two separate systems, each with two reference heights: an aspirated psychrometer system (system 1)

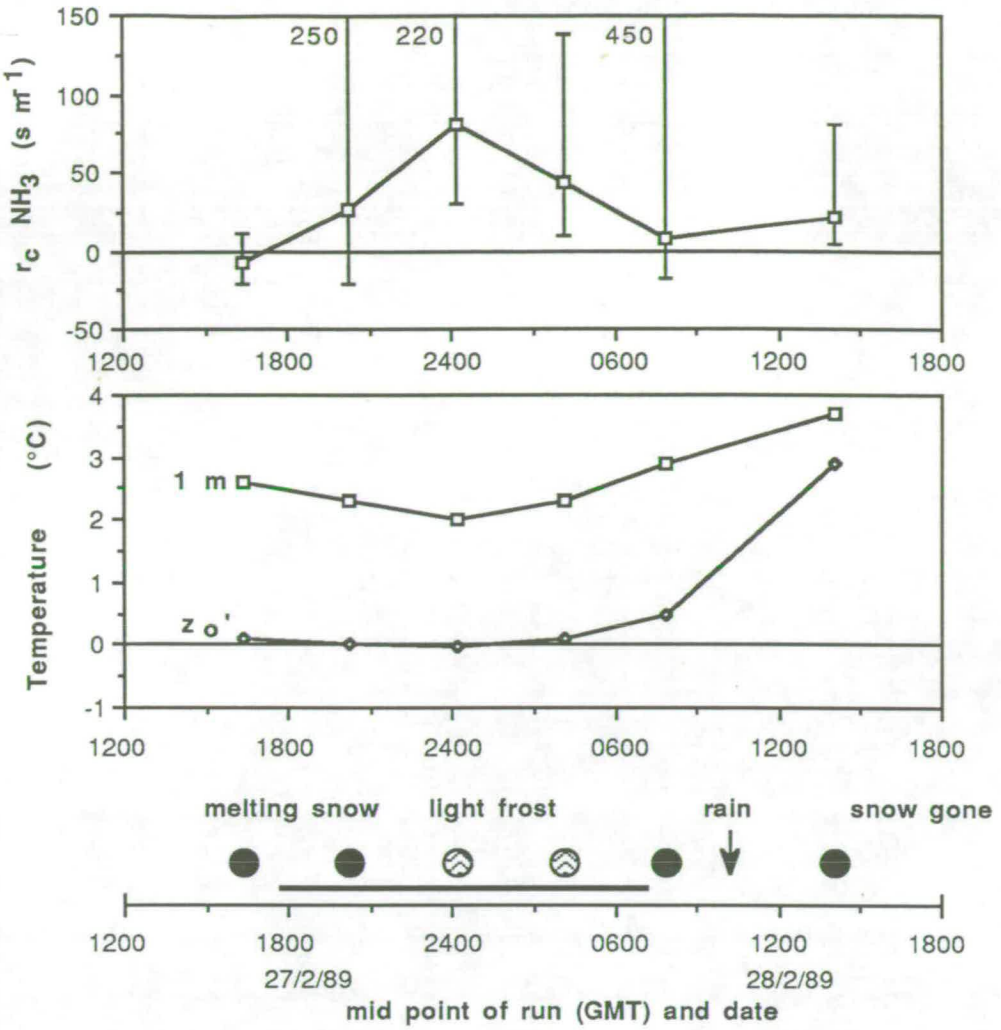

Figure 5.5c Course of NH_3 exchange and environmental conditions over time at Bush 2/1989. Explanation of surface conditions symbols given in Figure 5.3. Error bars are 95% confidence limits.

and a fine thermocouple and dewpoint hygrometer system (system 2), although the latter was not available for the whole experiment. In Figure 5.6, black symbols represent measurements using System 1, and open symbols System 2.

The general response of the two systems was similar, with good agreement of temperature gradients, as shown by the sensible and latent heat flux estimates. However, a consistent difference was evident in the absolute value of the temperature estimates ($\Delta T\{1\text{ m}\}$: 1.4 °C), which propagated into other estimates (*e.g.* $T\{z_o'\}$, $RH\{z_o'\}$, $SVCD\{z_o'\}$, r_{sEb}). It was thought that the discrepancy might result from a loss of calibration or wet/dry bulb interactions in System 1. However, applying corrections to the temperature estimates here actually removed existing good agreement of absolute humidity for the two systems. It is possible that the temperature sensors of System 2 (independent of the humidity measurement) were at fault, although this is not resolved.

As at Bush 6/1988, the interpretation of the NH_3 flux in relation to environmental conditions is complicated, since it shows agreement with trends in several variables. From the graphs in Figure 5.6, the tendency to larger emission fluxes, occurred in conditions where the surface conditions were warm and dry ($T\{z_o'\}$, RH$\{z_o'\}$, SVCD$\{z_o'\}$, wetness) with large sensible and latent heat emission fluxes, stomata were open (day-time/night-time) and turbulence was large ($u*$). Consequently it is again difficult to ascertain the relative importance of these different factors, though all may be expected to be relevant, either through modifying a surface χ_{cp}, or the resistance to transfer away from the surface.

For the emission runs, $\chi\{z_o'\}$ is the minimum surface potential for emission, and the values for these runs were 0.9–1.7 $\mu g\ m^{-3}$. For the deposition run, $\chi\{z_o'\}$ is the maximum emission potential, which was 0.6 $\mu g\ m^{-3}$. However, apart from the difference of this one run, $\chi\{z_o'\}$ shows little relationship to the environmental parameters noted above.

In an attempt to identify the source of the NH_3 emission, two within-canopy profiles were made, and are given in Figure 5.7. This shows NH_3 concentrations increasing steeply towards the ground, with emission occurring above the canopy (runs 8 and 9). However, since the canopy was rather open in this example, with bare ground visible from above, and leaf tissue down to ground level, it is difficult to attribute the cause of the emission with certainty to either the soil or the vegetation.

As a consequence, it is not possible to confirm the validity of the estimates of $\chi\{z_o''\}$ also shown in Figure 5.6. These are derived using the r_{sEb} results, and, given the difference between the estimates of the two temperature and humidity systems, both sets of $\chi\{z_o''\}$ are shown. The best estimates of $\chi\{z_o''\}$ for dry conditions are in the range 1.3–3.1 $\mu g\ m^{-3}$. If soil emission is occurring in addition to transfer through leaf stomata, these values will be over-estimates of a substomatal χ_{cp}. It is noticeable that despite large differences in the two system estimates of r_{sEb}, the general trends in $\chi\{z_o''\}$ are similar, and show a positive relationship with the environmental conditions noted above.

Alternatively, it is possible that emission from the soil dominates the exchange process. However, a resistance model for diffusion through the air from the soil surface is unavailable in this study, so that a χ_{cp} estimate in the case of soil emission is not given. Nevertheless, an extra resistance in addition to r_a and r_b terms, would be present, accounting for the diffusion through the lower crop layers. It is therefore possible that such a χ_{cp} would show broadly similar patterns to $\chi\{z_o''\}$, and again follow the trends of environmental conditions.

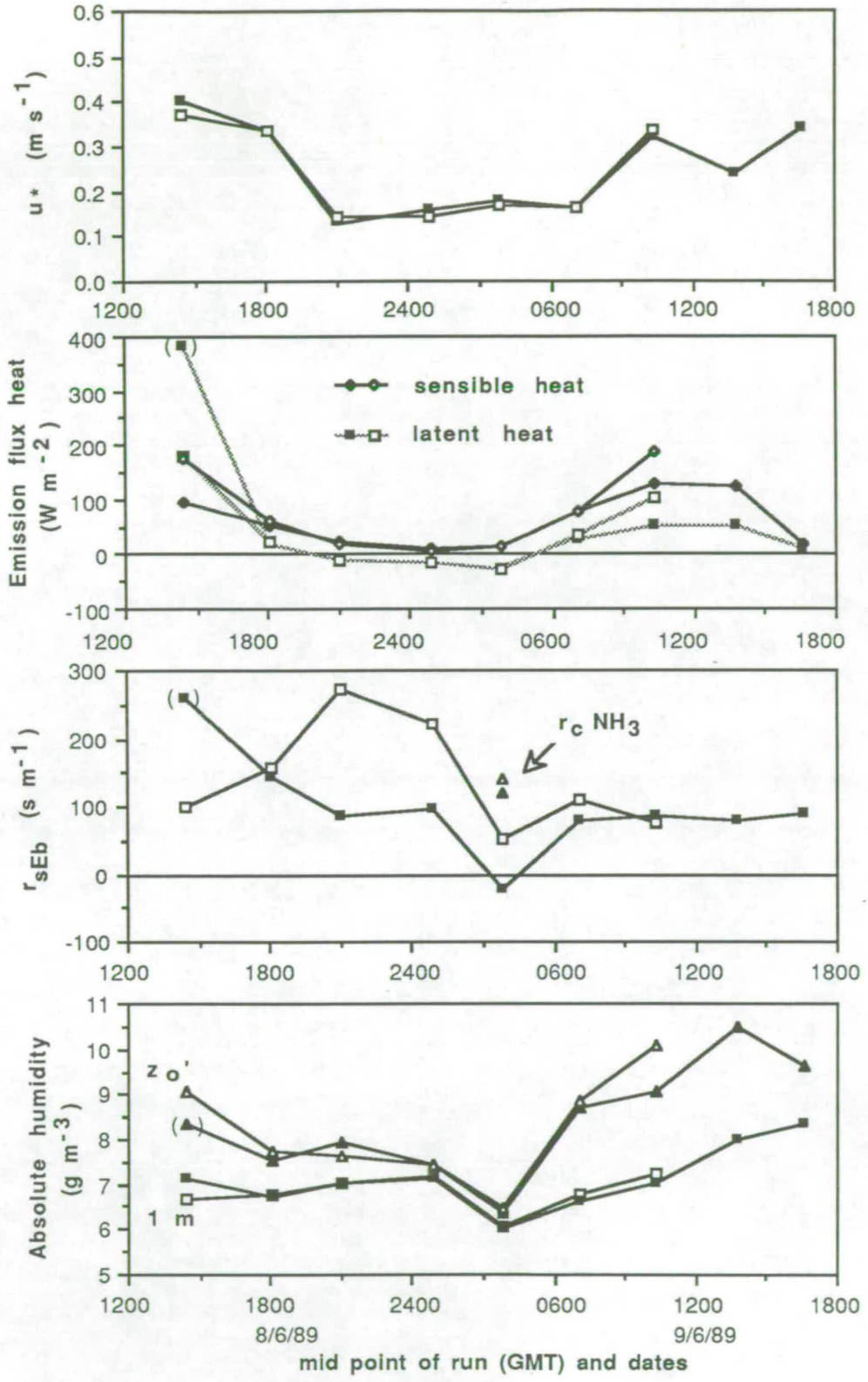

Figure 5.6a Course of ammonia exchange and environmental conditions over time at Stenton 6/1989 (barley). Note: filled symbols denote measurements calculated using System 1; open symbols denote System 2 (see text). Figure continued overleaf.

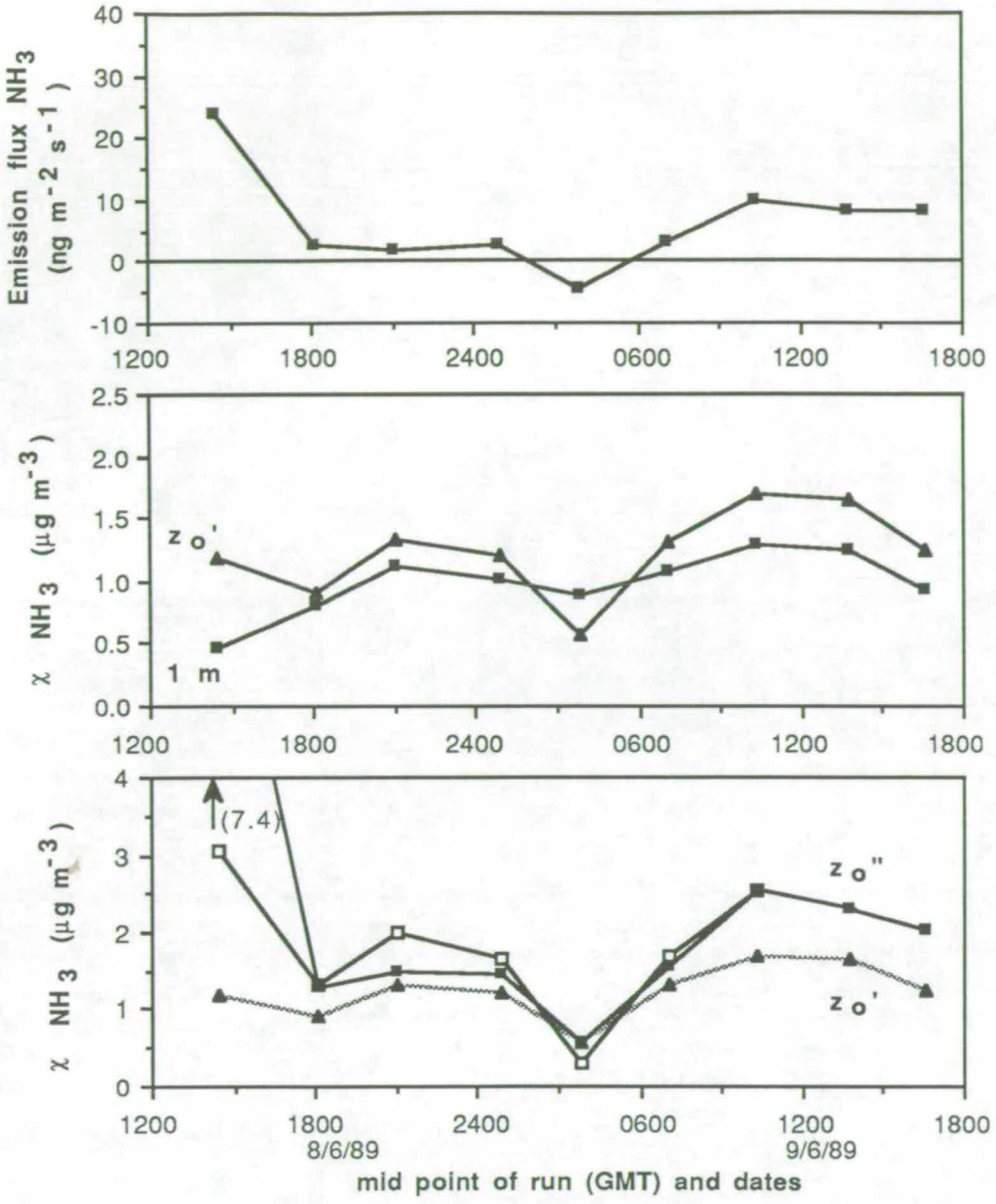

Figure 5.6b Course of ammonia exchange and environmental conditions over time at Stenton 6/1989 (barley). Notes: positive fluxes denote emission; filled symbols denote measurements calculated using System 1; open symbols denote System 2 (see text). Figure continued overleaf.

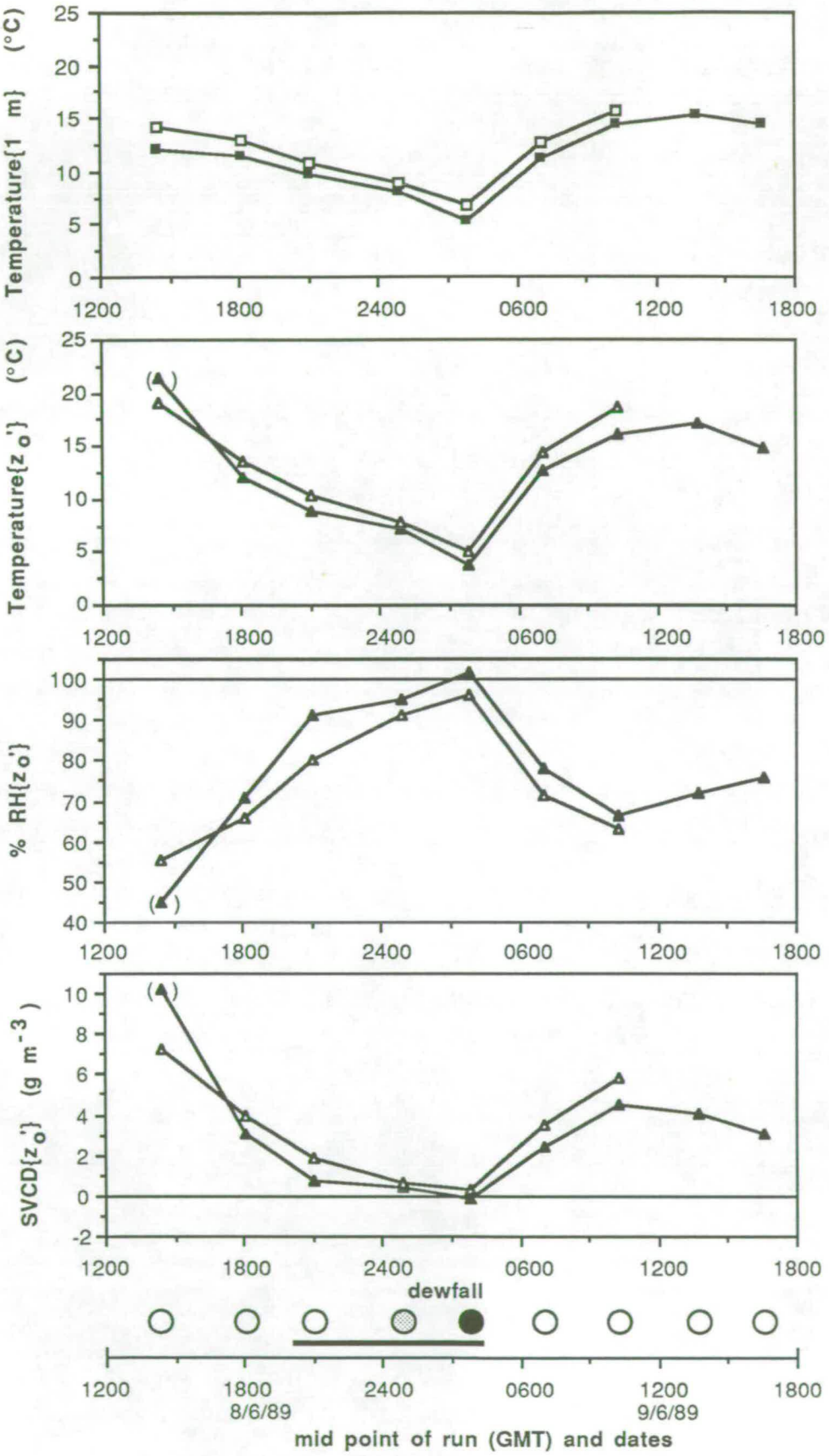

Figure 5.6c Course of ammonia exchange and environmental conditions over time at Stenton 6/1989 (barley). Note: filled symbols denote measurements calculated using System 1; open symbols denote System 2 (see text). Explanation of surface conditions symbols given in Figure 5.3.

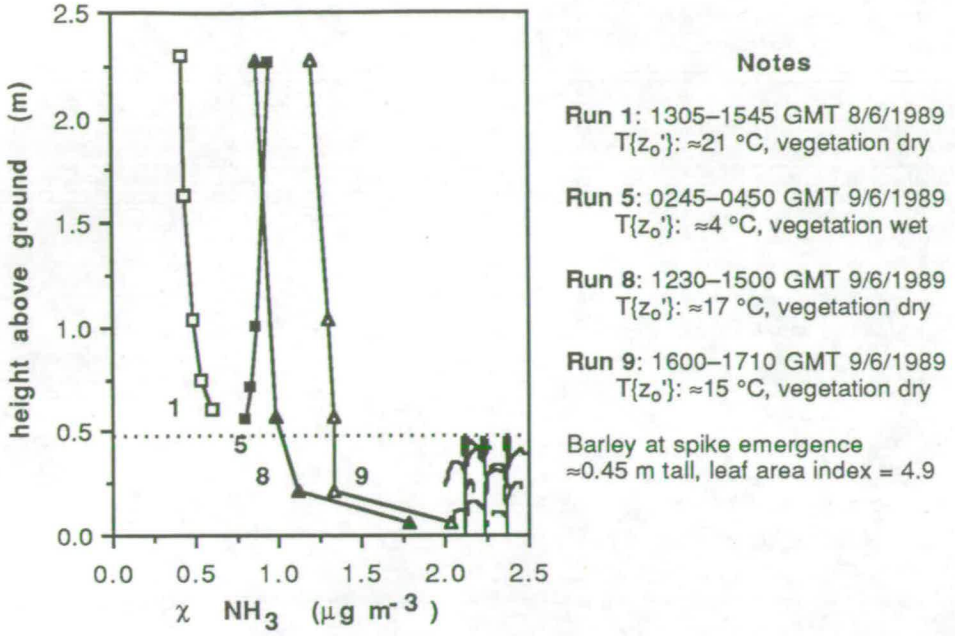

Figure 5.7 Profiles of ammonia within and above a barley crop at Stenton 6/1989. All runs gave emission of ammonia except run 5.

In summary, both stomatal and soil ammonia potentials, χ_{cp}, are possible causes of emission observed at this site. Emission from either or both would be consistent with environmental variables relating to surface temperature, humidity and wetness — variables which would be expected to be important from a knowledge of the behaviour of NH_4^+ in solution at the surface.

5.5.4 Stenton 6/1989: wheat

As a result of the uncertainty over the source of emission from the barley in the above example, it was decided to make more within-canopy profile measurements for a crop under similar management as the barley. These were made in a wheat crop adjacent to the barley that was at a later stage of development (grain filling stage, 0.9 m high), with full canopy closure. As a consequence of the similar management, it was expected that NH_3 emission would occur, while the tightly closed canopy would result in the NH_3 concentrations being largely controlled by processes within the canopy.

The profiles of four NH_3 sampling runs (runs 10–13) and a combined NH_4^+ profile are given in Figure 5.8. Temperature and humidity profiles were also measured using the psychrometers and results from these are given in Figure 5.10. In accordance with the other estimates of particulate exchange (section 4.4), the NH_4^+ gradient is approximately zero. Conversely NH_3 shows a rapid increase in concentration toward the ground, the gradient being approximately logarithmic with distance from the ground as is shown in Figure 5.8b. This suggests a diffusive gradient away from a soil emission site.

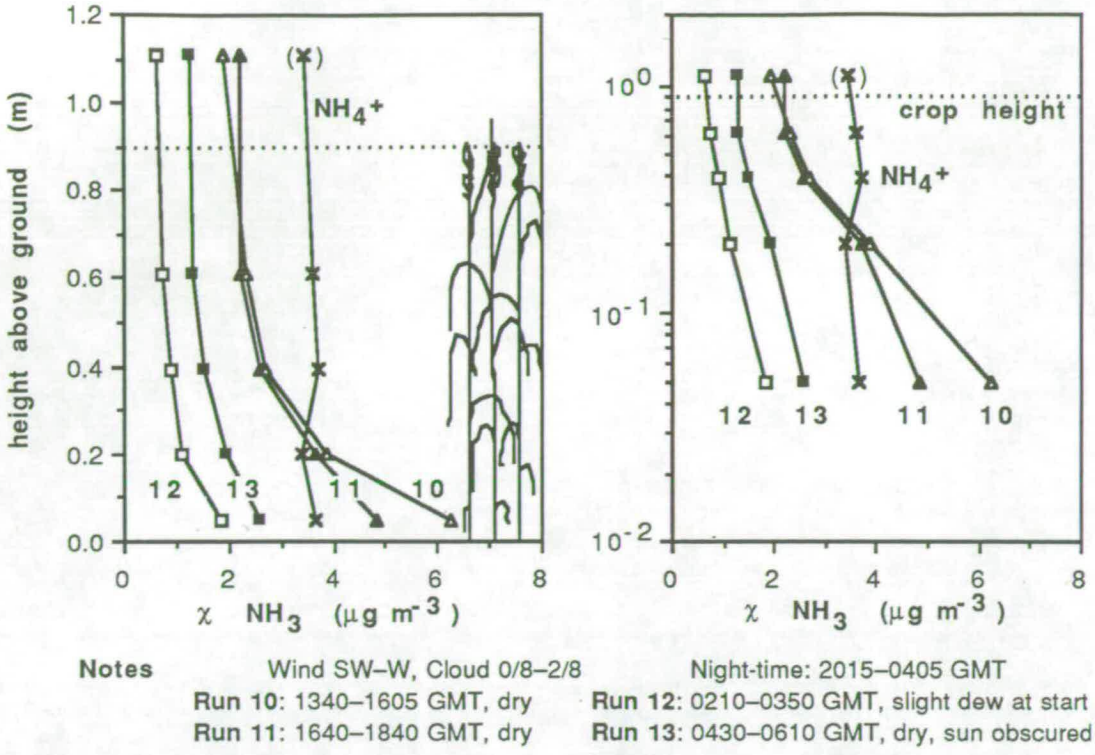

Figure 5.8 Profiles of NH_3 and NH_4^+ within a wheat crop at Stenton 20–21/6/1989.

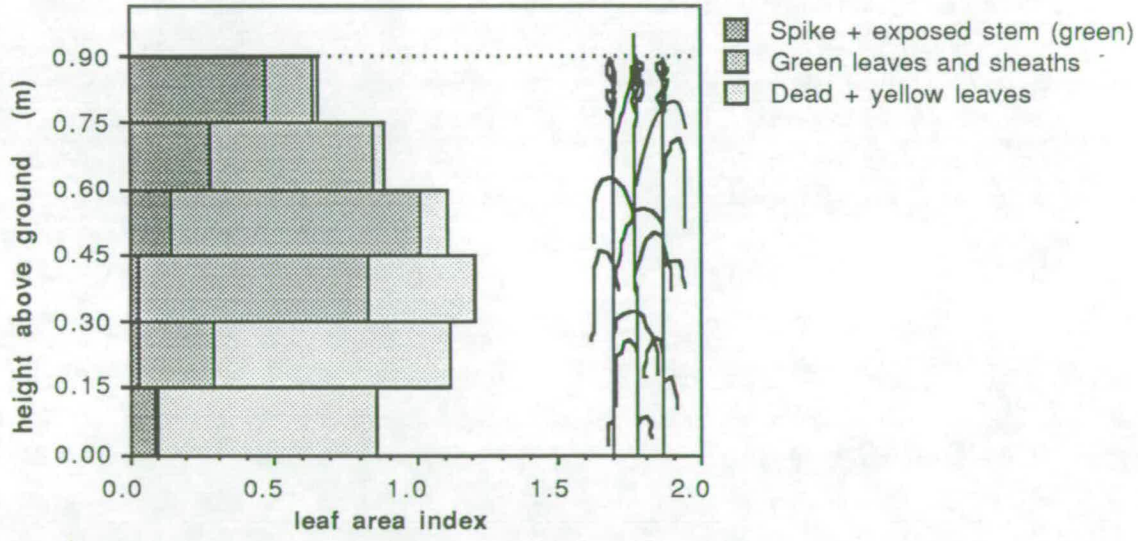

Figure 5.9 Distribution of component leaf area index for three classes of plant material in a wheat crop at Stenton 6/1989. Total leaf area index estimate = 5.9. This is probably a slight underestimate, since the sample material was partly dried by the time of analysis.

The leaf area index of the crop was also measured and this is shown in Figure 5.9. The vegetation sample material was divided into 0.15 m bands above the ground, and also into three classes. It may be seen that a considerable portion of the above-ground vegetation is dead or yellow leaves, situated mostly near the ground. This somewhat confounds the diagnosis of soil emission, since it has been observed elsewhere

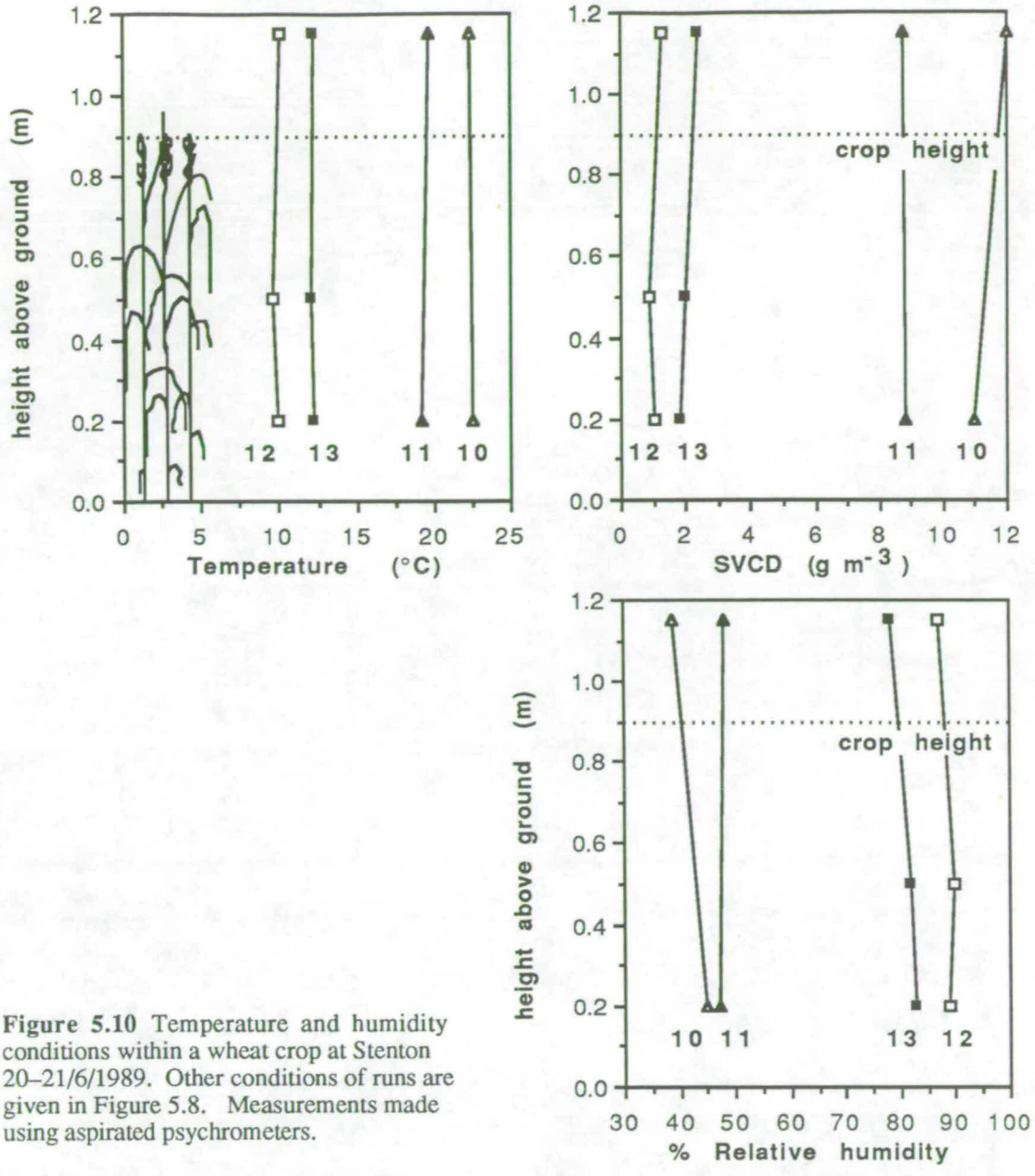

Figure 5.10 Temperature and humidity conditions within a wheat crop at Stenton 20–21/6/1989. Other conditions of runs are given in Figure 5.8. Measurements made using aspirated psychrometers.

that senescing vegetation may emit NH_3 (see section 1.4.3). Since this leaf class is most abundant near the ground, it is possible this was the cause of the emission. Consequently for this example also, it is not possible to be definite over the source of the emission; either or both of soil and vegetation emission are possible.

Despite this, the results are still useful to confirm the effect of environmental conditions on the NH_3 exchange process, on the assumption that the concentrations within the canopy reflect the size of the overall χ_{cp}. Again with these results, concentrations are largest in warm, low humidity runs in the day, with stomata open, and least in colder runs with high humidities and stomata closed, at night.

5.6. DISCUSSION

The results of the ammonia exchange measurements presented in this chapter separate clearly between the winter and summer-time campaigns, with ammonia deposition occurring throughout the former, and a bi-directional exchange, with emission predominating, in the latter.

The pattern of deposition to the wet vegetation or melting snow for the Bush 2/1989 measurements is largely in agreement with the results for natural and unfertilized surfaces in Chapter 4, with small surface resistances, all less than 30 s m^{-1}. No runs were made with a dry canopy in winter, but as the surface is rarely dry in winter, the results here are expected to typify the winter exchange pattern. The data also included a period of night frost, where significant r_c and $\chi\{z_o'\}$ were recorded, which probably relate to the freezing of the snow. It is not possible to conclude from these data which of these excesses is the most appropriate, but the relationship with freezing is most clear with r_c, which would also be consistent with the results over natural surfaces as at Great Dun Fell, Harwell, and Wether Law. In these cases, even in low concentrations no emission occurred, confirming a negligible surface concentration. However, measurements during periods of low concentrations in winter at Bush would be needed to confirm this.

The interpretation of the excess as r_c is also reasonable from a consideration of the transfer processes. The development of ice would be expected to limit free absorption of ions at the surface, as the lattice restricts diffusion into the surface water. Surface adsorption however, might still be efficient.

The exchange pattern at both sites studied in summer contrasts strongly with the winter results, with emission occurring for much of the time despite the large time period between the measurements and crop fertilization. Nevertheless, during periods in these experiments when the surface was wet, deposition was recorded. In these cases at Bush 6/1988 the data are approximate, so that r_c and $\chi\{z_o'\}$ are imprecise, however the deposition run at Stenton 6/1989 was well quantified, and here a large excess occurred (r_c = 130 s m^{-1}, $\chi\{z_o'\}$ = 0.6 $\mu g\ m^{-3}$).

The interpretation of the surface exchange process in the summer data also differs to that for the winter and natural surface data. Here, it is clear that since emission may occur, the assumption of a concentration independent rate of exchange (V_d) and zero surface concentration fails. Some form of crop or soil compensation point concentration (χ_{cp}) must exist to drive the emission. In this case, the resulting flux depends on the χ_{cp}, the concentration in the air, and the resistances to transfer between them.

It is therefore of interest to be able to estimate χ_{cp} so that the flux may be modelled using it, $\chi\{1\ m\}$ and the resistances. The estimate $\chi\{z_o'\}$ accounts solely for the atmospheric resistances and represents the mean surface concentration in the absence of any surface resistances to emission. Conversely where the emission entails further resistances, $\chi\{z_o'\}$ represents a minimum value of the surface concentration. This latter possibility is most probable, as the two expected sites for emission are either emission through stomata, or from the soil.

A stomatal emission process is the simpler to treat of these two possibilities, since the exchange elements are the leaves, with atmospheric transfer accounted for by r_a and r_b. The extra resistance for diffusion through the stomata, r_s, is also measurable by well known techniques using either chamber stomatal conductance estimates for water vapour, r_{sE}, or micrometeorological bulk stomatal resistance measurements, r_{sEb}. These may then be used to calculate the surface concentration estimate $\chi\{z_o''\}$. In the case of emission through the stomata, the suggestion is that the intercellular solution in the plant tissue has a concentration of NH_4^+ controlled by plant metabolism, which has an equilibrium atmospheric NH_3 concentration. Hence, with air concentrations below this, emission occurs through the stomata, and when concentrations are above it deposition occurs by the same route (see section 1.4.3).

For the measurements at Bush 6/1988, within-canopy profiles showed the vegetation canopy to be the source of the emission so that a stomatal χ_{cp} is the most probable mechanism for emission in this case. Here, soil emission was not important, so that the only interference to the estimate of $\chi\{z_o''\}$ would be possible leaf surface deposition. If dry conditions only are considered, since it is clear from the results that wetness changes the exchange pattern, the estimates of χ_{cp} using $\chi\{z_o''\}$ are in the range 2–7 $\mu g\ m^{-3}$ (mean: 4.8 $\mu g\ m^{-3}$) for this campaign. Since leaf surface deposition may still be important to some extent, these values probably represent a minimum estimate. Consequently for deposition to occur through stomata, for this vegetation surface, would require air concentrations above this level. These did not occur in this experiment, and are much greater than the typical concentrations for this site (Chapter 6).

The other possibility for emission, noted above, is a soil compensation point, where free NH_4^+ in the soil solution has an equilibrium atmospheric NH_3 concentration which is higher than air concentrations. This may have been the case with the ammonia emission measured over the barley crop at Stenton 6/1989, although the within-canopy profiles were unable to distinguish this from possible canopy emission. For the measurements over wheat at Stenton, emission may again be from the soil. However here senescing vegetation at the base of the canopy is another possible

source. For this crop it is unlikely that green leaf material was the source given its distribution in the canopy. By comparison, emission from senescing vegetation was not possible at either Bush 6/1988 or the barley at Stenton, since for both of these campaigns measurements were made before the onset of any senescence.

In the case of NH_3 emission from the soil or senescing vegetation at Stenton, neither site of exchange is the roughness elements of the canopy to which r_a and r_b model transfer. Here the exchange site is near or at ground level, so that further resistances to transfer through the lower layers of the canopy will be present. However, a parameterization of these resistances is unavailable in this study, and this would be necessary before χ_{cp} could be estimated in this situation.

The importance of leaf surface deposition of NH_3 in wet conditions was mentioned above for the exchange process at Bush 6/1988. In this situation, despite the large values of $\chi\{z_o"\}$, there is an offsetting of any emission from a sub-stomatal χ_{cp}, against this deposition process. In addition, as discussed in Chapter 4, since leaf surface deposition may also occur in dry conditions, to some extent this is probably also important here. Such processes are presumably equally important where soil or vegetation is the source, so that internal cycling of ammonia within the canopy may be occurring. The tendency to net emission or deposition would thus depend on the balance of sources and sinks within the soil/canopy system.

The other point of interest with the summer measurements is the relationship to environmental conditions. In addition to the wetness/dryness effect discussed above, the emission fluxes recorded were greatest in warm and low humidity surface conditions. In part, this effect is confounded by the presence of greater turbulence in these conditions. However, since the largest surface concentration estimates also occur in these conditions, this is probably a real effect. Given that in the field conditions here low humidity conditions accompany warming, it is not possible to separate these effects from these measurements.

Chapter 6

Monitoring of atmospheric ammonia concentrations

6.1. INTRODUCTION

In the previous chapters, measurements of surface exchange of ammonia were reported for a variety of vegetated surfaces. However, these covered only a few selected days, so that the fluxes derived are poor approximations to the annual values, given the variability of exchange and dependence on air concentrations and environmental conditions. Because of this, the rates and factors controlling exchange were also examined. From an understanding of these, it is possible to relate the exchange process to environmental conditions and air concentrations occurring over the longer term, and to estimate fluxes for given surfaces on an annual basis. This estimation is the most simple for deposition situations where concentration independent rates of exchange apply, and the exchange process may be described by a deposition velocity (V_d) and component resistances. In these situations representative V_d may be derived from appropriate values of r_a, r_b and r_c, and these used with concentrations from long term monitoring to estimate an annual flux (see section 2.4.1).

In order to make such estimates it is therefore necessary to know the longer term atmospheric concentrations, provided by gas monitoring. For ammonia, however, there is very little monitoring data available. In Scotland, the main location of this study, until recently the only available values were those of the EACN total NH_x measurements (Stevenson, 1968; see section 1.2.3). Although recently the results of a country-wide NH_3 monitoring study by Harwell Laboratory (Didcot, Oxfordshire, U.K.) have become available (Atkins, 1988, pers. comm.; RGAR, 1990). A monitoring study of ambient NH_3 concentrations was therefore made here in order to provide an independent estimate of air concentrations, and to complement the flux measurements reported in the previous chapters. This enables annual NH_3 fluxes to surfaces to be estimated.

The sampling program lasted 18 months, with measurements being made at four rural sites in S. Scotland. These sites were chosen to represent background NH_3 concentrations, in accordance with the main emphasis of the flux measurements, and were therefore located away from known point sources of NH_3. In addition to these sites, shorter term measurements were made at several other locations, including farm, urban and indoor measurements.

The gas sampling system chosen for this study was a passive molecular diffusion based sampler known as a diffusion tube. This system, now in frequent use for NO_2 measurements (*e.g.* Atkins *et al.*, 1986; Colls, 1986; Miller, 1988), has recently been developed for sampling NH_3 (Hargreaves and Atkins, 1987; Hargreaves, 1989) and is also the method used in the Harwell Laboratory monitoring study (Atkins, 1988, pers. comm.). It is a low-input method, requiring no electricity on site, with a sampling time of the order of one to several weeks. Consequently, it is well suited to sampling at remote sites, requiring little maintenance and only occasional visits.

In the following sections, the theory of diffusion tubes, methods of study, and restrictions and precision of data are considered, followed by presentation and discussion of the results.

6.2. THEORY

The principle of a diffusion tube is to provide a diffusion path, of known length and cross-sectional area, between the atmosphere and a sink for the gas of interest. In this study, cylindrical tubes 71.3 mm long × 11.0 mm diameter were used, these being orientated vertically, with the lower end open to the atmosphere and the upper end closed off by an inert cap covering an acidified matrix (see section 6.3). The matrix in this system acts as an efficient adsorbent of NH_3, which sets up a concentration gradient between zero at its surface and atmospheric concentrations at the open end of the tube. Given that the molecular diffusivity of NH_3 and the dimensions of the tube are known, and that the total amount of NH_3 captured in a given period is found by chemical analysis, the mean air concentration may be found. The calculations for this are described below.

The representation of the flux of an entrained property by turbulent transfer was introduced earlier (section 2.2.). A similar relationship holds for transfer by molecular diffusion. For a gas of concentration χ ($\mu g\ m^{-3}$):

$$F_\chi = D\frac{\partial \chi}{\partial z} \qquad 6.1$$

where F_χ is the flux, with units here of $\mu g\ m^{-2}\ s^{-1}$, D is the molecular diffusion coefficient ($m^2\ s^{-1}$) at a given temperature and pressure, and z is the diffusion path-length (m).

Equation 6.1 may be applied for diffusion through a tube, from an open to a closed end, where an adsorbent of the gas of interest is located. Given a cross-sectional area, A (m^2), a tube length, z (m), and an exposure period, t (s), the total quantity of gas caught, Q (μg), is given as:

$$Q = A\,t\,F_\chi = A\,t\,D\frac{\chi_1 - \chi_2}{z} \qquad 6.2$$

Here χ_1 and χ_2 are the concentrations of the gas at the open and closed ends of the tube respectively. Since an efficient adsorbent is used, χ_2 equals zero and the equation may be simplified:

$$Q = \frac{AD}{z} t\,\chi_1 \qquad 6.3$$

The term AD/z may be seen to be the effective sampling rate, with units $m^3\ s^{-1}$. This is a constant for fixed tube dimensions, gas species, temperature and pressure. Thus if the quantity of gas collected on the adsorbent is found, and the sampling period known, the air concentration of the gas may be calculated.

Reviewing the literature on diffusion rates of NH_3, Hargreaves and Atkins (1987) calculated the mean of 5 available estimates to be $2.09 \pm 0.15 \times 10^{-5}\ m^2\ s^{-1}$, referenced for 10 °C, and this is used in the calculations here. Accounting for the tube dimensions given above, this gives an effective sampling rate of $2.79 \times 10^{-8}\ m^3\ s^{-1}$, or more conveniently $0.100\ dm^3\ hour^{-1}$.

The effect of temperature on the value of D nevertheless gives some temperature dependence to the quantity captured, Q. The relationship with D is of the form:

$$\frac{D_1}{D_2} = \left[\frac{T_1}{T_2}\right]^{1.5} \qquad 6.4$$

where T is in Kelvin, and the subscripts 1 and 2 represent two example cases (Hargreaves, 1989). However, since mean monthly temperatures for the U.K. range over only 3–17 °C (range of January and July means over the U.K., reduced to sea level; Chandler and Gregory, 1976), this only accounts for a difference in D of ≈7%, which is small compared to other sources of error (section 6.4.).

In this study mass/volume concentrations are used (*e.g.* $\mu g\ m^{-3}$) so as to relate the data easily to surface fluxes. However, some authors prefer to use volume fractions (*e.g.* parts per billion (10^9) by volume, ppbv). Formulae for converting between these two measures are provided in Appendix 1. Applying the relationship there (equation A1.1), to equation 6.3 above gives:

$$Q = \frac{AD}{z} t s \left[\frac{P\,M}{10^3\,R\,T}\right] \qquad 6.5$$

where s is volume fraction in ppbv, P is atmospheric pressure (Pa), M is the molecular weight of the gas ($g\ mol^{-1}$), and R is the general gas constant ($8.314\ Pa\ m^3\ mol^{-1}\ K^{-1}$). As a result of the temperature dependence in the conversion to a volume fraction, the overall temperature dependence of Q reduces to:

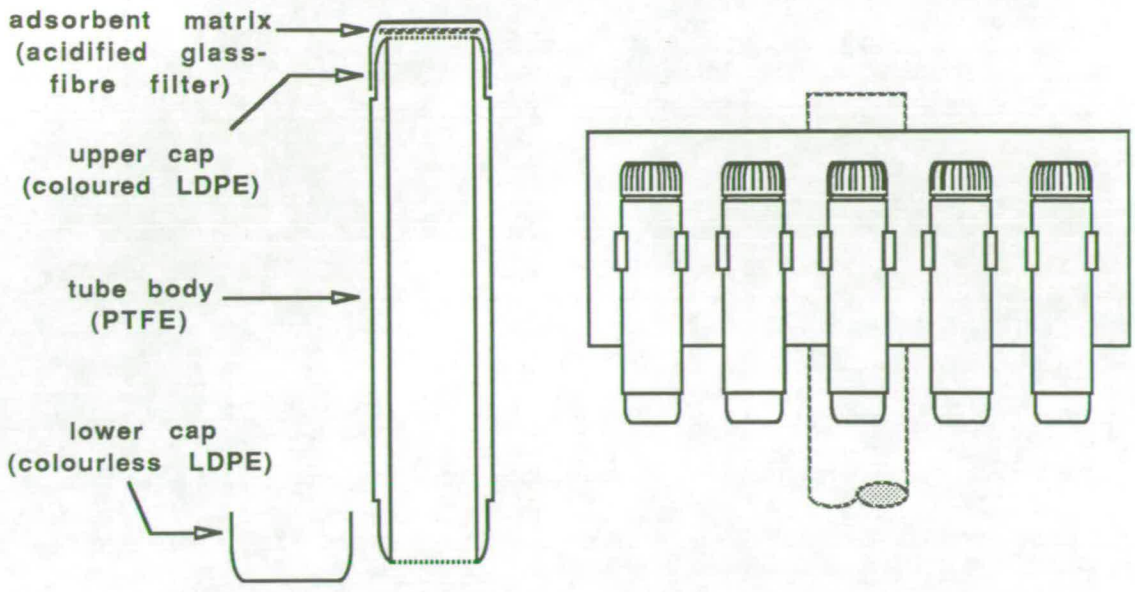

Figure 6.1 Diffusion tubes used for long term monitoring of ammonia. Tubes were set out in batches of 5 at 1.5 m above the ground. Sampling was started and stopped by removal and replacement of the colourless cap.

$$Q \propto sT^{0.5} \qquad 6.6$$

Consequently the temperature dependence is even less where volume fractions are used (2.5% for the example above), and this effect may again be ignored.

6.3. METHODS

A diagram of the diffusion tubes used in this study is given in Figure 6.1. The tubes were made of PTFE (polytetrafluoroethane), chosen as it is an inert material, so as to minimize deposition of the gas to the diffusion tube walls. The caps were of LDPE (low density polyethylene). Both were supplied by Gradko International Ltd., Winchester, U.K. In order to reduce confusion in the setting up of the tubes, a coloured cap was used to clamp the adsorbent matrix, while a colourless cap was used to seal the open end before and after sampling. The adsorbent matrix consisted of a glassfibre depth filter, impregnated with 1% H_2SO_4, so as to capture NH_3. The tubes were set out in batches of 5, clamped in a plastic holder, and mounted on a scaffold pole (Tubeclamps Ltd., Cradley Heath, West Midlands, U.K.) at 1.5 m above the ground.

The main tasks of the method were the preparation of the tubes, their setting up and exposure, the chemical analysis of the adsorbent matrix, and the calculation of air concentrations. These are outlined in the following sections.

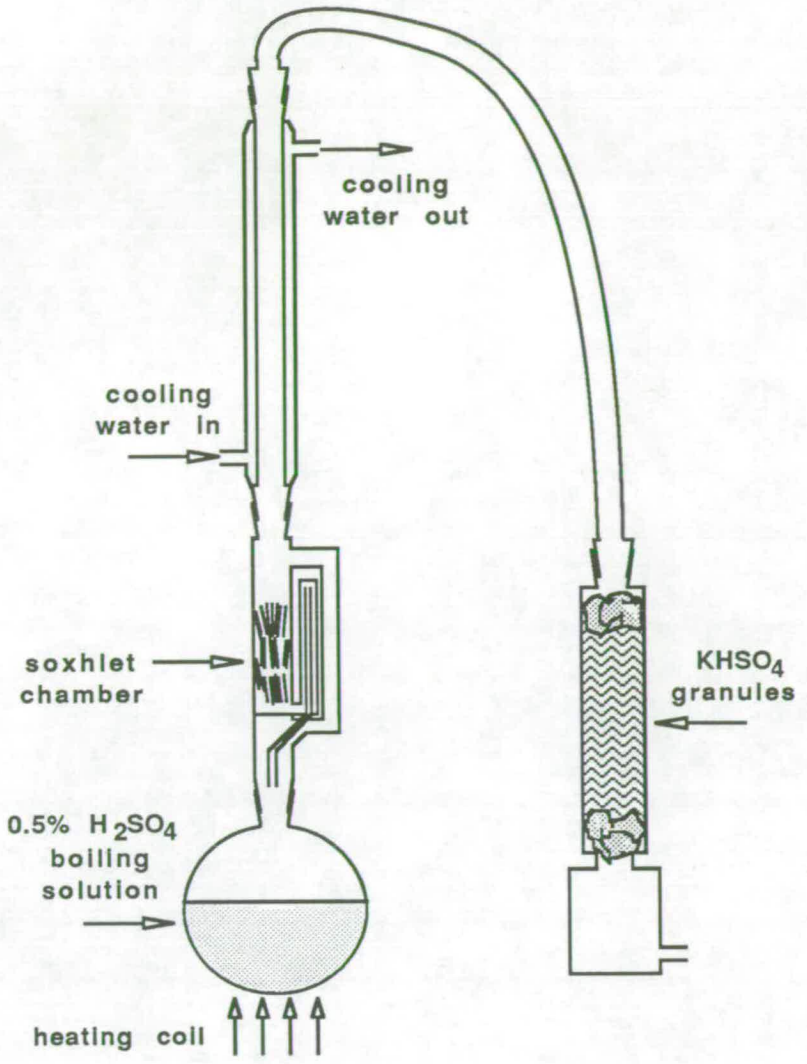

Figure 6.2 Apparatus for pre-extracting diffusion tube adsorbent discs. The discs in the Soxhlet chamber are cleaned by collected condensate which repeatedly flushes back into the boiling solution. The $KHSO_4$ tower serves to prevent recapture of ammonia from laboratory air. Approximate scale 1:5.

6.3.1 Preparation of ammonia diffusion tubes

Since both air concentrations of NH_3, and the effective sampling rate of the tubes are small, it is important to minimize the size and variability of the blank diffusion tubes. The focus of preparation of the tubes was therefore the pre-extraction of the adsorbent discs, and cleaning of the tube bodies and caps.

The adsorbent discs were stamped out of 90 mm Whatman GF/A filters using a 13.5 mm cork borer. This provided discs that fit well into the Gradko diffusion tube caps. These discs were then pre-extracted, in batches of 50–60 in a Soxhlet apparatus (Quickfit: EX5/21), over 0.5% sulphuric acid for ≈6 hours to remove blank NH_4^+ from the filters (Figure 6.2). The Soxhlet extraction is a refluxing operation, whereby the condensate is run into a chamber containing the items to be extracted, and regularly

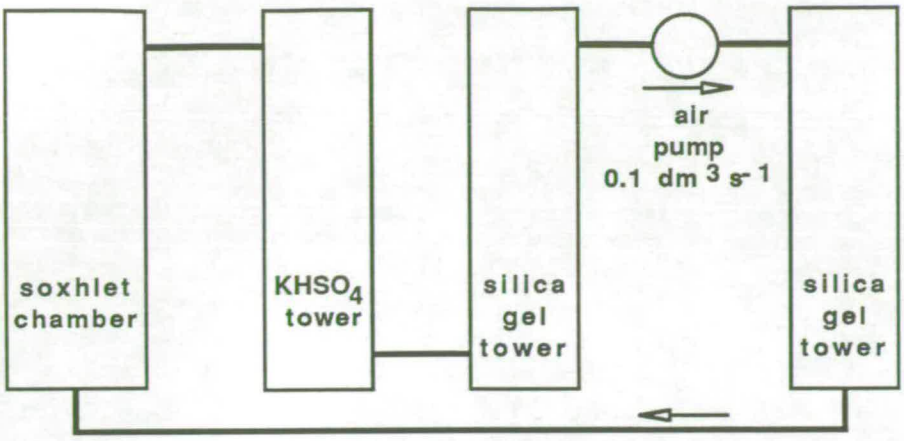

Figure 6.3 Schematic diagram of adsorbent disc drying apparatus. The cleaned and dried air is cycled through the chamber containing the discs for approximately 10–12 hours.

(about every 2 minutes) flushed out automatically by siphoning, when the chamber fills to a given level. In this way the filters were repeatedly washed in distilled water; the acidic boiling solution simply serves to trap the washed out NH_4^+.

In this study, a tower filled with $KHSO_4$ granules was connected to the open end of the condenser. This served to prevent entry and deposition of NH_3 from the laboratory back onto the extracting filters. The filters were then dried *in situ* in a closed cycle stream of air, which was passed through silica gel drying towers and again through the $KHSO_4$ tower to remove any NH_3 (Figure 6.3). This took several hours, and in practice was left overnight. The exclusion of NH_3 is important because of the long exposure times in these tasks, which would otherwise allow redeposition to the discs.

Tube bodies and caps were cleaned together in dilute Decon 90 detergent solution in water (≈0.5%; Decon Laboratories Ltd., Hove, Sussex., U.K.). They were then rinsed several times in tap water, followed by several rinses in de-ionized water. Excess water was shaken off, then the whole batch (50–60 tubes) dried in a fan oven at 70–80 °C. After cooling, the tubes and caps were assembled, ready for insertion of the discs.

Clean forceps were used to remove the discs from the Soxhlet apparatus. One disc was placed under each coloured cap, and the cap replaced. The filters were then acidified by the addition of 35 mm^3 1% analytical grade sulphuric acid, using a micropipette, and the caps again replaced. These last two stages took only a few seconds for each tube, and were therefore done in the open laboratory. Finally the tubes were labelled ready for exposure.

6.3.2 Sampling and exposure of diffusion tubes

For each batch of prepared diffusion tubes, at least 10 were kept as blanks and stored in NH_3 clean bags until the time of analysis (see section 3.3.3). The sampling tubes were set out in batches of 5 replicates at each site for approximately 3 weeks, these figures being chosen in response to NH_3 levels encountered and the error in measurements.

At each visit to a site, note was made as to the condition of the exposed tubes and these replaced with the next batch. The tubes mostly stayed in good condition in each exposure period, although at the urban sites the tubes became covered with a film of grey/brown dirt, while occasionally spiders would be found in a tube. At one site (Fala Moor) the samplers were located in open moorland, providing a good perch for birds, so that excrement occasionally contaminated the tubes. This was avoided by providing a spiked metal hood to the sampler to prevent perching.

6.3.3 Chemical analysis of adsorbent discs

The quantity of NH_3 captured by the adsorbent discs was measured by the same system as described in section 3.3.4 for the filter pack samples, although the implementation was adapted in detail. The continuous flow analysis (CFA) system was again run in a wash of 10% v/v propan-2-ol in water, using standards of 0, 50, 100, 200 and 500 μg NH_4^+ dm^{-3} water. Samples at the background sites measured for 3 weeks usually gave concentrations of less than 200 μg dm^{-3}. The sample carousel was again run in a clean air glove-bag, to minimize the deposition of NH_3 to exposed samples.

The polystyrene sample cups (2 cm^3 capacity) described in section 3.3.4 were used in the analysis here as both chambers for extracting samples, as well as to hold the prepared samples during analysis (Hargreaves and Atkins, 1987). The coloured cap with the adsorbent disc was removed from the diffusion tube body and fixed onto a freshly pre-rinsed sample cup containing 1 cm^3 of extractant. The whole vessel was then inverted and set in place in the sampling carousel. This was left to extract for ≈20 minutes, then re-inverted, the cap and disc removed, and the sample cup placed in the carousel ready for sampling.

A maximum of 10 prepared sample extracts were left (in the clean air chamber) waiting to be sampled at any time so as to further minimize NH_3 deposition. As a general procedure, standards were run every 15–20 samples, and the blanks measured in 3 separate groups, as a precaution in case the analysis should fail part way. Given that the solutions were not filtered (*c.f.* section 3.3.4), failure occasionally occurred due to a blocked tube. In order to minimize this, extracting discs were not shaken, since this encouraged disc disintegration.

Output from the CFA was recorded in a similar manner to that in section 3.3.4, using linear regression of chart recorder standard and sample peak heights to estimate concentration.

6.3.4 Calculation of air concentrations

Given that the discs were extracted in 1 cm^3 of liquid, and aqueous concentration expressed as q µg NH_4^+ dm^{-3} (≡ ng cm^{-3}), the mass of NH_4^+ in a disc was found as q ng. For each batch a mean blank value ($\bar{q}_b$) was calculated and then subtracted from the mean value of the exposed discs at a site ($\bar{q}_e$). This gave the quantity of NH_4^+ in the filters due to the air, which was then converted to the NH_3 equivalent by multiplying by the mass ratio NH_3/NH_4^+ (= 0.944). Finally this was divided by the effective sample volume (sample rate × exposure time, t) to give air concentration. This is summarized below, giving units:

$$\chi\ (\mu g\ NH_3\ m^{-3}\ air \equiv ng\ dm^{-3}) = \frac{0.944[\bar{q}_e - \bar{q}_b]\ (ng)}{0.100\ (dm^{-3}\ hour^{-1})\ t\ (hours)} \qquad 6.7$$

In practice the air concentrations were calculated and the precision of the estimates found by using a 1 tail (samples > blanks) unpaired t-test, implemented on the Minitab computer package. Confidence limits and standard errors are therefore given in the results.

6.4. Restrictions and precision of results

The precision of the air concentration data collected is shown in Figure 6.4. Standard errors are seen to increase with air concentration, reflecting variability due to sampling, as well as a fixed component due to the variability of blank filters. A typical standard error of the concentration estimates, (standard error of the difference of blanks to runs, from the t-test above) at the lowest concentrations is 0.1 µg NH_3 m^{-3}. Similarly, a typical minimum significant concentration (95% confidence limits) is 0.2 µg m^{-3}.

The usual comparisons in the determinations were 5 sampled tubes at a site to 10 blanks. However, for 11% of the exposed tubes, problems were encountered, so that these results are excluded from the mean calculations. These included tubes with known field contamination or loss of adsorbent disc, laboratory contamination, and loss of samples by mis-manipulation. Where contamination events are recorded, or the contamination is large (*e.g.* 3 µg $disc^{-1}$), exclusion is clear. However, where possible smaller contamination occurs, the situation is more uncertain.

In order to develop simple criteria for the exclusion of values the distributions of blank and sample discs were considered. Blanks were found to have a bi-modal distribution,

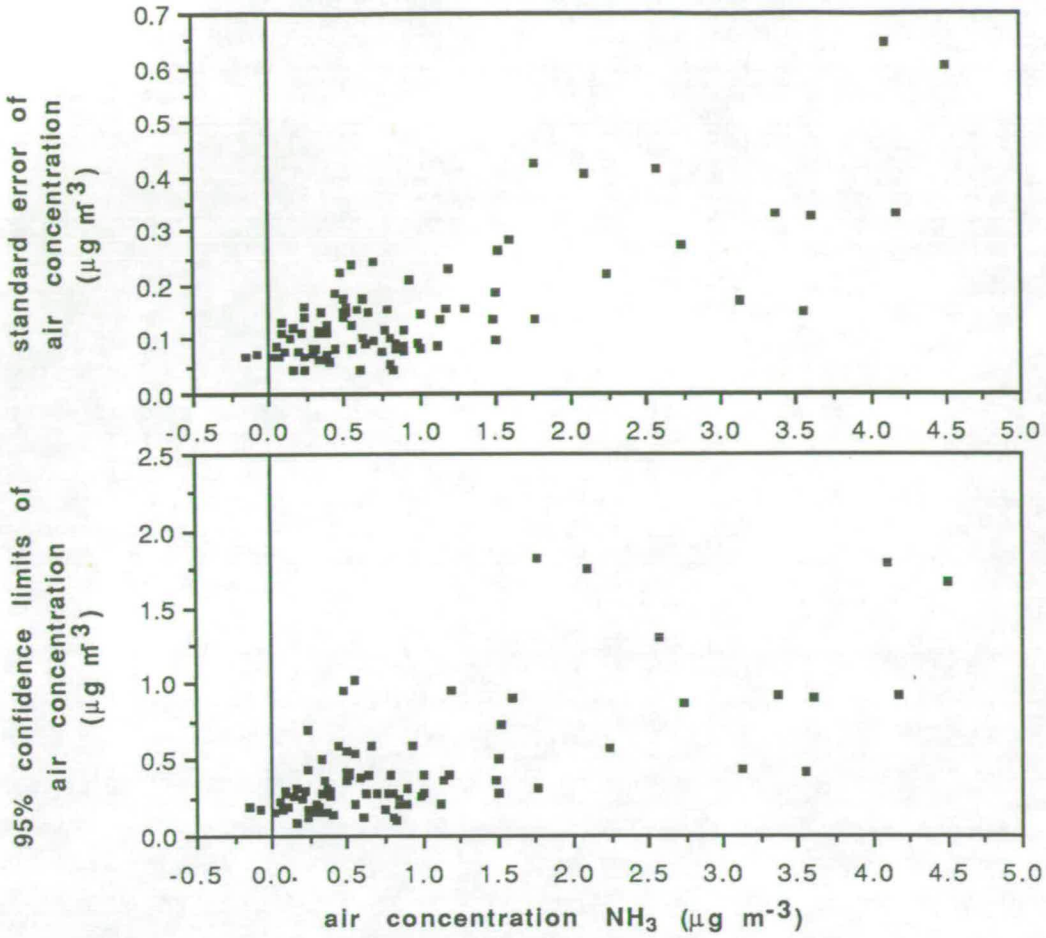

Figure 6.4 Precision of air concentrations measured by diffusion tubes. The errors are calculated by unpaired t-test comparisons of ≈10 blanks to ≈5 (batches of 3–6 included) exposed tubes.

with 12% of the discs being more than 25 ng disc^{-1} larger than the median for each batch, referred to as $\tilde{q}$. Removing these gave a normal distribution of (q_b - $\bar{q}_b$), with a mean of 0 ± 16 ng disc^{-1} (95% confidence limits of the distribution of values). The overall blank mean, $\bar{q}_b$, was 31 ng disc^{-1}. The degree of variation due to sampling was considered using high concentration runs ($\tilde{q}_e$ > 600 ng disc^{-1}). Using 4 runs which were judged to have no clear contaminations, the distribution of (q_e - $\bar{q}_b$) was considered, which gave the ratio: (95% confidence limits of the distribution of values)/ mean = 0.34, 0.46, 0.41, 0.49; with a mean of these of 0.43. An approximate system combining these two results was therefore developed; being to reject a value of q_e if:

$$(q_e - \tilde{q}_e) > 0.5[\tilde{q}_e - \bar{q}_b] + 25 \text{ ng} \qquad 6.8$$

Or more simply, and given $\bar{q}_b \approx 30$ ng disc^{-1} :

$$q_e > 1.5\tilde{q}_e - 0.5\bar{q}_b + 25 \text{ ng} \qquad 6.9$$

$$> 1.5\tilde{q}_e + 10 \text{ ng} \qquad 6.10$$

Here the value of 0.5 was chosen in order to be somewhat conservative about rejects, while the median was used to reduce the effect of skewness caused by contaminated values. Such a system is inevitably somewhat arbitrary, though it gives good agreement with removal by simple visual inspection (which was also used), and for minor contamination the effect of the decision will not be large anyway. Nevertheless, this does demonstrate the need for good replication when using diffusion tubes, so as to avoid the inclusion of falsely elevated values, which would otherwise result in an over-estimation of air concentrations.

Another possible cause of over-estimation of air concentrations is deposition of NH_3 in laboratory air to samples. The main site for this in the analysis, is deposition to extracted samples in the CFA carousel awaiting sampling. The deposition rate to sample cups was measured by analysing wash solution exposed for different periods of time. As discussed in section 3.3.4, this gave a deposition rate of ≈ 8 pg s^{-1} to samples in laboratory air, and ≈ 1 pg s^{-1} to samples in the clean air chamber. Following the protocol of this study, having a maximum exposure of 10 samples at one time in the clean air chamber ($\equiv$20 minutes exposure, at 2 minutes per sample), and exposing tubes in the field for 3 weeks ($\equiv$50 dm^{-3} effective sample volume), this gives a maximum concentration elevation of 0.02 $\mu g\ m^{-3}$. Compared to typical air concentrations of NH_3 of the order 1 $\mu g\ m^{-3}$ (section 6.5.2) this is acceptably small.

The importance of the precautions noted above may be demonstrated by the scenario in their absence. If the whole carousel (40 samples) were loaded and left to sample in an open laboratory, with similar air concentrations as here, the over-estimation would be 0.7 $\mu g\ m^{-3}$, which is a considerable fraction of typical air concentrations. This also points to a restriction upon short field exposure times; given a field exposure period of one week, the laboratory elevation of air concentration estimates would be $\approx 2\ \mu g\ m^{-3}$.

It should be stressed that these are the values for maximum laboratory exposure, so that only the last samples to be measured would experience such elevation. In addition, much of the effect may be removed by similar deposition to blank samples. However, where precautions against deposition are not made, care must be taken to expose blanks throughout the batch; where blanks are set out solely at the start or end of the analysis, a bias due to deposition will result.

Other possible restrictions include factors which modify the sampling performance of the diffusion tubes. These include, wind effects, possible sampling of NH_4^+, and losses of NH_3 to tube walls.

Hargreaves (1989) examined the possible effects of wind on diffusion tube performance. Wind tunnel studies, using similar NO_2 tubes orientated vertically, showed a sampling elevation following the relationship: % over-estimation = $14.15 \times u^{0.653}$, where u is windspeed in m s^{-1}. This, for example, predicts an over-estimation of 40% at 5 m s^{-1}. However, field studies were unable to show such a trend, a difference which he suggests may relate to the laminar nature of the wind-tunnel air flow, allowing the development of standing waves in the tubes. By comparison he suggests such waves do not have time to develop in the turbulent air flow of natural conditions, explaining the absence of detectable wind effects.

The possibility that NH_3 diffusion tubes over-record through the capture of NH_4^+ has also been suggested (Martin, 1988, pers. comm.). The basis for this is the results of a comparison of concentration measurements by diffusion tubes set out by Harwell laboratory (Atkins, 1988, pers. comm.) and filter pack measurements of Allen *et al.* (1988) in S.E. England. At Flatford in Essex measurements were made by both systems and gave 4.8 $\mu g\ m^{-3}$ NH_3 (diffusion tube) as compared to 2.5 $\mu g\ m^{-3}$ NH_3 (filter pack). NH_4^+ by filter pack was 4.1 $\mu g\ m^{-3}$. However, it is unclear whether this is the explanation of the difference observed. From a theoretical position, given the slow diffusion rates of sub-micron particles such as NH_4^+ (section 1.4.2), it would seem unlikely that much NH_4^+ would be deposited on the adsorbent disc.

Conversely, a possible cause of under-estimation of NH_3 concentrations would be deposition of NH_3 to the diffusion tube walls. This is a reasonable possibility given the results of the surface exchange studies (Chapters 4 and 5), which show high deposition rates may occur to vegetation. Deposition to the PTFE tube may, therefore be important, especially to water around the mouth of the tube in wet conditions. However, the PTFE may be inert, and its hydrophobic nature reduce water-associated deposition. Hargreaves (1989) extracted NH_4^+ from exposed tube walls but found only trace quantities deposited, so it may be that this is not a significant problem.

Despite each of these criticisms, extensive tests comparing NH_3 concentrations as measured by diffusion tubes and by denuder tubes of Hargreaves (1989) gave relatively good agreement and a regression not statistically different from 1:1, although considerable scatter was present. Conversely Vibelu-Anderson (1989, pers. comm.) found diffusion tubes to over-estimate, in a comparison against both filter packs and denuder tubes. The measurements, made at several sites in Denmark, gave an approximate relationship of: (Diffusion tube NH_3) = 2(Reference NH_3) + 0.4 $\mu g\ m^{-3}$. In summary then, some question remains at present as to the validity of NH_3 measurements by diffusion tubes, with an over-estimation of air concentrations being the most likely possible error.

Site Name	Site description	Dates	NGR
	Monitoring in S. Scotland		
Bush Estate	Lay field in agricultural area, Penicuik, Midlothian.	1/1988–6/1989	NT247639
Dunslair Heights (top site)	Clearing at top of hill (600 m AMSL) in Glentress Forest (conifer plantation), Peebles, Borders.	2/1988–6/1989	NT288405
Glentress Forest (bottom site)	Clearing on exposed ridge, S. of Dunslair Heights (300 m AMSL) in Glentress Forest, Peebles, Borders.	2/1988–6/1989	NT289405
Fala Moor	Open moorland (300 m AMSL) managed for low density sheep and grouse. Remote site 2 km N. of Brothershiels Farm. Nearest road 2 km S.E. Heriot, Midlothian.	1/1988–6/1989	NT423578
Brothershiels Farm	By trees in Farm yard. Silage and cattle nearby in yard. Silage smell continual. Nearest road 2 km S.W. Heriot, Midlothian.	12/1988–6/1989	NT420560
Edinburgh roadside	Main road kerbside. (3.5 m up on lamp post) Old College, South Bridge, Edinburgh.	3/1989–6/1989	NT260734
Edinburgh roof top	Roof of University Geography department. 200 m east of main road site. Edinburgh.	2/1989–6/1989	NT262734
Indoors I.T.E.	Indoor site in laboratory work place. No air conditioning, openable windows. Bush Estate, Penicuik, Midlothian.	12/1988–6/1989	NT246638
	Other sites		
Devilla Forest	Measurements within and above Scots Pine (*Pinus sylvestris*) canopy. 4 reference levels. Kincardine, Fife, C. Scotland.	6/1989–10/1989	NS959893
Great Dun Fell	Measurements at 4/5 sites in approximate NE-SW trajectory over hill. N. Pennines, Cumbria and Durham, England.	4/1989	
	Wharley Croft (200 m AMSL)		NY698246
	Fellside (550 m AMSL)		NY704295
	GDF summit (847m AMSL)		NY710322
	Tyne Head (550 m AMSL)		NY753350

Table 6.1. Sites used for monitoring ammonia by diffusion tubes. Notes: NGR, national grid reference; AMSL, above mean sea level.

6.5. RESULTS

6.5.1 Monitoring sites and studies

The measurements made in this study may be divided into 3 groups. The bulk of the results are for monitoring in S. Scotland, including locations in Midlothian and Borders, and site details for this are given in Table 6.1. Profile measurements within and above a forest canopy were also made to supply concentration data to another experiment on throughfall chemistry, as well as to see if gradients could be detected. This experiment was made at Devilla forest, Central Scotland. Finally, in an attempt to compare the implementation of the diffusion tubes between the methods used here, and those used by Harwell Laboratory, a field comparison was made. This took place at Great Dun Fell, N. England, in April 1989 as part of a separate investigation into atmospheric nitrogen chemistry. Site details of these measurements are also given in Table 6.1.

Site Name	Seasonal mean concentrations of NH_3 ($\mu g\ m^{-3}$)				
	Spring Mar., Apr., May	Summer Jun., Jul., Aug.	Autumn Sep., Oct., Nov.	Winter Dec., Jan., Feb.	Annual Mean *
Bush Estate	1.34 (6)	1.62 (6)	0.85 (4)	0.77 (6)	1.14
Dunslair Heights (600 m)	0.53 (6)	0.65 (6)	0.19 (4)	0.38 (4)	0.44
Glentress Forest (300 m)	0.68 (6)	0.95 (5)	0.32 (4)	0.37 (5)	0.58
Fala Moor	0.69 (6)	0.74 (5) 2.50 (6) †	0.19 (4)	0.59 (5)	0.55
Brothershiels Farm	11.2 (2)	—	—	3.68 (4)	—
Edinburgh roadside	3.41 (2)	—	—	—	—
Edinburgh roof top	3.02 (2)	—	—	0.84 (1)	—
Indoors (ITE)	7.34 (2)	—	—	7.46 (4)	—

Table 6.2 Seasonal arithmetic mean concentrations of atmospheric ammonia from diffusion tube monitoring in S. Scotland. Values in brackets are the number of runs from which each mean is calculated. * Mean of seasonal values. † This value is doubtful and results from the inclusion of one probably contaminated outlying run (run 8) of 10.5 $\mu g\ m^{-3}$.

6.5.2 Ammonia concentrations in S. Scotland

The results of air concentrations from the main monitoring study are summarized in Table 6.2. In this table, air concentrations are divided into seasonal means for each of the sites, and the number of determinations for each period at a site shown. The data for the four main background sites are also shown graphically in Figure 6.5. Following this, the individual run concentrations for each site are shown in histogram form, in Figures 6.6–6.7. In Figure 6.6, for the data from the Bush site, 95% confidence limits are given to show the significance of the air concentrations. These are not given for the other back-ground sites, but, the full data set including standard errors, confidence limits, number of exposed tubes and notes, is given in Appendix 6.

For all of the sites the mean seasonal concentrations were within the range 0.1–11 $\mu g\ m^{-3}$ NH_3. The highest of these were from the Brothershiels Farm site and the indoor measurements. The urban sites provided the next highest concentrations, while the four background rural sites gave the lowest concentrations.

The Brothershiels Farm results showed a clear distinction between very high concentrations in spring (and early summer) at $\approx 11\ \mu g\ m^{-3}$, and much lower concentrations in winter of ≈ 3–$4\ \mu g\ m^{-3}$. This seasonal difference probably reflects a tendency for emission of NH_3 from the cattle and silage at the farm to be greater in warmer conditions. No measurements were made at this site for the months July to November.

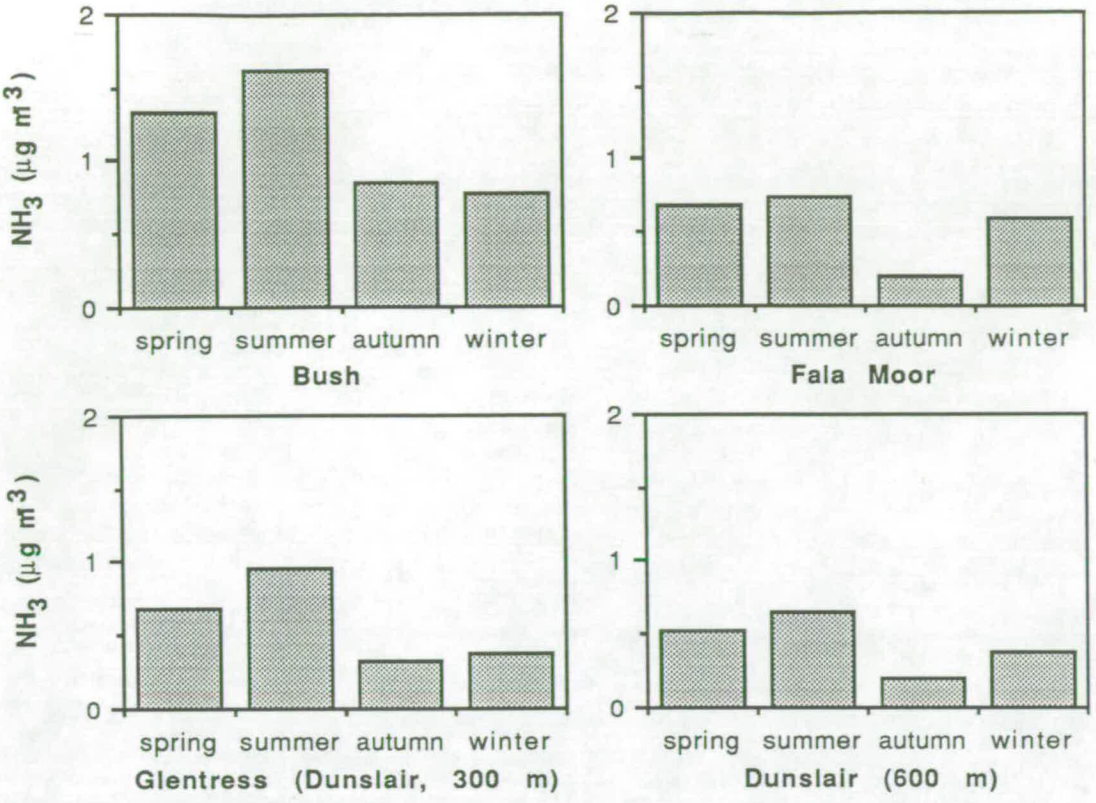

Figure 6.5 Bar charts of seasonal atmospheric NH_3 concentrations at four background rural sites in S. Scotland. Data from Table 6.2.

The indoor concentrations, measured in the laboratory at ITE Bush, were relatively constant throughout the period of study, with values within the range 6.3–8.3 $\mu g\ m^{-3}$ NH_3. These values were about 6–7 times the concentrations measured outdoors at the same site, and reflect the previous observation (NRC, 1979) that humans are a source of NH_3, emitting both through sweat and breath. The relatively constant concentrations in the laboratory probably reflect a uniform frequency of laboratory use and similar temperatures in the laboratory throughout the period of study.

Only a short period of monitoring was done at the two urban sites, which showed similar air concentrations to each other. It is likely that both combustion sources (*e.g.* vehicles and heating) and people are the source of the elevated concentrations at these sites (NRC, 1979). Given that the concentrations are larger than the rural back-ground sites it was expected that the roadside site might give larger concentrations than the roof-top. However, any such differences are not large enough to show any trends with the small amount of data collected here.

The main bulk of the measurement effort focused on four rural sites which were expected to represent background air concentrations in the region; each of the sites

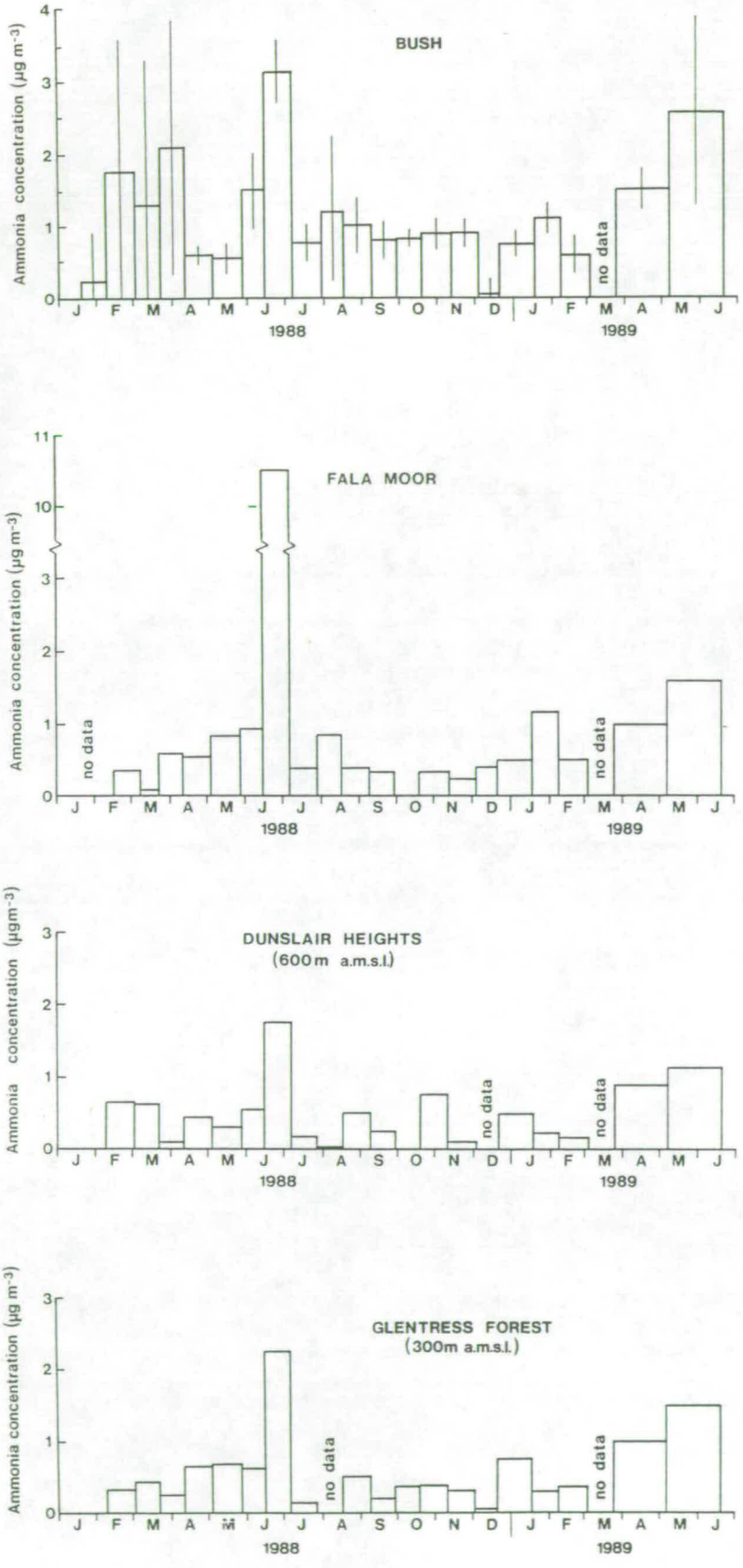

Figure 6.6 Histograms of measured ammonia concentrations at background rural sites in S. Scotland, 1988–89. Error bars, where given, are 95% confidence limits of the mean.

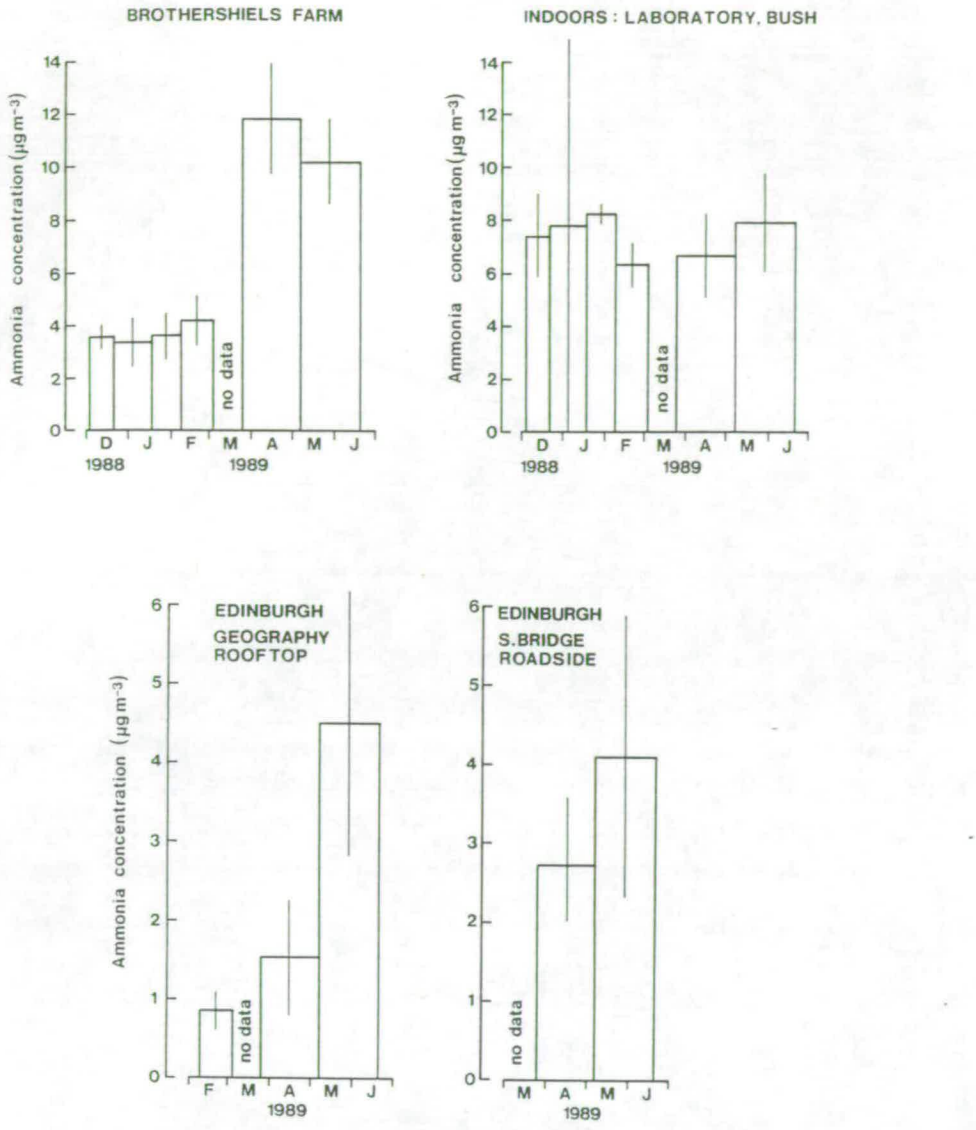

Figure 6.7 Histograms of measured ammonia concentrations at a farm site, indoor site, and two urban sites in S. Scotland, 1988–89. Error bars are 95% confidence limits of the mean.

being located away from expected point sources of NH_3. Of these, the Bush site gave the highest concentrations, with seasonal means of 0.8–1.3 μg m^{-3}, while each of the other sites gave lower seasonal concentrations, in the range 0.2–1.0 μg m^{-3}. This difference, which was statistically significant in each case (Table 6.3), probably relates to the Bush site being in an agricultural area, whereas the other sites were more remote upland sites.

From Table 6.2 and Figure 6.5, seasonal differences in concentrations may again be seen at each of these background sites, with highest concentrations in summer, the next highest in spring, and the lowest concentrations in autumn and winter.

	Fala Moor	Glentress (300 m)	Dunslair (600 m)
Bush	0.02 **0.19** NS *18*	0.0001 **0.66** ** *19*	0.0001 **0.34** NS *18*
Fala Moor	—	0.31 **0.42** NS *17*	0.11 **0.02** NS *17*
Glentress (300 m)	—	—	0.12 **0.79** *** *17*

Table 6.3 Summary table of statistical comparisons between NH_3 concentrations at the four background rural sites. Analyses were performed on $\ln(\chi)$ transformed data to normalize the distributions of values. The first value for each comparison is the probability that the mean concentrations of the sites are not different (two tail paired t-test). The figure in bold type is the value of the correlation coefficient, r; significance is denoted by: ***, $P < 0.001$; **, $P < 0.01$; *, $P < 0.05$; NS, $P > 0.05$, not significant. The final figure in italics is the number of runs included in the comparisons.

Inspection of Figure 6.6 shows the data frequently appear to have an approximate baseline concentration, with elevation above this in particular runs. At Bush a baseline concentration of ≈0.8 μg m^{-3} is present through much of the year, with a peak in early spring 1988 of 1.5–2.0 μg m^{-3} (not shown by other sites), and an early summer peak of up to 3 μg m^{-3}. At Fala Moor the baseline is ≈0.3–0.4 μg m^{-3}, with the most reliable concentrations in late spring and early summer being up to 1.6 μg m^{-3}. One run of 10.5 μg m^{-3} was found in summer 1988 at this site, but as noted in Table 6.2, this is probably the result of contaminated samples.

The Dunslair Heights/Glentress Forest sites were located close to each other (3 km apart in a North–South line), the main difference being the higher altitude (600 m) and remoteness from valley agriculture of the top Dunslair Heights site, as compared to the lower Glentress Forest site (300 m). The two sites had similar concentrations, which were not significantly different (Table 6.3), and a significant correlation of concentrations to $P < 0.001$. However, concentrations were somewhat less at the high altitude site in each of the seasons except winter (Figure 6.5). Neither of the concentrations were significantly different to the results at Fala Moor (Table 6.3), and an approximate baseline concentration for these sites was again ≈0.3–0.4 μg m^{-3}.

6.5.3 Ammonia concentrations within and above Devilla Forest

Atmospheric ammonia was measured at Devilla forest for a period of $3\frac{1}{2}$ months from 29/6 to 13/10/1989. Measurements were made at four heights, three within the canopy at 3.3, 5.5 and 8.9 m above the ground, and one above the canopy, 12.1 m above the ground. The trees were Scots Pine (*Pinus sylvestris*) and 11–12 m tall.

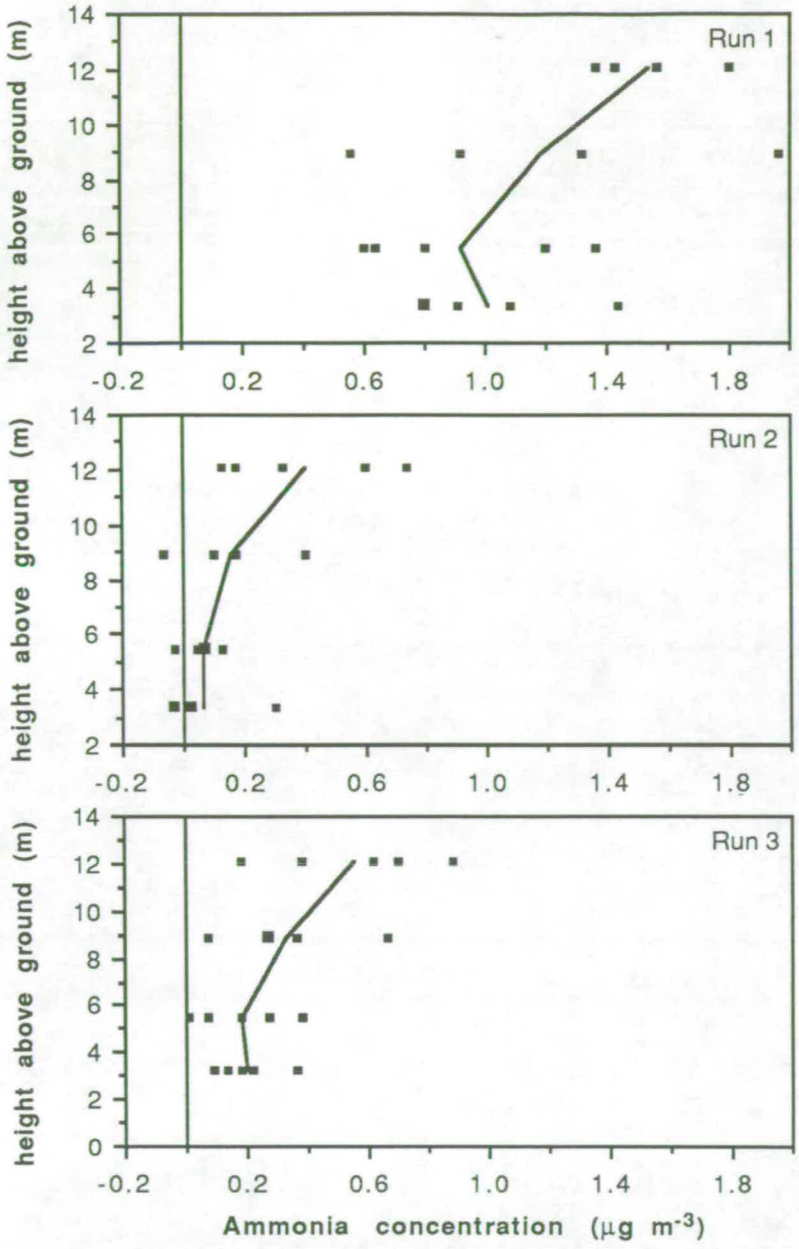

Figure 6.8 Ammonia concentration gradients above and within the canopy at Devilla Forest. Tree height 11–12 m. Individual determinations are given so as to show the precision of the results. Small squares (▪) represent single diffusion tube concentration estimates; large squares (■) represent the overlap of two points. The lines are interpolations between the mean concentrations at each height.

Three sample runs were taken and the results for these are shown in Figure 6.8 as concentration *versus* height above the ground. In each of these graphs individual concentration determinations are given in order to show the degree of scatter, while the tie lines are drawn from interpolation of the means at each height. The precision of the estimates was calculated comparing each height batch of tubes to 19 blanks. Standard errors, confidence limits and significance of concentrations are shown in Table 6.4. In all but three cases the concentrations at each height were significantly greater than zero ($P < 0.05$, 1 tail test).

Sample dates	height above ground (m)	mean concentrations ($\mu g\ m^{-3}$)	SE	95% Confidence limits	Significance (1 tail)	Notes
Run 1	12.1	1.54	0.11	[1.30, 1.97]	0.0003	1 cont.
29/6–8/8/1989	8.9	1.18	0.32	[0.23, 2.28]	0.015	1 cont.
	5.5	0.92	0.16	[0.52, 1.43]	0.002	
	3.3	1.01	0.13	[0.71, 1.42]	0.0006	
Run 2	12.1	0.40	0.13	[0.06, 0.77]	0.015	
8/8–25/9/1989	8.9	0.17	0.10	[-0.16, 0.46]	0.11	1 cont.
	5.5	0.06	0.03	[-0.01, 0.14]	0.049	
	3.3	0.06	0.06	[-0.12, 0.24]	0.20	
Run 3	12.1	0.55	0.13	[0.21, 0.90]	0.005	
25/9–13/10/1989	8.9	0.33	0.11	[0.06, 0.59]	0.012	
	5.5	0.18	0.08	[-0.01, 0.37]	0.03	
	3.3	0.20	0.07	[0.05, 0.34]	0.006	

Table 6.4 Mean values and precision of ammonia concentrations at Devilla forest. Statistics are calculated from two-sample t-tests comparing exposed filters to 19 blanks. At each height estimates are for 5 exposed tubes, except where values were excluded due to contamination (cont.).

The mean concentrations above the canopy for the 3 sampling periods were 1.54, 0.40 and 0.55 $\mu g\ m^{-3}$, with an overall mean of 0.86 $\mu g\ m^{-3}$. These values are in good agreement with the other measured values in summer and autumn given in section 6.5.3., supporting these values as being typical background concentrations in the region. While considerable scatter is present in the data, which is typical for such diffusion tube measurements, a decrease in concentration within the canopy is clearly present in each of the runs. This may be taken as supporting the finding that NH_3 deposits to natural and low input vegetation including forest, as described in Chapter 4. However, it is not possible from such gradients to estimate fluxes, since, in addition to the long term nature of the sampling, it is known that the simple flux-gradient relationships break down within the canopy.

One restriction which may be applied to this interpretation of the gradients is the possible wind enhancement of sampling. If this were occurring the gradients could simply result from greater sampling at higher levels. However, the only study available on this subject, that of Hargreaves (1989), as noted in section 6.4, suggests this is not important in field conditions.

6.5.4 Comparison of ammonia diffusion tubes at Great Dun Fell

In order to assess the performance of the diffusion tube system used in this study, a field comparison was made with the diffusion tubes of Harwell Laboratory (set out by G.J. Dollard). Two independent sets of diffusion tubes were set out; one set being prepared and subsequently analyzed using the methods described in this report, at the ITE, Bush Estate, Edinburgh, and the other being prepared and analyzed by Harwell Laboratory broadly following the methods described by Hargreaves and Atkins

site: / system:	blanks	Wharley Croft	Fellside	Summit	Tyne Head
ITE $\chi \pm$ SE	—	2.57 ± 0.44	2.20 ± 0.33	3.17 ± 0.61	2.40 ± 0.24
number of tubes*	10(8)	4(4)	5(4)	5(5)	5(5)
Harwell $\chi \pm$ SE	—	8.19 ± 1.77	5.92 ± 0.92	0.92 ± 0.53	1.56 ± 0.81
number of tubes*	2(1)	4(4)	5(5)	4(4)†	5(5)†
Significance by 2 sample (2 tail) t-test ‡	—	0.02	0.01	0.03	0.35
Filter pack ± SE selected days§	—	—	0.23 ± 0.05 (9 days)	0.15 ± 0.05 (8 days)	0.18 ± 0.04 (7 days)

Table 6.5 Comparison of diffusion tube estimates of NH_3 concentration ($\mu g\ m^{-3}$) at Great Dun Fell. Standard errors are calculated from the concentration estimates assuming a fixed blank value. (For the ITE data this differs little from a two sample comparison.) Notes: * The first value is the number of tubes set out; the value in brackets is the number of tubes included in the analysis. † Each of these runs include two samples where NH_3 was not detected in the exposed tube discs; the air concentrations of these are set to zero in the calculation of the means. ‡ Probability that the mean concentrations by the 2 laboratories are not different. Tubes were exposed from 13–14/4 to 30/4/1989 at 2 m above ground except Wharleycroft, set at 4 m above ground.

§ Comparison is also given with results of filter pack sampling made on selected days. Values are the means and standard errors of daily concentrations from at least 3 hours measurement per day.

(1987). In addition to being a simple comparison of results, the aim was to provide estimates of NH_3 concentration at different locations (in an approximate SW–NE line) over the Great Dun Fell field site, for the April 1989 campaign. Measurements were made at 4 sites, the locations of which are given in Table 6.1.

The details of tube exposure, blanks set out, and measured air concentrations at each of the sites are given in Table 6.5. Unfortunately the NH_3 analysis at ITE failed due to a blocked transmission tube in the continuous flow system, which took $4\frac{1}{2}$ hours to solve. As a result the the concentrations had to be corrected for laboratory deposition to samples (equivalent to 35 $\mu g\ NH_4^+\ dm^{-3}$ aqueous concentration), while, by the time the analysis worked, only a small volume of sample was available, making the analysis somewhat uncertain. As a consequence the ITE results do not reflect the quality of data typical of this study.

Consequently the comparisons here are somewhat tentative. Ammonia was also determined by ITE using filter packs (section 3.3) on several days at 3 of the sites. These results are therefore also available for observation of general trends and are given in Table 6.5.

The comparison of the two diffusion tube results appears rather poor, with only one site showing concentration estimates that were not significantly different to each other (Tyne Head). The ITE results show similar levels at each site, while the Harwell data show high concentrations at Wharleycroft and Fellside, and low concentrations at the

Summit and Tyne Head. Overall arithmetic mean concentrations for the 4 sites were ITE: 2.5 $\mu g\ m^{-3}$, and Harwell: 4.1 $\mu g\ m^{-3}$.

In addition to this, the filter pack measurements which were made — and may be assumed to give a much better measurement of air concentration — gave values much lower than both the diffusion tube estimates. For the 3 sites where both measurement methods were used, the filter packs gave $\approx 0.2\ \mu g\ m^{-3}$ compared to 2–3 $\mu g\ m^{-3}$ by ITE diffusion tubes and 1–6 $\mu g\ m^{-3}$ by Harwell diffusion tubes. It is possible that this difference is due to the limited sampling by filter pack not reflecting the overall mean concentration of the period. However, given the consistency of the filter pack results and that approximately half the days in the period were sampled, this seems unlikely.

It is not clear from this study whether the differences reflect a problem with the diffusion tube system itself, or with the implementation of the methods. However, the result is in opposition to the agreement found by Hargreaves (1989) in the development of the method. While this comparison is on a much smaller scale than that study, and contains major uncertainties (ITE analysis failure, discontinuous sampling by filter packs), it suggests further tests need to be done before the validity of NH_3 diffusion tubes can be fully accepted. If the trends in this comparison are real, NH_3 diffusion tube measurements give an over-estimation of air concentrations, with the over-estimation being larger for the Harwell results than for those of ITE.

6.6. Discussion

The main aim of this study was to use a simple method to provide estimates of background air concentrations of ammonia in S. Scotland. The diffusion tubes met this aim well, being particularly suitable for remote sites, and for low input monitoring, since no electricity supply is required at a site — a prerequisite for active sampling methods.

The implementation of the diffusion tube method used in this study allowed precise determination of NH_3 air concentrations. Using a system comparing ≈ 5 sample tubes exposed for three weeks to ≈ 10 blanks gave concentration estimates with a typical standard error at the lowest concentrations of 0.1 $\mu g\ m^{-3}$ NH_3, and typical 95% confidence limits of the mean of 0.2 $\mu g\ m^{-3}$ at the lowest concentrations, with the main error source being the variability in blanks. At the highest concentrations, where the error is dominated by sampling variability, the ratio: (95% confidence limits of the mean)/mean was ≈ 0.2.

In the development of the procedures used here a number of restrictions and precautions were found to be important. These included the requirement to keep the blank quantity of NH_4^+ in the discs to a minimum, achieved by pre-extracting the discs

in a Soxhlet apparatus, following the method of Hargreaves and Atkins (1987), and also drying the discs in a closed cycle of clean air (Figure 6.3). Using these methods, prepared blank diffusion tubes had a typical value of 30 ng $disc^{-1}$.

The need to minimize laboratory deposition of NH_3 to extracted sample solutions was also noted. This was done by enclosing the whole sampling stage of the CFA in a clean air chamber, and limiting the exposure period of open samples to a maximum of 20 minutes. Using this system, laboratory enhancement of air concentration estimates could be limited to a maximum of 0.02 $\mu g\ m^{-3}$, compared to 0.7 or 2 $\mu g\ m^{-3}$ for two possible exposure scenarios without these precautions.

In addition, the importance of replicating both exposed tubes and blanks was noted. Using the procedure outlined above, it was seen that occasional contamination of the tubes could occur, either in the field or in the laboratory, resulting in artificially inflated air concentration estimates. These were removed from the calculation of sample means in this study. The importance of such removal may be seen from a simple example; given 4 samples with a mean concentration of 1 $\mu g\ m^{-3}$, if a fifth contaminated sample of 5 $\mu g\ m^{-3}$ is included then the mean is raised to 1.8 $\mu g\ m^{-3}$, nearly double the real estimate. (See also example in Table 6.2.)

A number of possible restrictions to sampling NH_3 using diffusion tubes were also noted. These included wind enhancement of sampling rates, capture of NH_4^+ by the adsorbent discs, and loss of NH_3 to the tube walls. However, the second of these is theoretically unlikely, given the slow diffusion rates of sub-micron particles, while tests by Hargreaves (1989) have been unable to confirm the others in field conditions.

The results of the monitoring at each of the sites gave seasonal concentrations within the range 0.1–11 $\mu g\ m^{-3}$. As expected the highest concentrations were recorded at the farmyard site of Brothershiels, nearby to a cattle house and a silage store—both likely sources of atmospheric ammonia (section 1.3.). However, compared to other measurements in the literature at such sites, the values here, in the range 3–12 $\mu g\ m^{-3}$, are rather small. For example, at 2 farm sites in S. E. England Allen *et al.* (1988) recorded concentrations using filter packs of 3–66 $\mu g\ m^{-3}$ (monthly means) with an overall mean of 24 $\mu g\ m^{-3}$ (see Table 1.6), while Feeney (1988) found concentrations of up to 780 $\mu g\ m^{-3}$ at a pig farm in S. England using diffusion tubes set out for 2 week periods. Over the 4 runs of that study, a mean concentration at 100 m N.E. of the farm was 25 $\mu g\ m^{-3}$, while at 1000 m N.E. and beyond background levels of 5–8 $\mu g\ m^{-3}$ were recorded. It is clear that such sites represent sources of NH_3, though,

with the differences in farm sizes and management practices between farms, there is much scope for variation.

The next highest out-door air concentrations were those recorded in the city centre of Edinburgh, with values of between 0.8–4.5 $\mu g\ m^{-3}$ for a few runs in winter/spring 1989; this was approximately 2–4 times the air concentrations measured at the same time at the rural back-ground sites. Such differences have been previously observed. Early measurements separating NH_3 and NH_4^+ by Eggleton and Atkins (1972) gave a mean NH_3 concentration at Kew in S.W. London (urban) of 8.2 $\mu g\ m^{-3}$ as compared to Harwell, Oxfordshire (rural) of 5.4 $\mu g\ m^{-3}$. By comparison Cadle (1985) found much lower concentrations of 0.10–0.85 $\mu g\ m^{-3}$, in an urban area of Detroit, U.S.A., although no data was given for the surrounding countryside for comparison. In the study here, given that the values measured in the town are greater than the rural values, it suggests urban sources of NH_3 are present to give these elevated values. These may include both combustion and human sources. The existence of the latter is shown by the elevated indoor concentrations measured in the laboratory at Bush, although the relative importance of urban sources is not clear from this study.

Some uncertainty must remain however, with the diffusion tube measurements at the urban sites, since a film of dirt was present on the inside walls of the tube after exposure, especially at the roadside site. It is not known how this effects the sampling efficiency, and tests are needed to explore this.

As was expected the main background sites gave the lowest air concentrations, with reliable concentrations (typically 3 week averages) being in the range 0–3 $\mu g\ m^{-3}$. Of the 4 sites studied, Bush, in a mixed agricultural area, gave the highest values, with a mean annual concentration of 1.1 $\mu g\ m^{-3}$ NH_3. The three other sites, Fala Moor, Dunlsair Heights, Glentress Forest, were in upland areas and gave lower concentrations with similar mean annual values of 0.4–0.6 $\mu g\ m^{-3}$. The monitoring at Devilla Forest, which gave similar concentrations as these sites for the season also support these sites as being representative of background concentrations in the region.

The only other reported NH_3 concentrations in Scotland that are available for comparison to the data here are those of Harwell Laboratory, made at the Acid Rain Secondary Network sites (Warren Spring Laboratory, 1988). These used similar diffusion tubes, set out at 1 m above the ground, from which a concentration map of NH_3 over the UK has been produced (Atkins, 1988, pers. comm.; RGAR, 1990). The results for 1988–89 are reproduced in Figure 6.9. This gives a mean annual concentration of 2–4 ppbv for C. and S. Scotland, equivalent to 1.5–3 $\mu g\ m^{-3}$. This is clearly much higher than the concentrations found by the sampling in this study,

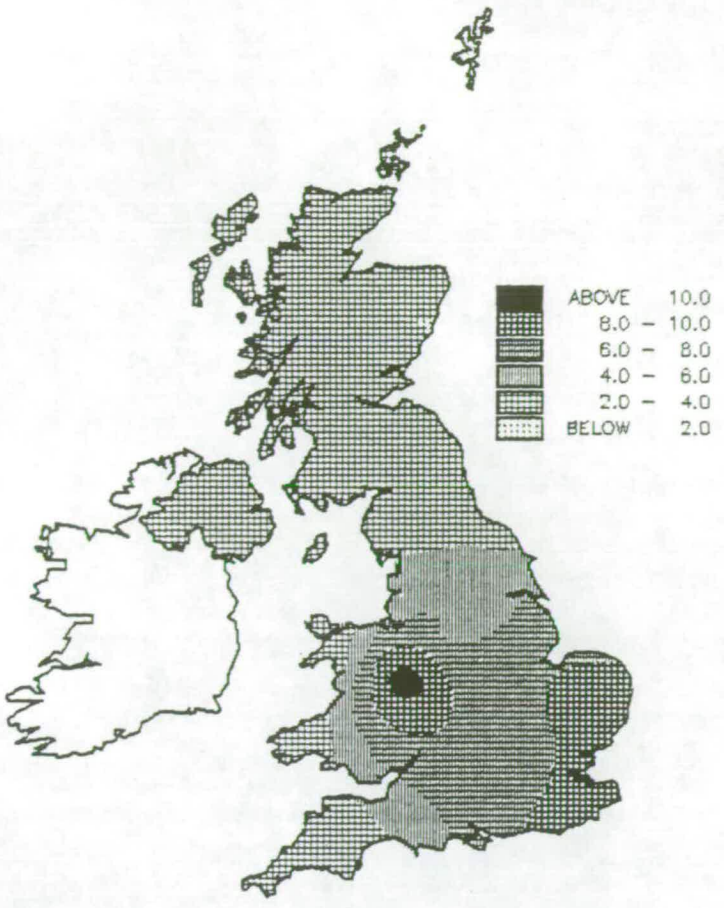

Figure 6.9 Ammonia concentration field for the United Kingdom (June 1988 to May 1989) from diffusion tube monitoring by Harwell Laboratory (Atkins, 1988, pers. comm.; RGAR, 1990). Isopleths are ppbv concentrations interpolated from measurements at the Acid Rain Secondary Network (Warren Spring Laboratory, 1988). Multiplication of these values by 0.75 gives approximate concentrations in $\mu g\ m^{-3}$.

and for the upland sites studied here, which are typical of the conditions over much of S. Scotland, represents a factor of difference of 2.5–7 times. The only other monitoring in Scotland is the total NH_x EACN data (Stevenson, 1968), which was given in Table 1.5. Comparisons here must be approximate, since the values are medians and for total NH_x, but assuming typical mean NH_4^+ concentrations to be at least 1 $\mu g\ m^{-3}$ (Table 1.6b; Appendix 4), this gives a maximum concentration at Eskdalemuir — a similar back-ground site in S. Scotland — to be 0.9 $\mu g\ m^{-3}$. This agrees well with the background values found in this study. It is therefore probable that the Harwell data is an over-estimate of typical air concentrations in the region. It is feasible in this respect that site criteria are not appropriate for background NH_3 levels, and that the sites may be located close to agricultural sources of NH_3. This may be the case with the Warren Spring Secondary Network sites, where the priority is for background levels of combustion source constituents, such as SO_2 and NO_x. Conversely, as a result of the comparison at Great Dun Fell (section 6.5.4), which

showed mean NH_3 concentrations by Harwell to be 1.6 times those recorded by ITE, it is probable that the Harwell diffusion tubes falsely over-estimate concentrations.

In comparison to other rural area measurements in the U.K. the concentrations presented for S. Scotland here are rather small. For example, Allen *et al.* (1988; See also Table 1.6) found a mean concentration for typical background sites in Essex, S.E. England, to be 2.6 $\mu g\ m^{-3}$. In comparison to concentrations in a livestock farming area in the Netherlands (Erisman *et al.*, 1988), the values are much less; in that study the mean concentration was 8 $\mu g\ m^{-3}$ (2 m above ground). These higher values may be related to the higher intensity of agriculture in these areas. Conversely, in remote areas much lower concentrations have been recorded. At Lerwick, in Shetland, Scotland, a median total NH_x of 1 $\mu g\ m^{-3}$ was recorded by the EACN (Table 1.5) suggesting very low NH_3, while in the U.S.A., in a forested area of Massachusetts, Tjepkema *et al.* (1981) found seasonal mean concentrations of NH_3 in the range 0.01–0.16 $\mu g\ m^{-3}$. The concentrations reported here are therefore midway between these other reported values. For the U.K., the pattern of small NH_3 concentrations in the north and large concentrations in the south is demonstrated by data in Figure 6.9, though again the concentrations are larger than other estimates.

It is of interest to compare the concentrations of NH_3 measured here with those predicted by model estimates. Asman and Janssen (1986, 1987) have developed a lagrangian model, calculating air concentrations on the basis of emission/deposition data and transformation to NH_4^+ for 100 × 100 km squares, with inputs being provided by an emissions inventory, approximations of deposition velocities, and conversion factors (NH_3 to NH_4^+) from available experimental data. The model predicts NH_3 concentrations of 1.3 and 1.6 $\mu g\ m^{-3}$ for the two grid squares over S. Scotland. This is in good agreement with the measured concentrations at the Bush site (1.1 $\mu g\ m^{-3}$), being in an agricultural area, but somewhat larger than the concentrations measured at the upland sites (Glentress, Fala Moor, 0.4–0.6 $\mu g\ m^{-3}$). This could relate to the model using a constant NH_3 deposition velocity (8 $mm\ s^{-1}$) for all surfaces. This has been shown in the previous chapters to be an over-simplification, with rapid deposition occurring to natural vegetation such as moorland and forest (Chapter 4; Devilla results section 6.5.3), and a bi-directional exchange occurring over intensive agricultural surfaces, depending on environmental conditions (Chapter 5). However, despite this limitation, and given the limited resolution of the model, the overall comparison is fairly good.

The data collected here also show seasonal patterns of air concentration, with the highest levels in summer, the second highest in spring, and the lowest concentrations in autumn and winter (Figure 6.5). This is in good agreement with other studies (*e.g.*

Tjepkema, 1980; see also Table 1.6) and probably relates to the change in temperature and surface wetness in the seasons, since it was shown in Chapter 5, and elsewhere (Allison, 1955; section 1.2.2) that NH_3 emission is greater in warm dry conditions. However, differences may also relate to agricultural practices, such as the flushing out of animal houses, and application of manures. It may be that the elevated concentrations at Bush in early spring 1988 are a result of this.

Such patterns also point to the usefulness of seasonal concentrations, over annual concentrations, in the calculation of surface flux budgets. Since air concentrations and exchange patterns vary together, appropriate seasonal concentrations, linked to the exchange processes occurring, will give an improved estimate of the annual budget.

For the four background sites of this study the correlation of sample concentrations between sites was calculated (Table 6.3). However, only two comparisons were significant. The most similar were the nearby Dunslair Heights (600 m AMSL) and Glentress Forest (300 m AMSL) sites. The only other significant comparison being between the Glentress site and Bush. The similarity of Dunslair Heights and Glentress may be attributed to their nearness (3 km apart N–S), and emphasizes the importance of local factors to air concentration levels, in common to both these sites. Such local influence is also shown by the difference of the Brothershiels Farm high concentrations and the Fala Moor (2 km north of Brothershiels) background levels. Conversely however, that the Bush site and Glentress Forest (300 m) show a correlation of concentrations, when they are 23 km apart (N–S), shows that factors controlling air concentrations also operate regionally, such as environmental conditions, and support these as being background sites. Given this pattern of local elevation of concentrations at sources, yet regional trends in background concentrations, it is clear that monitoring to imply concentrations at a regional scale can only be done for background sites; sites near specific sources of emission must be considered individually.

The background monitoring data collected here may be used for estimation of budgets of NH_3 over different vegetated surfaces, and this is done in the following chapter using the understanding of surface exchange developed in Chapters 4 and 5. However, some caution is needed because of the evidence that diffusion tubes over-estimate NH_3 concentrations. As discussed earlier, such over-estimation may either be a sampling artifact (*e.g.* wind enhancement, NH_4^+ capture) and therefore apply to all NH_3 diffusion tube sampling systems, or may result from analytical errors (*e.g.* laboratory deposition to samples, inclusion of contaminated values) that may be overcome by appropriate techniques and data treatment.

The analytical errors have been accounted for in this study and may be the cause of the differences observed between the ITE and Harwell diffusion tubes, suggesting that the latter over-estimate air concentrations; at Great Dun Fell the Harwell air concentrations were a factor of 1.6 larger than the ITE values, while for the annual estimates for S. Scotland this value ranged from 1.4 to 7. Further evidence that the Harwell diffusion tubes over-estimate air concentrations comes from the comparison of air concentrations in S.E. England noted by Martin (1988, pers. comm.) where the Harwell tubes over-estimated filter-pack air concentrations of NH_3 (Allen *et al.*, 1988) by a factor of 1.9. As an approximation, it seems reasonable to conclude that the Harwell NH_3 concentration map for the UK (see Figure 6.9) may over-estimate air concentrations by a factor of 2. It is possible that an additive correction may be more appropriate, though further study is needed to investigate this.

A major consequence of this conclusion is that estimates of deposition which use the Harwell concentration data, such as those given by RGAR (1990), probably over-estimate dry deposition by a factor of 2. As a consequence, the monitoring data collected in this study is considered to provide a more realistic estimate of air concentrations for S. Scotland, and is therefore used in the modelling of exchange fluxes in Chapter 7. Nevertheless, there is still some evidence that the values in this study may also over-estimate air concentrations (Great Dun Fell comparison, section 6.5.4). If this is sustained, it is presumably a result of the sampling artifacts noted above, and suggests that some correction of sampling rates may be needed in order for NH_3 diffusion tubes to provide an accurate measure of air concentrations. Further studies are needed to explore this possibility.

Chapter 7

General discussion: The surface/atmosphere exchange of ammonia

7.1. PREVIOUS STUDIES AND PRESENT APPROACH

At the start of this report the atmospheric cycle of ammonia was reviewed (Chapter 1), and it is useful to summarize briefly the main points made. Consideration was given to the chemistry, history of research, atmospheric concentrations, sources and sinks, and environmental effects of atmospheric NH_3 and NH_4^+. Of these, particular attention was paid to the 'background' surface/atmosphere exchange over vegetated surfaces, where, although much study had been made, important gaps were seen to exist in the understanding of the cycle, with many of the studies being largely isolated from one another. In that section studies motivated by an agricultural interest were therefore brought together with those from an air pollution interest, while field studies measuring NH_x dry deposition directly were compared with micrometeorological and laboratory exchange studies.

From this a picture emerged, that, while both NH_3 and NH_4^+ are present in the atmosphere in approximately similar concentrations (Table 1.6), the NH_3 component is potentially the more important in terms of dry exchange processes. The NH_4^+ aerosol is a secondary pollutant, resulting from the conversion of emitted atmospheric NH_3, which dry deposits very slowly, its main sink being removal by nucleation and scavenging, returning to earth in precipitation or cloud droplets (section 1.4.2).

For gaseous NH_3, a number of different patterns of surface exchange have been observed. Many of the early studies of total NH_x exchange over natural surfaces emphasized the importance of soil processes. Most of these authors found NH_x deposition (*e.g.* De Rossi, 1947; Malo and Purvis, 1964; Hanawalt, 1969; section 1.2.1). Conversely one study showed emission from some soils (Georgii and Lenhard, 1978), although these authors note that their soils had been fertilized at some point. Another study even went so far as to model emission from natural (ungrazed and unfertilized) surfaces on the assumption of soil emission (Dawson, 1977; section 1.3.1).

More recently, exchange measurements over natural surfaces have emphasized the role of vegetation. Field studies of NH_4^+ in forest throughfall, in areas of large NH_3 emission in the Netherlands, showed much larger deposition fluxes than by precipitation alone (Van Breeman *et al.*, 1982; Draaijers *et al.*, 1987). This was suggested to be due to NH_3 deposition onto leaf surfaces and subsequent washing off

by precipitation. This seems reasonable given the connection between large throughfall fluxes and atmospheric NH_3 concentrations, although canopy exchange processes may complicate observations (*e.g.* Heil *et al.*, 1987) so that this method cannot be used reliably to derive dry deposition fluxes. The only existing micrometeorological studies over natural surfaces (Duyzer *et al.*, 1987) have confirmed a process of rapidly depositing NH_3, and rather slow deposition of NH_4^+. The small surface resistances (r_c) calculated by these authors show that the NH_3 must have been depositing largely to leaf surfaces, rather than to the soil or through stomata (section 1.4.3).

By contrast to the exchange over natural surfaces, micrometeorological studies of total NH_x exchange over fertilized agricultural surfaces have shown that emission can occur. (Table 1.8). As expected, this is greatest immediately following fertilizer application (Harper *et al.*, 1983). Conversely, the background exchange for these surfaces encompasses both emission and deposition. The general trend is toward emission in dry conditions, while deposition may occur when the crop surface is wet (Dabney and Bouldin, 1985), although Denmead *et al.* (1978) found the reverse to be true in relation to soil wetness. Most of these studies considered the emission to come from the soil. This was demonstrated for one study by Denmead *et al.* (1976) who also showed that emitted NH_3 could be recaptured by the vegetation above, forming an 'internal cycle' within the canopy. Conversely other authors considered that emission of NH_3 could come from the vegetation itself by emission through stomata (*e.g.* Lemon and Van Houtte, 1980; Harper *et al.*, 1987).

Controlled laboratory experiments on plants have generally excluded soil from chambers, and have predominantly shown deposition of NH_3 to occur, the route of uptake being stomata (*e.g.* Hutchinson *et al.*, 1972; Aneja *et al.*, 1986; Van Hove *et al.*, 1987a; Table 1.7). However, these studies have generally used rather high NH_3 concentrations, often >50 $\mu g\ m^{-3}$. Low concentration studies have shown NH_3 emission can occur by the same route (*e.g.* Meyer, 1973; Farquahar *et al.*, 1980; Morgan and Parton, 1989), suggesting the existence of a substomatal 'compensation point' concentration of NH_3 (χ_{cp}), which may be of the same order as atmospheric concentrations. Deposition occurs when air concentrations exceed χ_{cp}, whereas emission occurs when they are less than χ_{cp}. The study of Farquahar *et al.* (1980) emphasized the role of temperature in controlling the value of χ_{cp}, while other studies have observed a dependence on growth stage, with larger fluxes at anthesis and during leaf senescence for annual plants (*e.g.* Farquahar *et al.*, 1979; Morgan and Parton, 1989). However, none of these chamber studies dealt with the effect of leaf surface wetness on exchange. More recent measurements by Van Hove *et al.* (1987b) have shown that at higher relative humidities some leaf surface deposition may occur.

The situation is further complicated by the role SO_2 may have in co-depositing with NH_3, so that each neutralizes the other on the surface, enabling a larger quantity of deposition. This was suggested as a result of the throughfall studies of Van Breeman *et al.* (1982), who observed large equivalent quantities of throughfall SO_4^{2-} alongside the NH_4^+. Van Hove *et al.* (1989, 1990) have also observed this enhancement in the laboratory, though at the high concentrations used (> 50 $\mu g\ m^{-3}$) they found the leaf surface sink to be saturated in several hours, the main route for deposition being through stomata (section 1.4.3). Conversely, in field conditions with much lower air concentrations, it is likely that this saturation period may take much longer, lasting several days or even weeks (Draaijers *et al.*, 1987).

Present approach

It is clear that these different ideas need tying together in a coherent manner. The study reported here aimed to build on the information base summarized above (and discussed in full in Chapter 1), by making micrometeorological measurements over vegetated surfaces. To examine the processes controlling the exchange of the gaseous and particulate fractions, NH_3 and NH_4^+ were sampled separately. Measurements were made over both natural and unfertilized surfaces, and fertilized agricultural surfaces in a wide range of conditions, both during the day and at night, while attention was paid to the condition of vegetation, including wetness/dryness, surface temperature and humidity. Fluxes were calculated using a standard but thorough implementation of the aerodynamic gradient method, as outlined in Chapter 2, the only new development being a convenient formulation of the Richardson number (equation 2.29).

The fluxes were analyzed using the usual form of the resistance analogy as described in section 2.4. In addition, a modified resistance analogy for estimating surface concentrations was also developed in order to examine the possibility and size of the 'compensation point' concentration (equations 2.56–2.58). The theory for micro-meteorological estimation of surface concentrations is well established and has largely been developed in ecophysiological research with respect to heat and water vapour (*e.g.* Thom, 1975). However, the application to NH_3 exchange represents a new extension of this theory. Recently Denmead (1990, pers. comm.) has independently also used this approach. Aside from this development, the study here reports unique measurements of NH_3 exchange over unfertilized neutral and calcareous grasslands, while the measurements over moorland contribute to a very limited dataset, especially for night-time runs, the only other data being that of Duyzer *et al.* (1987). Conversely, while the study of exchange over agricultural surfaces is not particularly new, the measurement as separate NH_3 and NH_4^+, rather than total NH_x, has not been reported before for surfaces of defined fertilization, and allows the resistance and surface

concentration estimates to be made. Finally, the integration of both natural and agricultural surfaces into one study is new, and allows a coherent picture of surface exchange to be developed.

The applied interest in developing an understanding of the exchange of ammonia is to quantify exchange budgets (long term fluxes) for different surfaces and locations. This is useful for providing data to models of air mass transfer and atmospheric chemistry, and to define the atmospheric inputs into ecosystems. For the latter, most concern centres on the ecological effects of nitrogen deposition to natural surfaces, so that the budgets over these surfaces are of particular interest. In order to estimate such budgets, where the resistance analysis model of transfer applies, monitored air concentrations may be related to transfer resistances to estimate long term fluxes (section 2.4.1). Consequently, in this study a small monitoring program of NH_3 concentrations was made to facilitate such estimates, which was reported in full in Chapter 6.

In accordance with this dual interest, of NH_3 exchange processes, and estimation of budgets, the following discussion is divided into two parts. In the first part, the surface exchange patterns reported in Chapter 4 and Chapter 5 are summarized and related, and then considered in terms of the different surface exchange mechanisms discussed above. In the second part, the understanding developed is used with the results of the NH_3 monitoring and other published concentrations to estimate annual budgets of NH_3 for different vegetated surfaces.

7.2. EXCHANGE PROCESSES

7.2.1 Surface exchange observed in this study

The particulate NH_4^+ component was found to deposit very slowly to the vegetated surfaces studied here, giving very small concentration gradients with height, which were generally not significantly different from zero. The mean of 19 determinations gave V_d = 1.9 mm s^{-1}, which is in good agreement with other published results. For example, Duyzer *et al.* (1987) calculated an average of 1.8 mm s^{-1}, while for similar SO_4^{2-} aerosol Nicholson and Davies (1987) recorded 0.7 mm s^{-1}. Given the approximate nature of the results here, no detectable variation with vegetation type or conditions was observed. The possibility of non-conservation of NH_4^+/NH_3 was also assessed. For the consistently small gradients of NH_4^+, and often maximal gradients of NH_3 (see below) this was not considered to be of great importance in the present context of background exchange of NH_3 (section 4.3–4.4).

The NH_3 fluxes and rates of transfer were generally much larger than those of NH_4^+. Consequently the study focused on the exchange of the former component. Two

different patterns of exchange were observed for the vegetated surfaces studied. For natural and unfertilized surfaces a consistent pattern of deposition was seen in all the conditions encountered. For fertilized agricultural surfaces, a bi-directional exchange was observed, with warm dry conditions favouring emission, and cool wet conditions favouring deposition. These different patterns are considered below.

Natural and unfertilized surfaces

Most of the natural and unfertilized surfaces showed rapid NH_3 deposition, with r_c generally approximating to zero for both day and night-time measurements. The measurements were most precise over the moorland and grassland sites, while results over a forest site, which were subject to much greater uncertainty, were also consistent with this pattern. Hence the main limitation to deposition was the atmospheric resistances, r_a and r_b, defined largely by site roughness and windspeed. By definition, the near zero r_c implies that the surface concentration estimate $\chi\{z_o'\}$ also approached zero. For cases of deposition, $\chi\{z_o'\}$ defines the maximum net compensation point (χ_{cp}) for the soil/plant system. Consequently, no compensation point applies in these cases, so that deposition velocities (V_d) are independent of air concentration between the concentrations studied (a maximum of 3.5 $\mu g\ m^{-3}$) and zero. Similarly, since only aerodynamic resistances are accounted for, the sink for the NH_3 must be the roughness elements of the canopy — the leaf surfaces. If deposition through stomata were the main route, a value of $r_c > 50\ s\ m^{-1}$ would be present in the day time increasing to the order of 1000 $s\ m^{-1}$ with the closing of stomata at night (Jarvis, 1981; Wallace *et al.*, 1981).

In some cases in dry and warm conditions, a small value of r_c was recorded. At Fala Moor 5/1988 reliable values were up to 8 $s\ m^{-1}$, which is very small, while at Huntingdon 8/1987, values up to 49 $s\ m^{-1}$ were found. Changes of r_c in these runs were seen to occur even when the vegetation was dry but where humidities and temperatures varied, with warm dry conditions favouring the development of a surface resistance. No runs were made during very dry or droughted conditions (with very low relative humidity), which would be useful for confirming this possibility.

The only clear exception to this pattern of exchange was the dataset recorded at Harwell 3/1988. Here r_c was consistently large with a mean of 125 $s\ m^{-1}$. A possible explanation is that this was due to the presence of calcareous soil (from recent harrowing) being distributed over the leaf surfaces (section 4.6.4). This is reasonable if the deposition is normally to water associated with the leaf surfaces, since the high soil pH (8.4) would limit NH_3 solubility, and hence deposition.

Fertilized agricultural surfaces

Measurements over fertilized agricultural crop surfaces gave a very different pattern of exchange to that for unfertilized surfaces. In wet and cool conditions deposition of NH_3 occurred, while in dry and warm conditions emission occurred.

Measurements in winter (Bush 2/1989), to a melting snow pack and wet grass showed rapid deposition with $r_c < 26$ s m^{-1} (mean 18 s m^{-1}), though V_d remained small due to the smooth nature of the snow surface. As a consequence of the small r_c, $\chi\{z_o'\}$ was also small, so that at low air concentrations (between zero and the highest concentrations encountered, 3 μg m^{-3}), V_d is independent of concentration. During a period of light frost a larger r_c was recorded of up to 80 s m^{-1}. It is not possible to say whether this change was due to an increased χ_{cp} when the surface froze ($\chi\{z_o'\}$ up to 0.4 μg m^{-3}), but the change was most clear in r_c, and the development of a resistance to transfer upon freezing might be expected as the ice precludes aqueous diffusion of deposited NH_3 away from the surface.

The general pattern of exchange in the summer measurements over fertilized vegetation (Bush 6/1988; Stenton 6/1989, barley) was emission of NH_3. Nevertheless, deposition of NH_3 was also recorded during wet conditions. In this situation r_c was not always near zero and in one well quantified run (Stenton, run 5) r_c was 130 s m^{-1}. Hence the presence of surface water on the vegetation appeared to be the main factor controlling the switch between emission and deposition. In addition, the emission potential, as measured by the surface concentration estimates $\chi\{z_o'\}$ and $\chi\{z_o''\}$ (see below), was greatest in conditions of highest temperature and lowest relative humidity.

Since emission occurred for much of the time it is clear that the resistance analogy using r_c and assuming zero surface concentration (section 2.4.1) is inappropriate. The exchange must depend on the size of the overall surface or net χ_{cp}, as well as air concentrations and transfer resistances. In the case of emission, the surface concentration estimate $\chi\{z_o'\}$ represents the minimum value this might have, since it accounts only for r_a and r_b. However, from the previous studies noted above, it is more likely that further resistances are involved, with emission from stomata or the soil. No parameterization is available in this study for emission from soil below the canopy, however, if emission is through stomata, χ_{cp} may be estimated by $\chi\{z_o''\}$ (equation 2.57).

At Bush 6/1988, within-canopy profiles showed that the soil was not emitting NH_3, so that leaf stomata are presumed to be the source of emission. As a consequence, $\chi\{z_o''\}$ was used as an estimate of the substomatal χ_{cp}. Values in dry conditions at this site were 1.7–7.3 μg m^{-3}. Conversely, in wet conditions, because of leaf surface deposition, $\chi\{z_o''\}$ approached zero. In this case it is clear that a substomatal χ_{cp} is

neither determinable nor relevant, since leaf surface processes dominate. In addition, given that leaf surface deposition may also be occurring in dry conditions, $\chi\{z_0"\}$ may again be an under-estimate of the substomatal χ_{cp}.

By comparison, it was not clear from the within-canopy profiles at Stenton 6/1989 (barley) whether the soil or vegetation was the main source of the emitted NH_3. To clarify this, further profiles were made within a similarly managed wheat crop at the same site — though with the crop at a later stage of development with a fully closed canopy. In this case the possible sources were the soil and senescing leaves near ground level. Consequently for this site, either or both of soil and stomatal emission may be important. For dry conditions reliable estimates of $\chi\{z_0"\}$ were 1.3–3.1 $\mu g\ m^{-3}$ for the barley crop, which is similar to the results at Bush 6/1988. If soil emission were occurring, this would be an over-estimate of a substomatal χ_{cp}, while as before, any leaf surface deposition would offset this to give an under-estimation.

7.2.2 Comparison with other studies

No other measurements of NH_3 exchange with unfertilized meadows (Huntingdon and Harwell sites) have been published, although the results over moorland may be compared with those of Duyzer *et al.* (1987). As noted earlier, these authors found a similar pattern of rapid NH_3 deposition, though they also found a more pronounced development of r_c in dry conditions. Accepting a considerable degree of variation, they summarized their results as $r_c = 9\ s\ m^{-1}$ for wet conditions and $28\ s\ m^{-1}$ for dry conditions (overall mean: $23\ s\ m^{-1}$). These authors did not report canopy humidities and found no clear relationship between exchange and air temperature.

Given the good general agreement of this study with that of Duyzer *et al.* (1987), both may be compared with some of the other studies of natural surfaces mentioned earlier. In the results presented here, the importance of vegetation exchange is emphasized, as compared with the soil exchange suggested, for example, by Di Rossi (1947), Malo and Purvis (1964) and Hanawalt (1969), while the consistent pattern of deposition suggests that the assumption of emission of Dawson (1977) is incorrect. Conversely, the leaf surface deposition observed in this study agrees well with the results of Van Breeman *et al.* (1982) and Draaijers *et al.* (1987), where they suggested that large observed throughfall fluxes of NH_4^+ were due high air concentrations of NH_3 causing increased dry deposition to leaf surfaces, which was subsequently washed off by rain. Nevertheless, because of canopy exchange processes, the use of throughfall studies to estimate deposition fluxes should be treated with caution.

The field results over natural surfaces may also be compared with plant exchange studies performed in the laboratory. Most of these studies found little leaf surface

deposition, with deposition through stomata dominating (*e.g.* Hutchinson *et al.*, 1972; Aneja *et al.*,1986; Lockyer and Whitehead, 1986; Van Hove *et al.*, 1987a; see Table 1.7), which disagrees with the findings of this study. However, these laboratory studies generally used unrealistically high concentrations (often >50 $\mu g\ m^{-3}$), so that it seems likely that saturation of the leaf surface sink must have occurred. Additionally, by comparison to the conclusion of Farquahar *et al.* (1980), the field results here show that no overall canopy or net 'compensation point' concentration (χ_{cp}) exists in the field for natural surfaces, as demonstrated by the analysis of $\chi\{z_o'\}$. It is possible that a substomatal χ_{cp} does exist, but not for the surface as a whole, as leaf surface deposition dominates. The studies of the effect of humidity on surface uptake of Van Hove *et al.* (1987b,1990) go some way toward the results observed here, but, probably as a result of their use of high concentrations, the effect was again limited.

The very different pattern recorded in this study for fertilized agricultural surfaces, of a bi-directional exchange of NH_3, is well supported by the literature. The fluxes recorded here, however, fall with in a much smaller range of -24 (emission) to 35 (deposition) ng $NH_3\ m^{-2}\ s^{-1}$ when compared with other studies (Table 1.8). For example, the only other U.K. measurements of NH_3 exchange over crop surfaces gave fluxes in the range -120 to 24 ng $NH_3\ m^{-2}\ s^{-1}$, although fertilization details were not provided nor the source ascertained (Harrison *et al.*, 1989). Denmead *et al.* (1978) measured background total NH_x fluxes over fertilized grassland in Australia of between -930 and 220 ng NH_x-$NH_3\ m^{-2}\ s^{-1}$. The opposite relationship which they observed to that expected for soil moisture may relate to the special case of hydrolysis of applied urea in the soil (see section 1.3.1). The soil (fertilized with ammonium nitrate) was probably also the source of the emission for the measurements at Stenton 6/1989 in this study, though it was not possible to confirm this. Conversely, the canopy emission at Bush 6/1988, supports the existence of a stomatal compensation point (Farquahar *et al.*, 1980), first suggested for field results by Lemon and Van Houtte (1980). The estimate for dry conditions in this study of ≈2–7 $\mu g\ m^{-3}$ — which may be an underestimate because of leaf surface deposition — is still much larger than the estimate of Farquahar *et al.*, whose results predict 0.5 $\mu g\ m^{-3}$ for the mean dry run $T\{z_o'\}$ of 15 °C at Bush (Figure 1.1). Other studies have also given larger estimates of χ_{cp}. The similar micrometeorological surface concentration estimates of Denmead (1990, pers. comm.) for rice give a χ_{cp} of 10–15 $\mu g\ m^{-3}$, although this may be an over-estimate due to the use of total NH_x measurement. Morgan and Parton (1989) also found a large χ_{cp}, with values ranging over 16 to >30 $\mu g\ m^{-3}$ depending on growth stage (Table 1.7).

No other NH_3 studies appear to be available for comparison with the winter deposition measurements at Bush 2/1989, although large values of r_c in frozen condtions

Plant species	N fertilization kg ha^{-1} $year^{-1}$	% N content	Reference and notes	
Lolium perenne	300	3	Whitehead and Lockyer (1989)	
typical fertilized grass	200–300	2.5	"	For U.K. conditions
Eriophorum vaginatum	none	1.83	Heal and Smith (1978) *	green leaves
	"	1.01	"	brown leaves
Calluna vulgaris	"	1.35	"	green shoots
Erica tetralix	"	0.86	"	green shoots

Table 7.1 Typical plant shoot percent nitrogen contents (% N) for fertilized agricultural cultivars and unfertilized native plants. Data are approximate since variations occur seasonally and as a function of the time period between fertilization and measurement (Whitehead, 1970). * Data for Moor House NNR, see Table 4.1

have been reported for both SO_2 and HNO_3 (Johansson and Granat, 1986). In addition Iribarne and Pyshnov (1990) showed no loss of NH_3 from NH_4^+-containing solutions upon freezing, which suggests that no χ_{cp} develops. Consequently, the interpretation of the results here as a surface resistance, r_c, seems most appropriate.

7.2.3 Comparison of background NH_3 exchange over fertilized and unfertilized ecosystems

The main difference between the natural and unfertilized sites and the fertilized agricultural sites in this study is that of the nitrogen fertilization received by the latter, although none of the measurements were made immediately following fertilizer application. The difference in the exchange patterns may therefore be attributed to the nitrogen (and presumably NH_3) status of the ecosystem; the higher the nitrogen status of the ecosystem the greater the tendency toward emission. This factor appears to have been largely ignored in most of the laboratory studies on plants, with most using well fed plants (*e.g.* Farquahar *et al.*, 1980; Van Hove *et al.*, 1987a; Table 1.7), although Parton *et al.* (1988) have studied the effect of different fertilization rate on NH_3 emission from wheat. They found fluxes (expressed on a leaf area basis) to be similar for both low and high N plants. Conversely, studies by Lockyer and Whitehead (1986) and Whitehead and Lockyer (1987, 1989) have observed clear effects of plant N status on both assimilation of atmospheric NH_3 and emission from decomposing vegetation, with higher N status reducing deposition and favouring emission.

The value of a stomatal χ_{cp} will be maintained by the NH_4^+ concentration, temperature and pH of the plant intercellular fluids (section 1.1). However, there appears to be a lack of such NH_4^+ data for different levels of N fertilization. Nevertheless, shoot % N content is commonly measured and might be considered an indicator of this. As shown in Table 7.1, there is some relationship between % N content and fertilization, although this is very approximate since variations also occur seasonally and for the time period

since the last fertilization. It is possible that the trend to higher % N contents in fertilized plants reflects a higher intercellular NH_4^+ concentration.

The existence of a NH_3/NH_4^+ pool in plant metabolism has been discussed by Farquahar *et al.* (1980) and Farquahar (1983). In addition, these authors discuss the observation that this concentration, and therefore χ_{cp}, may increase following anthesis and during leaf senescence in annual plants. This has been observed by a number of authors (Tables 1.7, 1.8) and may give an approximate doubling of the normal emission flux for these periods. It has been suggested (Morgan and Parton, 1989) that this reflects an increased $[NH_4^+]$ due to a change in the balance between NH_4^+ releasing reactions (de-amination reactions, nitrate reduction, senescence induced proeolysis) and NH_4^+ uptake reactions (N transport, and NH_4^+ assimilation *via* glutamate synthetase) which may occur during senescence.

By comparison with fertilized systems, natural and unfertilized vegetation probably has a much lower intercellular $[NH_4^+]$ and correspondingly smaller stomatal χ_{cp}. In addition, soil $[NH_4^+]$ is expected to be much smaller in the absence of fertilization, giving lower soil χ_{cp}. As a consequence, the overall χ_{cp} has little effect and leaf surface deposition dominates. Leaf surface deposition is also expected for the fertilized crop ecosystems. However, as with the laboratory studies using high NH_3 concentrations, the large quantities of NH_3 at these surfaces may also result in a degree of leaf surface saturation, so that emission is not as restricted as it otherwise might be. Nevertheless, in wet conditions the greater leaf surface sink results in net deposition occurring.

The different processes within the soil/canopy system may be envisaged as internal cycles of NH_3, such that it is the balance of these which determines the net exchange with the atmosphere. The different pathways, exchange sites and factors for such a system are summarized in Figure 7.1. The concept of an internal cycle of NH_3 within a plant canopy is not new; Denmead *et al.* (1976) introduced the idea for a flux of NH_x from soil to vegetation. However, other routes may also be included, such as stomata to the atmosphere, stomata to leaf surface, or stomata to the soil surface. In addition, NH_3 dry deposited to the leaf surfaces may subsequently be washed to the ground by precipitation (Van Breeman *et al.*, 1982; Draaijers *et al.*, 1987).

The $\chi\{z_o''\}$ estimate at Bush 6/1988 may be used to illustrate this net exchange. The value of 2–7 $\mu g\ m^{-3}$ is probably an under-estimate of a stomatal χ_{cp} given the existence of leaf surface deposition. Yet, even this is much larger than typical air concentrations at Bush (mean: 1.1 $\mu g\ m^{-3}$; Chapter 6) so that the normal tendency of the crop would be toward stomatal emission. However, because of the offsetting leaf surface depos-

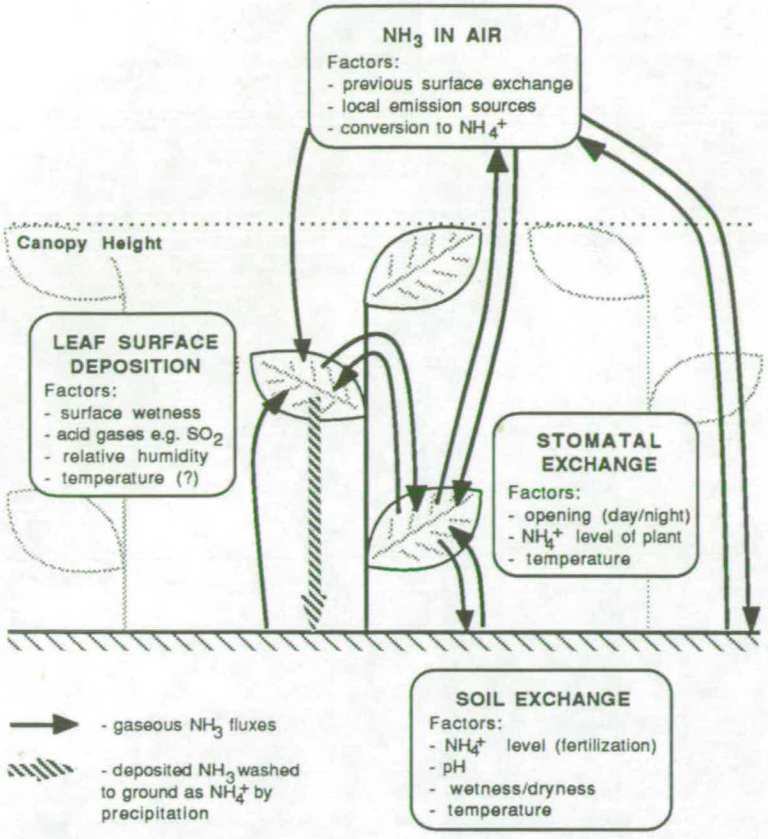

Figure 7.1 Proposed NH_3 cycles in a soil/vegetation/atmosphere system. Individual fluxes are denoted by arrows. Boxes denote surface exchange sites and NH_3 atmospheric concentration, for which factors controlling each are noted.

ition, this is only the case in warm dry conditions, when surface uptake is most easily overcome, and when the χ_{cp} is largest. In wet conditions, and over natural surfaces the leaf surface sinks outweigh (or short-circuit) the tendency to emission and net deposition occurs. This is clearly very different from the simple concept of a bi-directional exchange process dependent only on the relative magnitudes of the substomatal χ_{cp} and air concentrations (*e.g.* Farquahar *et al.*, 1980; Morgan and Parton, 1988), which is therefore seen to be an over-simplification. At Bush (in Summer) it is more likely that a continuous emission occurs through the stomata, but only in dry conditions does this result in net emission to the atmosphere.

7.2.4. Surface uptake mechanisms and acid gas interactions

The mechanism of leaf surface uptake is probably either physical adsorption to the surface waxes of the cuticle or dissolution in water films on the leaf surface. From the work of Van Hove *et al.* (1987a, 1989), it seems that the resistance to diffusion through the cuticle is large, and therefore of limited importance.

In wet conditions it is reasonable to assume that dissolution in surface water is important, given the high solubility of NH_3 described by Henry's Law. However, in this study and that of Duyzer *et al.* (1987) over natural surfaces, leaf surface uptake

was also important when leaf surfaces appeared dry. In this case it is possible that deposition occurs by adsorption onto leaf cuticles. It may be speculated that a limited number of adsorption sites exist on the leaf surface, which in practice for natural surfaces in background concentrations, are not saturated before a precipitation event washes the leaves clean. However, in the presence of high NH_3 concentrations, such as in many of the chamber studies mentioned or in fertilized agricultural situations, it is possible that these sites become saturated.

Another possibility involves the presence of water adsorbed on the leaf surfaces, which may exist on a micro-scale even when the leaves are visibly dry. Such a water-associated deposition process was demonstrated by Van Hove *et al.* (1987b) with the observation of a leaf surface capacitance for NH_3 which increased exponentially in size toward 100 % relative humidity. For the very high concentrations of their study (56, 100 $\mu g\ m^{-3}$ NH_3) the effect was limited compared to stomatal uptake, though for background concentrations this may become more important. It is therefore probable that both surface humidity (controlling adsorbed water) and free water are important in controlling deposition, which is consistent with the results of this study.

As has been mentioned earlier, this relatively simple pattern of deposition is complicated by the presence of acid gases, such as SO_2, which may interact with the NH_3 to increase deposition. For wet surfaces this was clearly demonstrated by Adema *et al.* (1986), who showed greatly increased fluxes of both NH_3 and SO_2 to distilled water in a wind tunnel when they were present together. Singly, these gases tend to raise or lower the pH of the water, respectively, eventually reaching equilibrium with the atmospheric concentration (section 1.1). However, the opposing pH of the gases means that equivalent deposition of each maintains the pH mid-way. Concurrently, oxidation of HSO_3^- (from dissolved SO_2) to SO_4^{2-} occurs, which results in the formation of ammonium sulphate (*e.g.* $(NH_4)_2SO_4$), as observed in large quantities in throughfall by Van Breeman *et al.* (1982). In comparison, the experiments of Van Hove *et al.* (1989, 1990) to investigate this in dry conditions and for different humidities, as noted earlier, found only a limited effect. Again it is possible that this process becomes more important at the lower concentrations typical of background conditions.

Conceptually, such surface deposits may be compared with atmospheric ammonium sulphate aerosols. It is known that at low relative humidities these are present as solid particles while at higher humidities they deliquesce to form droplets. The relative increase in droplet radius follows an approximate exponential increase similar to that found by Van Hove *et al.* (1987b) for surface NH_3 capacitance. Between ≈40–80 % relative humidity both solid and aqueous fractions are present. Above this all soluble material is dissolved, forming progressively more dilute droplets at higher humidities

Site, dates and times (GMT)		χ(1 m) ($\mu g\ m^{-3}$)	χ(1 m) ($nmol\ m^{-3}$)	F_χ * ($nmol\ m^{-2}\ s^{-1}$)	$r_a + r_b$ ($s\ m^{-1}$)	r_c ($s\ m^{-1}$)	Conditions and notes
Bush 28/2/1989							
NH_3	(1235–1535)	0.59	35	0.71	27.5	21.0	melting snow and wet
SO_2	(1355–1450)	0.89	14	0.78	27.9	-10.0	vegetation,
SO_2	(1450–1550)	1.1	17	0.50	38.9	-4.4	T(1 m): 3.7 °C
O_3	(1450–1550)	33.6	700	5.64	37.2	86.9	
Stenton 20–21/6/1989							
NH_3	afternoon †	≈2	≈120	≈-1 ‡	—	emission	day-time, dry,
SO_2	(1630–1640)	1.1	17	1.44	8.7	3.3	T(1 m): 22 °C
O_3	(1630–1640)	97.1	2023	17.5	8.5	107	
NH_3	night-time †	≈1	≈60	≈-0.1 ‡	—	emission	night-time, dry,
SO_2	(2245–2255) ¶	7.1	112	0.39	181	105	T(1 m): 11 °C
O_3	(2245–2255) ¶	62.0	1290	1.67	116	659	

Table 7.2 Measurements of NH_3, SO_2 and O_3 exchange over fertilized grassland (Bush) and barley (Stenton). SO_2 and O_3 data from unpublished results of Hargreaves *et al.* (1990). Results are discussed in the text. Notes: * deposition fluxes are positive; † estimated from measurements above an adjacent wheat crop, see Figures 5.8–5.10; ‡ estimated from measurements on 8–9/6/1989, see Appendix 3; ¶ data calculated from Bowen ratio measurements;

(Winkler, 1986). Hence for the frequently high humidities at leaf surfaces, even in dry conditions, this 'bound-aerosol' may be acting as the water layer for deposition.

The balance between the acid and base component may also be important. In the study here, for most of the measurements no SO_2 data was collected. However, given that the mean NH_3 concentration for the natural surface measurements was 0.8 $\mu g\ m^{-3}$ (≡ 47 $nmol\ m^{-3}$, range of campaign means: 6–120 $nmol\ m^{-3}$; Table 4.3) and typical background SO_2 concentrations for the areas studied are 3–17 $\mu g\ m^{-3}$ (≡ 47–270 $nmol\ m^{-3}$; RGAR, 1990), it is likely that SO_2 was generally in excess. As a consequence for these situations, it is likely that the excess SO_2 would tend to lower pH on leaf surfaces allowing rapid NH_3 deposition. Conversely, over the fertilized agricultural surfaces, with emission of NH_3, it is likely that NH_3 was in excess at the leaf surfaces. This might limit the rate of NH_3 leaf surface deposition, while SO_2 deposited rapidly. The importance of leaf surface pH is also supported by the observation of large r_c at Harwell 3/1988, since it is possible that this was a result of the buffering to a high pH by the disturbed soil, which limited surface NH_3 uptake.

Some measurements of SO_2 fluxes were also made at the same time as the NH_3 (Hargreaves *et al.*, 1990, unpublished data) and this is summarized in Table 7.2. For the measurements at Bush 2/1989, NH_3 and SO_2 were present in roughly equivalent air concentrations (SO_2 being di-basic). Minimal r_c was recorded for both gases over the wet surface. The fluxes were in similar molar quantities, so as to form NH_4HSO_4 rather than $(NH_4)_2SO_4$. These proportions must be accepted as approximate because

of the limited data, although the general pattern is consistent with the co-deposition hypothesis outlined above. Ozone (O_3) data are also given for comparison. Given the limited solubility of O_3 in water, this deposited rather slowly.

At Stenton 6/1989 the SO_2 measurements were made over the barley crop at the same time as the NH_3 within-canopy profiles for the wheat crop, so that the NH_3 fluxes are only estimated values. However, for the day-time example, with NH_3 emission occurring, and an excess air concentration of NH_3 to SO_2, rapid SO_2 deposition (near zero r_c) to the leaf surfaces was recorded. It is likely that the excess NH_3 provided a high pH so that the leaf surfaces acted as an efficient sink of SO_2, even in these dry conditions. These results may be compared with the night-time run where SO_2 air concentrations were in excess of the NH_3, and NH_3 emission much less. Here a considerable r_c for SO_2 was present, suggesting that, where relatively less NH_3 is available to neutralize the SO_2, some leaf surface saturation may occur. The O_3 deposition was again much slower, and as expected was consistent with stomatal rather than leaf surface uptake (Galbally and Roy, 1980; Kerstiens and Lendzian, 1989). Given that the r_c for SO_2 was much less than for O_3, it suggests some surface uptake was still occurring.

A further complicating factor which has received little attention is interaction with the acid gases HCl and HNO_3. The possibility of interactions *via* non-conservation of fluxes was discussed earlier, though considered not to be of large importance for background exchange processes here (see sections 3.8.1, 4.3–4.4). However, it is also possible that an interaction similar to that for SO_2 occurs on leaf surfaces. No evidence to test this hypothesis is available from for data collected in this study, though further calculations made here from the data presented by Harrison *et al.* (1989) reveal the possibility of an interaction (Figure 7.2). Given the limited number of parameters provided by these authors the calculations are limited and somewhat approximate. Nevertheless, as Figure 7.2 shows, it is possible that high surface concentrations or emission flux of NH_3 may promote more rapid HCl and HNO_3 deposition. This is contrary to the conclusion of these authors and that of others, that HCl and NHO_3 deposit to vegetation at with zero r_c for non-frozen conditions (*e.g.* Huebert and Robert, 1985; Dollard *et al.*, 1987). Conversely, it is possible that this data provides evidence that fluxes of HCl, HNO_3 and NH_3 are not conserved as they are deposited or emitted, and this again is contrary to the conclusion of Harrison *et al.* (1989), as discussed in the sections noted above. The existence of either of these processes would affect exchange rates of these components: leaf surface neutralization would reduce emission of NH_3 or increase deposition rates (affects r_c, $\chi\{z_o'\}$), whereas non-

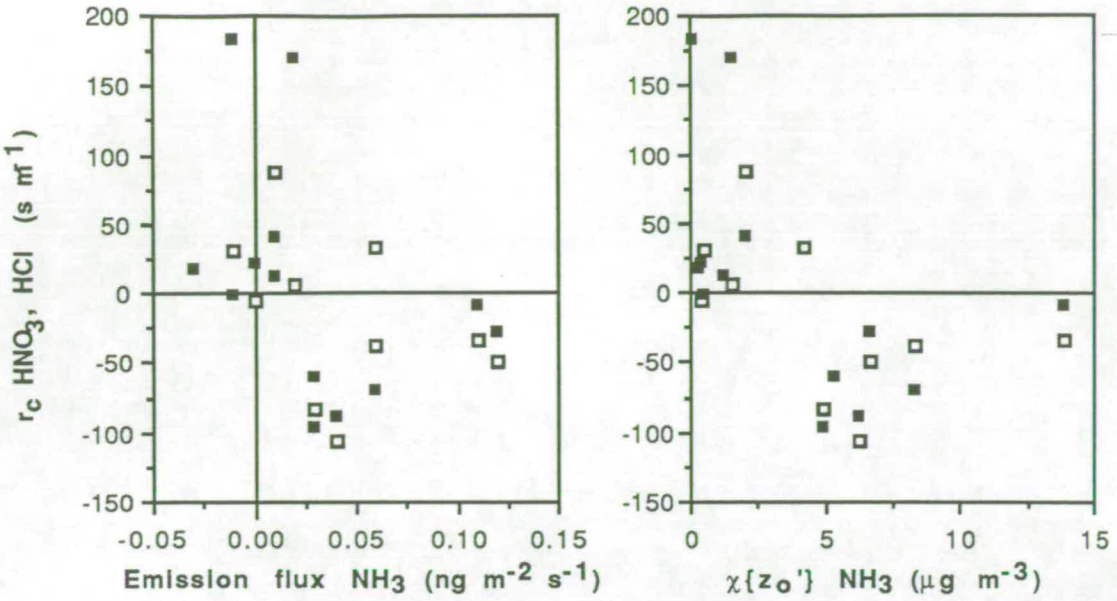

Figure 7.2 Surface resistance of HNO_3 and HCl as a function of NH_3 flux and surface concentration ($\chi\{z_o'\}$). The values are calculated from data given by Harrison *et al.* (1989). Given the limited number of parameters provided, the calculations used to derive these data are only approximate, taking no account of stability corrections. □ denotes HNO_3, ■ denotes HCl.

conservation would allow exchange in either direction to be more rapid than permitted by turbulent diffusion alone (analogous to reducing r_a).

It is clear that further work is needed to assess the importance of both surface neutralization processes (for SO_2, HCl and HNO_3) and non-conservation of chemical species. In particular, this should focus on understanding and quantifying the chemical mechanisms controlling each of these.

7.2.5 Concentration dependence of exchange rates

The possibility that exchange rates, as measured by a deposition velocity (V_d), are not independent of air concentrations of NH_3 for low concentration conditions has been discussed earlier (section 7.2.1). This arises where a compensation point concentration (χ_{cp}) exists at the surface, rather than zero concentration. It was shown that a net χ_{cp} could occur for fertilized agricultural vegetation, causing emission for much of the time, with the size of this depending on interacting factors at the surface. Conversely, over natural and unfertilized surfaces, leaf surface deposition dominates and no net χ_{cp} is observed. Here V_d is independent of air concentration for concentrations down to zero, and the usual resistance model of transfer (equation 2.45) may be applied with monitored air concentrations so as to estimate budgets.

However, NH_3 deposition rates, even over natural surfaces, are not expected to be independent of air concentrations for very high concentration situations. This was demonstrated by the saturation of leaf surface uptake in the high concentration chamber

studies, and also suggested for the agricultural surfaces emitting NH_3. While no concentrations high enough to saturate unfertilized leaf surface sinks were observed in this study, one set of measurements made by Duyzer *et al.* (1987) suggest this is possible. For 7 runs in dry conditions over heathland (T = 6–17 °C), with a mean concentration of 17 μg m^{-3} NH_3, they recorded a mean r_c of 64 s m^{-1}, which was much larger than their overall mean. Although measurements of r_s were not made, this figure is still small when compared to the day-time r_s of 50–290 s m^{-1} (median 110 s m^{-1}) found for similar vegetation by Miranda *et al.* (1984), which suggests some leaf surface uptake may still have been occurring. Nevertheless, this increase in r_c has important consequences for the data collected here and for that collected by Duyzer *et al.*(1987). It is likely that, where very high concentrations occur immediately adjacent to sources (*e.g.* > 50 μg m^{-3}), deposition of NH_3 encounters larger r_c than measured in either study.

The interaction with acid gases, such as SO_2, is also expected to be important to this high concentration limitation. It is likely that at high SO_2 concentrations, NH_3 leaf surface uptake remains unsaturated at higher NH_3 concentrations. Conversely, a similar pattern is expected for SO_2 transfer. Previously it has been thought that, while some leaf surface uptake of SO_2 may occur in dry conditions, the major route of uptake is through stomata. However, many of the measurements have been made in polluted atmospheres, where gas detection is easiest. For example, Fowler and Unsworth (1979) observed deposition according to the pattern described above in a study with atmospheric concentrations between 11–152 μg m^{-3} SO_2 (mean: 47 μg m^{-3}). By comparison, the air concentration for the day-time example at Stenton was 1 μg m^{-3} SO_2, and r_c approached zero (see Table 7.2). In the former case it is likely that SO_2 was generally in excess of NH_3, while the opposite was true for this run at Stenton. Consequently, model estimates predicting SO_2 dry deposition using conventional theory, are likely to give under-estimates at low concentrations.

In summary it may be concluded that the assumption of concentration independence of V_d is appropriate for NH_3 deposition to natural and unfertilized surfaces at background atmospheric concentrations ($\approx<$ 5 μg m^{-3}). However, it is not appropriate where a net compensation point exists, as with NH_3 emission from agricultural surfaces, or at higher air concentrations ($\approx>$10–20 μg m^{-3}), where saturation of leaf surface sinks becomes important. At even higher air concentrations in dry conditions ($\approx>$ 50 μg m^{-3}) stomata are expected to be the main route for deposition, though such concentrations are only applicable very near sources of NH_3 emission. Co-deposition or surface neutralization with SO_2 may modify these ranges, so that the balance between NH_3 and SO_2 at the surface is important in controlling deposition. As with NH_3, it is also likely that SO_2 deposition velocities are not independent of concentration. At low SO_2

concentrations, particularly in the presence of high concentrations of NH_3, it is likely that SO_2 deposition to leaf surfaces is not saturated, which allows much faster deposition than predicted by stomatal uptake alone. For rural areas with low SO_2 concentrations, this would result in dry deposition fluxes being substantially larger than currently estimated (*e.g.* RGAR, 1990). In addition, a reduced r_{cSO_2}, would allow larger deposition velocities to forests, which are already considered to be more efficient sinks than short vegetation for other pollutants (Fowler *et al.*, 1989).

7.3. SURFACE EXCHANGE BUDGETS OF ATMOSPHERIC AMMONIA

In the previous sections it was seen that NH_3 exchange over vegetated surfaces depends on the interaction between many factors at the surface, as summarized in Figure 7.1. Given the complexity of these different processes, it is clear that further research is needed if the functional responses of each are to be fully characterized. Nevertheless, the measurements in this study are representative of background exchange in a cool-temperate climate, and provide a good basis for the estimation of exchange budgets in these conditions.

Budgets of NH_3 surface/atmosphere exchange are of interest both for agricultural and natural surfaces. In the agricultural context, exchange represents a gain or loss of nitrogen which is required for crop growth. For natural surfaces concern centres on the quantities of nitrogen deposited, or the input of acidity which this may represent, either of which may give rise to undesirable ecological changes (see section 1.6). In addition to this surface orientated approach, budgets are also of interest in the modelling of atmospheric transport and chemistry, where exchange represents a gain or loss from the atmosphere. In this section, the understanding of surface exchange developed above is used to estimate annual background exchange budgets for typical example sites. This presentation is primarily of interest for ecosystem dynamics, although implications for atmospheric models are also drawn.

7.3.1 Example budgets for natural and unfertilized surfaces

Over natural and unfertilized ecosystems it has been concluded from this study that the usual resistance analogy for transfer is applicable. For the background exchange process described here, r_c approaches zero for most of the time. Consequently, V_d may be modelled assuming $V_d = 1/(r_a + r_b)$, values for which may be estimated (assuming overall neutral conditions) from appropriate values of $u\{z\}$ and z_o (section 2.4). V_d is then used in conjunction with monitored air concentrations, in this case from Chapter 6 and other published sources, to estimate the flux, which is given as an annual value.

Table 7.3 shows modelled fluxes of ammonia over example natural and unfertilized surfaces calculated on the basis of deposition velocities referenced at the height of NH_3 monitoring. (Data for calculations over wet agricultural surfaces are also included and discussed in section 7.3.2 below.) Over short vegetation the different methods discussed earlier for calculating r_b give similar values of V_d, and in this case the method of Garland (1977) is used (see Figure 3.5). However, over forests the differences are much larger, representing a major uncertainty in the calculation. On the basis of the review of Garratt and Hicks (1973), it is considered that the formulation of Wesely and Hicks (1977) gives more realistic results for forests. Both this and the method used for short vegetation by Garland (1977) are used here for comparison to show the magnitude of the errors that result from using the latter formulation for the exchange in this situation. The method of Monteith and Unsworth (1990) gives similar results to that of Wesely and Hicks (1977) and is not discussed in this section.

Another source of error is the applicability of estimated air concentrations at the given reference heights. For sites such as Fala Moor, where monitored air concentrations are available for the reference height and surface to be modelled, this error is avoided. However, where air concentrations are monitored over one surface in order to model exchange over another, it has to be assumed that the concentration gradients are the same over both surfaces, since concentrations monitored near ground level may be enhanced or depleted by surface exchange. Hence, monitoring should be made over surfaces with similar emission/deposition characteristics as the surfaces to be modelled, and this may be reasonably assumed for the data in Table 7.3.

In addition, the surface gradients also depend on the site roughness. This is discussed in full in Appendix 8, and depends on the method used to calculate r_b. Using the method of Garland (1977), gradients of concentration with height above d for surfaces with $r_c = 0$ are similar for a wide range of roughness (Short grass, long grass and forest are examined in Appendix 8). However, over forest the method of Wesely and Hicks (1977) predicts much larger gradients and therefore much larger surface depletion. As a consequence, where the Garland method is used, concentrations monitored over short vegetation may be used directly to imply those over forests. Conversely, the same procedure using the preferred Wesely and Hicks method results in over-estimation of air concentrations, and therefore deposition fluxes. This is relevant to the fluxes estimated in Table 7.3, since the concentrations used for the forest areas are generally monitored near ground level (*e.g.* 1.5 m) above short vegetation.

The resulting error in the estimation of fluxes to forests may be accounted for by estimating the concentration in the atmosphere at a height relatively unaffected by surface enhancement or depletion, and applying this with a deposition velocity

site type	location	$\approx z_o$ (m)	$u\{10\,m\}$ (m s^{-1})	ref. height (m)	V_d [b] (mm s^{-1})	χ NH_3 ($\mu g\ m^{-3}$)	Deposition flux NH_3–N [b] (kg ha^{-1} $year^{-1}$)
Moorland							
S. Scotland, upland	Fala Moor, Midlothian [a]	0.03	4.2 [d]	1.5	20.4	0.55 [f]	2.9
N. Scotland, remote	Lerwick, Shetland	0.03	7.1 [e]	1.5	33.0	≈0.4 [h]	3.4
Unfertilized meadow							
S. England, lowland	SSSI, Huntingdon [a]	0.02	3.6 [d]	2.5	16.0	≈2.6 [g]	10
Forest							
S. Scotland, upland	Glentress forest (300 m) [a]	0.5	3.3 [c]	1.5	34 (61)	0.58 [f]	5.1 (9.2)
	Glentress forest (600 m) [a]	0.3	5.3 [c]	1.5	48 (81)	0.44 [f]	5.4 (9.3)
C. Scotland, lowland	Glencorse wood, Bush [a]	1.0	3.9 [d]	1.5	46 (120)	1.1 [f]	13 (34)
E. England, lowland	Thetford forest, Norfolk	1.0	3.9 [d]	2.5	42 (99)	≈2.6 [g]	29 (67)
Agricultural crop	Calculations for when						
C. Scotland, lowland	grass wet (see Table 7.5)						
Bush [a]	winter (r_c = 0 s m^{-1})	0.02	3.9 [d]	1.5	17.2	0.77 [f]	—
	spring (r_c = 50 s m^{-1})	0.04	3.3 [d]	1.5	9.3	1.3 [f]	—
	summer (r_c = 100 s m^{-1})	0.06	3.3 [d]	1.5	6.6	1.6 [f]	—
	autumn (r_c = 50 s m^{-1})	0.02	4.4 [d]	1.5	9.8	0.85 [f]	—

Table 7.3 Ammonia surface exchange budgets for a range of U.K. natural and unfertilized vegetated surfaces. Calculations referenced at the height of NH_3 monitoring. Wet surface calculations for an agricultural crop at Bush are also given for inclusion in Table 7.5 below.

Notes: **a**, For further site details see Tables 4.1 and 5.1; **b**, For natural surfaces the deposition velocity is calculated assuming $r_c = 0$. In accordance with results for the wet crop surface, in Winter $r_c = 0$ and in Summer $r_c = 100$ s m^{-1}; for Spring and Autumn $r_c = 50$ s m^{-1}. r_b is calculated according to Garland (1977). For forest sites, the method of Wesely and Hicks (1977) gives better estimates (values in brackets), but these need to be corrected for surface depletion (see Table 7.4).

Windspeed data sources: **c**, transformed from $u\{2\ m\}$ data for 1988–89 (Crossley, 1990, unpublished results); **d**, From the MORECS database (see Ball *et al.*, 1983); **e**, From Chandler and Gregory (1976).

Concentration data sources: **f**, From Chapter 6 diffusion tube data; **g**, Estimated from Allen *et al.* (1988); **h**, Estimated from EACN total NH_x data (see Table 1.5) assuming 1/3 $NH_x = NH_3$.

site	$V_d\{10\ m\}$ (mm s^{-1})	$\chi\{10\ m\}$ ($\mu g\ m^{-3}$)	Deposition flux NH_3-N (kg ha^{-1} $year^{-1}$)
Glentress forest (300 m)	25, 38	0.77	5.0, 7.5
Glentress forest (600 m)	33, 47	0.58	5.0, 7.1
Glencorse wood, Bush	35, 67	1.45	13, 25
Thetford forest	35, 67	3.15	29, 55

Table 7.4 Ammonia deposition budgets for example forests in the U.K. calculated using a 10 m reference height above the surface. The deposition velocity,V_d, is calculated as $1/(r_a\{10\ m\} + r_b)$. Concentrations are rescaled for surface depletion assuming monitoring is made over short unfertilized vegetation where $r_c = 0$. To a good approximation $\chi\{10\ m\} = 1.32\ \chi\{1.5\ m\} = 1.21\ \chi\{2.5\ m\}$ (see Appendix 8).

Where paired values are given in the table, the first is calculated using the Garland (1977) formulation of r_b and the second using the Wesely and Hicks (1977) formulation. The latter method is considered to give better estimates of r_b over forest surfaces.

referenced at the same height (*e.g.* 10 m). Using the concentration profiles over surfaces with $r_c = 0$ for short vegetation, to a good approximation $\chi\{10\ m\} = 1.32 \times \chi\{1.5\ m\}$ (see Appendix 8). This re-scaling is used to give concentration estimates at 10 m in Table 7.4, from which revised flux estimates to forests are calculated using $V_d\{10\ m\}$. As expected, a comparison of Tables 7.3 and 7.4, shows little difference in the two flux estimates using the Garland method for r_b. Conversely, using the Wesely and Hicks method, the uncorrected fluxes in Table 7.3 over-estimate the corrected values in Table 7.4 by between 21 and 36 %. Hence, using this estimation of r_b (or the similar method of Monteith and Unsworth, 1990) alongside implied concentrations over forests, requires that the larger near-surface depletion of air concentrations should be accounted for in order to avoid over-estimation of fluxes.

The flux estimates in Table 7.3 and 7.4 are for the surface exchange experienced at example background sites. They therefore represent typical fluxes for natural vegetation surfaces over much of the U.K. The estimates are the most uncertain for forests, since the predicted deposition is very sensitive to the formulation of r_b that is used. For the estimates in Table 7.4 this uncertainty ranges from a factor of 1.4 to 1.9. Given that the Wesely and Hicks (1977) method is the more appropriate over forests, this shows that applying the estimate of r_b used for short vegetation by Garland (1977) to the case of forests results in a serious under-estimation of atmospheric inputs. In addition, it may be noted that the Wesely and Hicks formulation is based on the assumption that $k/B = 2$ for heat transfer over all values of Re*, which is only an approximation of observed determinations (Garratt and Hicks, 1973). Given the importance of r_b in defining the magnitude of fluxes to forests, particularly where r_c is minimal, it is therefore clear that further work is needed to define and quantify the factors controlling r_b.

A comparison of forests to shorter vegetation shows that the deposition velocities and fluxes are much greater to forests, due to the increased turbulence which allows increased deposition. This has been demonstrated elsewhere for a number of pollutants by Fowler *et al.* (1989). Using the deposition velocity approach, fluxes are also proportional to air concentration, so that the flux to an forest in E. England (Thetford: 55 kg NH_3-N ha^{-1} $year^{-1}$) is much greater than to forests in S. Scotland (*e.g.* Glentress: 7.5 kg ha^{-1} $year^{-1}$) due to the larger air concentrations at Thetford.

The effect of air concentration may also be seen for the deposition to short vegetation. Hence, despite the smaller deposition velocity estimated for for the unfertilized meadow at Huntingdon, the flux at this site (10 kg ha^{-1} $year^{-1}$) is much larger than to the moorland examples: Fala Moor, 2.9 kg ha^{-1} $year^{-1}$; Lerwick, 3.4 kg ha^{-1} $year^{-1}$. Conversely, the larger windspeeds on Shetland compared to S. Scotland, result in the

larger flux to moorland at Lerwick compared to Fala Moor. Given the similar deposition rates to unfertilized grassland and moorland, much moorland or heathland in S. England is likely to receive similar deposition to that at Huntingdon.

From the above it is seen that deposition to natural and unfertilized surfaces depends on air concentration, windspeed and site roughness. In addition, the estimates here are for representative background concentrations. Near sources of emission, fluxes will be much larger than these. It is difficult to generalize for such sites given the degree of variability of concentrations (see Table 1.6), however, fluxes several times larger than these may be expected. Conversely, saturation of leaf surface sinks at high concentrations is expected to reduce deposition velocities so as to moderate this increase.

7.3.2 An example budget for a fertilized agricultural grassland

For fertilized agricultural surfaces the approach used above, assuming concentration independent exchange rates, was noted to fail because of the existence of a compensation point (χ_{cp}) at the surface, with emission occurring for much of the time. In this case the flux depends not only on the air concentration and resistances, but also on the value of the net χ_{cp}. Consequently, the main interest for estimating the value of χ_{cp} was so that it could be included in models of exchange, as for example by Derwent (1987). However, since the net χ_{cp} may vary greatly both in time and for different sites, the simple approach of assuming a mean χ_{cp} is of little practical value. As was noted in section 7.2.5, there is potential for the development of more complex models accounting for this variation, though this is beyond the scope of this study.

As a simplified approach here, the flux is estimated seasonally. For each season the average flux during dry, wet or frozen periods is calculated. These are then summed for the percentage occurrence of each environmental condition so as to give seasonal fluxes, which are then summed to give an annual value. In dry conditions, emission rates are estimated for the mean seasonal temperature from the data collected at Bush 6/1988 and Stenton 6/1989. In wet and frozen conditions, deposition fluxes are calculated using the resistance analogy and monitored air concentrations. For wet conditions different seasonal values of r_c are assumed in accordance with exchange results: in Winter $r_c = 0$ s m^{-1} while in Summer $r_c = 100$ s m^{-1}. For Spring and Autumn $r_c = 50$ s m^{-1} is assumed, while for frozen surfaces $r_c = 100$ s m^{-1} is used.

The estimation of a typical exchange budget over an agricultural surface is given in Table 7.5 for a fertilized grass crop at Bush. Details of the calculation for periods when the surface is wet are given in Table 7.3. The calculation of fluxes in frozen conditions is similar, though details are not given. It is seen that the background NH_3 flux varies

season	mean T (°C)	mean flux NH_3 dry conditions (ng m^{-2} s^{-1}) [a]	mean flux NH_3 wet conditions (ng m^{-2} s^{-1}) [b]	mean flux NH_3 frozen conditions (ng m^{-2} s^{-1}) [c]	% time surface: dry, wet, frozen [d]	mean seasonal flux NH_3 (ng m^{-2} s^{-1}) [e]
Winter	4	—	13.2	4.9	0, 88, 12	12.2
Spring	8	-5	12.1	8.3	34, 61, 5	6.1
Summer	15	-15	10.6	—	60, 40, 0	-4.8
Autumn	10	-5	8.3	5.6	33, 61, 6	3.7
					Annual background flux (ng NH_3 m^{-2} s^{-1}):	4.3
					Annual background flux (kg NH_3-N ha^{-1} $year^{-1}$):	1.1
					Additional emission following fertilization with NH_4NO_3 (kg NH_3-N ha^{-1}):	-1.2
					Additional emission during senescence/hay drying (kg NH_3-N ha^{-1}):	-0.3
					Overall annual flux (kg NH_3-N ha^{-1} $year^{-1}$):	-0.4

Table 7.5 Example exchange budget of NH_3 for a fertilized grass crop at Bush. Positive fluxes denote deposition. The main body of the table considers background exchange processes occurring throughout the year. Estimates of the increased emission following fertilizer application and during plant senescence/hay drying are included at the base of the table.

Notes: a, Typical values for the temperatures from the data collected at Bush 6/1988 and Stenton 6/1989; b, Calculated from Table 7.3; c, Calculated similarly to wet surface data but assuming r_c = 100 s m^{-1}; d, Data from 3 hourly values of state of ground at Edinburgh airport for 1989; e, Sum of % components: wet, dry or frozen.

considerably for the different seasons. In this example, net emission occurs in summer, while net deposition occurs in all the other seasons. Accounting for only background exchange, as examined in this study, this site receives a small net deposition of 1.1 kg NH_3-N ha^{-1} $year^{-1}$.

This estimate is probably biased toward deposition compared to the overall annual exchange. Factors not accounted for include emission following fertilizer application and possible increased emission following anthesis and during vegetation senescence or hay drying. No measurements of the exchange during these periods were made in this study, while data from the literature are very limited and variable (see Tables 1.7 and 1.8) with values depending on both environmental conditions and management. In the U.K., fertilization with ammonium nitrate is usual, and this was the case for the grass crop at Bush. In this example a single batch of 150 kg N ha^{-1} was applied in late April. Harper *et al.* (1987) showed that emission rates following fertilization to wheat with 112 kg N ha^{-1} applied as ammonium nitrate in the southern U.S.A. were up to 4 times the normal emission rate, accounting for a total of 8.3 kg N ha^{-1} emission in the 2 weeks following application (≡ 800 ng NH_3 m^{-2} s^{-1}). Since the normal emission rates in that study (see Table 1.8) were much larger than here, this value is probably also larger. Over vegetation including crops in S.E. England Harrison *et al.* (1989) recorded emission of up to 120 ng NH_3 m^{-2} s^{-1} though fertilization details were not given. For the post-fertilization emission in the example here, an emission of 100 ng

NH_3 m^{-2} s^{-1} for 2 weeks is assumed. This gives a total of 1.2 kg N ha^{-1} emission, though there is considerable uncertainty in this estimate.

Emission of NH_3 may also be larger from senescing crop vegetation. However, most study has been made for the senescence of annual rather than perennial crops. In a study of exchange over a wheat crop Harper *et al.* (1987) estimated a loss of 7 kg N ha^{-1} during senescence, though, as with the case of losses following fertilization, this may again be an over-estimate for U.K. conditions. Conversely, Wetselaar and Farquahar (1980) have suggested such losses may be much smaller for perennial plants, where translocation to roots can occur. In support of this Whitehead *et al.* (1988) showed negligible loss from shade induced senescence of perennial rye grass. Hence for perennial grass crops, such that at Bush, total emission may be less than that from annual plants such as cereals. Nevertheless, further emission is possible where cut grass is left to dry in the field to make hay. Little information is available on this, although controlled laboratory drying of perennial rye grass by Whitehead *et al.* (1988) showed little emission. Conversely, these authors showed that emission could be large where rain allows decomposition of the cut grass, although these figures are difficult to extrapolate to field losses. The chamber experiments in Table 1.7 generally show an approximate doubling of NH_3 emission from senescing annual plants. If this is applied for the drying of the cut grass crop at Bush for a 3 week period, a further emission of 0.3 kg N ha^{-1} is predicted.

These additional exchange processes are included in Table 7.5. Overall this shows a small annual emission of 0.4 kg NH_3-N ha^{-1} $year^{-1}$. As has been noted, there is considerable uncertainty in this estimate, particularly for fertilizer and senescence related emission. Variation will also occur between annual and perennial crops, for different management practices and for different environmental conditions. In terms of using this estimate to typify exchange over U.K. crops, the uncertainty may be several kg N ha^{-1} $year^{-1}$. The results of Harrison *et al.* (1989) in S.E. England are not strictly applicable given that the surface fertilization was not defined. However, the mean of 19 runs at different times of year was an emission of 31 ng NH_3 m^{-2} s^{-1}, equivalent to 9.8 kg NH_3-N ha^{-1} $year^{-1}$, which suggests that emission from crops in the U.K. may frequently be larger than the estimate here. It is clear that more work is needed in order to characterize exchange over fertilized crop surfaces, especially for fertilizer, senescence and vegetation drying related emissions.

7.3.3 Comparison of NH_3 budgets over different vegetation surfaces and implications for atmospheric models.

The difference in NH_3 surface exchange processes over natural and unfertilized vegetation and fertilized agricultural vegetation, as discussed in section 7.2, is reflected in the different annual exchange budgets estimated above; unfertilized surfaces showing consistent rapid deposition, and fertilized showing bi-directional fluxes, resulting in annual net emission. The exchange over grazed vegetation has not been examined in this study, apart from the very low-density grazing at some of the unfertilized surfaces. As with fertilized crops, emission also occurs from more heavily grazed surfaces. For example, in a study by Jarvis *et al.* (1989) the net annual emission for 3 different cattle grazed pastures was estimated to be 7–25 kg N ha^{-1} $year^{-1}$ (see section 1.3.2).

These observations have important implications for models of atmospheric transport and deposition of NH_3, since models generally include a fixed deposition velocity estimate for all land surfaces (*e.g.* 8 mm s^{-1}, Asman and Janssen, 1987). Inventory estimates of emission are used as inputs to such models (*e.g.* Buijsman *et al.*, 1987; ApSimon *et al.*, 1987) and these include inputs from point source emissions, such as animal houses, and also surface exchange processes, such as emission from grazing animals in the field. In the case of the latter, it is clear from the results in this study that a deposition velocity should not be applied to the same land area, as is done with existing models.

It is possible that this in part explains the tendency of some European models to predict less wet deposition of NH_4^+ than recorded in monitoring studies (Derwent, 1987; Fisher, 1987). This is often attributed to an under-estimation of European emissions by the inventory of Buijsman *et al.* (1987) which is used in these models (Buijsman, 1987; Derwent, 1987). From the above, an alternative explanation is that regional NH_3 dry deposition is over-estimated by imposing a deposition velocity to emitting crop and grazed surfaces. Removing this from these surfaces would reduce the discrepancy, although Fisher (1987) has suggested that the disagreement could not entirely be accounted for by re-scaling deposition velocities.

Surface exchange differences may also explain observed geographical inconsistencies between models and field monitoring. For example, using an inventory approach in England and Wales, ApSimon *et al.* (1987) have shown that emissions are largest in the west, due to high livestock densities. As a consequence deposition may be predicted to be highest in these areas (Asman and Drukker, 1988). However, this is inconsistent with monitored NH_4^+ wet deposition, which is largest in the east of the country (Warren Spring Laboratory, 1988; Buijsman and Erisman, 1988). It is probable that

part of this discrepancy results from the different surface exchange processes in the west and east. Much of the land in the west is grazed pasture and therefore accounted for in the emission inventory. However, large areas here are also unfertilized uplands for which rapid NH_3 deposition is expected. Conversely, in the east, most of the land is either pasture or fertilized crop surfaces, where net annual emission rather than dry deposition is expected. If the extra deposition in the west and the emission rather than deposition in the east are accounted for, it is possible that much of the geographical inconsistency would be removed.

7.3.4 Comparison of sources and magnitude of deposition to natural and unfertilized vegetation.

Ammonia deposition is of interest both for the input of nitrogen which it represents and for its potential to acidify ecosystems (see section 1.6). In order to identify its importance for each of these processes, comparison with other inputs of N and acidifying pollutants is necessary. Comparison of the relative inputs of N is straightforward since this is found directly from the fluxes of each of the components of deposition. Conversely, an assessment of the acidifying input into ecosystems can only be approximate since this depends on the fate of the deposited species as governed by the status of the ecosystem. In addition, because of atmospheric transformations, it is important to distinguish between the deposited sources of acidity at a site, and attribution of this acidity to different emission sources.

Nitrogen deposition

A comparison of the different fixed nitrogen inputs into natural and unfertilized ecosystems is given in Tables 7.6 and 7.7. Inputs include dry, wet and cloud-water deposition of both oxidized and reduced N, resulting in the addition of NO_3^- and NH_4^+ respectively. In each table, deposition to a forest site is compared with that to short vegetation. This is done in Table 7.6 for two typical upland examples in S. Scotland, and in Table 7.7 for two lowland examples in S.E. England.

It can be seen that, for both the lowland examples and for the upland forest, dry deposition of NH_3 is the largest single input. The largest input at the upland moor (Fala Moor) is wet deposition of NH_4^+, which is also the second largest at the other sites. The importance of dry deposition of NH_3 is most pronounced for the lowland forest example (Thetford Forest) where it accounts for 75% of the total N input. Given that these examples are for background air concentrations, it is clear that dry deposited NH_3 will completely dominate the N input near NH_3 sources. These examples demonstrate the importance of understanding NH_3 surface exchange processes.

Site (height AMSL) and nitrogen species	wet deposition [a]	dry deposition: gaseous [b]	dry deposition: particulate [c]	cloud-water deposition [d]	total deposition
Upland forest *e.g.* **Glentress (600 m)**					
NO_3^-	3.5	1.0 (NO_2) 1.5 (HNO_3)	0.2	0.9	7.1
NH_4^+	4.5	7.1 (NH_3)	0.6	1.0	13.2
					20.3
Upland moorland *e.g.* **Fala Moor (330 m)**					
NO_3^-	3.5	1.0 (NO_2) 0.6 (HNO_3)	0.2	0.2	5.5
NH_4^+	4.5	2.9 (NH_3)	0.6	0.2	8.2
					13.7

Table 7.6 Budgets of fixed nitrogen deposition for example forest and moorland sites in S. Scotland (upland). For site details see Table 4.1. Figures in kg N ha^{-1} $year^{-1}$ deposited. NH_3 and HNO_3 fluxes to the forest surface are calculated using the Wesely and Hicks (1977) formulation of r_b, and are corrected for surface depletion effects.

Notes: **a**, wet deposition data from Warren Spring Laboratory (1988); **b**, Calculated using 10 m and 1.5 m reference heights for forest and grassland respectively. Concentrations of NO_2 (7 μg m^{-3}) and HNO_3 (0.5 μg m^{-3}) from RGAR (1990) are not re-scaled for height. Assumes NO_2: V_d = 1.5 mm s^{-1} and HNO_3: $V_d = 1/(r_a + r_b)$. NH_3 data from Tables 7.3 and 7.4. **c**, Assumes V_d = 1.5 mm s^{-1} and χ = 1.5 μg m^{-3} for particulate NH_4^+ and NO_3^-, see Table 1.6b, Appendix 4; **d**, from Fowler *et al.* (1989).

Site (height AMSL) and nitrogen species	wet deposition [a]	dry deposition: gaseous [b]	dry deposition: particulate [c]	cloud-water deposition [d]	total deposition
Lowland forest *e.g.* **Thetford (30 m)**					
NO_3^-	4.5	4.3 (NO_2) 3.2 (HNO_3)	0.4	—	12.4
NH_4^+	6.5	55 (NH_3)	0.8	—	62.3
					74.7
Lowland meadow *e.g.* **Huntingdon (15 m)**					
NO_3^-	4.5	4.3 (NO_2) 0.7 (HNO_3)	0.4	—	9.9
NH_4^+	6.5	10.0 (NH_3)	0.8	—	17.3
					27.2

Table 7.7 Budgets of fixed nitrogen deposition for example forest and unfertilized grassland sites in S.E. England (lowland). For site details see Tables 4.1 and 7.3. Figures in kg N ha^{-1} $year^{-1}$ deposited. NH_3 and HNO_3 fluxes to the forest surface are calculated using the Wesely and Hicks (1977) formulation of r_b, and are corrected for surface depletion effects.

Notes: **a**, wet deposition data from Warren Spring Laboratory (1988); **b**, Calculated using 10 m and 2.5 m reference heights for forest and grassland respectively. Concentrations of NO_2 (30 μg m^{-3}) and HNO_3 (0.8 μg m^{-3}) from RGAR (1990) are not re-scaled for height. Assumes NO_2: V_d = 1.5 mm s^{-1} and HNO_3: $V_d = 1/(r_a + r_b)$. NH_3 data from Tables 7.3 and 7.4. **c**, Assumes V_d = 1.5 mm s^{-1} and χ = 2.2, 3.5 μg m^{-3} for particulate NH_4^+ and NO_3^- respectively, RGAR (1990); **d**, Cloud water deposition negligible.

The relative inputs of oxidized and reduced N may also be compared. This is of interest since the oxidized inputs result from NO_x emission and reduced inputs from NH_3 emission. In each of the examples, reduced N deposition (NH_x) accounts for between 60 and 80% of the N input. This shows that, in terms of N eutrophication, NH_3 emission and deposition is much more important than NO_x.

Acid deposition

A comparison of the components of acid or acidifying deposition may be made either in terms of the emitted primary pollutants (mainly SO_2, NO_x and NH_3), or in terms of the different components of deposition received by ecosystems. The first case is of interest in order to identify the contribution of different emission sources to the acidification of ecosystems, while the second is appropriate when defining the suite of deposited pollutants and the relative contribution to acidification among these.

A major complication in either approach is that the acidifying potential of NO_x, NH_3 and their products depends on their fate when deposited onto ecosystems (Binkley and Richter, 1987; Gundersen and Rasmussen, 1988; Driscoll and Shaefer, 1989). This was demonstrated in Figure 1.4 for an input of NH_3 or NH_4^+. In particular, nitrification (bacterial oxidation) in the soil of NH_x to NO_3^- is an acidifying process. Nitrification generates two H^+ ions from each deposited NH_4^+ and one H^+ ion from each NH_3 molecule. Input of NH_4^+ followed by plant or microbial assimilation is also acidifying, since the NH_4^+ is converted to the organic R-NH_2 form. Conversely, uptake of NH_3 and conversion to R-NH_2 has no net acidifying effect. The different possible fates of deposited HNO_3 or NO_2 (equivalent to HNO_3) or NO_3^- also affect the degree of acidification. When taken up by plants and microbes, reduction of NO_3^- to R-NH_2 results in HNO_3 and NO_2 having no net acidifying effect, whereas uptake of NO_3^- may reduce the acidity. Acidification from HNO_3 and NO_2 occurs where these remain in or are leached from the soil. As with oxidized N, plant or microbial uptake and reduction of SO_2 or H_2SO_4 to organic R-SH forms may also have no acidifying effect, whereas SO_4^{2-} may reduce acidity. However, this uptake is much less important for S than for N, and most of the deposited S remains in or is leached from the soil (Binkley and Richter, 1987; Eriksson, 1988). As a consequence, equivalent deposition from S is generally more acidifying than that from N.

An inventory of the acid and acidifying components of deposition into the four example ecosystems considered in Tables 7.6 and 7.7 is given in Table 7.8. Direct sources of acidity are given in the table for wet and cloud-water deposition, as well as from dry deposition. In addition, potential sources and sinks of acidity are included, with NH_4^+ and NH_3 generating acidity, and NO_3^- with the potential to consume acidity. In Table

	wet deposition [a]			dry deposition						cloud water deposition [d]			H^+ input	
Chemical species	H^+	NH_4^+	NO_3^-	SO_2 [b]	NO_2 [c]	HNO_3 [c]	NH_3 [c]	NH_4^+ [c]	NO_3^- [c]	H^+	NH_4^+	NO_3^-	Total H^+ (mmol m^{-2} $year^{-1}$)	% of positive inputs from NH_x
H^+ produced (mol/mol)	+1	+1 or +2	-1 or 0	+2	0 or +1	0 or +1	0 or +1	+1 or +2	-1 or 0	+1	+1 or +2	-1 or 0	—	—
SITES (height AMSL)														
Upland forest	0.35	4.5	3.5	3	1	1.5	7.1	0.6	0.2	0.11	1.0	0.9		
***e.g.* Glentress (600 m)**	*35*	*32–64*	*-25–0*	*19*	*0–7*	*0–11*	*0–51*	*4–9*	*-1–0*	*11*	*7–14*	*-6–0*	*76–221*	40–62
Upland moorland	0.35	4.5	3.5	3	1	0.6	2.9	0.6	0.2	0.02	0.2	0.2		
***e.g.* Fala Moor (330 m)**	*35*	*32–64*	*-25–0*	*19*	*0–7*	*0–4*	*0–21*	*4–9*	*-1–0*	*2*	*1–3*	*-1–0*	*66–164*	39–59
Lowland forest	0.25	6.5	4.5	10	4.3	3.2	55	0.8	0.4	—	—	—		
***e.g.* Thetford (30 m)**	*25*	*46–93*	*-32–0*	*63*	*0–31*	*0–23*	*0–393*	*6–11*	*-3–0*				*105–639*	37–78
Lowland meadow	0.25	6.5	4.5	10	4.3	0.7	10	0.8	0.4	—	—	—		
***e.g.* Huntingdon (15 m)**	*25*	*46–93*	*-32–0*	*63*	*0–31*	*0–5*	*0–71*	*6–11*	*-3–0*				*105–299*	37–59

Table 7.8 Acid deposition loadings for example unfertilized ecosystems in the U.K. For site details see Tables 4.1 and 7.3. For each site the first figure is the deposition (kg ha^{-1} $year^{-1}$) expressed as H, N or S. The second figure (in italics) is the equivalent H^+ ion input (mmol m^{-2} $year^{-1}$). Considerable uncertainty exists for the potential input of acidity depending on the fate of the deposited ion. For nitrogen species, ranges are given: the first figure represents the case where complete nitrogen uptake by plants or soil microbes occurs, the second is where all the deposited NH_x is oxidized to NO_3^-, and negligible plant and microbial uptake of N occurs.

A diagram of the possible fate and acidification following NH_x deposition is given in Figure 1.4. Other relationships for oxidized N are given by Binkley and Richter (1987) from which the H^+ balances are calculated. Plant uptake of sulphur species is less important and ranges are not calculated. Dry deposition of H^+ in aerosols is assumed to be small and is not calculated

Notes: **a**, from Warren Spring Laboratory (1988); **b**, from RGAR(1990); **c**, from Tables 7.6 and 7.7.; **d**, calculated from Fowler *et al.* (1989).

Table 7.8 alternative acid production ratios (mol H^+ produced/mol ion deposited) are given for the N species. In accordance with the above, minimum acidifying potential results from complete plant and microbial uptake, whereas maximum acidifying potential results from no uptake of N, with all deposited NH_x being nitrified. Minimal assimilation of S is assumed and ranges are not given.

Examination of the potential acid loadings in Table 7.8 from each of the deposited pollutants shows that the fate of the deposited N species has a major effect on the acid loading. In practice, acidification from N deposition only occurs where the deposition exceeds N uptake by plants and microbes, and N is no longer the limiting nutrient. This state is termed N saturation. Where deposition exceeds this level, NO_3^- may remain in or be leached from the soil, resulting in acidification.

The percentage of the potential acidifying input from NH_x deposition is also given in Table 7.8. Even where plant uptake dominates and minimal nitrification occurs, NH_x represents ≈40% of the acidifying input, mainly as wet deposition of NH_4^+. Where deposition exceeds plant uptake and nitrification is efficient, deposited NH_x has the potential to account for up to 60–80% of the acidifying input. The highest percentage is for the lowland forest example (Thetford, 78%), which results from the very large dry deposition fluxes of NH_3. In these cases it is clear that the bulk of the acidifying input is not deposited directly in acid form, such as acidic wet or dry deposition, but results from plant uptake and nitrification of deposited NH_4^+ and NH_3.

Although much of the acidifying input is deposited as NH_4^+, this is itself a product of neutralization of H_2SO_4 and HNO_3 in the atmosphere from emitted SO_2, NO_x and NH_3. In order to attribute the acidifying input into ecosystems to different sources of emission, the potential acidifying effect of each of the primary pollutants needs to be considered. This has been given elsewhere as (Duyzer *et al.*, 1987; Ivens *et al.*, 1989):

$$H^+ = 2SO_x + NO_y + NH_x \qquad 7.1$$

where SO_x = dry deposited SO_2 + wet and dry deposited SO_4^{2-}
NO_y = dry deposited NO_2 and HNO_3 + wet and dry deposited NO_3^-
NH_x = dry deposited NH_3 + wet and dry deposited NH_4^+.

From the above discussion it is clear that this formula should not be used to identify the relative components of deposition, and that the actual acidifying potential of each of these depends on the fate of the deposited species. If the latter is accounted for, assuming that assimilation of N species may be important, whereas assimilation of S is minimal, then the relationship may be modified to:

	deposited species (kg S, N ha^{-1} $year^{-1}$) (*mmol H^+ m^{-2} $year^{-1}$*)				% acidifying input attributable to pollutant emission		
Sites (height AMSL)	SO_x[a]	NO_y[b]	NH_x[b]	Total H^+ input	SO_2	NO_x	NH_3
Upland forest	12	7.1	13.2				
***e.g.* Glentress (600 m)**	*75*	*0–51*	*0–94*	*75–220*	34–100	0–23	0–43
Upland moorland	12	5.5	8.2				
***e.g.* Fala Moor (30 m)**	*75*	*0–39*	*0–59*	*75–173*	43–100	0–23	0–34
Lowland forest	20	12.4	62.3				
***e.g.* Thetford (30 m)**	*125*	*0–89*	*0–445*	*125–659*	19–100	0–14	0–68
Lowland meadow	20	9.9	17.3				
***e.g.* Huntingdon (15 m)**	*125*	*0–71*	*0–124*	*125–320*	39–100	0–22	0–39

Table 7.9 Total acidifying potential of deposited S and N species and attribution to emitted pollutants. Ranges of acidifying effect are given for N deposition. Where complete plant or microbial uptake of deposited N occurs, no acidification is attributable to N emission, and the lower figure is appropriate. Where no N uptake occurs, and where all the deposited NH_x is nitrified the upper figure is appropriate. In practice neither extreme is likely. For larger N fluxes, non-uptake and nitrification are more likely, so that the acidifying effect will tend towards the upper figure. Minimal S uptake is assumed so that ranges are not given. Notes: a, from RGAR (1990); b, from Tables 7.6 and 7.7.

$$H^+ = 2SO_x + (0–1)NO_y + (0–1)NH_x \qquad 7.2$$

Using this formula the relative acidifying contribution of the different emitted pollutants (SO_2, NO_x and NH_3) may be calculated and compared. This is done in Table 7.9.

A comparison of Tables 7.8 and 7.9 shows that the estimated ranges of the total acidifying input agree well with each other, which confirms the approaches used. However, given the ranges of possible acidifying effect, it is clear that only limited information on the relative sources of acidity from SO_2, NO_x and NH_3 may be made without a consideration of probable scenarios for the fate of the deposited N, which is beyond the scope of this work. Nevertheless, it may be seen that NH_3 emission has the potential to account for a maximum of 30–70% of the acidifying deposition in the examples given. Conversely, NO_x emission accounts for a maximum of 20–25%, so it is likely to be less important to acidification than NH_3, although it may become more important where nitrification of NH_x is limited.

7.3.5 Effects of N deposition and implications for emission control policies

The extent to which ecological effects result from atmospheric deposition has recently been formalized in the concept of a 'critical load', which is the maximum deposition flux of a pollutant which causes no significant harmful ecological effects (Nilsson and

Grennfelt, 1988). The estimation of the critical load is necessarily an approximate task and values are expected to be revised (generally downwards) as further experiments identifying effects are performed. Conversely, poor definition of the deposition occurring in critical loads experiments, such as the use of bulk wet deposition and under-estimation of dry deposition inputs, may result in values being revised upwards.

Nilsson and Grennfelt (1988) have estimated critical loads for eutrophication and acidification for different ecosystems. Ecosystems differ in sensitivity, though an upper value at the least sensitive sites is 20 kg N ha^{-1} $year^{-1}$. At more sensitive sites critical loads may approach zero, as any deposition is likely to have an effect. A conversion of heathlands to grasslands is expected where deposition exceeds 20 kg ha^{-1} $year^{-1}$, whereas acidification of heathlands may occur with a much lower deposition of less than 5 kg ha^{-1} $year^{-1}$. Critical loads for forests are suggested to be in the range 3–20 kg ha^{-1} $year^{-1}$, and for neutral unfertilized grassland 3–10 kg ha^{-1} $year^{-1}$.

A comparison of these figures with the total fluxes presented in Tables 7.6 and 7.7 shows that N deposition at each of the example sites exceeds the critical load estimates for the most sensitive ecosystems. If the examples are taken as approximately representative of sites in the U.K. — although it is stressed that much variation is likely — it suggests that background deposition of N is likely to cause harmful ecological effects. The lowest deposition estimate is for upland moorland (*e.g.* Fala Moor) with an input of 14 kg N ha^{-1} $year^{-1}$. For such sites a change of heathland to grassland vegetation is therefore unlikely, although deposition may have acidifying effects. Conversely, deposition to heathlands in S. England (with similar fluxes to the unfertilized meadow, Huntingdon) is approximately twice this (27 kg N ha^{-1} $year^{-1}$) and a transition to grasslands may be expected. The deposition to the unfertilized meadow is equally likely to cause ecological effects. A comparison of the two forest examples shows that while deposition at upland sites, such as Glentress Forest, is only moderately in excess of the critical load, that to lowland forests such as Thetford forest is much larger (75 kg N ha^{-1} $year^{-1}$). It is therefore likely that lowland forests in the U.K. are at significant risk from N deposition, on the basis of current critical loads estimates. Effects may include eutrophication, leading to a change in ground flora, acidification of soils and ground-water, as well as nutrient imbalances in the trees (Nilsson and Grennfelt, 1988). In addition, since these flux estimates are for background deposition, near sources of emission significantly larger fluxes and ecological effects may be expected.

These conclusions have important consequences for emission control policies. From Tables 7.6 and 7.7 it is seen that between 60–80 % of the N input is deposited as NH_x

from emitted NH_3, as compared to 20–40 % as oxidized N from emitted NO_x. In Europe NH_3 emission results predominantly from livestock farming activities, whereas NO_x emission arises largely from combustion sources, such as from motor vehicles and electricity generation. Hence, in terms of atmospheric N inputs into unfertilized ecosystems the combustion source input is much less important than that from agricultural emission. As a result, control measures aimed at reducing NO_x emission, such as the European Community Large Combustion Plants Directive (EC-LCP Directive, CEC, 1989) will only have limited effectiveness at reducing N deposition. In order to achieve major reductions in N deposition, measures to control NH_3 emission are required.

As has been shown in Table 7.9 and the discussion above, calculation of the relative importance of NH_3 emission to the acidification of ecosystems, in relation to SO_2 and NO_x, is a much more complicated and uncertain task. Assimilation of deposited N by plants limits the acidifying effect attributable to emitted NH_3 and NO_x. By comparison, minimal assimilation of deposited S occurs, so that deposition of an equivalent quantity of S is usually more acidifying than N. Despite this, where N deposition exceeds plant uptake, and nitrification of deposited NH_x occurs, N species can contribute significantly to the acidification of ecosystems alongside S. For the sites in Table 7.9 a maximum of between 30–70% of the acidifying input may be attributable to NH_3 emission. This demonstrates that NH_3 emission should also be considered in emission control measures designed to reduce acidifying deposition. Again, the EC-LCP Directive (CEC, 1989), which includes reductions in both SO_2 and NO_x emissions, is expected to have only partial effectiveness in the absence of measures to reduce NH_3 emission.

Of the European NH_3 emission, over 80% is estimated to result from livestock farming activities (Buijsman *et al.*, 1987). The emission is connected with the fate of the livestock waste, with major sources being losses from grazing animals in the field, from housed livestock and stored waste, and from the application of liquid manure as a fertilizer. As a result, measures to control NH_3 emission need to focus on these sources. Voorburg and Monteny (in preparation), as part of the Dutch Priority Programme on Acidification, have reviewed such procedures and conclude that the most effective control is to limit emission from the spreading of liquid manure, which accounts for 50 % of the agricultural NH_3 emission in the Netherlands. Incorporation of the manure, by injection in the case of grasslands and by ploughing or harrowing for arable surfaces, can reduce emission by between 50–99% depending on the method used, although some caution is needed since this may increase denitrification losses of N_2O (Freney *et al.*, 1990). Other techniques include minimizing losses by using closed storage or by acidifying manure.

7.4. AREAS REQUIRING FURTHER STUDY

More information is required on:

- The extent of increased r_c for unfertilized surfaces in very dry conditions (low humidity) or in the presence of high atmospheric NH_3 concentrations. The effect of acid gases (SO_2, HNO_3, HCl) on this response and the chemical mechanism of deposition.
- The confirmation of increased r_c over unfertilized vegetation surfaces with exposed calcareous soil.
- The size of r_c for different temperatures in frozen conditions.
- The relative importance of surface wetness/dryness (free water and humidity) and temperature in controlling the bi-directional exchange over fertilized crop surfaces.
- The relative size of soil and plant compensation points for fertilized agricultural and unfertilized natural ecosystems, and the response to different fertilizer application rates.
- The magnitude of NH_3 emission following fertilizer application to agricultural surfaces, from cut vegetation left in the field, and during senescence for both annual and perennial plant species.
- The concentration of NH_3 in the atmosphere.
- The validity of passive diffusion tube measurements of NH_3 concentrations.
- The extent of non-conservation of NH_3 fluxes for different exchange situations.
- The magnitude of r_b over forests.
- The effect of CO_2 on reducing NH_3 solubility in water (separate from pH effects).

7.5. RECOMMENDED CRITERIA FOR FUTURE MEASUREMENTS OF NH_3 SURFACE/ATMOSPHERE EXCHANGE

Further studies of the exchange of NH_3 over vegetated surfaces should:

- define the vegetation, soil type and management, especially the use or absence of fertilizers.
- measure NH_3 and NH_4^+ separately so as to identify the exchange processes of each. This allows resistance and surface concentration analyses to be made.
- measure environmental variables during exchange measurements, particularly surface temperature, wetness and humidity.
- include both day and night-time measurements.
- where possible identify the source of any NH_3 emission.

7.6. SUMMARY

• The atmosphere contains trace quantities of ammonia gas (NH_3) and particulate ammonium (NH_4^+) in approximately similar concentrations. Background concentrations are usually in the range 0.01–10 $\mu g\ m^{-3}$, though near sources much higher NH_3 concentrations (>100 $\mu g\ m^{-3}$) may occur.

• Monitoring of NH_3 concentrations in this study using passive diffusion tubes showed mean background concentrations in rural areas in S. Scotland to range between 0.4 and 1.1 $\mu g\ m^{-3}$.

  ◦ This is much smaller than the concentrations measured, using similar diffusion tubes to those here, by a national monitoring network in the U.K., the results of which have been reported by RGAR (1990). These give a regional average of 1.5 to 3 $\mu g\ m^{-3}$ for S. Scotland. A sampling comparison performed in this study confirmed that the methods used in the national network provide larger estimates of air concentration than those here. Other available data suggest that the results reported by RGAR (1990) typically over-estimate air concentrations (and therefore deposition) by at least a factor of 2. As a consequence, the national network data are are not used here for the estimation of dry deposition budgets (see below).

  ◦ Possible errors in NH_3 diffusion tube sampling arise from sampling artifacts (NH_3 deposition to tube walls, capture of NH_4^+, wind enhancement of sampling) and analytical artifacts (deposition to samples from laboratory air, inclusion of contaminated samples). Measures to reduce analytical artifacts may account for the difference between the results here and those given by RGAR (1990).

• Evidence in the literature suggests that emissions to the atmosphere occurs as NH_3, the main source being from livestock agriculture, which may be converted in the atmosphere to NH_4^+.

• The dry deposition of NH_4^+ particles is expected be a very slow process, which is confirmed by micrometeorological field measurements in this study. Most of the NH_4^+ therefore becomes dissolved in precipitation and is returned to earth as wet deposition.

• The major part of this study focused on the measurement of the surface exchange of gaseous NH_3 using micrometeorological methods. The background exchange over different vegetated surfaces in a temperate climate was considered and included measurements over natural and unfertilized surfaces, and fertilized agricultural surfaces:

  ◦ Measurements over natural and unfertilized vegetation generally recorded rapid deposition of NH_3 with minimal surface resistance (r_c), which shows that the

surface behaves largely as a perfect sink, with NH_3 being deposited onto leaf surfaces rather than through stomata. Some exceptions to this pattern were seen. In dry conditions a small r_c (< 50 s m^{-1}) was sometimes recorded, while over a surface with exposed calcareous soil a mean r_c of 125 s m^{-1} was found.

- Measurements over fertilized agricultural vegetation showed both emission and deposition to occur. Emission was favoured in warm dry conditions, with fluxes in summer of up to 24 ng m^{-2} s^{-1} being measured. In wet conditions deposition was recorded. Measurements to wet surfaces in summer showed r_c to be variable (0–130 s m^{-1}), while winter-time measurements showed rapid deposition to wet surfaces (r_c < 30 s m^{-1}). During a period of light frost an increased r_c of up to 80 s m^{-1} was observed.

- The different surface exchange patterns observed are interpreted in terms of the net effect of leaf surface, stomatal and soil exchange processes:

  - Deposition to leaf surfaces is a major uptake mechanism, which may be enhanced in wet conditions. Acid gases, particularly SO_2, may enhance leaf surface uptake, often referred to as co-deposition. HNO_3 and HCl may also have some effect. Partial or complete saturation of this sink may occur in very dry (low humidity) conditions or in the presence of very high concentrations of NH_3, such as with a crop emitting NH_3 or in the presence of high atmospheric concentrations.

  - Stomata and soil can act as either sources or sinks of NH_3, depending on the Henry equilibria of NH_3 and NH_4^+ in plant tissues and soil water with atmospheric concentrations of NH_3. The atmospheric concentration in equilibrium with the surface is often referred to as the 'compensation point' (χ_{cp}). Where air concentrations are less than χ_{cp} emission occurs, whereas with air concentrations larger than χ_{cp} deposition occurs. The compensation point concept is most usually applied to the exchange of NH_3 through stomata, though equally soil χ_{cp} and overall canopy or net χ_{cp} may be defined.

  - Over natural and unfertilized vegetation it is probable that the low N status results in small stomatal and soil χ_{cp}, with the result that leaf surface deposition dominates and the net χ_{cp} is small. Where $r_c = 0$ the net χ_{cp} is by definition zero.

  - Over fertilized agricultural vegetation the higher N status results in larger χ_{cp}, and emission may occur through either stomata or soil. However, during wet conditions these χ_{cp} have little effect on the net exchange as leaf surface deposition dominates, and the net χ_{cp} again approaches zero.

- Surface concentrations may be predicted by extrapolation of the concentration gradient using a modified resistance analysis, and these may be used as estimates of χ_{cp}. Where emission is through stomata alone and stomatal resistance known, estimates of the stomatal χ_{cp} may be made (referred to as $\chi\{z_o"\}$). For an agricultural crop in dry summer conditions $\chi\{z_o"\}$ was 2–7 $\mu g\ m^{-3}$. Given that some leaf surface deposition may also have been present, this may be an underestimate of the stomatal χ_{cp}.

• This understanding is used with the results of the air concentration monitoring from this study and other published values to estimate annual budgets for different example U.K. ecosystems. Examples are for typical exchange not affected by local sources.

- Over the natural and unfertilized surfaces examined, estimated NH_3 deposition ranges from 3 to 55 kg N ha^{-1} $year^{-1}$. Estimates are sensitive to air concentration, site roughness (*e.g.* short grass or forest) and prevailing windspeed at a site.

- The largest deposition is expected to forests in lowland Britain where NH_3 concentrations are frequently higher than in upland areas. However, estimates over forests are very sensitive to the value of the laminar boundary-layer resistance, r_b, which is a major uncertainty in the calculations.

- Where a χ_{cp} exists for fertilized surfaces it is attractive to be able to include this in models of exchange alongside monitored air concentrations and transfer resistances. However, given the spatial and temporal variability of the net χ_{cp}, this is beyond the scope of simple models with only long term air concentration inputs.

- To model annual exchange over an agricultural surface a simplified approach is used in this study. The percentage time the surface is dry, wet or frozen in different seasons is found, and fluxes for each condition summed to provide net seasonal and annual fluxes. Typical emission estimates are used for dry conditions, while a deposition velocity approach is used in wet and frozen conditions.

- A calculated example budget of background exchange for a fertilized agricultural surface shows that in summer net emission occurs, whereas the other seasons show net deposition. If the emission following fertilizer application and probable extra losses during crop senescence or hay drying are included, the net annual NH_3 emission of is < 1 kg N ha^{-1} $year^{-1}$. Large uncertainty applies in using this as typical for fertilized crop surfaces in the U.K. Other sites with larger levels of N fertilization may show emission of > 5 kg N ha^{-1} $year^{-1}$.

- Implications for atmospheric models are drawn from the difference between fertilized and unfertilized surfaces and it is concluded that applying a fixed

deposition velocity for all land surfaces contributes to the discrepancy between predicted and observed deposition.

- The total N inputs into specific natural and unfertilized ecosystems are estimated and comparisons made of the contribution from different sources. Dry deposition of NH_3 is frequently the largest single N input, which emphasizes the importance of understanding NH_3 surface exchange processes. Including wet deposited NH_4^+, NH_x accounts for 60–80 % of the total N input to the examples considered, as compared to 20–40 % from oxidized N species (NO_2, HNO_3, NO_3^-), giving a total deposition of 10–75 kg N ha^{-1} $year^{-1}$. Near sources of NH_3 emission (mainly livestock agriculture) the deposition could be several times larger than this.

- A comparison of the relative acidifying inputs into the example ecosystems is also given, though since the acidifying effect of pollutants depends on their fate when deposited only general conclusions may be made. In particular nitrification of deposited NH_x to NO_3^- is an acidifying process. Comparison may be made either of the suite of deposited pollutants, or according to the origin of the acidity as emitted pollutants (SO_2, NO_x, NH_3). Because of atmospheric neutralization of oxidized S and N by NH_3 to form NH_4^+, much of the acidifying deposition in the examples (up to 60–80%) is as NH_x rather than free acidity. Emission of NH_3 accounts for between a maximum of 30–70% of the potential acidity. Plant uptake of deposited N may reduce these figures substantially. This applies for the products of both NO_x and NH_3, so that SO_2 emission is frequently the dominant acidifying input. Conversely, where N deposition exceeds plant uptake, NH_3 emission may have a sizeable or even dominant acidifying effect.

- A comparison of the background deposition estimates of total N with current estimates of critical loads given in the literature shows that N deposition in the U.K. is typically is excess of the critical loads. This is especially clear for forests in lowland Britain where deposition may be several times the critical load. Given the importance of NH_3 in dominating the N deposition and contributing to the acidification of natural and unfertilized ecosystems, it is clear that emission control policies aimed at reducing SO_2 and NO_x emissions will only have limited effectiveness. In order to achieve major reductions in deposition, particularly in the case of N inputs, additional polices controlling NH_3 emission are required. Given the agricultural origin of the NH_3 emission, measures would require changes in farming practice. Major reductions in emission may be achieved by soil incorporation or injection of surface spread liquid manure, acidification of manure, and the use of closed manure storage.

References

Adema E.H., Heeres P. and Hulskotte J. (1986) On the dry depositon of NH_3, SO_2 and NO_2 on wet surfaces in a small scale wind tunnel. In: *Proceedings 7th World Clean Air Congress, vol. 2* (Ed: Hartmann H.F.) pp 1–8. Clean Air Soc. Australia and New Zealand.

Alkezweeny A.J., Lawes G.L. and Jones W. (1986) Aircraft and ground measurements of ammonia in Kentucky. *Atmos. Environ.* **20**, 357–360.

Allegrini I., De Santis F., Di Palo V. and Liberti A. (1984) Measurement of particulate and gaseous ammonia at a rural site by means of newly developed high performance diffusion tubes. *J. Aerosol Sci.* **15**, 465–71.

Allen A.G., Harrison R.M. and Erisman J.-W. (1989) Field measurements of the dissociation of ammonium nitrate and ammonium chloride aerosols. *Atmos. Environ.* **23**, 1591–1599.

Allen A.G., Harrison R.M., Wake M.T. (1988) A meso-scale study of the behaviour of atmospheric ammonia and ammonium. *Atmos. Environ.* **22**, 1347–1353.

Allison F.E. (1955) The enigma of soil nitrogen balance sheets. *Adv. Agron.* **7**, 213–251.

Aneja V.P., Rogers H.H. and Stahel E.P. (1986) Dry deposition of ammonia at environmental concentrations on selected plant species. *J. Air Pollut. Contr. Assoc.* **36**, 1338–1341.

Anlauf K., MacTavish D., Wiebe A. and Mackay G. (1987) Measurement of atmospheric nitric acid and ammonia by the filter method and a comparison to the tunable diode laser method. In: *Proceedings of the 1987 EPA/APCA Symposium on Measurement of Toxic and Related Air Pollutants*. pp 373–378. EPA Report No. 600/9-87-010.

Appel B.R., Wall S.M., Tokiwa Y. and Haik M. (1980) Simultaneous nitric acid, particulate nitrate and acidity measurements in ambient air. *Atmos. Environ.* **14**, 549–554.

ApSimon H.M., Kruse M. and Bell J.N.B. (1987) Ammonia emissions and their role in acid deposition. *Atmos. Environ.* **21**, 1939–1946.

Asman W.A.H. and Drukker B. (1988) Modelled historical concentrations and depositions of ammonia and ammonium in Europe. *Atmos. Environ.* **22**, 725–735.

Asman W.A.H. and Janssen A.J. (1986) A long range model for ammonia and ammonium for Europe and some model experiments. IMOU Report R-86-6. Institute for Meteorology and Oceanography (IMOU), 5 Princetonplein, 3584 CC Utrecht, The Netherlands.

Asman W.A.H. and Janssen A.J. (1987) A long-range transport model for ammonia and ammonium for Europe. *Atmos. Environ.* **21**, 2099–2119.

Atkins D.H.F. (1988) Personal communication. AERE, Harwell Laboratory, Didcot, Oxon, UK. Present address: Commission EC / JCR, Environment Institute, Chemistry Division, I-21020 Ispra, Italy.

Atkins D.H.F., Sandalls J., Law D.V., Hough A.M. and Stevenson K. (1986) The measurement of nitrogen dioxide in the outdoor environment using passive diffusion tube samplers. Report AERE-R-12133, Harwell Laboratory, Didcot, Oxon, UK.

Ayers G.P. and Gras J.L. (1983) The concentration of ammonia in Southern Ocean air. *J. Geophys. Res.* **88**, 10655–10659.

Ball D.F., Radford G.L and Williams W.M. (1983) A land characteristic data bank for Great Britain. Bangor Occasional Paper No. 13. Institute of Terrestrial Ecology, Bangor Research Station, Penrhos Road, Bangor, Gwynedd, UK.

Beauchamp E.G., Kidd G.E. and Thurtell G. (1982) Ammonia volatilization from liquid dairy cattle manure in the field. *Can. J. Soil Sci.* **62**, 11–19.

Bietz J.A. (1974) Micro-Kjeldahl analysis by an improved automated ammonium determination following manual digestion. *Analytical Chem.* **46**, 1617–1618.

Bineau A. (1854) *Études chimiques, sur les eaux pluviales et sur l'atmosphere de Lyon et de quelques points des environs*. Lyon (in French; see Hall and Miller, 1911).

Binkley D. and Richter D. (1987) Nutrient cycles and H^+ budgets of forest ecosystems. *Adv. Ecol. Res.* **16**, 1–51.

Biscoe P.V., Clark J.A., Gregson M., McGowan M., Monteith J.L. and Scott R.K. (1975) Barley and its environment. I. Theory and practice. *J. App. Ecology* **12**, 227–257.

Bobbink R. (1989) Brachypodium pinnatum and the species diversity in chalk grassland. Ph.D thesis, University of Utrecht, Drukkerij Elinkwijk BV, Utrecht, The Netherlands.

Boussingault J.B. (1856) Recherches sur la végétation. Troisiéme mémoire. De l'action du salpêtre sur le développement des plantes. *Ann. Chim. Phys. Ser. 3*, **46**, 5–41 (in French).

Bonis K., Mészáros E. and Putsay M. (1980) On the atmospheric budget of nitrogen compounds over Europe. *Időjárás* **84**, 57–68.

Bretschneider P. (1872) Ueber die Quantitäten Ammoniak welche die hauptsächlichsten Konstituenten des Kulturbodens aus der Atmosphäre innerhalb eines Jahres auf gemessener Fläche absrbieren. *Der Lantwirt* **8**, 225, 234, 238 and 241 (in German).

Brost R.A., Delany A.C. and Huebert B.J. (1988) Numerical modeling of concentrations and fluxes of HNO_3, NH_3, and NH_4NO_3 near the surface. *J. Geophys. Res.* **93**, 7137–7152.

Brunsting A.M.H. and Heil G.W. (1985) The role of nutrients in the interactions between a herbivorous beetle and some competing plant species in heathlands. *Oikos* **44**, 23–26.

Buenos Aires (1906) The climate of Buenos Aires. *Statis. Ann. City Buenos Aires*, **16**, 3–8.

Buijsman E. (1987) Ammonia emission calculation: fiction and reality. In: *Ammonia and acidification: Proc. EURASAP Symp.* 13–15 April 1987, Bilthoven, The Netherlands. (Eds: Asman A.H. and Diederen S.M.A.) pp 13–27. RIVM, Bilthoven and TNO Delft, The Netherlands.

Buijsman E. and Erisman J.-W. (1988) Wet deposition of ammonium in Europe. *J. Atmos. Chem.* **6**, 265–280.

Buijsman E., Maas H.F.M., Asman W.A.H. (1987) Anthropogenic NH_3 emissions in Europe. *Atmos. Environ.* **21**, 1009–1022.

Buijsman E., Mass H.F.M. and Asman W.A.H. (1984) Een gedetailleerde ammoniak-emissiekaart van Nederland (A detailed ammonia emission map of the Netherlands). Report V-84-20. Institute for Meteorology and Oceanography, State University, Utrecht, The Netherlands. (in Dutch with English summary).

Businger J.A. (1966) Transfer of momentum and heat in the planetary bounday layer. In: *Arctic heat budget and atmospheric circulation* (Symposium proceedings) pp 305–332. The Rand Corporation.

Bytnerowicz A., Miller P.R. and Olszyk D.M. (1987) Dry deposition of nitrate, ammonium and sulfate to a *Ceanothus crassifolius* canopy and surrogate surfaces. *Atmos. Environ.* **21**, 1749–1757.

Cadle S.H. (1985) Seasonal variations in nitric acid, nitrate, strong aerosol acidity, and ammonia in an urban area. *Atmos. Environ.* **19**, 181–188.

Cass G.R., Gharib S., Peterson M. and Tilden J.W. (1982) The origin of ammonia emissions to the atmosphere in an urban area. Open File Report 82-6. Environmental Quality Laboratory, California Institute of Technology, USA.

CEC (1988) Council directive on the limitation of emissions of certain pollutants into the air from large combustion plants. *Official J. European Communities.* No. L 336, 1–13. (Council of the European Communities).

Chamberlain A.C. (1966) Transport of gases to and from grass and grass like surfaces. *Proc. Roy. Soc. London.* A. **290**, 236–265.

Chamberlain A.C. (1968) Transport of gases to and from surfaces with bluff and wave-like roughness elements. *Quart. J. Roy. Meteor. Soc.* **94**, 318–332.

Chamberlain A.C. and Little P. (1981) Transport and capture of particles by vegetation. In: *Plants and their atmospheric environment* (21 st. Syposium of the British Ecological Society) (Eds: Grace J., Ford E.D. and Jarvis P.G.) pp 147–173. Blackwell Scientific, Oxford.

Chandler T.J. and Gregory S. (1976) *The climate of the British Isles.* (Eds.) Longman, London. 390 pp.

Clapham A.R., Tutin T.G. and Moore D.M. (1987) *Flora of the British Isles.* Third edition. Cambridge University Press, Cambridge. pp 688.

Colls J.J. (1986) Measurement of nitrogen dioxide profiles by diffusion tube within a barley canopy. *Atmos. Environ.* **20**, 239–242.

Court M.N., Stephen P.C. and Waid J.S. (1964) Toxicity as a cause of the inefficiency of urea as a fertilizer. *J. Soil Sci.* **15**, 42–48.

Cowling D.W. and Lockyer D.R. (1981) Increased growth of Ryegrass exposed to ammonia. *Nature* **292**, 337–338.

Crossley A.C. (1990) Unpublished results. Institute of Terrestrial Ecology, Edinburgh Research Station, Bush Estate, Penicuik, Midlothian, UK.

Dabney S.M. and Bouldin D.R. (1985) Fluxes of ammonia over an alfalfa field. *Agron. J.* **77**, 572–578.

Dasch J.M. (1987) Measurement of dry deposition to surfaces in deciduous and pine canopies. *Environ. Pollut.* **44**, 261–277.

Dawson G.A. (1977) Atmospheric ammonia from undisturbed land. *J. geophys. Res.* **82**, 3125–3133.

De Rossi G. (1947) Absorption of ammonia from the atmosphere (Abs.) *Soils and Fert.* **10**, 400.

De Temmerman L., Ronse A., Van Den Cruys K. and Meeus-Verdinne K. (1987) Ammonia and pine tree dieback in Belgium. In: *Air pollution and Ecosystems. Proceedings of an international symposium*, 18–22 May 1987, Grenoble, France. (Ed: Mathy P.) pp 774–779. D. Reidel Publishing Company, Dordrecht.

Delwiche C.C. (1977) Energy relations in the global nitrogen cycle. *Ambio* **6**, 106–111.

Denmead O.T. (1983) Micrometeorological methods for measuring gaseous losses of nitrogen in the field. In: *Gaseous loss of nitrogen from plant-soil systems*. (Eds: Freney J.R. and Simpson J.R.) pp 133–158. Martinus Nijhoff / Dr W. Junk, The Hague.

Denmead O.T. (1990) Personal communication. CSIRO, Division of Environmental mechanics, Canberra, A.C.T., Australia.

Denmead O.T., Freney J.R. and Simpson J.R. (1976) A closed ammonia cycle within a plant canopy. *Soil Sci. Biochem.* **8**, 161–164.

Denmead O.T., Nulsen R. and Thurtell G.W. (1978) Ammonia exchange over a corn crop. *Soil Sci. Soc. Am. J.* **42**, 840–842.

Denmead O.T., Simpson J.R. and Freney J.R. (1974) Ammonia flux into the atmosphere from a grazed pasture. *Science* **185**, 609–610.

Derwent R.G. (1987) Modelling the long-range transport of ammonia and ammonia compounds. In: *Ammonia and acidification: Proc. EURASAP Symp.* 13–15 April 1987, Bilthoven, The Netherlands. (Eds: Asman A.H. and Diederen S.M.A.) pp 223–238. RIVM, Bilthoven and TNO Delft, The Netherlands.

Dollard G.J., Atkins D.H.F., Davies T.D. and Healy C. (1987) Concentrations and dry deposition velocities of nitric acid. *Nature* **326**, 481–483.

Dollard J.G., Unsworth M.H. and Harvey M.J. (1983) Pollutant transfer in upland regions by occult deposition. *Nature* **302**, 241–247.

Draaijers G.P.J., Ivens W.P.M.F. and Bleuten W. (1987) The interaction of NH_3 and SO_2 in the process of dry deposition on plant surfaces. In: *Ammonia and acidification: Proc. EURASAP Symp.* 13–15 April 1987, Bilthoven, The Netherlands. (Eds: Asman A.H. and Diederen S.M.A.) pp 141–148. RIVM, Bilthoven and TNO Delft, The Netherlands.

Driscoll C.T. and Schaefer D.A. (1989) Background on nitrogen processes. Chapter 4 In: *The role of nitrogen in the acidification of soils and surface waters.* (Eds: Malanchuk J.L. and Nilsson J.) pp 4.1–4.12. Nordic Council of Ministers, Copenhagen, Denmark.

Duyzer J.H., Bouman A.M.H., Diederen H.S.M.A. and Van Aalst R.M. (1987) Measurement of dry deposition velocities of NH_3 and NH_4^+ over natural terrains. Report R 87/273 Netherlands organisation for applied scientific research. MT-TNO, Delft, The Netherlands.

Dyer A.J. and Hicks B.B. (1970) Flux-gradient relationships in the constant flux layer. *Quart. J. Roy. Meteor. Soc.* **96**, 715–721.

Eggleton A.E.J. and Atkins D.H.F. (1972) Results of the Tees-side investigation . Report AERE-R6983, Harwell Laboratory, Didcot, Oxon, UK.

Egnér H. and Eriksson E. (1955) Current data on the chemical sampling of air and precipitation. *Tellus* **7**, 134–137.

Eriksson E. (1952) Composition of atmospheric precipitation: A. Nitrogen compounds. *Tellus* **4**, 215–232 and 296–303(references).

Eriksson E. (1988) Retention and release of sulphate in soils. In: *Critical loads for sulphur and nitrogen.* (Report from a workshop at Skokloster, Sweden, 19–24 March 1988) (Eds: Nilsson J. and Grennfelt P.) pp 151–184. Nordic Council of Ministers, Copenhagen, Denmark.

Erisman J.-W., Vermetten A.W.M., Asman W.A.H., Waijers-Ijpelaan A. and Slania J. (1988) Vertical distribution of gases and aerosols: the behaviour of ammonia and related components in the lower atmosphere. *Atmos. Eviron.* **22**, 1153–1160.

Farquahar G.D., Firth P.M., Wetselaar R. and Wier B. (1980) On the gaseous exchange of ammonia between leaves and the environment: determination of the ammonia compensation point. *Plant Physiol.* **66**, 710–714.

Farquahar G.D., Wetselaar R. and Firth P.M. (1979) Ammonia volatilization from senescing leaves of maize. *Science* **203**, 1275–1258.

Farquahar G.D., Wetselaar R. and Weir B. (1983) Gaseous nitrogen losses from plants. In: *Gaseous loss of nitrogen from plant-soil systems.* (Eds: Freney J.R. and Simpson J.R.) pp 159–180. Martinus Nijhoff / Dr W. Junk, The Hague.

Feeney A. (1988) Biological immpacts of ammonia in the atmosphere. M.Sc. Thesis., Centre for Environmental Technology, Imperial College, London.

Fenn L.B., Taylor R.M. and Tatocha J.E. (1981) Ammonia losses from surface-applied nitrogen fertilizer as controlled by soluble calcium and magnesium: general theory. *Soil Sci. Soc. Am. J.* **45**, 777–781.

Ferm M. (1979) Method for the determination of atmospheric ammonia. *Atmos. Environ.* **13**, 1385–1393.

Fisher B.E.A.(1987) Assessing recent ammonia inventories using a statistical long-range model. In: *Ammonia and acidification: Proc. EURASAP Symp.* 13–15 April 1987, Bilthoven, The Netherlands. (Eds: Asman A.H. and Diederen S.M.A.) pp 239–258. RIVM, Bilthoven and TNO Delft, The Netherlands.

Fodor J. (1881) *Hygienische untersuchungen über Luft, boden und wasser. I. Die luft.* Braunschweig (in German).

Forestry and Timber Bureau (1957) *Forest trees of Australia.* Department of the Interior, Commonwealth of Australia, Canberra. pp 230.

Fowler D. (1976) Uptake of SO_2 by crops and soil. Ph.D. thesis, University of Nottingham, UK.

Fowler D. and Cape J.N. (1984) The contamination of rain samples by dry deposition on rain collectors. *Atmos. Environ.* **18**, 183–189.

Fowler D., Cape J.N. and Unsworth M.H. (1989) Deposition of atmospheric pollutants on forests. *Phil. Trans. Roy. Soc. London.* B **324**, 247–265.

Fowler D. and Duyzer J.H. (1989) Micrometeorological techniques for the measurement of trace gas exchange. In: *Exchange of trace gases between terrestrial ecosystems and the atmosphere.* (Eds: Andreae M.O. and Schimel D.S.) pp 189–207. Wiley, Chichester.

Fowler D. and Unsworth M.H. (1979) Turbulent transfer of sulphur dioxide to a wheat crop. *Quart. J. Roy. Meteor. Soc.* **105**, 767–783.

Freney J.R., Simpson J.R. and Denmead O.T. (1983) Volatilization of ammonia. In: *Gaseous loss of nitrogen from plant-soil systems.* (Eds: Freney J.R. and Simpson J.R.) pp 1–32. Martinus Nijhoff / Dr. W. Junk, The Hague.

Freney J.R., Trevitt A.C.F., De Datta S.K., Obcemea W.N. and Real J.G. (1990) The interdependence of ammonia volatilization and denitrification as nitrogen loss processes in flooded rice fields in the Philippines. *Biol. Fertil. Soils* **9**, 31–36.

Galbally I.E. and Roy C.R. (1980) Destruction of ozone at the earth's surface. *Quart. J. Roy. Meteor. Soc.* **106**, 599–620.

Gallagher M.W., Choularton T.W., Morse A.P. and Fowler D. (1988) Measurements of the size dependence of cloud droplet deposition at a hill site. *Quart. J. Roy. Meteor. Soc.* **114**, 1291–1203.

Garland J.A. (1977) The dry deposition of sulphur dioxide to land and water surfaces. *Proc. Roy. Soc. London.* A. **354**, 245–268.

Garratt J.R. and Hicks B.B. (1973) Momentum, heat and water vapour transfer to and from natural and artificial surfaces. *Quart. J. Roy. Meteor. Soc.* **99**, 680–687.

Georgii H.W. and Gravenhorst G. (1977) The ocean as a source and sink of reactive trace gases. *Pure and App. Geophys.* **115**, 503–511.

Georgii H.W. and Lenhard U. (1978) Contribution to the atmospheric NH_3 budget. *Pure and App. Geophys.* **116**, 385–392.

Georgii H.W. and Müller W.J. (1974) On the distribution of ammonia in the middle and lower troposphere. *Tellus* **26**, 180–184.

Goldan P.D., Kuster W.C., Albritton D.L., Fehsenfeld F.C., Connell P.S. and Norton R.B. (1983) Calibration and tests of the filter-collection method for measuring clean-air, ambient levels of nitric acid. *Atmos. Environ.* **17**, 1355–1364.

Gras J.L. (1983) Ammonia and ammonium concentrations in the Antarctic atmosphere. *Atmos. Environ.* **17**, 815–818.

Gundersen P. and Rasmussen L. (1988) Nitrification, acidification and aluminium release in forest soils. In: *Critical loads for sulphur and nitrogen.* (Report from a workshop at Skokloster, Sweden, 19–24 March 1988) (Eds: Nilsson J. and Grennfelt P.) pp 225–268. Nordic Council of Ministers, Copenhagen, Denmark.

Hales J.M. and Drewes D.R. (1979) Solubility of ammonia in water at low concentrations. *Atmos. Environ.* **13**, 1133–1147.

Hall A.D. and Miller N.H.J. (1911) On the absorption of ammonia from the atmosphere. *J. Agr. Sci.* **4**, 56–68.

Hanawalt R.B. (1969) Environmental factors influencing the sorption of atmospheric ammonia by soils. *Soil Sci. Soc. Am. Proc.* **33**, 231–234.

Hargreaves K.J. (1989) The development and application of diffusion tubes for air pollution measurements. Ph.D. thesis, University of Nottingham, UK.

Hargreaves K.J. and Atkins D.H.F. (1987) The measurement of ammonia in the outdoor environment using passive diffusion tube samplers. Report AERE-R-12568, Harwell Laboratory, Didcot, Oxon, UK.

Hargreaves K.J., Fowler D. and Storeton-West R.L. (1990) Unpublished results. Institute of Terrestrial Ecology, Edinburgh Reseach Station, Bush Estate, Penicuik, Midlothian, UK.

Harper L.A., Catchpoole V.R., Davis R. and Weir K.L. (1983) Ammonia volatilization: soil, plant, and microclimate effects on diurnal and seasonal fluctuations. *Agron. J.* **75**, 212–218.

Harper L.A., Sharpe R.R., Langdale G.W. and Giddens J.E. (1987) Nitrogen cycling in a wheat crop: soil, plant and aerial nitrogen transport. *Agron. J.* **79**, 965–973.

Harrison R.M. (1986) Personal communication. Institute of aerosol science, University of Essex, Colchester, Essex, UK.

Harrison R.M., Rapsomanikis S. and Turnbull A. (1989) Land-surface exchange in a chemically reactive system; surface fluxes of HNO_3, HCl and NH_3. *Atmos. Environ.* **23**, 1795–1800.

Haynes R.M. (1982) *Environmental science methods.* (Ed.) Chapman and Hall, London. pp 404.

Heal O.W. and Smith R.A.H. (1978) Introduction and site description. Chapter 1. In: *Production ecology of British moors and montane grasslands.* Section 1. The Moor House programme. (Eds: Heal O.W. and Perkins D.F.) Ecological Study **27**, 3–16. Springer-Verlag, Berlin.

Healy T.V., McKay H.A.C., Pilbeam A. and Scargill D. (1970) Ammonia and ammonium sulphate in the troposphere over the United Kingdom. *J. Geophys. Res.* **75**, 2317–2321.

Heil G.W. and Diemont W.H. (1983) Raised nutrient levels change healthland into grassland. *Vegetatio* **53**, 113–120.

Heil G.W., Van Dam D. and Heijne B.(1987) Catch of atmospheric deposition in relation to vegetation structures of heathland. In: *Ammonia and acidification: Proc. EURASAP Symp.* 13–15 April 1987, Bilthoven, The Netherlands. (Eds: Asman A.H. and Diederen S.M.A.) pp 107–123. RIVM, Bilthoven and TNO Delft, The Netherlands.

Heinrich R. (1881) Ueber die Ammoniakmengen welche der Atmosphäre im Lauf eines Jahres durch Salzäure entzogen werden. *Wollnys Forschungen* **4**, 446–452 (in German).

Hooker M.L., Sander D.H., Peterson G.A. and Daigger L.A. (1980) Gaseous N losses from winter wheat. *Agron. J.* **72**, 789–792.

Horváth L. (1982) On the vertical flux of gaseous ammonia over water and soil surfaces. In: *Deposition of atmospheric pollutants.* (Eds: Georgii H.W. and Pankrath J.) pp 17–22. D. Reidel Publishing Company.

Horváth L. (1983) Concentration and near surface vertical flux of ammonia in the air in Hungary. *Időjárás* (Journal of the Hungarian Meteorological Service) **87**, 65–70.

Hov Ø., Allegrini I., Beilke S., Cox R.A., Eliassen A., Elshout A.J., Gravenhorst G., Penkett S.A. and Stern R. (1988) Air pollution research report 10. Evaluation of atmospheric processes leading to acid deposition in Europe, 1987. Report from the COST 611 task force on acid deposition. EUR 11441 EN, Environment and quality of life, CEC, Luxembourg.

Huebert B.J. and Robert C.H. (1985) The dry deposition of nitric acid to grass. *J. Geophys. Res.* **90**, 2085–2090.

Huebert B.J., Luke W.T., Delany A.C. and Brost R.A. (1988) Measurements of concentrations and dry surface fluxes of atmospheric nitrates in the presence of ammonia. *J. Geophys. Res.* **93**, 7127–7136.

Hutchinson G.L. and Viets F.G.Jr. (1970) Nitrogen enrichment of surface water by absorbtion of ammonia volatilized from cattle feedlots. *Science* **166**, 514–515.

Hutchinson G.L., Millington R.J. and Peters D.B. (1972) Atmospheric ammonia: absorption by plant leaves. *Science* **175**, 771–772.

Incoll L.D., Long S.P. and Ashmore M.R. (1977) SI units in publications in plant science. *Commentaries in Plant Sci.* No. 28. *Current Adv. Plant Sci.* 331–343.

Ingham G. (1950) Effect of materials adsorbed from the atmosphere in maintaining soil fertility. *Soil Sci.* **70**, 205–212.

Iribarne J.V. and Pyshnov J. (1990) The effect of freezing on the composition of supercooled droplets —. Retention of HCl, HNO_3, NH_3 and H_2O_2. *Atmos. Environ.* **24A**, 383–387.

Istas J.R., De Borger R., De Temmerman L., Guns M., Meeus-Verdinne K., Ronse A., Scokart P. and Temonia M. (1988) Effect of ammonia on the acidification of the environment. Environment and Quality of Life, Report EUR 11857 EN, Commission of the European Communities, Luxembourg.

Ivens W.P.M.F., Draaijer G.P.J., Bleuten W. and Bos M.M. (1989) The impact of air-borne ammonia from agricultural sources on fluxes of nitrogen and sulphur towards forest soils. *Catena* **16**, 535–544.

Jarvis P.G. (1981) Stomatal conductance, gaseous exchange and transpiration. In: *Plants and their atmospheric environment* (21st Symposium of the British Ecological Society) (Eds: Grace J., Ford E.D. and Jarvis P.G.) pp 175–204. Blackwell Scientific, Oxford.

Jarvis S.C., Hatch D.J. and Lockyer D.R. (1989) Ammonia fluxes from grazed grassland: annual losses from cattle production systems and their relation to nitrogen inputs. *J. Agric. Sci. Camb.* **113**, 99–108.

Johansson C. and Granat L. (1986) An experimental study of the dry deposition of gaseous nitric acid to snow. *Atmos. Environ.* **20**, 1165–1170.

Jones H.G. (1983) *Plants and microclimate. A quantitative approach to environmental plant physiology.* Cambridge University Press, Cambridge. pp 323.

Junge C.E. (1963) Air Chemistry and Radioactivity. Academic Press, New York. pp 382.

Junge C.E. and Ryan T.G. (1958) Study of the SO_2 oxidation in solution and its role in atmospheric chemistry. *Quart. J. Roy. Meteor. Soc.* **84**, 46–55.

Kadowaki S. (1976) Size distribution of atmospheric total aerosol sulphate, ammonium and nitrate particulates in the Nagoya area. *Atmos. Environ.* **10**, 39–43.

Kellner O., Savano J., Yoshii T. and Makina R. (1886) I. Untersuchungen über der gehalt den atmosphärishen niederschlägen an stickstoffverbindungen. II. Über das maximum an gebundenen stickstoff welches des ackerboden der atmosphäre zu entziehen vermag. *Lantwirt schaftlich Jahrb.* **15**, 701–711 (in German).

Kerstiens G. and Lendzian K.J. (1989) Interactions between ozone and plant cuticles: I. Ozone deposition and permeability. *New Phytol.* **112**, 13–19.

Lawes J.B. and Gilbert J.H. (1851) On agricultural chemistry. *J. Roy. Agr. Soc.* **12**, 1–40.

Le Bel P.J., Hoell J.M., Levine J.S. and Vay S.A. (1985) Aircraft measurements of ammonia and nitric acid in the lower troposphere. *Geophys. Res. Lett.* **12**, 401–404.

Lemon E. and Van Houtte R. (1980) Ammonia exchange at the land surface. *Agron. J.* **72**, 876–883.

Lenhard U. and Gravenhorst G. (1980) Evaluation of ammonia fluxes into the free atmosphere over Western Germany. *Tellus* **32**, 48–55.

Leuning R., Denmead O.T., Simpson J.R. and Freney J.R. (1984) Processes of ammonia loss from shallow floodwater. *Atmos. Environ.* **18**, 1583–1592.

Levine J.S., Augustsson T.R. and Hoell J.M. (1980) The vertical distribution of tropospheric ammonia. *Geophys. Res. Lett.* **7**, 317–320.

Levy A.A. (1880) Ammoniaque de l'air et des eaux. *Compte Rendus Acad. Sci., Paris.* **91**, 94–97 (in French).

Liebig J. (1847) Liebig on manures, v. Bousingault and Kuhlman (Extract from a letter to the *Revue Scientifique et Industrielle*) *Farmers Magazine* **16**, 511.

Liss P.S. (1983) Gas transfer: Experiments and geochemical implications. In: *Air-sea exchange of gases and particles* (Eds: Liss P.S. and Slinn N.N.). NATO. D. Reidel, Boston.

Lockyer D.R. and Whitehead D.C. (1986) The uptake of gaseous ammonia by the leaves of Italian Rygrass. *J. Experim. Botany* **37**, 919–927.

Lockyer D.R., Pain B.F. and Klarenbeek J.V. (1989) Ammonia emissions from cattle, pig and poultry wastes applied to pasture. *Environ. Pollut.* **56**, 19–30.

Malo B.A. and Purvis E.R. (1964) Soil absortion of atmospheric ammonia. *Soil Sci.* **97**, 242–247.

Martin A. (1988) Personal communication. Central Electricity Generating Board, Operational Engineering Division - Midlands Area, Ratcliffe-on-Soar, Nottingham, UK.

McConnell J.C. (1973) Atmospheric ammonia. *J. Geophys. Res.* **78**, 7812–7821.

McMahon T.A. and Denison P.J. (1979) Empirical atmospheric deposition parameters — a survery. *Atmos. Environ.* **13**, 571–585.

Meyer M.W. (1973) Absorption and release of ammonia from and to the atmosphere by plants. Ph.D. thesis, University of Maryland, College Park, Maryland, USA.

Mészaros E. (1981) *Atmospheric Chemistry: Fundamental Aspects.* Elsevier, Amsterdam.

Mészaros E. and Horváth L. (1984) Concentration and dry deposition of atmospheric sulphur and nitrogen compounds in Hungary. *Atmos. Environ.* **18**, 1725–1730.

Miller D.P. (1988) Low-level determination of nitrogen dioxide in ambient air using the Palmes Tube. *Atmos. Environ.* **22**, 945–948.

Miller N.H.J. (1913) The composition of rain water collected in the Hebrides and in Iceland. *J. Scot. Meteor. Soc.* **3**, 141–158.

Miranda A.C. (1982) A micrometeorological study of transpiration and evaporation from *Calluna vulgaris* (L.) Hull. Ph.D. thesis, University of Edinburgh, Edinburgh, UK.

Miranda A.C., Jarvis P.G. and Grace J. (1984) Transpiration and evaporation from heather moorland. *Boundary-Layer Meteor.* **28**, 227–243.

Monteith J.L. (1973) *Principles of environmental physics.* Edward Arnold, London. pp 241.

Monteith J.L. and Unsworth M.H. (1990) *Principles of environmental physics.* Second edition. Edward Arnold, London. pp 291.

Morgan J.A. and Parton W.J. (1989) Characteristics of ammonia volatilization from spring wheat. *Crop Sci.* **29**, 726–731.

Möller D. and Schieferdecker H. (1985) A relationship between agricultural NH_3 emissions and the atmospheric SO_2 content over industrial areas. *Atmos. Environ.* **19**, 695–700.

Möller D. and Schieferdecker H. (1989) Ammonia emission and deposition of NH_x in the G.D.R. *Atmos. Environ.* **23**, 1187–1193.

Müntz A. and Aubin E. (1882) De la distribution de l'ammoniaque dans les météores aqueux aux grandes altitudes. *Compt.Rend. Acad. Sci., Paris.* **95**, 788 (in French).

Nicholson K.W. (1988) The dry deposition of small particles: a review of experimental measurements. *Atmos. Environ.* **22**, 2653–2666.

Nicholson K.W. and Davies T.D. (1987) Field measurements of the dry deposition of particulate sulphate. *Atmos. Environ.* **21**, 1561–1571.

Nihlgard B. (1985) The ammonium hypothesis. An additional explanation to the forest dieback in Europe. *Ambio* **14**, 2–8.

Nilsson J. and Grennfelt P. (1988) *Critical loads for sulphur and nitrogen.* (Report from a workshop at Skokloster, Sweden, 19–24 March 1988) (Eds.) Nordic Council of Ministers, Copenhagen, Denmark. 418 pp.

NRC (1979) *Ammonia.* Subcommittee on ammonia, Committee on medical and biologic effects of environmental pollutants. National Research Council. University Park Press, Baltimore. 305 pp.

Owen P.R. and Thomson W.R. (1963) Heat transfer across rough surfaces. *J. Fluid Mech.* **15**, 321–334.

Pain B.F. and Thompson R.B. (1989) Ammonia volatilization from livestock slurries applied to land. In: *Nitrogen in organic wastes applied to soils.* (Eds: Hansen J.A. and Henriksen K.) pp 202–211. Academic Press, London.

Pang S.W. and Tong Y.G. (1985) Separation and measurement of gaseous ammonia in air. *J. Environ. Sci.* (China) **6**, 70–74 (in Chinese).

Panofsky H.A. (1963) Determination of stress from wind and temperature measurements. *Quart. J. Roy. Meteor. Soc.* **89**, 85–94.

Parton W.J., Morgan J.A., Altenhofen J.M. and Harper L.A. (1988) Ammonia volatilization from spring wheat plants. *Agron. J.* **80**, 419–425.

Paulson C.A. (1970) The mathematical representation of wind speed and temperature profiles in the unstable atmospheric surface layer. *J. App. Meteor.* **9**, 857–861.

Porter L.K., Viets F.G.Jr. and Hutchinson G.L. (1972) Air containing nitrogen-15 ammonia: foliar absorbtion by corn seedlings. *Science* **175**, 759–761.

Quinn P.K., Charlson R.J., Zoller W.H. (1987) Ammonia, the dominant base in the remote marine troposphere: a review. *Tellus* **39B**, 413–425.

Raupach M.R. (1979) Anomalies in flux-gradient relationships over forest. *Boundary Layer Meteor.* **16**, 467–486.

RGAR (1990) *Acid deposition in the United Kingdom 1986–1988.* Third report of The United Kingdom Review Group on Acid Rain. Department of the Enviroment, London. In press.

Robinson E. and Robbins R.C. (1970) Gaseous nitrogen compound pollutants from urban and natural sources. *J. Air Pollut. Contr. Ass.* **20**, 303–306.

Rodgers G.A. (1978) Dry deposition of atmospheric ammonia at Rothamsted in 1976 and 1977. *J. Agr. Soc. Camb.* **90**, 537–542.

Roelofs J.G.M. (1986) The effect of airborne sulphur and nitrogen deposition on aquatic and terrestrial heathland vegetation. *Experientia* **42**, 372–377.

Roelofs J.G.M., Kempers A.J., Houdijk A.L.F.M. and Jaansen J. (1985) The effect of airborne ammonium sulphate on *Pinus nigra* var. maritima in The Netherlands. *Plant and Soil* **84**, 45–56.

Roswall T. (1976) The internal nitrogen cycle between microorganisms, vegetation and soil. In: *Nitrogen, phosphorus and sulphur - global cycles.* (Eds: Svensson B.H. and Söderlund R.) SCOPE Report 7. *Ecol. Bull. Stockholm* **22**: 157–176.

Russell E.J. and Richards E.H. (1919) The amounts and composition of rain and snow falling at Rothamsted. *J. Agr. Sci.* **9**, 309–337.

Ryden J.C. (1984) The flow of nitrogen in grassland. *Proc. Fert. Soc., Lond.* (229). The Fertiliser Society, London. pp 44.

Ryden J.C., Whitehead D.C., Lockyer D.R., Thompson R.B., Skinner J.H. and Greenwood E.A. (1987) Ammonia emission form grassland and livestock production systems in the UK. *Environ. Pollut.* **48**, 173–184.

Saugier B. and Ripley E.A. (1978) Evaluation of the aerodynamic method of determining fluxes over natural grassland. *Quart. J. Roy. Meteor. Soc.* **104**, 257–270.

Saxena V.K. and Lin N.-H. (1990) Cloud chemistry measurements and estimates of acidic deposition on an above cloudbase coniferous forest. *Atmos. Environ.* **24A**, 329–352.

Schaug J., Pacyna J., Harstad T., Krognes T. and Skjelmoen J.E. (1987) ECE Co-operative programme for monitoring and evaluation of the long range transmission of air pollutants in Europe. Report EMEP/CCC 2/87, Norwegian Institute for Air Research, Lillestrøm, Norway.

Schlösing Th. (1874) Sur l'absortion de l'ammoniaque de l'air par les végétaux. *Compte Rendus Acad. Sci., Paris.* **78**, 1700–1703 (in French).

Schlösing Th. (1875) Sur l'ammoniaque de l'atmosphere. *Compte Rendus Acad. Sci., Paris* **80**, 175–185 (in French).

Schneider T. and Bresser A.H.M. (1987) Verzuringsonderzoek eerste fase. Tussentijdse evaluatie augustus 1987, Dutch priority programme on acidification, Report 00-04, RIVM, Bilthoven, The Netherlands. (in Dutch).

Searle P.L. (1984) The Berthelot or Indophenol Blue reaction and its use in the analytical chemistry of nitrogen. *Analyst* **109**, 548–568.

Sehmel G.A. (1980) Particle and gas dry deposition. A review. *Atmos. Environ.* **14**, 983–1012.

Seinfeld J.H. (1986) *Atmospherc chemistry and physics of air pollution.* John Wiley, New York. pp 738.

Sickles J.E. II, Hodson L.L., McClenny W.A., Paur R.J., Ellestad T.G., Mulik J.D., Anlauf K.G., Wiebe H.A., Mackay G.I., Schiff H.I. and Bubacz D.K. (1990) Field comparison of methods for the measurement of gaseous and particulate contributors to acidic dry deposition. *Atmos. Environ.* **24A**, 155–165.

Skeffington R.A. and Wilson E.J. (1988) Excess nitrogen deposition: issues for consideration. *Eviron. Pollut.* **54**, 159–184.

Smith A.J.E. (1978) *The moss flora of Britain and Ireland.* Cambridge University Press, Cambridge. pp 706.

Sokal R.R. and Rohlf F.J. (1969) *Biometry: the principles and practice of statistics in biological research.* W.H. Freeman and Co., San Fransisco. pp 776.

Söderlund R. (1977) NO_X pollutants and ammonia emissions - a mass balance for the atmosphere over N.W. Europe. *Ambio* **6**, 118–122.

Söderlund R. and Granat L. (1982) Ammonium in precipitation - a presentation of data from the European Air Chemistry Network. Report CM-59, Dept. of Meteorology, University of Stockholm, Sweden.

Söderlund R. and Svensson B.H. (1976) The global nitrogen cycle. In: *Nitrogen and Sulphur-Global Cycles* (eds: Svensson B.H. and Söderlund R.), SCOPE report 7, *Ecol. Bull., Stockholm* **22**, 23–73.

Sommer S., Klausen P.S., Tholstrup Christensen B., Hansen J., Jensen N. and Olsen H. (1984) Beregning af ammoniak-fordampning fra naturgodning i Danmark (Calculation of the

ammonia volatilization from animal manure in Denmark). Miljoministeriet, Center for Jordokologi, Soborg (in Danish).

Stevenson C.M. (1968) An analysis of the chemical composition of rain-water and air over the British Isles and Eire for the years 1959–1964. *Quart. J. Roy. Meteor. Soc.* **94**, 57–70.

Thom A.S. (1972) Momentum, mass and heat exchange of vegetation. *Quart. J. Roy. Meteor. Soc.* **98**, 124–134.

Thom A.S. (1975) Momentum, mass and heat exchange of plant communities. In: *Vegetation and the atmosphere.* Volume 1. (Ed: Monteith J.L.) pp 57–109. Academic Press, London.

Thom A.S. and Oliver H.R. (1977) On Penman's equation for estimating regional evaporation. *Quart. J. Roy. Meteor. Soc.* **103**, 345–357.

Thom A.S., Stewart J.B., Oliver H.R. and Gash J.H.C. (1975) Comparison of aerodynamic and energy budget estimates of fluxes over a pine forest. *Quart. J. Roy. Meteor. Soc.* **101**, 93–105.

Thomas R. (1986) Personal communication. Macaulay Land Use Research Institute, Bush Estate, Penicuik, Midlothian, UK.

Tjepkema J.D., Cartica R.J. and Hemond H.F. (1981) Atmospheric concentrations of ammonia in Massachusetts and deposition on vegetation. *Nature* **294**, 445–446.

Tutin T.G., Heywood V.H., Burges N.A., Valentine D.H., Walters S.M. and Webb D.A. (1964) *Flora Europaea.* (Eds.) Cambridge University Press, Cambridge. (6 volumes).

Unsworth M.H. (1981) The exchange of carbon dioxide and air pollutants between vegetation and the atmosphere. In: *Plants and their atmospheric environment.* (21st symposium of the British Ecological Society.) (Eds: Grace J., Ford E.D. and Jarvis P.G.) pp 111–138. Blackwell Scientific, Oxford.

Van Breeman N. and Van Dijk H.F.G. (1988) Ecosystem effects of atmospheric deposition of nitrogen in The Netherlands. *Environ. Pollut.* **54**, 249–274.

Van Breeman N., Burrough P.A., Velthorst E.J. Van Dobben H.F., De Wit T., Ridder T.B. and Reijnders H.F.R. (1982) Soil acidification from atmospheric ammonium sulphate in forest canopy throughfall. *Nature* **299**, 548–550.

Van den Abbeel R., Claes A. and Vlassak K. (1989) Gaseous nitrogen losses from slurry-manured land. In: *Nitrogen in organic wastes applied to soils.* (Eds: Hansen J.A. and Henriksen K.) pp 212–224. Academic Press, London.

Van der Eerden (1982) Toxicity of ammonia to plants. *Agric. and Environ.* **7**, 223–235.

Van der Molen J., Bussink D.W., Vertregt N., Van Faassen H.G. and den Boer D.J. (1989) Ammonia volatilization from arable and grassland soils. In: *Nitrogen in organic wastes applied to soils.* (Eds: Hansen J.A. and Henriksen K.) pp 185–201. Academic Press, London.

Van Dijk H.F.G. and Roelofs J.G.M. (1988) Effects of excessive ammonium deposition on the nutritional status and condition of pine needles. *Physiologia plantarum* **73**, 494–501.

Van Hove L.W.A., Adema E.H. and Vredenberg W.J. (1987b) The uptake of atmospheric ammonia by leaves. In: *Air pollution and Ecosystems. Proceedings of an international symposium,* 18–22 May 1987, Grenoble, France. (Ed: Mathy P.) pp 734–738. D. Reidel Publishing Company, Dordrecht.

Van Hove L.W.A., Adema E.H., Vredenberg W.J. and Pieters G.A. (1989) A study of the adsorption of NH_3 and SO_2 on leaf surfaces. *Atmos. Environ.* **23**, 1479–1486.

Van Hove L.W.A., Koops A.J., Adema E.H., Vredenberg W.J. and Pieters G.A. (1987a) Analysis of the uptake of atmospheric ammonia by leaves of *Phaseolus vulgaris* L. *Atmos. Environ.* **21**, 1759–1763.

Van Hove L.W.A., Vredenberg W.J. and Adema E.H. (1990) The effect of wind velocity, air-temperature and humidity on NH_3 and SO_2 transfer into Bean-leaves (*Phaseolus vulgaris* L.). *Atmos. Environ.* **24**, 1263–1270.

Vibelu-Anderson H. (1989) Personal communication. Natural Environment Research Institute, Frederiksborgvej 399, DK 4000, Roskilde, Denmark.

Ville G. (1850) Note sur l'assimilation de l'azote du l'air, par les plantes, et sur l'influence qu'excerce l'ammoniaque dans la végétation. *Compte Rendus Acad. Sci., Paris.* **31**, 578–580 (in French).

Vlek P.L.G. and Craswell E.T. (1981) Ammonia volatilization from flooded soils. *Fert. Res.* **2**. 227–245.

Voorburg J.H. and Monteny G.J. (in preparation) Emissions of NH_3. Chapter 1. In: *Review Report, Dutch Priority Programme on Acidification.* Ministry of Housing, Physical and Natural Environment, The Hague, The Netherlands.

Wallace J.S. Batchelor C.H. and Hodnett M.G. (1981) Crop evaporation and surface conductance calculated using soil moisture data from central India. *Agric. Meteor.* **25**, 83–96.

Warren Spring Laboratory (1988) United Kingdom acid rain monitoring. Ocassional paper. Warren Spring Laboratory, Department of Trade and Industry, Stevenage, Herts, UK.

Way J.T. (1855) The atmosphere as a source of nitrogen to plants being an account of recent researches into this subject. *J. Roy. Agr. Soc.* **16**, 249–267.

Webb E.K. (1970) Profile relationships: The log–linear range and extension to strong stability. *Quart. J. Roy. Meteor. Soc.* **96**, 67–90.

Webb E.K., Pearman G.I. and Leuning R. (1980) Correction of flux measurements for density effects due to heat and water vapour transfer. *Quart. J. Roy. Meteor. Soc.* **106**, 85–100.

Wesely M.L. and Hicks B.B. (1977) Some factors that affect the deposition rates of sulfur dioxide and similar gases on vegetation. *J. Air Pollut. Control Assoc.* **27**, 1110–1116.

Wetselaar R. and Farquahar G.D. (1980) Losses of nitrogen from the tops of plants. *Adv. Agron.* **33**, 263–302.

Whitehead D.C. (1970) *The role of nitrogen in grassland productivity: a review of information.* Commonwealth Agricultural Bureau, Farnham Royal, Buckinghamshire, UK. pp 202.

Whitehead D.C. and Lockyer D.R. (1987) The influence of the concentration of gaseous ammonia on its uptake by the leaves of Italian Ryegrass, with and without an adequate supply of nitrogen to the roots. *J. Experim. Botany* **38**, 818–827.

Whitehead D.C. and Lockyer D.R. (1989) Decomposing grass herbage as a source of ammonia in the atmosphere. *Atmos. Environ.* **23**, 1867–1869.

Whitehead D.C., Lockyer D.R. and Raistrick N. (1988) The volatilization of ammonia from perennial ryegrass during decomposition, drying and induced senescence. *Ann. Bot.* **61**, 567–571.

Winkler P. (1986) Relations between aerosol acidity and ion balance. In: *Chemistry of multiphase atmospheric systems.* (Ed: Jaeschke W.) NATO ASI Series **G6**, 269–298. Springer-Verlag, Berlin.

WMO (1984) Global atmospheric background monitoring for selected environmental parameters, BAPMoN data for 1980, World Meteorological Organization, Geneva, Switzerland.

Yamamoto N., Kabeya N., Onodera M., Takahahi S., Komori Y., Nakazuka E. and Shirai T. (1988) Seasonal variation of atmospheric ammonia and particulate ammonium concentrations in the urban atmosphere over a 5 year period. *Atmos. Environ.* **22**, 2621–2623.

Yosida Z. (1953) General survey of the studies on fog-preventing forest. *Studies on Fogs in relation to fog-resisting forests.* (Ed: Hori T.) pp 1–23. Tanne Trading Co. Ltd., Sapporo, Japan.

Appendices

Contents

Appendix 1

Reconciliation of units and presentation of results

Units and the SI

In an attempt to provide a consistent and economic presentation of units, the advantages of the SI (Système International d'Unites), as discussed in full by Incoll *et al.* (1977), are recognized and the system broadly followed in this study. However, in several cases strict adherence to the SI provides cumbersome expressions, making it desirable to diverge. This occurs where powered units are used, and where there is a particular scale of interest to the result.

The unit prefixes in the SI account for multiples of 10^3 so that, for example, μm, mm, m and km are all legitimate measures of length. However, where powered units, such as areas or volumes are to be described, this results in larger multiples, here 10^6 and 10^9 respectively, giving rise to the need for exponents in the presentation of results. It is because of this that many authors still use non-standard units such as litres. In this study the litre is avoided, however dm^3 (equivalent to a l), and cm^3 (equivalent to a ml) are used where necessary to overcome this problem.

Measure	units used here	SI	Other equivalent non-standard units / notes
aqueous mass concentration	$\mu g\ dm^{-3}$ $mg\ dm^{-3}$ $g\ dm^{-3}$	$mg\ m^{-3}$ $g\ m^{-3}$ $kg\ m^{-3}$	$\mu g\ l^{-1}$, $ng\ ml^{-1}$, ppb(mass) $mg\ l^{-1}$, $\mu g\ ml^{-1}$, ppm(mass) 0.1 % (weight/volume)
mass concentration in air	$\mu g\ m^{-3}$	$\mu g\ m^{-3}$	(refers to total molecule or ion)
volumes	cm^3 dm^3	$10^3\ mm^3$; $10^{-6}\ m^3$ $10^6\ mm^3$; $10^{-3}\ m^3$	ml l
volume flow	$mm^3\ s^{-1}$ $dm^3\ s^{-1}$	$mm^3\ s^{-1}$ $10^6\ mm^3\ s^{-1}$; $10^{-3}\ m^3\ s^{-1}$	$0.06\ ml\ min^{-1}$ $60\ l\ min^{-1}$
pressure	Pa mPa	Pa mPa	0.01 mbar; 0.0075 mm Hg 10 nbar
deposition velocity, V_d	$mm\ s^{-1}$	$mm\ s^{-1}$	$0.1\ cm\ s^{-1}$
deposition resistance, r	$s\ m^{-1}$	$s\ m^{-1}$	$0.01\ s\ cm^{-1}$
flux, F_χ	$ng\ m^{-2}\ s^{-1}$	$ng\ m^{-2}\ s^{-1}$	$3.6\ g\ m^{-2}\ hour^{-1}$; $36\ mg\ ha^{-1}\ hour^{-1}$ (refers to total molecule or ion)
flux of element, *e.g.* NH_3-N	$kg\ NH_3$-N $ha^{-1}\ year^{-1}$	3.1 ng NH_3-N $m^{-2}\ s^{-1}$	$2.74\ g\ NH_3$-N $ha^{-1}\ day^{-1}$ (refers to mass of specified element)

Table A1.1 Comparison of units used in this study, SI, and other commonly used units.

The scale of interest of the SI units may also be inconvenient. This is the case for measures of time, where for example, seconds are inconvenient to describe a process taking several hours. In this study therefore periods of time are expressed in the most convenient time scale. However, in measures with multiple units, this can become complicated, so that in general the SI units are used in the study. In addition, following the recommendation of Incoll *et al.*, prefixed units are confined to numerators. Exceptions to these are aqueous concentrations and annual fluxes of N.

The set of units used in this study are given in Table A1.1, along with SI equivalents, and other commonly used non standard units.

Ammonia concentration units

In accordance with general practice in air pollution research, air concentrations of NH_3 and NH_4^+ are expressed as $\mu g\ m^{-3}$ throughout the study. The exception to this is during discussion of chemical solubility. In this case both aqueous and gaseous concentrations are given as $mol\ dm^{-3}$ (molar, M), so as to maintain consistency in the use of the Henry constant, conventionally expressed as M(gas)/M(aqueous).

Other authors use parts per billion (10^9) volume fraction (ppbv), here termed s, to describe the quantity of a trace gas in air. The relationship between this and concentration ($\mu g\ m^{-3}$) may be found from the general gas law:

$$s\ (\text{ppbv}) = \left[\frac{10^3\ R\ T}{P\ M}\right] \chi \quad (\mu g\ m^{-3}) \qquad \text{A1.1}$$

where R is the general gas constant (8.314 Pa m^3 mol^{-1} K^{-1}), T is temperature (K), P is atmospheric pressure (Pa), and M is the molecular weight of the entity (g mol^{-1}). For NH_3 at standard temperature and pressure (STP: 273.15 K, 101.325 kPa) this gives:

$$s_{NH_3}\ (\text{ppbv}) = 1.316\,\chi\ (\mu\text{g m}^{-3})$$

At 10 °C (283.15 K) this becomes $s_{NH_3} = 1.364\,\chi$. Partial pressures are also sometimes used to describe trace NH_3 levels. Again from the gas law:

$$P_{NH_3}\ (\text{mPa}) = \left[\frac{10^{-3}\,R\,T}{M}\right]\chi\ (\mu\text{g m}^{-3}) \qquad \text{A1.2}$$

where P_{NH_3} is partial pressure of ammonia. At STP this gives:

$$P_{NH_3}\ (\text{mPa}) = 0.1334\,\chi\ (\mu\text{g m}^{-3})$$

which at 10 °C becomes $P_{NH_3} = 0.1382\,\chi$.

Direction of fluxes

In chapter 2 the derivation of formulae for calculating fluxes using the aerodynamic gradient method was considered. From this, accepting standard mathematical convention, it may be seen that a deposition flux, with concentrations smaller near the ground, has a positive value, while an emission flux, with concentrations larger near the ground, has a negative value (section 2.3.1). This convention is consistent with the development of the resistance analogy and deposition velocities (section 2.4), where a positive V_d implies deposition, and a negative V_d implies emission. Given this consistency, this system, as also used by Garland (1977), is used as the basis for presentation of the results here. For the flux data sets given in Appendices 2–4 this applies to **H**, λE and F_χ.

It is noted however, that in micrometeorology, fluxes of entrained properties, such as heat, water vapour and CO_2 are usually treated with the signs reversed, so that deposition is negative and emission positive (*e.g.* Monteith, 1973). This is because fluxes are considered as inputs and outputs from the atmosphere, rather than the surface. The exception is momentum fluxes, which are treated by the first method above. This system, in addition to being inconsistent here, is not consistent with the system for V_d used in air pollution research, noted above. Consequently the first method is preferred in this study and is used throughout in the presentation of the data in tables. Nevertheless, this second method provides a convenient form for the presentation of values, and following the micrometeorological convention the values of **H** and λE are graphed this way. To avoid confusion, note is made on the graphs that the axes are for 'emission fluxes'. Similarly in Chapter 5, where both emission and

deposition fluxes of NH_3 occur, it is convenient to plot cases of emission in this way. Here again axes are labelled appropriately.

Notes on symbols used in Appendices 2–4

In appendices 2–4, which follow this section, details of the results for the flux gradient studies are presented. Given the large number of possible parameters which could be given, only the most important and relevant to this study are included. Error limits are provided for a number of the most interesting variables ($\chi\{1\ m\}$, F_χ, r_c, $\chi\{z_o'\}$), these being 95% confidence limits of the mean values. The error estimates are derived from the profile regressions as set out in Appendix 5 and must be accepted as somewhat approximate due to the small number of points in the regressions. For r_c, upper and lower limits are given separately since the intervals for each differ. Here 'em' denotes emission, in which case r_c is not relevant, while negative values of r_c imply deposition at rates faster than permissible by turbulence.

In the tables, figures in brackets represent very approximate or doubtful values, while profiles with less than four NH_3 values are noted with an asterisk and the number of NH_3 points available. Symbols used, other than those described in the main list of symbols, are:

n	number of values included in the calculation of a mean
NM	not measured
ND	not detected (for temperature gradients in calculation of stability)
em	emission
*	values approximate or doubtful
LS	long sampling period
S	ground-vegetation surface
V	vegetation
G	ground
0/8, 8/8	cloud cover of sky in octas (eighths)
NE, SW	wind direction, *e.g.* north east, south west

Appendix 2

Tables of NH_3 surface exchange results over natural and low input surfaces

Huntingdon (Neutral-calcareous grassland) 8/1987 — Night-time: 1935–0440 GMT

Run	Date and time (GMT)	L (m)	SF{1} —	U{1} (m s^{-1})	U* (m s^{-1})	z_o (mm)	r_a{1} (s m^{-1})	r_b (s m^{-1})	T{z_o'} (°C)	χ{1} (μg m^{-3})	Flux χ (ng m^{-2} s^{-1})	V_d{1} (mm s^{-1})	r_c (s m^{-1})	χ{z_o'} (μg m^{-3})	Conditions and notes
	11–13/8/1987														light W–S flow
1	11/8 1120–1350	NM	1.0	2.98	0.28	13.1	37.5	14.3	—	1.94 ± 0.31	40.8 ± 29.3	21.0	-4.2 [-24.4, 129]	-0.17 ± 1.36	V drying, thin 8/8
2	1445–1540	NM	1.0	2.66	0.25	12.4	43.1	15.6	—	1.49 ± 0.79	19.9 ± 59.5	13.4	16.1 [-40.1, em]	0.32 ± 2.93	V dry, rain stopped run at end
3	12/8 0925–1105	NM	1.0	3.59	0.31	9.1	36.5	12.1	—	2.19	59.8	27.3	-12.1	-0.72	* 2 pt NH_3, V dry, 8/8 bright
4	1335–1535	NM	1.0	1.82	0.16	8.8	73.0	20.3	—	—	—	—	—	—	* 1 pt NH_3, ditto
5	1600–1800	(-25)	(1.45)	1.56	0.18	25.8	45.6	23.6	(20.8)	1.84 ± 0.18	15.6 ± 13.6	8.5	48.7 [-6.4, 899]	0.76 ± 0.84	V dry, 8/8
6	1835–2025	26.6	0.70	1.03	0.16	83.5	41.6	34.9	16.3	3.43 ± 0.86	57.2 ± 44.6	16.7	-16.7 [-43.6, 254]	-0.95 ± 2.97	V dry, 3/8, dusk
7	12–13/8 2130–0035	34.2	0.75	1.98	0.19	14.8	57.2	20.3	14.9	2.19 ± 0.50	34.4 ± 47.4	15.7	-13.9 [-51.0, em]	-0.48 ± 3.50	V wet, dew fall, 1/8
8	13/8 0130–0500	158	0.94	1.94	0.19	15.8	53.7	20.3	16.0	2.11 ± 1.53	46.9 ± 91.9	22.2	-29.0 [-59.2, em]	-1.36 ± 5.92	V wet, much dew, 1–8/8
9	0940–1140	-215	1.06	3.33	0.31	12.8	33.5	13.1	18.7	1.34 ± 0.13	8.0 ± 14.7	6.0	120 [12.4, em]	0.97 ± 0.62	V wet, rain before run, 8/8
10	1225–1425	-125	1.09	3.60	0.33	11.2	32.7	12.2	20.9	1.44 ± 0.22	22.9 ± 24.2	15.9	17.9 [-14.5, em]	0.41 ± 0.98	V wet, drying at end, 8/8

MEAN VALUES		U{1}	n	V_m †	r_{a+b} ‡	T{z_o'}	χ{1}	Flux χ	V_d{1}	r_t{1}	r_c ¶	χ{z_o'}	
		2.52	9	17.2	58.2	(17.9)	2.00	33.9	16.3	61.4 ¥	3.1	-0.14	Excluding run 4
		2.39	8	16.8	59.7	"	1.97	30.7	14.9	67.0 ¥	7.3	-0.06	Excluding runs 3 & 4
									17.0 §	58.9 §	0.7		Excluding run 4
									15.6 §	64.2 §	4.5		Excluding runs 3 & 4

Notes: † arithmetic mean; ‡ reciprocal of mean V_m; ¥ reciprocal of mean V_d ; ¶ from mean r_t and mean r_{a+b}. § Alternative mean from mean χ{1} & mean flux χ.

Harwell (Calcareous grassland) 3/1988 $d = 0.03$ m — Night-time: 1810–0615 GMT

Run	Date and time (GMT)	L (m)	SF{1} n/a	U{1} (m s^{-1})	U* (m s^{-1})	z_o (mm)	r_a{1} (s m^{-1})	r_b (s m^{-1})	T{z_o'} (°C)	χ{1} (μg m^{-3})	Flux χ (ng m^{-2} s^{-1})	V_d{1} (mm s^{-1})	r_c (s m^{-1})	χ{z_o'} (μg m^{-3})	Conditions and notes
	16–18/3/1988														
1	16/3 1000–1200	-93.4	1.13	4.59	0.34	4.00	38.6	8.7	10.2	2.97 ± 0.17	22.0 ± 15.8	7.4	87.4 [31.0, 433]	1.92 ± 0.62	S partly wet, 7/8 NW
2	1300–1445	-261	1.05	4.84	0.37	4.56	35.4	8.1	10.3	3.71 ± 0.27	28.5 ± 26.3	7.7	86.6 [24.1, 1710]	2.47 ± 0.96	V dry, G damp, 8/8 NW
3	1535–1645	ND	1.0	4.04	0.28	2.73	51.4	10.7	7.6	3.21 ± 0.69	34.0 ± 51.0	10.6	32.1 [-24.6, em]	1.09 ± 2.68	S dry, NW 8/8
4	16–17/3 1735–0820	ND	1.0	1.07	0.08	4.37	164.1	27.9	4.2	0.33 ± 0.00	0.23 ± 0.11	0.7	1290 [808, 2750]	0.29 ± 0.02	* LS, S wet, NW–NE
5–7	17/3 1015–1655	-15.7	1.70	2.37	0.19	5.45	60.7	15.5	9.7	0.25 ± 0.13	1.08 ± 2.38	4.4	154 [-47.5, em]	0.17 ± 0.49	*LS, S dry, 1–8/8, SE
8	17–18/3 1800–0915	ND	1.0	3.01	0.24	6.30	50.6	12.3	3.5	0.12 ± 0.04	0.12 ± 2.81	1.0	916 [-23.4, em]	0.11 ± 0.15	*LS, S wet, E
MEAN VALUES				U{1}	n		V_m †	r_{a+b} ‡	T{z_o'}	χ{1}	Flux χ	V_d{1}	r_t{1}	r_c¶	χ{z_o'}
				3.32	6		15.7	63.5	7.6	1.77	14.3	5.3	189 ¥	125	1.01
												8.1 §	123 §	59.7	

Notes: † arithmetic mean; ‡ reciprocal of mean V_m; ¥ reciprocal of mean V_d ; ¶ from mean r_t and mean r_{a+b}. § Alternative mean from mean χ{1} & mean flux χ.

Example of sensitivity of data to varying value of d for run 1.

1	d = 0.00	-96.2	1.12	4.57	0.36	5.68	34.0	9.6	10.3	2.96 ± 0.18	26.4 ± 21.0	8.9	68.7 [18.8 , 517]	1.81 ± 0.78	
1	d = 0.03	-93.4	1.13	4.59	0.34	4.00	38.6	8.7	10.2	2.97 ± 0.17	22.0 ± 15.8	7.4	87.4 [31.0, 433]	1.92 ± 0.62	
1	d = 0.06	-91.6	1.13	4.62	0.32	2.66	44.4	8.9	10.1	2.96 ± 0.14	17.1 ± 10.3	5.8	119.8 [54.7 , 383]	2.05 ± 0.45	

Great Dun Fell 5/1987, 3/1988, 4/1988 and 4/1989

Run	Date and time (GMT)	L (m)	SF{1} —	U{1} ($m\ s^{-1}$)	U*	z_o (mm)	r_a{1}	r_b ($s\ m^{-1}$)	T{z_o'} (°C)	χ{1} ($\mu g\ m^{-3}$)	Flux χ ($ng\ m^{-2}\ s^{-1}$)	V_d{1} ($mm\ s^{-1}$)	r_c ($s\ m^{-1}$)	χ{z_o'} ($\mu g\ m^{-3}$)	Conditions and notes
	27/5/1987			Night-time: 2020–0345 GMT											V dry, G damp, W, 3/8, hazy
2	1250–1500	NM	1.0	4.10	0.40	14.3	26.2	11.3	≈15	1.24 ± 0.51	64.5 ± 74.1	52.1	-18.3 [-28.9, em]	-1.18 ± 2.38	*3 pt NH_3
3	1630–1910	NM	1.0	4.10	0.40	14.3	26.2	11.3	≈15	1.21 ± 1.30	35.1 ± 96.6	28.9	-2.9 [-28.8, em]	-0.10 ± 2.76	* wind data approximate
	29–30/3/1988			Night-time: 1840–0545 GMT											SW flow, low cloud base (≈10–100 m height)
1	29/3 1725–1910	ND	1.0	4.90	0.42	8.53	27.5	9.5	2.2	0.81 ± 0.75	19.0 ± 258	23.6	5.4 [-34.2 , em]	0.10 ± 9.50	* 3 pt NH_3, S wet, 8/8
2	1955–2220	ND	1.0	3.50	0.30	8.84	38.0	12.3	0.7	0.47 ± 0.09	7.2 ± 7.4	15.2	15.5 [-18.2 , em]	0.11 ± 0.32	S wet, 8/8
3	30/3 1010–1235	-120	1.10	4.65	0.40	8.41	28.6	9.8	2.1	0.61 ± 0.03	14.1 ± 3.9	23.2	4.6 [-4.9 , 21.6]	0.07 ± 0.13	S wet, 7/8
4	1330–1530	-112	1.11	5.80	0.51	9.15	22.1	8.4	6.1	1.02 ± 0.20	31.3 ± 31.8	30.8	2.0 [-14.5 , em]	0.06 ± 0.86	S wet, 5/8
5	1700–1840	-124	1.10	4.05	0.34	7.41	34.7	10.8	2.8	0.68 ± 0.17	12.2 ± 18.0	18.0	10.1 [-23.3 , em]	0.12 ± 0.73	S wet, 3/8
6	1925–2210	ND	1.0	3.28	0.28	8.25	41.8	12.9	-0.1	0.12 ± 0.03	0.8 ± 4.8	6.7	94.6 [-33.5 , em]	0.07 ± 0.25	S wet, 2/8
	21/4/1988			Night-time: 1920–0455 GMT											WNW hazy
1	1045–1245	-24.3	1.46	3.88	0.40	16.6	23.2	11.6	15.0	0.67 ± 0.17	15.9 ± 27.5	23.8	7.3 [-19.5 , em]	0.12 ± 0.86	V dry, G wet, 6/8 CuSt
2	1330–1530	-11.3	1.94	2.95	0.27	9.12	37.6	13.5	15.1	0.55 ± 0.42	2.9 ± 51.3	5.3	139 [-40.9 , em]	0.40 ± 2.39	V dry, G wet, 8/8 CuSt
	25/4/1989			Night-time: as above											Measurements over snow
1	0835–1000	-11.5	1.92	2.57	0.14	0.62	118	11.6	(1.0)*	0.10 ± 0.02	0.0 ± 1.1	0.5	2049 [-45.2, em]	0.09 ± 0.13	snow frozen, ESE, 3/8
2	1200–1330	-19.3	1.57	2.69	0.19	2.36	74.4	12.9	(3.7)*	0.60 ± 0.08	4.3 ± 4.2	7.2	52.3 [-17.0, 9217]	0.22 ± 0.33	melting snow, WNW, 4/8, hazy
MEAN VALUES				U{1}	n		V_m †	r_{a+b} ‡	T{z_o'}	χ{1}	Flux χ	V_d{1}	r_t{1}	r_c¶	χ{z_o'}	
				3.87	12		22.2	45.0	(6.6)	0.67	17.3	19.6	51.0 ¥	5.9	0.01	All values
				3.75	10		21.3	46.9	(6.1)	0.60	12.4	16.0	62.3 ¥	15.7	0.12	Excluding 3 point profiles
												25.7 §	38.9 §	-6.1		All values
												20.5 §	48.7 §	1.8		Excluding 3 point profiles

Notes: * Absolute values of temperature in doubt; † arithmetic mean; ‡ reciprocal of mean V_m; ¥ reciprocal of mean V_d ; ¶ from mean r_t and mean r_{a+b}.
§ Alternative mean from mean χ{1} & mean flux χ.

Appendix 2

Fala Moor 11/1987

Night-time: 1625–0725 GMT

Run	Date and time (GMT)	L (m)	SF{1} n/a	U{1} ($m\ s^{-1}$)	u_*	z_o (mm)	r_a{1}	r_b ($s\ m^{-1}$)	T{z_o'} (°C)	χ{1} ($\mu g\ m^{-3}$)	Flux χ ($ng\ m^{-2}\ s^{-1}$)	V_d{1} ($mm\ s^{-1}$)	r_c ($s\ m^{-1}$)	χ{z_o'} ($\mu g\ m^{-3}$)	Conditions and notes
	5–6/11/1987														G damp throughout
1	5/11 1300–1500	-6.5	2.55	1.18	0.16	35.7	38.8	27.5	10.1	0.08 ± 0.02	1.1 ± 2.5	13.6	7.3 [-44.4, em]	0.01 ± 0.10	* 3 pt NH_3, V dry, SE, 2/8 hazy
2	1545–1745	(1.9)	(0.07)	0.75	0.04	4.6	536	51.7	1.2	0.06	—	—	—	—	* U + NH_3 unsure, V wet, fog
3	1820–2020	97.2	0.90	1.27	0.14	22.3	69.5	28.4	1.7	0.03 ± 0.02	-1.1 ± 1.4	—	—	0.14 ± 0.13	V wet, fog thinning, 0/8 above
4	2125–2335	-152	1.08	0.88	0.10	27.6	87.3	37.6	3.3	0.12 ± 0.06	2.4 ± 3.4	19.5	-73.5 [-104, em]	-0.17 ± 0.40	V wet, W, 8/8, light mist
5	6/11 0015–0340	98.6	0.90	1.84	0.22	32.2	38.1	21.5	2.8	0.07 ± 0.24	1.2 ± 25.1	16.7	0.2 [-56.8, em]	0.00 ± 1.43	* 3 pt NH_3, V wet, W, 8/8, clear
6	0430–0725	167.4	0.94	2.28	0.27	31.6	31.1	18.3	3.4	0.29 ± 0.16	10.9 ± 23.5	37.2	-22.4 [-41.0, em]	-0.24 ± 1.11	V wet, W, 8/8
7	0815–1020	-947	1.01	2.08	0.23	26.4	37.8	19.5	4.8	0.40 ± 0.06	9.1 ± 7.7	22.6	-13.0 [-33.4, 242]	-0.12 ± 0.42	V drying, NW, 8/8, dull
8	1110–1200	-144	1.08	2.29	0.25	24.5	35.0	18.0	6.4	0.60 ± 0.25	11.7 ± 36.5	19.3	-1.2 [-40.6, em]	-0.01 ± 1.89	V dry, 8/8, hazy
MEAN VALUES				U{1}	n		V_m †	r_{a+b} ‡	T{z_o'}	χ{1}	Flux χ	V_d{1}	r_t{1}	r_c ¶	χ{z_o'}	
				1.69	7		15.2	65.6	4.6	0.23	5.04	21.5	46.5 ¥	-19.1	-0.06	Excluding run 2
												22.2 §	45.0 §	-20.6		"

Notes: † arithmetic mean; ‡ reciprocal of mean V_m; ¥ reciprocal of mean V_d ; ¶ from mean r_t and mean r_{a+b}. § Alternative mean from mean χ{1} & mean flux χ.

Fala Moor 5/1988 $d = 0.05$ m Night-time: 2030–0345 GMT

Run	Date and time (GMT)		L (m)	SF{1} n/a	U{1} (m s^{-1})	U* (m s^{-1})	z_o (mm)	r_a{1} (s m^{-1})	r_b (s m^{-1})	T{z_o'} (°C)	χ{1} (μg m^{-3})	Flux χ (ng m^{-2} s^{-1})	V_d{1} (mm s^{-1})	r_c (s m^{-1})	χ{z_o'} (μg m^{-3})	Conditions and notes
	24–25/5/1988															SW flow, Canopy drying cycle, ground damp
1	24/5	1445–1645	-261	1.05	5.01	0.59	30.9	14.2	10.0	13.4	0.53 ± 0.20	-8.3 ± 83.2	-15.7	—	0.73 ± 2.03	* 3 pt NH_3, V dry, 8/8 bright
2		1710–1900	1342	0.99	4.89	0.59	32.7	14.3	10.2	10.6	1.15 ± 0.16	64.4 ± 48.3	55.8	-6.6 [-14.3, 51.1]	-0.42 ± 1.11	Vdry, 8/8
3	25/5	0415–0625	517	0.98	4.18	0.49	29.8	17.6	11.5	4.7	0.62 ± 0.03	29.2 ± 9.7	47.2	-8.0 [-13.3, 2.7]	-0.23 ± 0.27	V wet, 1/8
4		0705–0900	-144	1.08	5.80	0.68	30.0	12.3	8.9	12.8	0.69 ± 0.14	37.0 ± 58.0	53.6	-2.6 [-14.0, em]	-0.10 ± 1.18	V drying, 3/8
5		0930–1130	-83	1.14	5.72	0.68	30.8	12.1	9.0	17.6	0.59 ± 0.10	25.7 ± 58.6	43.6	1.8 [-14.1, em]	0.05 ± 1.23	V dry, 3/8
6		1205–1405	-101	1.12	6.47	0.77	30.3	10.9	8.2	19.5	0.51 ± 0.58	8.0 ± 447.7	15.8	44.1 [-18.0, em]	0.35 ± 8.78	* 3 pt NH_3, V dry, 3/8
7		1430–1715	-101	1.12	5.79	0.69	31.1	12.0	8.9	18.0	0.46 ± 0.06	16.1 ± 26.7	35.2	7.5 [-10.3, em]	0.12 ± 0.53	V dry, 4/8
8		1755–1955	-226	1.05	3.83	0.47	34.7	17.3	12.3	10.5	0.55 ± 0.09	15.5 ± 22.6	28.4	5.7 [-15.3, em]	0.09 ± 0.64	rain 1840, V wet , 4/8
MEAN VALUES					U{1}	n		V_m †	r_{a+b} ‡	T{z_o'}	χ{1}	Flux χ	V_d{1}	r_t{1}	r_c ¶	χ{z_o'}	
					5.21	8		43.1	23.2	13.4	0.64	23.5	33.0	30.3 ¥	7.1	0.07	All values
					5.04	6		41.9	23.8	12.4	0.68	31.3	44.0	22.7 ¥	-1.1	-0.08	Excluding 3 point profiles
													36.8 §	27.2 §	4.0		All values
													46.3 §	21.6 §	-2.2		Excluding 3 point profiles

Notes: † arithmetic mean; ‡ reciprocal of mean V_m; ¥ reciprocal of mean V_d; ¶ from mean r_t and mean r_{a+b}. § Alternative mean from mean χ{1} & mean flux χ.

Example of data sensitivity to a varying value of d for run 3.

3	d = -0.10 m	572	0.98	3.96	0.57	58.8	12.1	12.0	4.6	0.59 ± 0.03	41.5 ± 11.8	70.3	-9.9 [-13.1,- 4.2]	-0.41 ± 0.27	
3	d = 0.00 m	529	0.98	4.11	0.51	37.8	15.6	11.7	4.7	0.61 ± 0.03	33.0 ± 10.2	54.1	-8.9 [-13.3, -0.4]	-0.29 ± 0.27	
3	d = 0.05 m	517	0.98	4.18	0.49	29.8	17.6	11.5	4.7	0.62 ± 0.03	29.2 ± 9.7	47.2	-8.0 [-13.3, 2.7]	-0.23 ± 0.27	
3	d = 0.10 m	501	0.98	4.25	0.46	22.4	20.3	11.3	4.8	0.63 ± 0.04	25.4 ± 9.2	40.4	-6.9 [-13.5, 7.4]	-0.17 ± 0.27	
3	d = 0.15 m	488	0.98	4.32	0.43	16.0	23.7	11.0	4.8	0.64 ± 0.04	21.6 ± 8.7	34.0	-5.3 [-13.8, 15.1]	-0.11 ± 0.28	
3	d = 0.20 m	482	0.98	4.38	0.39	10.7	28.1	10.6	4.9	0.64 ± 0.05	17.9 ± 8.3	27.9	-2.8 [-14.3, 29.3]	-0.05 ± 0.29	

Wether Law (heather moor) 2/1989 — Night-time: 1730–0725 GMT

Run	Date and time (GMT)	L (m)	SF{1} n/a	U{1} ($m s^{-1}$)	U* ($m s^{-1}$)	z_o (mm)	r_a{1} ($s m^{-1}$)	r_b ($s m^{-1}$)	T{1} (°C)	T{z_o'} (°C)	H ($W m^{-2}$)	λE ($W m^{-2}$)	E_ST{z_o'} ($g m^{-3}$)	E{z_o'} ($g m^{-3}$)	r_{sEb} ($s m^{-1}$)	χ{1} ($\mu g m^{-3}$)	Flux χ ($ng m^{-2} s^{-1}$)	V_d{1} ($mm s^{-1}$)	r_c ($s m^{-1}$)	χ{z_o'} ($\mu g m^{-3}$)	Conditions and notes
	21/2/1989																				SW flow
1	1410–1715	187 0	0.99	4.65	0.56	33.4	14.8	10.6	2.6	2.5	8.1	-27.6	5.71	5.02	62.2	0.18 ± 0.05	-0.3 ± 9.6	-2.0	—	0.19 ± 0.21	V dry, G wet, 8/8
	22–23/2/1989																				SW flow
2	1435–1610	ND	1.0	8.48	0.95	25.8	9.4	6.7	2.3	2.4	-5.5	-7.7	5.69	3.68	656	0.11 ± 0.03	7.2 ± 11.0	66.9	-1.1 [-10.2, em]	-0.01 ± 0.16	V dry, G damp, 3/8
																					≈5 mm snow 16 20
3	1715–1930	307 .5	0.97	5.73	0.64	25.1	14.2	9.0	-1.1	-2.4	70.6	-8.4	3.99	4.02	-14.6	0.08 ±0.03	-1.1 ±8.0	-13.6	—	0.11 ± 0.17	dry snow, 1/8
4	2015–0005	460.2	0.98	6.48	0.73	26.2	12.2	8.2	-1.5	-2.7	71.0	—*	—	—	—	0.06 ± 0.04	3.3 ± 11.8	55.6	-2.5[-16.6, em]	-0.01 ± 0.23	snow still on V, 5/8
5	0045–0405	710.4	0.99	7.38	0.83	25.8	10.8	7.5	-1.8	-2.8	67.1	—*	—	—	—	0.03 ± 0.02	1.0 ± 5.3	37.1	8.6 [-14.0, em]	0.01 ± 0.09	Snow blown to G
6	0515–0740	735.0	0.99	7.11	0.80	26.3	11.1	7.7	-1.9	-2.8	59.0	—*	—	—	—	0.07 ± 0.13	-1.7 ± 31.9	-24.3	—	0.10 ±0.53	* 3pt NH_3, *, 4/8
7	0930–1240	-517	1.02	8.47	0.96	26.9	9.1	6.7	0.6	2.5	-148	-11.0	5.73	4.36	310	0.05 ±0.01	6.9 ± 5.2	149.9	-9.2 [-12.1, 18.6]	-0.06 ± 0.08	V dry, 3/8
8	1315–1615	ND	1.0	7.44	0.84	26.9	10.5	7.4	0.8	1.4	-36.7	-10.9	5.31	3.61	392	0.03 ± 0.01	-1.6 ± 3.7	-48.3	—	0.06 ±0.06	V dry, 3–6/8
MEAN VALUES			n	U{1}		V_m †	r_{a+b} ‡		T{1}	T{z_o'}						χ{1}	Flux χ	V_d{1}	r_t{1}	r_c ¶	χ{z_o'}	
			8	6.97		52.6	19.0		0.0	-0.2						0.076	1.71	27.7	36.2¥	17.1	0.049	
																		22.5 §	44.5 §	25.5		

Notes: * Psychrometers not fully aspirated for runs 4–6. † arithmetic mean; ‡ reciprocal of mean V_m; ¥ reciprocal of mean V_d; ¶ from mean r_t and mean r_{a+b}.
§ Alternative mean from mean χ{1} & mean flux χ.

Dunslair (Glentress Forest) 11/1988 — Night-time: 1610–0740 GMT

Run	Date and time (GMT)		L * (m)	SF n/a	U{1} (m s^{-1})	U* (m s^{-1})	z_o (mm)	r_a{1} (s m^{-1})	r_b** (s m^{-1})	T{z_o'} (°C)	χ{mean z-d} (μg m^{-3})	Flux χ (ng m^{-2} s^{-1})	V_d{1} (mm s^{-1})	r_c (s m^{-1})	χ{z_o'} (μg m^{-3})	Conditions and notes
	NH_3 data															
1	12/11	1130–1335	-3170	1.00	3.43	1.24	320	2.2	3.8	5.2	0.12 ± 0.05	14.4 ± 122	167	-0.0	0.00	*3 pt NH_3, V dry, SW, 8/8
2		1415–1630	-7710	1.00	4.96	1.47	250	2.3	3.2	4.8	0.11	—	—	—	—	*1 pt NH_3, V partly wet, 8/8
3	14/11	1255–1600	ND	1.0	4.78	1.06	160	4.2	4.5	—	0.43 ± 0.06	27.7 ± 103	82	3.5	0.10	V mostly dry, SW, 8/8
4	15/11	1110–1355	ND	1.0	4.12	0.93	160	4.8	5.1	≈6.2	0.06 ± 0.02	—	—	—	—	*2 pt NH_3, V drying
5		1445–1640	ND	1.0	2.27	0.54	180	7.6	8.8	≈5.7	0.13 ± 0.61	0.8 ± 527	6.6	137	0.11	*3 pt NH_3, V wet, thin 8/8 Ci
6	16/11	1115–1350	-246	1.06	2.68	0.63	170	6.7	7.6	7.5	0.13 ± 0.05	1.0 ± 59.1	8.0	111	0.11	V wet, dew, WSW, 4/8, hazy
7	17/11	1305–1605	ND	1.0	2.12	0.53	190	7.6	9.0	≈7	0.06 ± 0.04	-13.1 ± 29.1	(-218)	—	0.37	*in cloud, NH_3 uncertain, V wet, S, 8/8

MEAN VALUES			U{1}	n	V_m †	r_{a+b} ‡	T{z_o'}	χ{1}	Flux χ	V_d{1}	r_t{1}	r_c ¶	χ{z_o'}	V_d/V_m	
			3.06	5	94.6	10.6	(6.4)	0.174	6.16	9.12	110 ¥	99.4	0.14	0.10	Excluding runs 2 & 4
			3.29	4	103	9.7	(6.1)	0.203	10.98	65.9	15.2 ¥	5.5	0.08	0.64	Excluding runs 2, 4 & 7
										35.4 §	28.2 §	17.6		0.37	Excluding runs 2 & 4
										54.1 §	18.5 §	8.8		0.53	Excluding runs 2, 4 & 7

Run	Date and time (GMT)		L (m)	SF n/a	U{1} (m s^{-1})	U* (m s^{-1})	z_o (mm)	r_a{1} (s m^{-1})	r_b** (s m^{-1})	T{z_o'} (°C)	χ{mean z-d} (μg m^{-3})	Flux χ (ng m^{-2} s^{-1})	V_d{1} (mm s^{-1})	r_t (s m^{-1})	Conditions and notes
	NH_4^+ data														
1–2	12/11	1130–1630	-5140	1.00	4.30	1.36	270	2.3	—	5.0	0.32 ± 0.03	10.9 ± 94.5	37.5	26.7	
3	14/11	1255–1600	ND	1.0	4.78	1.06	160	4.2	—	—	0.46 ± 0.09	2.1 ± 146	4.8	208	
4–5	15/11	1110–1640	ND	1.0	3.39	0.77	160	5.7	—	≈6	1.22 ± 0.05	18.7 ± 55.9	16.5	61	
6	16/11	1115–1350	-246	1.06	2.68	0.63	170	6.7	—	7.5	3.26 ± 0.13	9.1 ± 146	2.8	360	
7	17/11	1305–1605	ND	1.0	2.12	0.53	190	7.6	—	≈7	0.43± 0.06	7.9 ± 59.2	21.6	46	

MEAN VALUES			U{1}	n	$V_m(NH_3)$ †	$r_{a+b}(NH_3)$ ‡	T{z_o'}	χ{1}	Flux χ	V_d{1}	r_t{1}	$V_d/V_m(NH_3)$	
			3.45	5	100	10.0	(6.4)	1.14	9.74	16.6	60.1 ¥	0.17	
										8.6 §	117 §	0.09	

Notes: * L from eddy correlation data. ** r_b calculated according to Wesely and Hicks (1977). Equivalent V_m for NH_3 calculated for NH_4^+ data for comparison of rates by V_d/V_m. Further notes as for other tables.

Appendix 2

Appendix 3

Tables of NH_3 surface exchange results over agricultural surfaces

Bush (Intensive agricultural grassland) 2/1989 — Night-time: 1740–0710 GMT

Run	Date and time (GMT)	L (m)	SF{1} n/a	U{1} ($m\,s^{-1}$)	u^* ($m\,s^{-1}$)	z_o (mm)	r_a{1} ($s\,m^{-1}$)	r_b ($s\,m^{-1}$)	T{1} (°C)	T{z_o'} (°C)	H ($W\,m^{-2}$)	λE ($W\,m^{-2}$)	E_ST{z_o'} ($g\,m^{-3}$)	E{z_o'} ($g\,m^{-3}$)	r_{sEb} ($s\,m^{-1}$)	χ{1} ($\mu g\,m^{-3}$)	Flux χ ($ng\,m^{-2}\,s^{-1}$)	V_d{1} ($mm\,s^{-1}$)	r_c ($s\,m^{-1}$)	χ{z_o'} ($\mu g\,m^{-3}$)	Conditions and notes
	27–28/2/1989																				Melting snow, W
1	1450–1745	28.9	0.72	4.71	0.23	0.26	90.2	6.5	2.6	0.1	33.2	4.1	4.85	4.93	48.5	3.14 ± 0.05	35.1 ± 6.2	11.2	-7.5 [-20.9, 11.5]	-0.26 ± 0.25	100% S
2	1845–2150	34.1	0.75	4.66	0.23	0.31	86.7	6.8	2.3	0.0	29.7	1.2	4.85	4.88	67.3	1.92 ± 0.18	16.1 ± 10.4	8.4	25.9 [-21.3, 251]	0.42 ± 0.87	97% S
3	2230–0150	54.0	0.83	5.35	0.28	0.43	68.5	6.4	2.0	-0.0	33.5	4.1	4.84	4.81	-20.1	0.80 ± 0.03	5.2 ± 2.5	6.5	79.8 [29.9, 221]	0.41 ± 0.16	97% S, 5/8, l. frost
4	0235–0535	67.6	0.86	6.24	0.33	0.46	57.3	5.7	2.3	0.1	44.4	(0.8)	4.85	4.73	—	0.54 ± 0.03	5.1 ± 2.4	9.4	43.8 [9.7, 138]	0.22 ± 0.13	97% S, 4/8, l. frost
5	0615–0925	103	0.91	7.88	0.42	0.52	43.8	4.8	2.9	0.5	62.4	-2.7	5.00	4.88	116	0.76 ± 0.10	13.3 ± 11.7	17.6	8.0 [-18.6, 447]	0.11 ± 0.51	99–80% S, 8/8
6	1235–1535	548	0.98	7.65	0.60	5.63	20.9	6.6	3.7	2.9	34.8	-39.6	5.89	5.84	3.2	0.59 ± 0.04	12.1 ± 6.7	20.6	21.0 [3.8, 80.8]	0.26 ± 0.16	50–5% S, V wet 8/8 rain before run
MEAN VALUES		n		U{1}		V_m†	r_{a+b} ‡		T{1}	T{z_o'}						χ{1}	Flux χ	V_d{1}	r_t{1}	r_c ¶	χ{z_o'}	
		6		6.08		17.9	56.0		2.6	0.6						1.29	14.5	12.3	81.4 ¥	25.4	0.19	
		4		6.23		19.5	51.3		2.9	0.9						1.60	19.2	14.4	69.2 ¥	17.9		exluding 3, 4 (frozen)
		6																11.2 §	89.1 §	33.1		
		4																12.0 §	83.6 §	32.3		exluding 3, 4 (frozen)

Notes: † arithmetic mean; ‡ reciprocal of mean V_m; ¥ reciprocal of mean V_d; ¶ from mean r_t and mean r_{a+b}. § Alternative mean from mean χ{1} & mean flux χ.

Bush (Intensive agricultural grassland) 6/1988 — Night-time: 2055–0330 GMT

Run	Date and time (GMT)		L (m)	SF{1} n/a	U{1} (m s^{-1})	U* (m s^{-1})	z_o (mm)	r_a{1} (s m^{-1})	r_b (s m^{-1})	T{z_o'} (°C)	r_{sE} * (s m^{-1})	χ{1} (μg m^{-3})	Flux χ (ng m^{-2} s^{-1})	V_d{1} (mm s^{-1})	r_c (s m^{-1})	χ{z_o'} (μg m^{-3})	χ{z_o"}	Conditions and notes
	14–17/6/1988																	
1	14/6	1430–1645	-19.5	1.57	2.49	0.33	40	21.1	13.4	21.1	224	0.96 ± 0.08	-12.6 ± 23.0	—	—	1.39 ± 0.76	4.2	V,G dry, N 0/8, hazy
2		1700–1820	-29.8	1.38	2.07	0.27	41	26.4	16.3	16.0	204	0.56 ± 0.07	-19.4 ± 16.7	—	—	1.39 ± 0.68	5.3	ditto
3		1850–1940	-43.6	1.26	1.84	0.25	45	28.7	18.0	12.7	207	0.12 ± 0.10	-8.2 ± 19.0	—	—	0.50 ± 0.81	2.2	V, G dry, NNE 0–8/8
4		2010–2130	-34.6	1.33	1.39	0.20	49	35.0	22.9	10.4	(350)	0.15 ± 0.16	-17.1 ± 25.1	—	—	1.14 ± 1.32	(7.1)	V ,G dry, N 8/8
5		2150–2245	ND	1.0	1.25	0.16	41	48.6	28.1	10.0	(1000)	≈0.44	≈1.2	≈2.6	≈308	≈0.35	(-0.9)	* 2 pt NH_3, V wet, N 8/8, haar
6	15/6	0920–1100	ND	1.0	1.15	0.14	33	60.1	32.6	10.9	(250)	0.15 ± 0.08	(1.3 ±0.3)	12.8	-14.9	-0.02 ± 0.03	(-0.3)	*3 pt NH_3 unsure, V wet, N 8/8
7		1155–1305	ND	1.0	1.34	0.16	32	52.7	28.1	13.2	(250)	0.15 ± 0.28	-1.1 ± 25.2	—	—	0.25 ± 1.91	(0.5)	* 3 pt NH_3, V drying, N 88
8		1420–1620	-15.7	1.70	1.93	0.27	43	25.3	16.8	17.7	(250)	0.14 ± 0.14	-5.3 ± 38.0	—	—	0.36 ± 1.53	(1.7)	V dry, N 6/8, bright
9		1650–1910	-10.9	1.97	1.34	0.20	47	31.8	22.9	16.6	288	0.08 ± 0.05	-7.8 ± 12.5	—	—	0.51 ± 0.64	2.8	V dry, N 4/8, hazy
10		1925–2105	≈1.4	≈0.04	0.59	≈0.02	0	1467	224	(9.8)	299	—	—	—	—	—	—	L & NH_3 unsure, sunset, dew
11	15–16	2205–0225	ND	1.0	0.35	≈0.04	31	208	110	(11.5)	—	0.16, 0.16	—	—	—	—	—	2 @ χ{1.4 m}, V wet, calm
12	16/6	0315–0620	ND	1.0	0.96	0.12	37	67.9	37.9	10.8	(700)	0.10 ± 0.13	0.6 ± 11.6	6.7	44.5	0.03 ± 1.17	(-0.4)	V wet, NNE 8/8, haar
13		0710–0910	NM	1.0	1.28	0.15	32	55.1	29.5	—	(250)	0.04 ± 0.05	-0.4 ± 6.3	—	—	0.07 ± 0.51	(0.2)	V wet, N 8/8
14		0945–1140	NM	1.0	1.19	0.14	28	63.4	32.9	—	(250)	≈0.00	≈-2.1	—	—	≈0.21	(0.7)	*2 pt NH_3 , V drying, N 8/8
15		1200–1400	-5.1	2.89	0.79	0.13	56	37.4	33.7	17.9	(250)	0.26 ± 0.15	-22.1 ± 29.1	—	—	1.82 ± 1.99	(7.3)	V dry, NNE 8/8 bright, hazy
16		1430–1630	-15.2	1.71	1.74	0.25	50	25.0	17.7	18.7	(300)	0.16 ± 0.78	-19.0 ± 159	—	—	0.64 ± 6.47	(6.3)	*3 pt NH_3, V dry, N 8/8, bright
17		1700–1905	-305	1.04	1.77	0.24	48	31.4	18.9	14.7	322	0.17 ± 0.24	-10.8 ± 43.3	—	—	0.72 ± 2.10	4.2	V dry, NNE 8/8
18		1945–2150	ND	1.0	1.26	0.18	56	39.6	25.3	12.9	(950)	0.08 ± 0.04	-4.2 ± 5.8	—	—	0.35 ± 0.36	(4.3)	V dry, NNE 8/8, dusk
19	16–17	2220–0125	ND	1.0	1.26	0.18	56	39.6	25.3	11.2	(1700)	0.13 ± 0.07	-4.0 ± 10.2	—	—	0.38 ± 0.64	(7.1)	V dry, NNE 8/8
MEAN VALUES			n		U{1}			V_m †	r_{a+b} ‡	T{z_o'}		χ{1}	Flux χ			χ{z_o'}	χ{z_o"}	
			17		1.47			17.0	58.8	14.3		0.211	-7.71			0.59	3.1	Excluding runs 10 & 11

Notes. * r_{sE} by Parkinson leaf chamber measurements, see overleaf; † arithmetic mean; ‡ reciprocal of mean V_m.

Bush 6/1988 Measurements of stomatal conductance to water vapour (r_{sE}).

Data collected by Parkinson leaf chamber. Leaf area index (LAI) = 6 (2 samples: 6.6, 5.6).
Canopy r_{sE} = leaf area r_{sE}/LAI. Most runs n = 10. Means are calculated from reciprocal values ($1/r_{sE}$).
Confidence limits are calculated from the fractional errors and are therefore only approximate.
Given the similar molecular diffusion rates of NH_3 and H_2O, $r_{sNH_3} \approx r_{sE}$.

Run	Date and time (GMT)		Canopy r_{sE} ± 95% Confidence limits ($s\ m^{-1}$)
1	14/6	1620–1640	224 ± 71
2a		1710–1740	228 ± 50
2b		1800–1815	180 ± 62
3		1855–1915	207 ± 14
4		2120–2140	591 ± 181
9	15/6	1705–1730	288 ± 63
10		1930–1950	299 ± 86
17a	16/6	1705–1730	326 ± 88
17b		1830–1850	318 ± 86
18a		1955–2010	676 ± 154
18b		2110–2130	1628 ± 597
19		2230–2255	1697 ± 672

Stenton 6/1989 (barley) Night-time: 2005–0415 GMT

Run	Date and time (GMT)	L (m)	SF{1} n/a	U{1} ($m s^{-1}$)	u_* ($m s^{-1}$)	z_o (mm)	r_a{1} ($s m^{-1}$)	r_b ($s m^{-1}$)	T{1} (°C)	$T\{z_o'\}$ (°C)	H ($W m^{-2}$)	λE ($W m^{-2}$)	$E_s T\{z_o'\}$ ($g m^{-3}$)	$E\{z_o'\}$ ($g m^{-3}$)	r_{sEb} ($s m^{-1}$)	χ{1} ($\mu g m^{-3}$)	Flux χ ($ng m^{-2} s^{-1}$)	V_d{1} ($mm s^{-1}$)	r_c ($s m^{-1}$)	$\chi\{z_o'\}$ ($\mu g m^{-3}$)	$\chi\{z_o''\}$ ($\mu g m^{-3}$)	Conditions and notes
	8–9/6/1989																					
	System 1 *																					
1	1305–1545	-13.4	1.80	2.53	0.40	59.9	14.5	15.8	12.0	21.3	-381	-96.1	18.58	8.36	260	0.47 ± 0.02	-23.9 ± 6.9	—	—	1.19 ± 0.20	(7.4)	V, G dry, NE, 4/8
2	1645–1920	-191	1.06	2.36	0.33	54.5	20.9	17.7	11.5	12.1	-17.0	-53.9	10.67	7.55	143	0.81 ± 0.04	-2.7 ± 8.0	—	—	0.91 ± 0.29	1.30	*3 pt NH_3, ", E
3	1955–2205	19.0	0.62	1.12	0.13	37.6	67.2	33.5	9.8	8.9	11.9	-22.7	8.71	7.94	85.0	1.13 ± 0.07	-2.0 ± 3.9	—	—	1.33 ± 0.37	1.50	V, G dry, SE
4	2330–0210	27.6	0.71	1.08	0.16	74.8	42.7	33.7	8.1	7.2	14.3	-9.6	7.81	7.44	96.8	1.01 ± 0.06	-2.7 ± 4.5	—	—	1.21 ± 0.32	1.47	dew at end, SW, 6/8
5	0245–0450	20.1	0.63	1.20	0.18	83.7	37.0	31.4	5.4	3.8	29.5	-12.5	6.25	6.36	-22.7	0.89 ± 0.01	4.7 ± 0.5	5.3	121 [103, 144]	0.57 ± 0.03	(0.57)	dew, SW, 1/8
6	0545–0815	-11.4	1.93	1.01	0.16	59.8	35.1	31.5	11.2	12.7	-28.0	-77.2	11.12	8.69	78.0	1.09 ± 0.03	-3.3 ± 3.2	—	—	1.31 ± 0.20	1.57	V, G dry, W–SW, 4/8
7	0850–1140	-51.9	1.22	2.12	0.32	62.5	20.0	18.9	14.4	16.0	-54.1	-130	13.62	9.08	85.8	1.30 ± 0.07	-10.0 ± 13.3	—	—	1.69 ± 0.49	2.55	V, G dry, SW, 2/8
8	1230–1500	-20.9	1.53	1.52	0.24	61.6	25.5	23.7	15.2	17.2	-51.0	-124	14.58	10.50	80.6	1.26 ± 0.19	-8.2 ± 29.5	—	—	1.66 ± 1.39	2.32	3 pt NH_3, ", 7/8
9	1600–1710	-330	1.04	2.32	0.34	61.8	19.6	17.9	14.5	14.9	-10.8	-20.7	12.67	9.61	90.6	0.94 ± 0.50	-8.4 ± 89.4	—	—	1.26 ± 3.24	2.02	3 pt NH_3, ", SE, 8/8
MEAN VALUES		n		U{1}		V_m †		r_{a+b} ‡	T{1}	$T\{z_o'\}$						χ{1}	Flux χ			$\chi\{z_o'\}$	$\chi\{z_o''\}$	
		9		1.70		20.5		48.8	11.3	12.7						0.989	-6.28			1.24	2.3	
	System 2 *																					
1	1305–1545	-26.2	1.43	2.52	0.37	55.0	17.3	16.4	14.3	19.1	-178	-177	16.32	9.08	100	0.47 ± 0.02	-19.4 ± 6.2	—	—	1.12 ± 0.20	3.06	As above
2	1645–1920	-153	1.08	2.36	0.34	55.0	20.7	17.7	12.9	13.6	-22.0	-62.9	11.71	7.74	156	0.81 ± 0.04	-2.7 ± 8.0	—	—	0.91 ± 0.29	1.33	
3	1955–2205	29.3	0.72	1.13	0.14	45.5	56.5	32.7	10.9	10.3	9.0	-17.0	9.53	7.65	274	1.12 ± 0.07	-2.4 ± 4.6	—	—	1.34 ± 0.38	2.00	
4	2330–0210	16.0	0.57	1.07	0.14	61.7	54.0	35.3	9.0	7.8	16.6	-7.6	8.13	7.44	223	1.01 ± 0.06	-2.1 ± 3.7	—	—	1.20 ± 0.31	1.67	
5	0245–0450	15.5	0.56	1.20	0.17	76.2	42.0	32.3	6.7	5.0	29.4	-13.0	6.75	6.48	53.0	0.89 ± 0.01	4.2 ± 0.4	4.7	140 [119, 160]	0.58 ± 0.03	(0.31)	
6	0545–0815	-10.5	2.00	1.01	0.16	60.6	34.1	31.3	12.7	14.5	-35.4	-78.9	12.42	8.88	111	1.09 ± 0.03	-3.4 ± 3.3	—	—	1.32 ± 0.20	1.70	
7	0850–1140	-31.3	1.36	2.13	0.33	65.7	18.3	18.6	15.6	18.7	-104	-190	15.96	10.1	75.7	1.30 ± 0.07	-10.9 ± 14.9	—	—	1.70 ± 0.53	2.53	

* Temperature and humidity profiles were recorded with two systems. **System 1**: aspirated psychrometers (2 heights – other psychrometers not in working order). **System 2**: fine thermocouples and a dewpoint hygrometer system from Campbell Scientific Ltd. (2 heights). System 2 not available for runs 8–9. Notes: † arithmetic mean; ‡ reciprocal of mean V_m;

Appendix 4

Tables and graphs of particulate and acid gas surface exchange results

Aerosol data

Site and NH_3 sampl0ing run numbers		L (m)	SF{1} n/a	U{1} ($m\ s^{-1}$)	U* ($m\ s^{-1}$)	z_o (mm)	r_a{1} ($s\ m^{-1}$)	T{z_o'} (°C)	χ{1} ($\mu g\ m^{-3}$)	Flux χ ($ng\ m^{-2}\ s^{-1}$)	V_d{1} ($mm\ s^{-1}$)	r_t{1} ($s\ m^{-1}$)	Conditions and notes
Fala 11/88	(1–6) NH_4^+	ND	1.0	1.44	0.17	33.2	47.9	3.5	5.75 ± 0.08	3.8 ± 7.6	0.7	1500	
	(1–6) Cl^-		"	"	"	"	"	"	2.60 ± 0.16	-5.9 ± 15.4	-2.3	-437	
	(1–6) NO_3^-	"	"	"	"	"	"	"	1.86 ± 0.10	0.0 ± 9.6	0.0	41400	
	(1–6) SO_4^{2-}	"	"	"	"	"	"	"	3.82 ± 0.22	7.5 ± 21.6	2.0	511	
	(7–8) NH_4^+	ND	1.0	2.12	0.24	25.4	37.8	5.3	9.47 ± 0.22	-2.1 ± 29.7	-0.2	-4480	
	(7–8) Cl^-		"	"	"	"	"	"	3.83 ± 0.49	54.6 ± 64.5	14.2	70.3	
	(7–8) NO_3^-	"	"	"	"	"	"	"	3.63 ± 0.23	1.6 ± 31.0	0.4	2280	
	(7–8) SO_4^{2-}	"	"	"	"	"	"	"	4.44 ± 0.40	2.2 ± 52.6	0.5	2120	
Fala 5/88	(1–8) NH_4^+	-110	1.11	5.25	0.63	32.0	13.0	14.4	0.49 ± 0.02	-2.4 ± 7.9	-4.9	-207	
Wether Law	(1) NH_4^+	1870	0.99	4.65	0.56	33.3	14.8	2.5	0.33 ± 0.01	2.5 ± 2.7	7.6	132	
	(2–6) NH_4^+	632.5	0.98	6.96	0.77	25.4	11.6	-2.1	0.34 ± 0.01	-0.7 ± 2.0	-1.9	-520	
	(7–8) NH_4^+	-712	1.02	7.79	0.86	24.5	10.5	1.8	0.35 ± 0.02	-0.6 ± 5.2	-1.7	-574	

Site and NH_3 sampling run numbers		L (m)	SF{1} n/a	U{1} ($m\ s^{-1}$)	U* ($m\ s^{-1}$)	z_o (mm)	r_a{1} ($s\ m^{-1}$)	T{z_o'} (°C)	χ{1} ($\mu g\ m^{-3}$)	Flux χ ($ng\ m^{-2}\ s^{-1}$)	V_d{1} ($mm\ s^{-1}$)	r_t ($s\ m^{-1}$)	Conditions and notes
Bush 6/88	(1–5) NH_4^+	-26	1.43	1.93	0.26	42.5	27.1	15.5	2.44 ± 0.26	13.3 ± 58.6	5.5	183	
Bush 6/88	(6–10) NH_4^+	-15	1.72	1.31	0.16	30.9	45.9	13.1	3.47 ± 0.07	12.7 ± 11.2	3.7	272	
Bush 6/88	(11–19) NH_4^+	—	—	—	—	—	—	—	—	—	—	—	filters wetted at end
Bush 2/89	(1–6) NH_4^+	82.3	0.88	6.09	0.35	0.86	49.6	0.7	0.55 ± 0.02	-0.5 ± 1.9	-0.9	-1120	
Stenton 6/89	(1–8) NH_4^+	ND	1.0	1.67	0.25	61.5	27.6	13.0	0.77 ± 0.01	-1.6 ± 2.0	-2.1	-474	heights altered at end

Aerosol data

Site and sampling run numbers		L (m)	SF{1} n/a	U{1} ($m\,s^{-1}$)	U^*	z_o (mm)	r_a{1} ($s\,m^{-1}$)	T{z_o'} (°C)	χ{1} ($\mu g\,m^{-3}$)	Flux χ ($ng\,m^{-2}\,s^{-1}$)	V_d{1} ($mm\,s^{-1}$)	r_t ($s\,m^{-1}$)	Conditions and notes
GDF 5/87	(2–3) NH_4^+	NM	1.0	4.10	0.40	14.3	26.2	≈15	1.51 ± 0.11	-3.0 ± 9.5	-2.0	-503	
	(2–3) NO_3^-	"	"	"	"	"	"	"	1.07 ± 0.41	-5.8 ± 33.5	-5.4	-184	
GDF 3/88	(1–2) NH_4^+	ND	1.0	4.07	0.35	8.78	32.8	1.4	0.57 ± 0.03	5.5 ± 3.0	9.8	103	
	(1–2) Cl^-	"	"	"	"	"	"	"	0.63 ± 0.68	13.4 ± 118	21.4	46.7	
	(1–2) NO_3^-	"	"	"	"	"	"	"	0.61 ± 0.12	9.9 ± 12.6	16.2	61.6	
	(1–2)SO_4^{2-}	"	"	"	"	"	"	"	2.94 ± 0.57	41.7 ± 61.3	14.2	70.4	
GDF 3/88	(3–6) NH_4^+	-120	1.10	4.29	0.37	8.50	30.9	2.9	0.46 ± 0.06	3.6 ± 7.0	7.9	127	
	(3–6) Cl^-	"	"	"	"	"	"	"	1.52 ± 0.18	32.4 ± 21.3	21.3	46.9	
	(3–6) NO_3^-	"	"	"	"	"	"	"	0.67 ± 0.07	3.7 ± 8.0	5.5	181	
	(3–6) SO_4^{2-}	"	"	"	"	"	"	"	1.38 ± 0.12	-10.1 ± 13.5	-7.3	-137	
GDF 4/88	(1) NH_4^+	-24.3	1.46	3.88	0.40	16.6	23.2	15.0	0.74 ± 0.02	2.7 ± 3.9	3.9	274	
	(1) NO_3^-	"	"	"	"	"	"	"	0.74 ± 0.30	4.4 ± 43.4	5.9	168	
	(2) NH_4^+	-11.3	1.94	2.95	0.27	9.1	37.6	15.1	1.22 ± 0.10	17.6 ± 12.8	14.5	69.0	
	(2) NO_3^-	"	"	"	"	"	"	"	1.40 ± 0.74	22.1 ± 89.1	15.8	63.3	
GDF 4/89	(1–2) NH_4^+	-15.3	1.71	2.58	0.17	1.61	86.8	2.1	1.16 ± 0.14	-1.0 ± 7.5	-0.9	-1175	
	(1–2) Cl^-	"	"	"	"	"	"	"	0.25 ± 0.12	2.4 ± 6.5	9.7	103	
	(1–2) NO_3^-	"	"	"	"	"	"	"	1.20 ± 0.19	-11.8 ± 10.4	-9.8	-102	
	(1–2) SO_4^{2-}	"	"	"	"	"	"	"	2.20 ± 0.22	-9.0 ± 11.9	-4.1	-244	

Aerosol data

Site and sampling run numbers		L (m)	SF{1} n/a	U{1} ($m\ s^{-1}$)	u^* ($m\ s^{-1}$)	z_o (mm)	r_a{1} ($s\ m^{-1}$)	T{z_o} (°C)	χ{1} ($\mu g\ m^{-3}$)	Flux χ ($ng\ m^{-2}\ s^{-1}$)	V_d{1} ($mm\ s^{-1}$)	r_t{1} ($s\ m^{-1}$)	Conditions and notes
Huntingdon	(1–8) NH_4^+	—	—	—	—	—	—	—	3.58	—	—	—	filter pack order varied
Huntingdon	(9–10)NH_4^+	-171	1.07	3.47	0.32	11.9	33.7	19.7	1.33 ± 0.05	-1.0 ± 5.4	-0.8	-1330	
	(9–10)NO_3^-	"	"	"	"	"	"	"	1.33 ± 0.10	12.8 ± 12.1	9.6	104	
	(9–10)SO_4^{2-}	"	"	"	"	"	"	"	3.34 ± 0.52	-18.9 ± 59.8	-5.7	-177	
Harwell 3/88	(1–4) NH_4^+	ND	1.0	1.88	0.14	4.02	96.1	5.5	3.08 ± 0.11	-3.0 ± 4.2	-1.0	-1030	
	(1–4) Cl^-	"	"	"	"	"	"	"	1.49 ± 0.18	-6.2 ± 6.7	-4.2	-240	
	(1–4) NO_3^-	"	"	"	"	"	"	"	4.45 ± 0.29	2 .8 ± 10.6	0.6	1613	
	(1–4) SO_4^{2-}	"	"	"	"	"	"	"	7.41 ± 0.89	5.3 ± 32.6	0.7	1389	
Harwell 3/88	(5–8) NH_4^+	ND	1.0	2.87	0.21	3.45	66.6	4.5	3.28 ± 0.12	-5.0 ± 6.4	-1.5	-657	
	(5–8) Cl^-	"	"	"	"	"	"	"	1.43 ± 0.22	5.0 ± 11.8	3.5	283	
	(5–8) NO_3^-	"	"	"	"	"	"	"	7.68 ± 1.54	17.3 ± 84.3	2.2	444	
	(5–8) SO_4^{2-}	"	"	"	"	"	"	"	5.80 ± 0.75	-5.3 ± 40.9	-0.9	-1091	
AEROSOL MEAN VALUES				n			r_a{1} †		X{1}	Flux χ	V_d{1}	r_t{1}	r_a/r_t ‡
	NH_4^+			19			26.2		1.96	2.15	1.88	532 ¥	0.05
	Cl^-			7			47.6		1.68	13.7	9.09	110 ¥	0.43
	NO_3^-			11			38.6		2.24	5.18	3.73	268 ¥	0.14
	SO_4^{2-}			8			45.2		3.92	1.68	-0.08	-12500 ¥	-0.00
	NH_4^+										1.1 §	915 §	0.03
	Cl^-										8.1 §	123 §	0.39
	NO_3^-										2.3 §	432 §	0.09
	SO_4^{2-}										0.4 §	2340 §	0.02

Notes: † reciprocal arithmetic mean; ¥ reciprocal of mean V_d; ‡ from mean r_a and mean r_t; § Alternative mean from the arithmetic means of χ{1} & flux χ.

Distributions of $V_d\{1\ m\}$ estimates for aerosol data (see section 4.4)

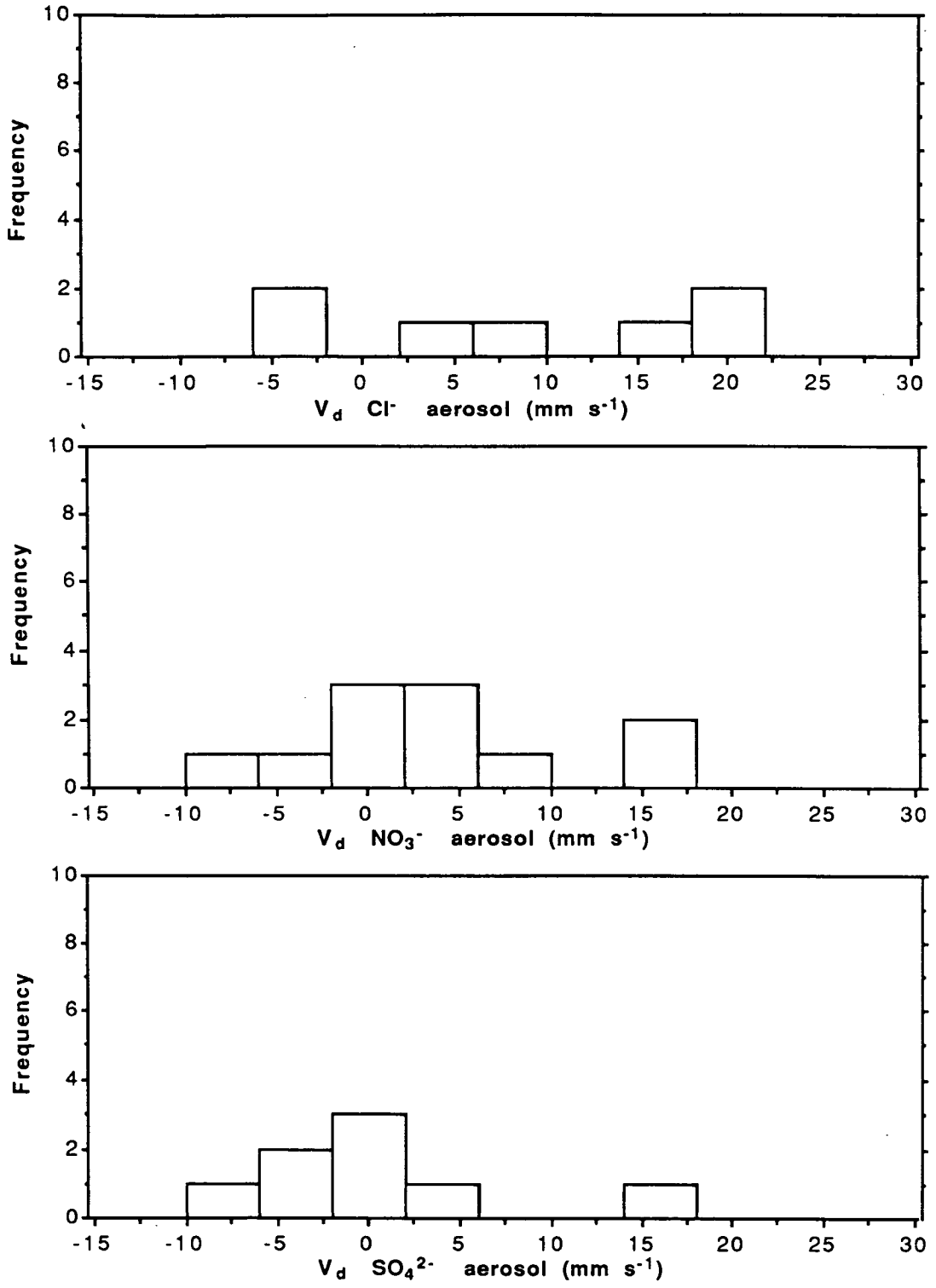

Harwell (Calcareous grassland) 3/1988: Acid gases (HNO_3, HCl)

Run	Date & time: see NH_3 runs (App. 2)	L (m)	SF{1} n/a	U{1} ($m\ s^{-1}$)	U*	z_o (mm)	r_a{1}	r_b ($s\ m^{-1}$)	T{z_o'} (°C)	χ{1} ($\mu g\ m^{-3}$)	Flux χ ($ng\ m^{-2}\ s^{-1}$)	V_d{1} ($mm\ s^{-1}$)	r_c ($s\ m^{-1}$)	χ{z_o'} ($\mu g\ m^{-3}$)	Conditions and notes
1–3	HCl	-177	1.07	4.53	0.34	3.87	40.0	11.7	9.6	2.65 ± 1.28	48.3 ± 115.4	18.2	3.2 [-35.7, em]	0.26 ± 4.82	
1–3	HNO_3	"	"	"	"	"	"	14.5	"	0.97 ± 0.85	38.7 ± 76.8	39.7	-29.4 [-46.1, em]	-0.94 ± 3.21	
4	HCl	-52.0	1.22	1.07	0.08	4.37	164	35.3	4.8	3.04 ± 0.55	8.8 ± 11.9	2.9	150 [-49.4, em]	1.35 ± 1.89	
4	HNO_3	"	"	"	"	"	"	43.9	"	1.82 ± 1.72	6.1 ± 36.6	3.4	90.4 [-184, em]	0.64 ± 5.88	
5–7	HCl	-12.0	1.89	2.39	0.18	3.54	69.6	18.1	10.0	6.66 ± 1.69	84.4 ± 99.0	12.7	-8.8 [-51.5, em]	-0.44 ± 7.13	
5–7	HNO_3	"	"	"	"	"	"	22.5	"	5.42 ± 2.18	138 ± 128	25.4	-52.8 [-71.7, 450]	-6.18 ± 9.21	
8	HCl	269	0.96	3.04	0.22	3.94	60.0	15.9	3.5	1.41 ± 0.27	-2.6 ± 15.8	-1.8	em [-0.1, em]	1.60 ± 0.97	
8	HNO_3	"	"	"	"	"	"	19.7	"	1.49 ± 0.66	2.3 ± 39.0	1.6	568 [-43.6, em]	1.32 ± 2.39	

MEAN VALUES		n		V_m †	r_{a+b} ‡	T{z_o'}	χ{1}	Flux χ	V_d{1}	r_t{1}	r_c ¶	χ{z_o'}	
HNO_3 & HCl bulked		8		11.9	83.8	7.0	2.93	40.5	12.8	78.4 ¥	-5.4	-0.3	
									13.8 §	72.5 §	-11.0		

Notes: † arithmetic mean; ‡ reciprocal of mean V_m; ¥ reciprocal of mean V_d; ¶ from mean r_t & mean r_{a+b}. § Alternative mean from mean χ{1} & mean flux χ.

Appendix 5

Estimation of random errors in flux gradient analysis

It is of interest to know the precision of the individual runs, and to be able to give standard errors and confidence limits to the parameters of interest such as F_χ, V_d, r_c, $\chi\{z_o'\}$. Multiple sources of error exist for these values, arising from the different regression coefficients used in their calculation — the regressions being calculated here as set out by Sokal and Rohlf (1969). To estimate the errors in the surface exchange parameters, the component errors must be combined or a dominating error source used where this occurs. An approximate method of combining errors is to calculate the square root of the sum of the squares of the individual errors (Haynes, 1982). For combinations involving addition or subtraction actual errors are used, while for multiplication and division fractional errors (error of value/value) are used.

In the case of division, however, the use of fractional errors is approximate as the mean error limits are estimated. Thus given y ± n, the error in the reciprocal would be given as 1/y ± (n/y)1/y. In fact, the upper and lower limits will differ in this case, with the error more precisely being given by calculating the reciprocals of the individual error limits of y.

In this section, therefore, the 'root sum of squares' method is used to estimate combined errors and to identify dominant errors so as to derive simplified relations. However, where these final expressions contain reciprocal errors, individual limits are calculated.

Errors in the flux

Using the 'root mean sum of squares' method, the fractional error in the flux in neutral conditions may be found. Given the flux as:

$$F_\chi = k^2 \Gamma_u \Gamma_\chi \qquad \text{A5.1}$$

where $\Gamma_u = \dfrac{\partial u}{\partial \ln(z-d)}$ $\Gamma_\chi = \dfrac{\partial \chi}{\partial \ln(z-d)}$

then $$\frac{E_{F\chi}}{F_\chi} = \sqrt{\left[\frac{E_{\Gamma u}}{\Gamma_u}\right]^2 + \left[\frac{E_{\Gamma \chi}}{\Gamma_\chi}\right]^2} \qquad \text{A5.2}$$

Here E denotes an error estimate, while the constant, k, is omitted since it is not a source of random error.

In conditions where a stability correction applies, random error associated with the wind and temperature profiles also contributes to the combined error of results, through the estimation of the stability functions. It is difficult to calculate this error using the integrated profile technique, since it is introduced into the regressions of the other quantities. However, a good approximation may be achieved by estimating the error in the stability correction of equation 2.23, $(\Phi_M.\Phi_H)^{-1}$, denoted f, and including this in the estimate of the error of the flux. To do this the error in Ri is first estimated, and using the empirical stability relationships, this is used to give the error in f. Given the formula for Ri (equation 2.29) the appropriate fractional error is:

$$\frac{E_{Ri}}{Ri} = \sqrt{\left[\frac{E_{\Gamma T}}{\Gamma_T}\right]^2 + 2\left[\frac{E_{\Gamma u}}{\Gamma_u}\right]^2 + \left[\frac{E_{T\{1\,m\}}}{T\{1\,m\}}\right]^2} \qquad \text{A5.3}$$

From this the error in f is found from the relationships of equations 2.24, 2.25:

$$Ri < 0 \qquad \frac{E_f}{f} = \sqrt{0.75\left[\frac{\sqrt{16(E_{Ri})^2}}{1 - 16Ri}\right]^2} \qquad \text{A5.4}$$

$$Ri > 0 \qquad \frac{E_f}{f} = \sqrt{2\left[\frac{\sqrt{5.2(E_{Ri})^2}}{1 - 5.2Ri}\right]^2} \qquad \text{A5.5}$$

Applying this to an example run, which was of moderate instability (Bush, 1800 GMT, 14/6/1988), gives Ri = 0.034 ± 0.014 and f = 1.380 ± 0.043, where the errors are 95% confidence limits. The latter terms may be included in a modified form of equation A5.2, alongside the wind and ammonia profile errors for this run, to give a combined error for the flux:

$$\frac{E_{F\chi}}{F_\chi} = \sqrt{(1.62 \times 10^{-3}) + 0.738 + (9.71 \times 10^{-4})} = 0.860$$

(wind) (ammonia) (stability)

Hence

$$F_\chi = -19.4 \pm 16.6 \text{ ng m}^{-2} \text{ s}^{-1} \text{ (95\% confidence limits)}$$

This could equally have been considered using standard errors, which would have given F_χ = -19.4 ± 5.2 (SE). It is clear that the error in the ammonia concentration gradient dominates the combined error in this example. This is a general feature of the data here, which reflects a general ability to measure windspeed and temperature with much greater precision than ammonia. This may be used to simplify the error analysis here since the error associated with the stability factor, f, may be acceptably omitted.

Errors in deposition resistances

Similar calculations may be used to estimate the errors in V_d and the component resistances of deposition. The error in r_c includes components from the other resistances. From equation 2.46:

$$E_{r_c} = \sqrt{E_{r_t}^2 + E_{r_a}^2 + E_{r_b}^2} \qquad \text{A5.6}$$

The mean fractional error of r_t, which is the same as that for V_d, is given as:

$$\frac{E_{r_t\{1\,m\}}}{r_t\{1\,m\}} = \frac{E_{V_d\{1\,m\}}}{V_d\{1\,m\}} = \sqrt{\left[\frac{E_{F_\chi}}{F_\chi}\right]^2 + \left[\frac{E_{\chi\{1\,m\}}}{\chi\{1\,m\}}\right]^2} \qquad \text{A5.7}$$

To calculate the error in r_a, the neutral case may again be acceptably used (equation 2.47):

$$\frac{E_{r_a\{1\,m\}}}{r_a\{1\,m\}} = \sqrt{\left[\frac{E_{u\{1\,m\}}}{u\{1\,m\}}\right]^2 + 2\left[\frac{E_{\Gamma_u}}{\Gamma_u}\right]^2} \qquad \text{A5.8}$$

The error in r_b is more complicated. From equations 2.51 and 2.52:

$$\frac{E_{r_b}}{r_b} = \sqrt{0.24\left[\left(\frac{E_{z_o}}{z_o}\right)^2 + \left(\frac{E_{\Gamma_u}}{\Gamma_u}\right)^2\right] + \left[\frac{E_{\Gamma_u}}{\Gamma_u}\right]^2} \qquad \text{A5.9}$$

To solve this the error in z_o is needed. This may be approximated by taking the anti-logarithm of the error limits in $\ln(1/z_o)$, given as:

$$\frac{E_{\ln(1/z_o)}}{\ln(1/z_o)} = \sqrt{\left[\frac{E_{u\{1\,m\}}}{u\{1\,m\}}\right]^2 + \left[\frac{E_{\Gamma_u}}{\Gamma_u}\right]^2} \qquad \text{A5.10}$$

A second example may serve to illustrate the application of these formulae. For measurements at Harwell, 1100 GMT, 16/3/1988, giving 95% confidence limits, with all values in units of s m^{-1}: $r_t = 134.8 \pm 97.0$; $r_a = 38.6 \pm 7.5$; $r_b = 8.7 \pm 3.8$. From these, using equation A5.6, $r_c = 87.4 \pm 97.3$. Again standard errors could equally be used, which would give $r_c = 87.4 \pm 26.7$. In this analysis r_t is the only component term to include ammonia concentration estimates, and correspondingly, this dominates the sources of error. A good approximation, therefore, that may be seen to hold throughout the data collected is:

$$E_{r_c} \approx E_{r_t} \qquad \text{A5.11}$$

These estimates are only approximate however, because r_t has the main source of error (the flux) as a reciprocal, so that the upper and lower errors for r_t and r_c differ. The individual limits may be found by taking the reciprocal of the limits of V_d. Using 95% confidence limits, this gives $r_t = 134.8$ [78.4, 480.8] s m^{-1}. These limits are then

inserted into equation 2.46 which gives r_c = 87.4 [31.4, 433.0] s m^{-1}. Since the limits of r_c do not contain zero, it is clear that in this case r_c is significantly different to zero (P = 0.05). In Appendices 2–4 it is this method which is used to describe the errors of r_c.

Error in surface concentration estimates

The error associated with the surface concentration estimate, $\chi\{z_0'\}$ may be estimated by the 'root sum of squares' method according to equation 2.56, taking into account all sources of error. However, as it has been established above that the errors arising from the concentration profile dominate, the analysis may be simplified by ignoring the errors arising from the wind profile. In this case it is more accurate to be able to estimate the error directly from the regression, estimating the error in χ at the height z_0' above d. A method for estimating the error in any predicted value at a given value of the X-axis, in the regression here ($\ln(z-d) - \psi_H$), is provided by Sokal and Rohlf (1969). Applying this to the example run at Harwell, using a stability corrected value of z_0' (since the integrated stability correction is used) gives $\chi\{z_0'\} = 1.92 \pm 0.62$ (95% confidence limits).

Appendix 6

Ammonia monitoring results using diffusion tubes

Bush data

Run No.	Date of end of run	mean χ(1.5 m) ($\mu g\ m^{-3}$)	± SE	± 95% confidence limits	No. of tubes averaged	Notes
1	8/2/88	0.23	0.162	0.70	3	as, set out 19/1/88
2	2/3/88	1.76	0.425	1.83	3	as
3	22/3/88	1.30	0.157	2.00	2	1 cont.
4	11/4/88	2.10	0.405	1.75	3	as
5	3/5/88	0.60	0.044	0.12	3	1 cont.
6	27/5/88	0.55	0.083	0.21	5	
7	14/6/88	1.51	0.183	0.51	5	
8	6/7/88	3.13	0.169	0.44	5	
9	29/7/88	0.77	0.116	0.27	5	
10	16/8/88	1.19	0.230	0.96	3	1 cont.
11	8/9/88	1.01	0.144	0.40	3	1 cont.
12	28/9/88	0.80	0.101	0.28	4	1 cont.
13	18/10/88	0.81	0.052	0.12	4	1 cont.
14	11/11/88	0.89	0.080	0.21	5	
15	3/12/88	0.90	0.087	0.20	5	
16	20/12/88	0.05	0.088	0.22	5	
17	17/1/89	0.76	0.079	0.18	4	1 cont.
18	7/2/89	1.11	0.087	0.21	5	
19	3/3/89	0.69	0.099	0.27	5	
20	24/3/89	—	—	—	—	lost batch
21	6/5/89	1.51	0.095	0.27	5	
22	19/6/89	2.57	0.411	1.30	4	1 cont.

Dunslair Heights data: top site (600 m)

Run No.	Date of end of run	mean χ(1.5 m) ($\mu g\ m^{-3}$)	± SE	± 95% confidence limits	No. of tubes averaged	Notes
2	2/3/88	0.64	0.093	0.41	3	as, set out 8/2/88
3	22/3/88	0.62	0.175	2.22	2	1 cont.
4	11/4/88	0.09	0.113	0.29	3	as
5	3/5/88	0.44	0.183	0.58	4	as
6	27/5/88	0.30	0.082	0.21	5	
7	15/6/88	0.55	0.239	1.03	3	1 cont.
8	5/7/88	1.76	0.135	0.31	5	
9	26/7/88	0.16	0.121	0.31	3	1 cont.
10	16/8/88	0.02	0.066	0.16	5	
11	8/9/88	0.51	0.160	0.42	4	1 cont.
12	28/9/88	0.24	0.045	0.11	4	1 cont.
13	18/10/88	-0.08	0.074	0.18	4	1 lost
14	9/11/88	0.76	—	—	1	4 cont.
15	2/12/88	0.11	0.077	0.19	5	
16	20/12/88	—	—	—	—	not opened
17	17/1/89	0.49	0.150	0.41	4	1 cont., fell to ground
18	7/2/89	0.22	0.110	0.30	4	1 cont. .
19	3/3/89	0.17	0.042	0.08	5	
20	24/3/89	—	—	—	—	lost batch
21	6/5/89	0.90	0.117	0.32	5	
22	19/6/89	1.14	0.134	0.37	5	

Dunslair Heights data: bottom site (300 m)

Run No.	Date of end of run	mean χ(1.5 m) ($\mu g\ m^{-3}$)	± SE	± 95% confidence limits	No. of tubes averaged	Notes
2	2/3/88	0.32	0.116	0.50	3	as, set out 8/2/88
3	22/3/88	0.43	0.081	0.19	2	1 cont.
4	11/4/88	0.24	0.139	0.44	3	as
5	3/5/88	0.65	0.151	0.58	3	1 lost
6	27/5/88	0.69	0.243	3.09	2	3 bad cont.
7	15/6/88	0.62	0.101	0.28	4	as
8	5/7/88	2.24	0.221	0.57	5	
9	26/7/88	0.15	0.102	0.26	3	1 cont.
10	16/8/88	—	—	—	—	post blew over
11	8/9/88	0.51	0.153	0.40	4	1 cont.
12	28/9/88	0.20	0.078	0.25	3	1 cont., 1 lost
13	18/10/88	0.37	0.119	0.31	5	
14	9/11/88	0.39	0.074	0.93	2	3 bad cont.
15	2/12/88	0.31	0.084	0.20	5	
16	20/12/88	0.07	0.068	0.17	5	
17	17/1/89	0.79	0.154	0.40	5	
18	7/2/89	0.30	0.072	0.16	4	1 lost
19	3/3/89	0.37	0.062	0.15	5	
20	24/3/89	—	—	—	—	lost batch
21	6/5/89	1.00	0.084	0.27	4	1 cont.
22	19/6/89	1.49	0.135	0.37	5	

Fala Moor data

Run No.	Date of end of run	mean χ(1.5 m) ($\mu g\ m^{-3}$)	± SE	± 95% confidence limits	No. of tubes averaged	Notes
2	7/3/88	0.35	0.152	0.37	6	as, set out 15/2/88
3	22/3/88	0.08	0.131	0.28	6	as
4	11/4/88	0.58	0.157	0.38	5	1 cont.
5	4/5/88	0.54	0.125	0.54	3	as
6	27/5/88	0.83	0.045	0.11	4	1 cont.
7	15/6/88	0.93	0.210	0.59	5	1 cont.
8	5/7/88	10.5	1.360	4.34	4	contam odd?
9	26/7/88	0.38	0.124	0.29	5	2 cont.
10	16/8/88	0.85	0.085	0.22	4	as
11	8/9/88	0.38	0.113	0.26	6	1 cont.
12	28/9/88	0.33	0.112	0.28	6	1 cont.
13	18/10/88	-0.15	0.070	0.19	4	1 cont., 2 lost
14	11/11/88	0.33	0.065	0.16	5	
15	3/12/88	0.23	0.070	0.17	5	
16	20/12/88	0.40	0.059	0.14	5	
17	17/1/89	0.50	0.143	0.37	5	
18	7/2/89	1.18	0.154	0.40	5	
19	3/3/89	0.50	0.174	0.56	4	1 lost
20	24/3/89	—	—	—	—	lost batch
21	6/5/89	0.99	0.094	0.26	5	
22	19/6/89	1.60	0.282	0.90	4	1 lost

Brothershiels Farm data

Run No.	Date of end of run	mean χ(1.5 m) ($\mu g\ m^{-3}$)	± SE	± 95% confidence limits	No. of tubes averaged	Notes
16	20/12/88	3.55	0.151	0.42	5	set out 3/12/88
17	17/1/89	3.37	0.329	0.92	5	
18	7/2/89	3.61	0.327	0.91	5	
19	3/3/89	4.17	0.331	0.92	5	
20	24/3/89	—	—	—	—	data lost
21	6/5/89	11.8	0.762	2.08	5	
22	19/6/89	10.14	0.570	1.58	5	

Laboratory data (indoor ITE, Bush) and other sites

Run No.	Date of end of run	mean χ(1.5 m) ($\mu g\ m^{-3}$)	± SE	± 95% confidence limits	No. of tubes averaged	Notes
16	20/12/88	7.42	0.510	1.60	4	as, set out 3/12/88
17	17/1/89	7.80	1.620	20.6	2	as, poss cont?
18	7/2/89	8.26	0.128	0.36	4	as
19	3/3/89	6.35	0.271	0.87	4	as
20	24/3/89	—	—	—	—	lost batch
21	6/5/89	6.70	0.508	1.62	4	as
22	19/6/89	7.97	0.570	1.88	4	as
	OTHERS:					
17	17/1/89	0.47	0.222	0.95	3	1 cont., **MCB-FM**
4	30/3–30/4/88	0.71	0.112	0.48	2	2 cont., **GDF 1988**
	EHG (roof)					
19	3/3/89	0.84	0.093	0.25	5	as, set out 7/2/89
20	24/3/89	—	—	—	—	data lost
21	12/5/89	1.52	0.264	0.73	4	1 cont.
22	19/6/89	4.51	0.602	1.67	5	
	EHR (road)					
20	24/3/89	—	—	—	—	lost batch,set out 3/3
21	12/5/89	2.73	0.274	0.87	4	1 lost
22	19/6/89	4.09	0.646	1.78	5	as(poss 1 cont.?)

Notes to diffusion tube data tables.

Means and errors of concentrations of NH_3 are given. These are estimated by comparing the values of batch blanks (≈10) with the exposed tubes at a site using an unpaired t-test. Generally 5 exposed tubes are used for each batch at a site. The number of exclusions due to loss of tubes or sample are noted with *n* lost; the number of exclusions due to contamination noted by *n* cont.; as denotes that the number used is the number set out where this does not equal 5.

Other sites: **MCB-FM**, Master Cleuch Burn, midway between Fala Moor and Brothershiels Farm; **GDF**, Silverband, on Fellside, Great Dun Fell; **EHG (roof)**, Edinburgh town centre on roof top of University Geography Department; **EHR(road)**, Edinburgh town centre by main road, South Bridge (3.5 m above pavement).

Appendix 7

Plant species referred to in the text

The nomenclature for vascular plants follows Clapham *et al.* (1987) and, for plants not native or naturalized in Britain, Tutin *et al.* (1964; denoted by *) and the Forestry and Timber Bureau (1957; denoted by †). For bryophytes nomenclature follows Smith (1978).

SCIENTIFIC NAME AND AUTHORITY	COMMON NAME
Bryophyta (mosses and liverworts)	
Drepanocladus fluitans (Hedw.) Warnst.	
Sphagnum spp.	Bog moss
Pteridophyta (ferns)	
Isoetes spp. L.	Quillwort
Gymnospermae (includes conifers)	
Abies procera Rehder (*A. nobilis* (Douglas ex D. Don) Lindley, non A. Dietr.)	Noble Fir
Larix decidua Miller	European Larch
Picea sitchensis (Bong.) Carr.	Sitka Spruce
Pinus sp. L.	Pine
Pinus contorta Douglas ex Loudon	Lodgepole Pine
Pinus sylvestris L.	Scots Pine
Angiospermae (flowering plants)	
Cyperaceae and Juncaceae (sedges and rushes)	
Eriophorum vaginatum L.	Cotton-grass, Hare's-tail
Juncus bulbosus L.	Bulbous Rush
Juncus squarrosus L.	Heath Rush
Gramineae (grasses)	
Agrostis spp. L.	Bent-grass
Brachypodium pinnatum (L.) Beauv.	Tor-grass, Heath False-brome
Briza media L.	Quaking grass, Doddering Dillies
Dactylus glomerata L.	Cock's-foot
Deschampsia flexuosa (L.) Trin.	Wavy Hair-grass
Elymus repens (L.) Gould (syn. *Agropyron repens* auct., non Gaertner)	Couch-grass
Festuca ovina L.	Sheep's-fescue
Holcus lanatus L.	Yorkshire Fog
Hordeum vulgare L.	Cultivated Barley
Lolium multiflorum Lam.	Italian Rye-grass

L. perenne L.	Rye-grass
Molinia caerulea (L.) Moench	Purple moor-grass
Nardus stricta L.	Mat-grass
Phleum pratense L.	Timothy, Cat's-tail
Poa spp. L.	Meadow-grass
Triticum aestivum L.	Wheat
Zea mays L. *	Maize

other herbaceous plants

Centaurea nigra L.	Lesser Knapweed, Hardheads
Amaranthus edulis L. (syn. *Carpobrotus edulis* (L.) N.E.Br.)	Hottentot Fig
Filipendula vulgaris Moench	Dropwort
Glycine max (L.) Merr *	Soya bean
Gossypium hirsutum L. *	Cotton
Helianthus anuus L.	Common Sunflower
Littorella uniflora (L.) Ascherson	Shore-weed
Lobelia dortmanna L.	Water Lobelia
Medicago sativa L.	Lucerne, Alfalfa
Orchis morio L.	Green-winged Orchid
Phaseolus vulgaris L. *	French bean, Haricot bean
Ranunculus spp. L.	Buttercup
Sanguisorba officinalis L. (syn. *Poterium officinale* (L.) A. Gray	Great Burnet
Sanguisorba minor Scop.: subsp. *minor* (syn. *Poterium dictyocarpum* Spach; *P. sanguisorba* L.)	Salad Burnet
Taraxicum sp. Weber	Dandelion
Trifolium sp. L.	Clover, Trefoil
Trifolium repens L.	White Clover, Dutch Clover

flowering trees and shrubs

Calluna vulgaris (L.) Hull	Heather, Ling
Eucalyptus pauciflora sieb. ex Spreng. (syn. *E. coriacea* A. Cunn.)†	Snow Gum
Erica tetralix L.	Cross-leaved Heath, Bog Heather
Populus sp. L.	Poplar

Appendix 8

Model concentration profiles over surfaces of different roughness

In cases where pollutant deposition occurs with $r_c = 0$, as with NH_3 deposition over natural (unfertilized) surfaces, then by definition, $\chi\{z_o'\} = 0$ (section 2.4). Given that the concentration profile is defined as:

$$\chi\{z\text{-}d\} = (\chi_*/k) \ln[(z\text{-}d)/z_\chi] \qquad \text{A8.1}$$

where z_χ is the height above the zero plane of predicted zero concentration and assuming neutral conditions. Then, where $r_c = 0$:

$$\chi\{z\text{-}d\} = (\chi_*/k) \ln[(z\text{-}d)/z_o'] \qquad \text{A8.2}$$

This equation may be used to construct hypothetical concentration profiles, which are useful for predicting maximum possible concentration changes within an available measurement height range, or for rescaling concentrations for different heights above a surface.

In order to use equation A8.2 the value of z_o' needs to be found. This is related to z_o through the quasi-laminar boundary-layer resistance, r_b, where this is defined and found as:

$$r_b = \ln[z_o/z_o']/(u_*k) = (u_*B)^{-1} \qquad \text{A8.3}$$

and B is the empirically estimated boundary layer Stanton number. In this study B is found following the method of Garland (1977; section 2.4), which gives good agreement with other estimations over smooth surfaces (Figure 3.5). According to Garland, for vegetated surfaces:

$$B^{-1} = 1.45\ Re_*^{0.24}\ Sc^{0.8} \qquad \text{A8.4}$$

where $Re_* = (z_o\ u_*)/\nu$ and $Sc = \nu/D$. However, over aerodynamically rough surfaces, such as forests, this agreement breaks down and other formulations give very different results. According to Wesely and Hicks (1977):

$$B^{-1} = 2/k\ (\kappa/D)^{0.67} \qquad \text{A8.5}$$

which for NH_3 gives $B^{-1} = 4.768$ for all vegetation roughnesses.*

---

* On the basis of the of experimentally determined values of B^{-1} reviewed by Garratt and Hicks (1973), equation A8.5 is expected to give a better estimate of B^{-1} than equation A8.4 for the large Re_* typical of forest canopies.

From equation A8.3, z_0' may be found from its relationship to z_0:

$$z_0/z_0' = e^{k/B} \qquad \text{A8.6}$$

This is used in Figure A8.1 for three example surface roughnesses, typical of short grassland (z_0 = 0.005 m), long grassland or cereals (z_0 = 0.05 m) and forest (z_0 = 0.5 m). For each case the Garland formulation of B^{-1} is used, with the Wesely and Hicks method also being used for the forest surface.

The Wesely and Hicks method provides z_0' as a constant fraction of z_0 for all vegetation roughnesses and windspeeds, such that for NH_3: $z_0/z_0' = 7.06$. Conversely, the value of this ratio for the Garland formulation varies both with z_0 and windspeed. In Figure A8.1 values of z_0' are given for $u\{10\text{ m}\}$ = 1–10 m s^{-1}. Given that $r_c = 0$, concentration profiles may be drawn between the appropriate value of z_0' and any concentration. As an example, this is done in each of the three diagrams for $u\{10\text{ m}\} = 5$ m s^{-1} and $\chi\{1\text{ m}\} = 1$ μg m^{-3}. The profiles represent maximum possible gradients, since where $r_c > 0$ then $\chi\{z_0'\} > 0$, which reduces the gradients.

Application

a) Maximum measurable concentration changes with height

The profiles plotted in Figure A8.1 are useful for demonstrating the effect of surface roughness on the ability to detect concentration gradients and fluxes above the surface. In order for the one dimensional flux gradient theory to apply, profile determinations must be made within the fully developed boundary layer. The maximum measurement height (z_{max}) is often approximately given by $z_{max} = x/100$, where x is the length of fetch over the surface to be measured (*e.g.* Monteith, 1973). Similarly, minimum heights apply in order that the effects of individual roughness elements are averaged out. Approximately, $z_{min} = 10\ z_0$ (Raupach, 1979). Consequently, gradient measurements must be made within this height range.

Typical available measurement ranges are given in Figure A8.1. With increasing roughness, the range becomes much smaller, so that the gradient is progressively difficult to detect over rougher surfaces in the absence of extremely large fetch. For example, for the lines drawn in Figure A8.1, the maximum concentration changes, $\Delta\chi$, are 0.56 μg m^{-3} (z_0 = 0.005 m), 0.25 μg m^{-3} (z_0 = 0.05 m) and 0.08 μg m^{-3} (z_0 = 0.5 m). Using the Wesely and Hicks method over forest $\Delta\chi$ is larger, 0.18 μg m^{-3} (z_0 = 0.5 m), though this is still small compared to the values possible over short vegetation. As a consequence, estimates of concentration gradients and fluxes over forests tend to be more approximate than over short vegetation.

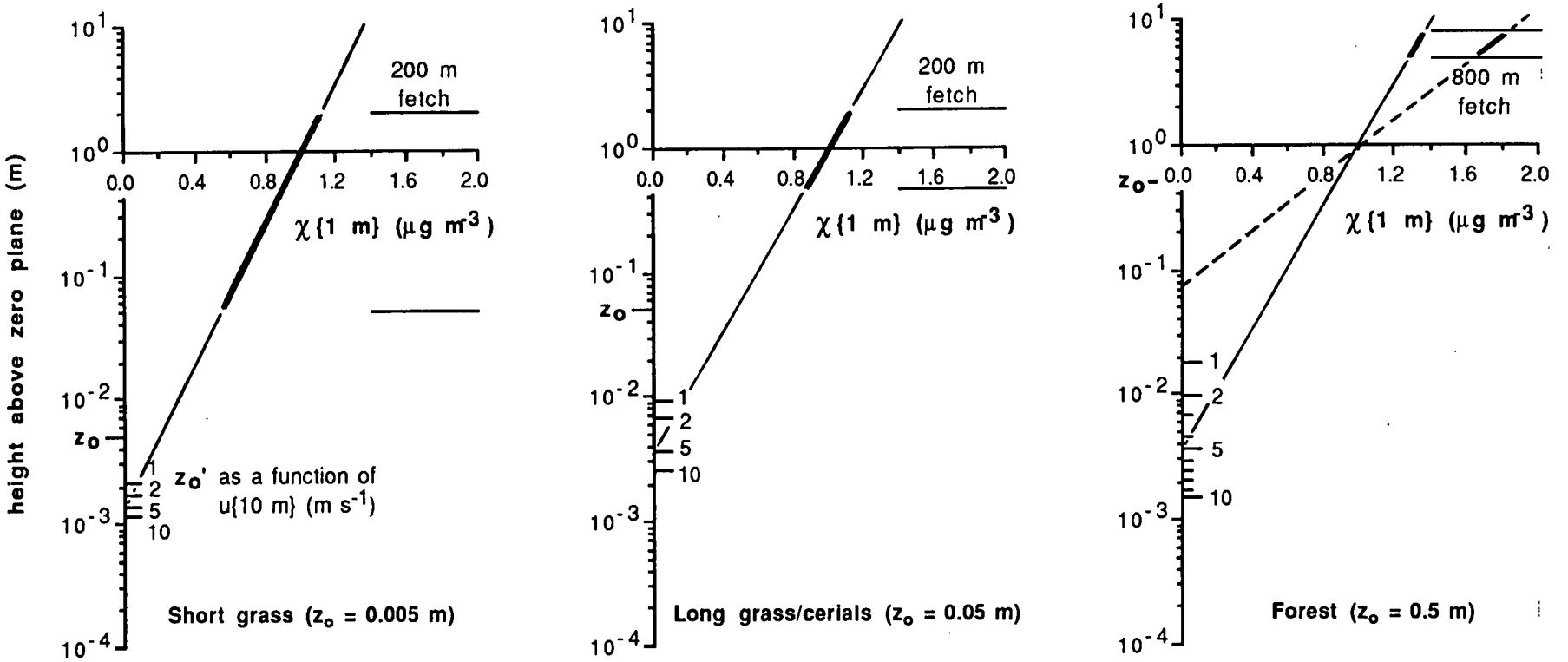

Figure A8.1 Model concentration profiles over surfaces of different roughness. Where $r_c = 0$ then $\chi\{z_o'\} = 0$. The example tie lines are drawn for $u\{10\ m\} = 5\ m\ s^{-1}$ and $\chi\{1\ m\} = 1\ \mu g\ m^{-3}$. The continuous lines are calculated according to $B^{-1} = 1.45\ Re_*^{0.24}\ Sc^{0.8}$ (Garland, 1977), while the dashed line by $B^{-1} = 2/k\ (\kappa/D)^{0.67}$ (Wesely and Hicks, 1977). The lines are described by $\chi\{z\text{-}d\} = \chi_*/k\ \ln[(z\text{-}d)/z_o']$. Bold sectors denote available measurement range for given fetch. See text for full details.

b) Rescaling concentrations with height above the surface.

The other use of this approach is to rescale concentrations for different heights above a surface. For the profiles here, it is clear that this is only possible where the assumption of $r_c = 0$ holds, as with NH_3 deposition to natural surfaces. For both the short vegetation examples in Figure A8.1, the value of z_o' varies little, so that a good approximation may be made with a single rescaling factor. In the estimation of budgets over forests, the effect on the flux of rescaling monitored concentrations from 1.5 m to 10 m above short vegetation is discussed (Chapter 7). For short vegetation a good approximation is given by:

$$\chi\{10\ \text{m}\} = (1.32 \pm 0.06) \times \chi\{1.5\ \text{m}\} \qquad \text{A8.7}$$

where the error is for the limits of $u\{10\ \text{m}\} = 1\text{–}10\ \text{m s}^{-1}$ and for short vegetation with $z_o = 0.005\text{–}0.05$ m. For another example rescaling from 2.5 to 10 m the multiplying factor is 1.21. This rescaling may be done either graphically or by substitution of values into equation A8.2.

Appendix 9

Continuous flow analysis system for NH_X

The continuous flow system used in this study was set up as shown schematically in Figure A9.1. The composition of reagents and details of preparation are given below:

Sodium hydroxide solution in water (25 g dm^{-3} ≡ 2.5% w/v): Add 66 cm^3 46/48% sodium hydroxide to 1 dm^3 of water, make up with water to 1.9 dm^3 and mix thoroughly.

Sodium salicylate (85 g dm^{-3}) and sodium nitroprusside (0.5 g dm^{-3}) solution in water: Dissolve 42.5 g sodium salicylate and 0.3 g sodium nitroprusside in 0.5 dm^3 of water and mix thoroughly.

Sodium hydroxide (25 g dm^{-3}) and sodium dichloroisocyanurate (5 g dm^{-3}) in water: Add 18 cm^3 46/48% sodium hydroxide to 0.2 dm^3 of water. Dissolve 2.5 g sodium dichloroisocyanurate in this solution, make up with water to 0.5 dm^3 and mix thoroughly.

Propan-2-ol solution in water (0.1 dm^3 dm^{-3} ≡ 10% v/v): Mix directly.

De-ionized water and analytical grade reagents used throughout.

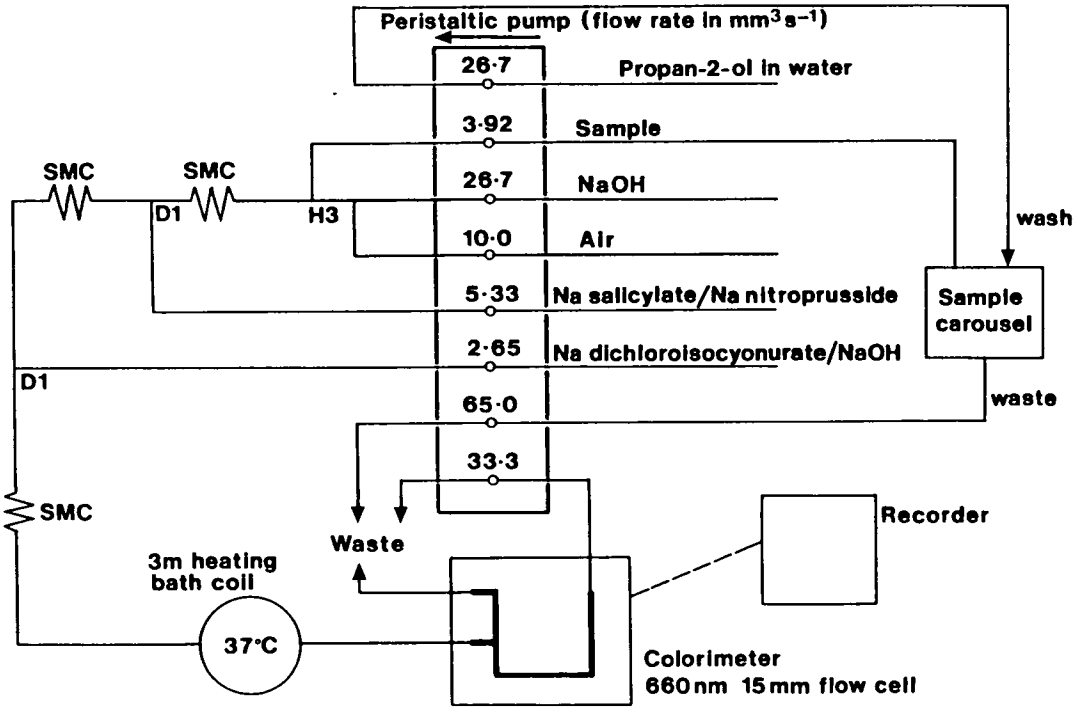

Figure A9.1 Continuous flow analysis system used for the analysis of NH_X. SMC = single mixing coil. D1 and H3 are standard fittings.